Characterisation of cells in the postnatal neurogenic niche of the murine spinal cord

Laura Frances Corns

Submitted in accordance with the requirements for the degree of
Doctor of Philosophy

The University of Leeds

School of Biomedical Sciences

Faculty of Biological Sciences

September 2012

The candidate confirms that the work submitted is her own and that appropriate credit has been given where reference has been made to the work of others.

This copy has been supplied on the understanding that it is copyright material and that no quotation from the thesis may be published without proper acknowledgement.

Acknowledgements

First and foremost, I would like to thank my supervisor Susan Deuchars who has been an excellent supervisor and a great role model. I would also like to thank my co-supervisor Jim Deuchars whose enthusiasm and ideas have always been welcome.

Thanks go out to all the members of Deuchars and Ichiyama labs who have been there to provide either technical advice or moral support, but a few deserve special mentions. In particular I would like to thank Brenda Frater, a brilliant technician, who taught me how to recover the filled slices, contributed to the recovery herself and was always on hand for advice. Thanks must go to Ian Edwards whose help was invaluable, as he was always there to help solve tricky technical rig or computer issues. I would also like to acknowledge and thank Mukti Singh and Jeremy Burgess who performed some of the immunohistochemistry that is part of this thesis.

Finally thanks must go to my wonderful friends and family, to my girls and Sally, who are always there to remind me to have fun, to Don and Julie who have provided many supportive cups of tea or glasses of wine, to my mum and dad who have always supported me in whatever I have wanted to do and are always on hand with excellent advice and food when it is needed, and last but certainly not least to Matt who, even on the bad cell days, has been there to cheer me up, keep me calm and provide amazing support.

Abstract

The area surrounding the central canal of the spinal cord is a highly plastic region containing a range of poorly defined cell types, including ependymal cells and cerebrospinal fluid-contacting cells (CSFcCs). This study aims to characterise ependymal cells and CSFcCs, determining whether they are capable of responding to neurotransmitters. To test the hypothesis, whole cell patch clamp electrophysiology and intracellular dye-loading in *in-vitro* Wistar rat and C57/bl6 mouse spinal cord slices were combined with immunohistochemistry.

CSFcCs could be categorised into three subtypes based on their voltage responses to positive current pulses. CSFcCs did not show an immediate electrophysiological response to 5HT or substance P but could respond to GABA with a $GABA_A$ receptor mediated depolarisation or hyperpolarisation. Ependymal cells were defined by their passive response properties and high degree of gap junction coupling and could depolarise in response to GABA; this could only be partially antagonised by the $GABA_A$ antagonist, bicuculline. CSFcCs and ependymal cells were both depolarised by ACh, with the size of the cholinergic response increasing from ependymal cells and subtype 1 CSFcCs to subtype 3 CSFcCs. Evidence indicated that the response was direct and mediated by nicotinic ACh receptors (nAChRs). Antagonism by the non α7*nAChR antagonist dihydro-β-erythroidinne or potentiation by the α7*nAChR modulator PNU-120596 revealed that non α7*nAChRs predominantly mediate the cholinergic responses but there is also a contribution from α7*nAChRs. These contributions varied between ependymal cells and the different CSFcC subtypes, reflecting variation in the functional responses of these cells.

GABA and ACh modulate neurogenesis and plasticity in other neurogenic niches and these results demonstrate that they are also capable of modulating cells within the neurogenic niche of the postnatal spinal cord. Manipulation of these neurotransmitter systems could influence ependymal cell proliferation and differentiation resulting in beneficial implications for the treatment of spinal cord pathologies.

Table of Contents

List of Figures

List of Tables

Abbreviations

[H]NMS[3]	[H]-*N*-methylscopolamine[3]
8-OH-DPAT	(±)-8-Hydroxy-2-dipropylaminotetralin
18β-Glycyrrhetinic acid	3β-Hydroxy-11-oxo-18β,20β-olean-12-en-29-oic acid
AADC	L-aromatic acid decarboxylase
α-BgT	α-Bungarotoxin
Acc	CC-contacting astrocyte
AChR	acetylcholine receptor
aCSF	artificial cerebrospinal fluid
AP-5	D-(-)-2-Amino-5-phosphonopentanoic acid
Atropine	α-(Hydroxymethyl)benzeneacetic acid 8-methyl-8-azabicyclo[3.2.1]oct-3-yl ester
BAC	bacterial artificial chromosome
Baclofen	(R)-4-Amino-3-(4-chlorophenyl)butanoic acid
Bicuculline	[R-(*R**,*S**)]-5-(6,8-Dihydro-8-oxofuro[3,4-*e*]-1,3-benzodioxol-6-yl)-5,6,7,8-tetrahydro-6,6-dimethyl-1,3-dioxolo[4,5-*g*]isoquinolinium
BLBP	brain lipid binding protein
BrdU	5-bromo-2'-deoxyuridine

BzATP	2'(3')-O-(4-benzoylbenzoyl)adenosine 5'-triphosphate
CAA	central autonomic area
CC	central canal
ChAT	choline acetyl transferase
CSF	cerebrospinal fluid
CSFcC	cerebrospinal fluid-contacting cell
CSFcN	cerebrospinal fluid-contacting neurone
D-AP5	D-(-)-2-amino-5-phosphonopentanoic acid
DA	dopamine
DAB	3, 3'-diaminobenzidine
DβH	dopamine-β-hydroxylase
Dcx	doublecortin
DG	dentate gyrus
DHβE	dihydro-β-erthyrodine / 3β-1,6-didehydro-14,17-dihydro-3-methoxy-16(15H)-oxaerythrinan-15-one
DiI	1,1'-dioctadecyl-6,6'-di(4sulphopentyl)-3,3,3',3'tetramethylindocarbocyanin
DMPP	1,1-dimethyl-4-phenylpiperazinium iodide
EAP	extravidin peroxidise

EPSP	excitatory postsynaptic potential
Gabazine	SR-95531 / 6-Imino-3-(4-methoxyphenyl)-1(6H)-pyridazinebutanoic acid
GAD	glutamic acid decarboxylase
GAT	GABA transporter
GENSAT	gene expression nervous system atlas
GFAP	glial fibrilliary acid protein
GFP	green fluorescent protein
GAP 43	growth associated protein 43
HuC/D	neurone specific RNA binding protein
IC	intercalated nucleus
IML	intermediolateral column
KCC2	K^+-Cl^- cotransporter
L-DOPA	L-3,4-dihydroxyphenylalanine
mAChR	muscarinic acetylcholine receptor
MCA	mecamylamine / N,2,3,3-tetramethylbicyclo[2.2.1]heptan-2-amine
mIPSPs	miniature inhibitory post-synaptic potentials

MLA	methyllycaconitine / [1α,4(S),6β,14α,16β]-20-Ethyl-1,6,14,16-tetramethoxy-4-[[[2-(3-methyl-2,5-dioxo-1-pyrrolidinyl)benzoyl]oxy]methyl]aconitane-7,8-diol
nAChR	nicotinic acetycholine receptor
NBQX	2,3,-dioxo-6-nitro-1,2,3,4-tetrahydrobenzo[f]quinoxaline-7-sulphonamide
NeuN	neuronal nuclei
NKCC1	Na^+-K^+-$2Cl^-$ cotransporter
NSC	neural stem cell
PB	phosphate buffer
PFA	paraformaldehyde
PKD2L1	polycystic kidney disease-2-like 1
PNMT	phenylethanolamine-N-methyltransferase
PNU-120596	N-(5-Chloro-2,4-dimethoxyphenyl)-N'-(5-methly-3-isoxazolyl)-urea
PPADS	pydridoxal phosphate-6-azo(benzene-2,4-disulfonic acid)
PSA-NCAM	polysialylated-neural cell adhesion molecule
Rhodamine	dextran tetramethylrhodamine
RT-PCR	reverse transcription-PCR

SVZ	subventricular zone
SPN	sympathetic preganglionic neurone
SV2	synaptic vesicle protein 2
TH	tyrosine hydroxylase
TRP	transient receptor potential
Tuj1	neurone-specific class III β-tubulin
VAChT	vesicular ACh transporter
VGAT	vesicular GABA transporter
VGluT1	vesicular glutamate transporter 1
VGlut2	vesicular glutamate transporter 2
VIP	vasoactive intestinal polypeptide.

Chapter 1 - General Introduction

1.1 The spinal cord

The spinal cord has been predominantly regarded as a relay centre within the CNS for many years. It is essential for the relaying of sensory information from the periphery to the brain, the subsequent relay of motor information from the brain to the periphery and the co-ordination of sensorimotor reflexes. However, it is becoming increasingly evident that the spinal cord is far more than a simple relay centre. The complex and diverse network of spinal cord neurones can modulate both the sensory input, and the autonomic and motor outputs, thus influencing the brain's perception of the sensory information and the magnitude of the autonomic or motor responses. Furthermore, certain groups of neurones within the spinal cord are capable of generating their own pattern of firing, such as the central pattern generators that are involved in controlling the muscle activity that underlies locomotion (for review see Kiehn (2006)).

Structurally, the spinal cord is divided into white matter, consisting of fibre tracts, and grey matter, containing neuronal cell bodies and their associated processes. The grey matter is further divided into laminae based on the cytoarchitecture of the specific areas (Rexed, 1952). The dorsal horn, which receives sensory input, can be divided into laminae I-VI. The ventral horn, where the somatic motor neurones and their associated interneurones reside, can be divided into laminae VIII and IX. The intermediate zone is found between the dorsal and ventral horn and incorporates the lateral horn, which contains the intermediolateral column (IML) and is associated with autonomic output; the intermediate zone can be divided into laminae VII and X. Lamina X was originally known as the *substantia grisea centralis* as it is the area of the grey matter at the centre of the spinal cord surrounding the central canal (CC), and it is this area that the following research focuses on.

1.2 Lamina X

Lamina X forms its dorsal border with the white substance of the dorsal funiculus and its ventral border with the commissura alba ventralis. The lateral borders of lamina X are formed with lamina VII; these borders are indistinct but are roughly where the central grey matter starts to widen towards the dorsal and ventral

columns. Lamina X itself can be further sub-divided into the commissural dorsalis grisae (the dorsal gray commissure), the commissural ventralis grisea (the ventral gray commissure) and the substantia gelatinosa centralis.

The substantia gelatinosa centralis is the ring of grey matter directly surrounding the CC and was considered by Rexed to consist almost wholly of glial cells and unmyelinated neuronal processes whilst being poor in neurones. It is this specific area that my research focuses on; therefore, the current knowledge about the cell types within this area will be most thoroughly examined. In addition, there are many other cell types within lamina X that must be considered, as they are likely to impact on the cells within the substantia gelatinosa centralis. Finally, the neuronal inputs to lamina X and the possible receptors that could mediate the responses to these inputs will be discussed.

1.3 Cell types of lamina X

The cells of lamina X can be divided into four categories: sympathetic preganglionic neurones (SPNs), interneurones, cerebrospinal fluid-contacting cells (CSFcCs) and ependymal cells.

1.3.1 Sympathetic preganglionic neurones

SPNs are peripherally projecting neurones whose axons exit the spinal cord by the ventral horn and synapse with the sympathetic postganglionic neurones, which in turn synapse with target organs. This sympathetic system is essential for the correct functioning of numerous vital organs, including the heart, vascular smooth muscle and kidneys. Using various techniques including the retrograde axonal transport of horseradish peroxidase (Chung et al., 1975), pseudorabies virus (Strack et al., 1989) and fluorogold (Strack et al., 1988) from different autonomic ganglia, including the adrenal medulla, SPNs have been identified in three areas of the spinal cord. Studeis in both the cat and rat have demonstrated that the majority of SPNs reside in the IML in the lateral horn of the spinal cord; others are located in the intercalated nucleus (IC), located between the IML and CC and in the central autonomic area (CAA) which is found dorsal to the CC in lamina X (Chung et al., 1975; Strack et al., 1988). SPNs are restricted to the thoracic and upper lumbar regions, from segments C8 to L3 (Strack et al., 1988). SPNs can also be identified

by their expression of choline acetyl transferase (ChAT), the enzyme necessary to produce ACh which thus identifies cholinergic cells (Houser et al., 1983; Barber et al., 1984). In the rat these cells are, however, intermingled with numerous other ChAT positive interneurones within the CAA. SPNs cannot definitively be distinguished by their morphology from these interneurones at autonomic levels, although they do commonly have larger cell bodies (Barber et al., 1984). They can be distinguished following the intraperitoneal injection of fluorogold, which labels only those neurones which have axons terminating in the periphery (Ambalavanar and Morris, 1989). SPNs of the IML can also be identified from neighbouring interneurones by their electrophysiological properties, for example, in the rat spinal cord SPNs have a longer action potential duration than interneurones due to a slower repolarisation phase (Deuchars et al., 2001). Although, the action potential duration of SPNs in the CAA of the rat was much shorter (3 ms) than that observed in SPNs of the IML (9 ms; Bordey et al., (1996a)). The SPNs of the CAA have dendrites orientated in numerous directions including laterally projecting dendrites that form large ChAT positive transverse dendritic bundles and dendrites that form longitudinal dendritic bundles (Barber et al., 1984). Through these dendrites and their cell bodies, SPNs receive inputs from supraspinal neurones and local interneurones. In the rat, SPNs respond to stimulation of glutamatergic and γ-aminobutyric acid (GABA)-ergic neurones of the rostral ventrolateral medulla (Deuchars et al., 1995; Deuchars et al., 1997) and GABAergic interneurones of the CAA (Deuchars et al., 2005). SPNs also respond to substance P (Dun and Mo, 1988), vasopressin, oxytocin (Backman and Henry, 1984; Hosoya et al., 1995), noradrenaline, adrenaline, dopamine (DA) (Lewis and Coote, 1990; Llewellyn-Smith et al., 2006), and 5HT (Ma and Dun, 1986; Bacon and Smith, 1988; Pickering et al., 1994). Many of the functional studies were observing SPNs of the IML, thus it is yet to be confirmed whether SPNs in the CAA respond in the same way to all of these stimuli. It has been confirmed that SPNs of the CAA respond to 5HT (Pickering et al., 1994) and ACh (Bordey et al., 1996a; Bradaia and Trouslard, 2002b; Bradaia et al., 2005) and produce glycinergic (Bradaia and Trouslard, 2002a) and GABAergic (Seddik et al., 2006) mediated miniature inhibitory postsynaptic potentials (mIPSPs).

1.3.2 Interneurones

There are numerous spinal interneurones within lamina X and although some of these neurones have been sub-typed using neurochemistry, there is little understanding of their function. To date subtypes of GABAergic, cholinergic and glutamatergic interneurones have been identified, with the possibility of 5HTergic interneurones also being present.

1.3.2.1 GABAergic interneurones

GABAergic interneurones are distributed throughout many areas of the CNS, including the spinal cord. These interneurones are most commonly identified through their expression of glutamic acid decarboxylase (GAD), the enzyme which synthesises GABA from glutamate. There are two isoforms of this enzyme, GAD65 and GAD67, and antibodies detecting these enzymes have been used to detect GABAergic neurones. More recently, transgenic mice have been generated that express green fluorescent protein (GFP) under the control of promoters for GAD65 and GAD67 (Tamamaki et al., 2003; Lopez-Bendito et al., 2004). This means that any neurones that usually express GAD should now express GFP, enabling GABAergic neurones to be visualised by fluorescence. In both the GAD65-GFP mice and GAD67-GFP mice, numerous GABAergic neurones can be observed in lamina X (Conte, 2009). This distribution is similar to that seen when using GAD antibodies or detecting GAD mRNA in rats (Barber et al., 1982; Feldblum et al., 1995). In the rat, GAD positive soma have a mean area of 153 μm^2 and appear to be organised into two longitudinal columns either side of the CC, one dorsolaterally and one ventrolaterally to the CC (Barber et al., 1982). Although there are GAD positive processes in numerous orientations from these neurones, there are more processes in a dorsoventral orientation from the dorsolaterally located cells, and more longitudinal processes from the ventrolaterally located cells (Barber et al., 1982). In the rat, a group of presympathetic GABAergic interneurones have been identified in the CAA by transneuronal labelling (Deuchars et al., 2005). These neurones provide ongoing monosynaptic inhibition to SPNs, which can be abolished by the GABA$_A$ receptor antagonist bicuculline. Other functions of these GABAergic interneurones are, to date, unknown.

1.3.2.2 Cholinergic interneurones

There are two types of cholinergic interneurone located in lamina X throughout the entire length of the spinal cord, namely partition neurones and CC cluster cells. The partition neurones are such named since they divide the dorsal and ventral aspects of the spinal cord as they extend across the intermediate grey matter from the CC to the lateral edges of the grey matter (Barber et al., 1984; Phelps et al., 1984). The partition neurones can be further divided into lateral, intermediate and medial depending on their position within the spinal cord, with the medial partition neurones being located in lamina X. Immunohistochemistry for ChAT established that these neurones possess complex dendritic arborisations and ventrolaterally projecting axons. Combining the immunohistochemistry with retrograde tracing using True blue in the rat demonstrated that they can project rostrocaudally up to six spinal cord segments from the segment in which the cell body is located (Sherriff and Henderson, 1994). As a result of this projection system they have been suggested to play a role in activities that require the co-ordination of numerous spinal segments (Sherriff and Henderson, 1994). Following fictive locomotion, which initiates the circuitry controlling movement without movement actually occurring, some partition neurones in the cat spinal cord express the activity dependent c-fos transcription factor, demonstrating that they are part of the circuitry involved in locomotion (Huang et al., 2000). A subpopulation of the ChAT positive medial partition neurones in the postnatal mouse spinal cord can be defined by their expression of the promoter for developing brain homeobox protein 1, Dbx1, and the expression of paired-like homeodomain transcription factor, Pitx2, during their development, and their lack of expression of nitric oxide synthase (Miles et al., 2007; Zagoraiou et al., 2009). The axons from this subpopulation of partition neurones form c-bouton synapses with motor neurones enabling them to regulate motor neurone excitability (Miles et al., 2007; Stepien et al., 2010). Genetic inactivation of ChAT in these specific neurones impairs the locomotor task-dependent modulation of hindlimb muscle activity (Zagoraiou et al., 2009; Stepien et al., 2010).

The CC cluster cells are a group of small neurones found in the grey matter surrounding the CC. ChAT positive processes from these cells contribute to small, longitudinal fascicles located near the ependymal layer in the rat spinal cord. These fascicles are most commonly observed ventral to the CC (Barber et al., 1984). These cells, like the partition neurones, have been observed to send projections up to six spinal cord segments away (Sherriff and Henderson, 1994). Although little is

known about these CC cluster cells it appears that at least a subpopulation are involved in locomotion, as evidenced by the fact that in the cat spinal cord they too express the activity dependent marker, c-fos, following fictive locomotion (Huang et al., 2000).

Due to the intersegmental projections of these cholinergic interneurones and their location in lamina X, it has been suggested that they provide a relay between dorsal, intermediate and ventral grey matter, providing integration between sensory, motor and autonomic functions (Borges and Iversen, 1986; Deuchars, 2007).

1.3.2.3 Glutamatergic interneurones

A population of small interneurones expressing the homeodomain transcription factor, Hb9, were identified predominantly in medial lamina VIII but also in ventral lamina X in mice (Hinckley et al., 2005; Wilson et al., 2005). These interneurones express vesicular glutamate transporter 2 (VGlut2) mRNA and are immunoreactive for the VGlut2 protein, therefore they are glutamatergic. They also receive glutamatergic inputs from both peripheral sources, identified by the expression of vesicular glutamate transporter 1 (VGluT1), and central sources, identified by the expression of VGlut2, as well as receiving input from 5HT-containing terminals (Wilson et al., 2005). These cells exhibit numerous characteristics expected of interneurones participating in locomotor rhythm generation. For example, there are pronounced membrane potential oscillations in these cells following the application of chemical stimuli that induce locomotor activity (Wilson et al., 2005), the activity dependent marker c-fos is expressed in these neurones following walking (Wilson et al., 2005) and the activity of these interneurones is synchronised to rhythmic ventral root output (Hinckley et al., 2005; Hinckley et al., 2010).

1.3.2.4 5HTergic interneurones

There is much debate over the presence of intraspinal 5HT interneurones. A few studies have shown 5HT positive interneurones within lamina X of the spinal cord in monkeys and rats (Lamotte et al., 1982; Newton et al., 1986; Takeoka et al., 2009).

These interneurones were located in levels associated with autonomic function, including T4-L2 and L6-S1, with the greatest numbers in T7-T10 (Newton et al., 1986). In the rat, these interneurones were always observed either dorsal or lateral to the CC and never ventral to the CC (Newton et al., 1986), however, in the monkey these interneurones were predominantly observed ventral to the CC (Lamotte et al., 1982). To support the presence of these interneurones, following a spinal cord transection at T9, 5HT immunoreactive fibres were observed in lamina X at T12, L3 and S1 in the rat (Takeoka et al., 2009). Despite these positive identifications of 5HT immunoreactive interneurones in the spinal cord many groups, including the Deuchars's lab, have been unable to detect any intraspinal 5HT interneurones; this could be due to a difference in antibodies used, the fact that these neurones have a small profile in transverse sections or due to their sparse numbers (Takeoka et al., 2009).

1.3.3 Cerebrospinal fluid-contacting cells

CSFcCs are an unusual cell type found within the substantia gelatinosa centralis. The cell bodies of CSFcCs are found predominantly in the subependymal layer surrounding the CC, but are also found within the ependymal layer itself (Figure 1.1). These cell bodies are roughly 92 μm^2, much smaller than nearby interneurones in rats (Barber et al., 1982). The defining feature of all CSFcCs is the process that extends from the cell body and through the ependymal layer to contact the cerebrospinal fluid (CSF) in the CC; this is commonly referred to as the CSF-contacting process (Vigh et al., 1977). The CSF-contacting process terminates in an enlarged bulb, 4-5 μm wide, which possesses stereocilia (Vigh et al., 1977). Although CSFcCs appear to be remarkably well conserved throughout evolution, this feature of CSFcCs varies between mammalian and non-mammalian vertebrates. The terminal bulbs of CSFcCs of non-mammalian vertebrates have numerous stereocilia and a larger kinocilium; in contrast mammalian CSFcCs possess fewer stereocilia and no kinocilium (Vigh et al., 1983). The CSFcCs also have axons that extend from the cell bodies to terminate on the ventral and ventrolateral surfaces of the cord in numerous species (Vigh et al., 1977; Shimosegawa et al., 1986; Lamotte, 1987; Stoeckel et al., 2003). These axons contain synaptic vesicles and express synaptic machinery such as synaptotagmin and synaptophysin, however in the rat, electron microscopy revealed that the
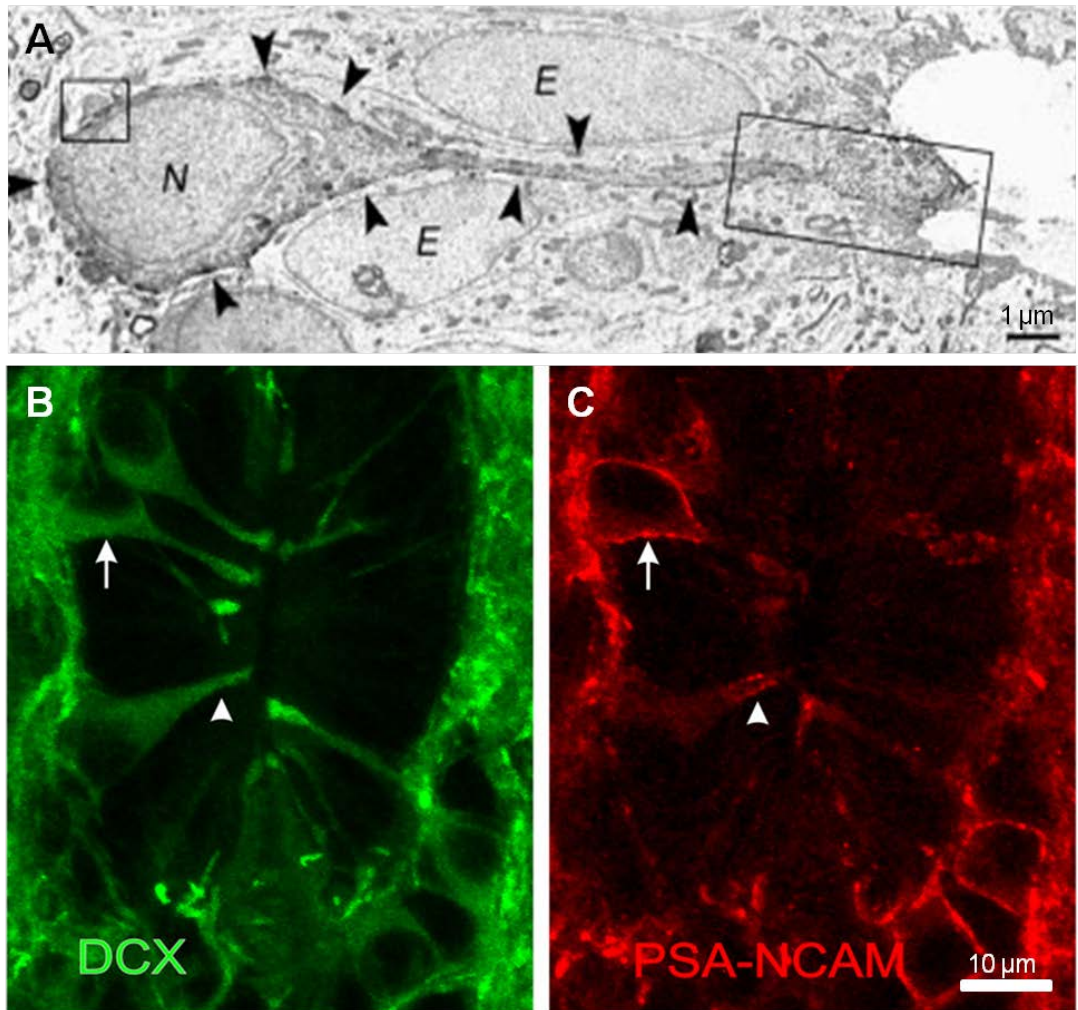
Figure 1.1: Morphology of CSFcCs.

A) Electron microscope image of a CSFcC with a round nucleus (N) and the CC-contacting process extending between two ependymal cells (E) to contact the lumen of the CC, arrowheads indicate $P2X_2$ labelling (Stoeckel et al., 2003). B and C) Immunohistochemistry for doublecortin (Dcx) and polysialylated-neural cell adhesion molecule (PSA-NCAM), highlighting the distribution of CSFcCs around the CC, arrows indicate CSFcC cell bodies and arrowheads indicate CSF-contacting processes (Marichal et al., 2009).

distribution of these proteins was throughout the axonal tracts but not in synaptic endings (Stoeckel et al., 2003). Using immunohistochemistry and electron microscopy in rats, unmyelinated axons believed to belong to CSFcCs were observed in close apposition to the basal bodies of ependymal cells; these axons were immunoreactive for GAD, GABA, P2X$_2$, synaptotagmin and growth associated protein (GAP)-43 (Stoeckel et al., 2003). The lack of synaptic endings observed in these axons combined with the expression of GAP 43, a protein which is expressed at high levels throughout axon genesis and is believed to play a role in synaptogenesis (Benowitz and Routtenberg, 1997), suggests that these axons are immature in nature or are involved in axonal remodelling.

CSFcCs have previously been classified into subtypes based on their morphology, including the shape of the cell body or on the relationship between the CSF-contacting and axonal processes. The cell bodies can be either oval, polygonal or elongated (Shimosegawa et al., 1986). The axonal processes extend from (1) the basal surface of the cell body, directly opposite the CSF-contacting process; (2) the lateral surface of the cell body; (3) the same origin as the CSF-contacting process; and (4) regions further along the CSF-contacting process (Shimosegawa et al., 1986). This demonstrates the variations in morphology that are present within the CSFcC population, although it is unknown whether these morphologically different CSFcCs perform specific functions.

1.3.3.1 Possible functions of CSFcCs

Most of the hypotheses regarding the function of CSFcCs have been based on their expression of different enzymes, neurotransmitters, neuromodulators and receptors that has been determined through immunohistochemical studies. The expression of such molecules is different between non-mammalian and mammalian vertebrates, however, the variation may appear greater than it is due to a lack of investigation of all molecules in all species. To outline the actual variation, as opposed to lack of data, Table 1 states those species that were positively immunoreactive for a molecule and those that were found to be negatively immunoreactive for the same molecule. Although mammalian CSFcCs are the focus of this research, it is important to look at non-mammalian vertebrate CSFcCs to compare the

Table 1.1: Immunoreactivity of CSFcCs to several neurotransmitters, enzymes and receptors in numerous species.

[1] (Nagatsu et al., 1988); [2] (Jaeger et al., 1983); [3] (Roberts et al., 1995); [4] Deuchars's Lab; [5] (Barber et al., 1982); [6] (Fernandez et al., 2002); [7] (Margeta-Mitrovic et al., 1999); [8] (Lamotte, 1987); [9] (Fuji et al., 1983); [10] (Gibson et al., 1981); [11] (Shimosegawa et al., 1986); [12] (Stoeckel et al., 2003); [13] (Huang et al., 2006).

Enzyme, Neurotransmitter or Receptor	Species with CSFcCs immunoreactive for	Species with CSFcCs not immunoreactive for
L-aromatic acid decarboxylase (AADC)	Mouse [1], Rat [2]	
Tyrosine Hydroxylase (TH)	Eel, Trout [3]	Mouse, Rat [1,2]
Dopamine-β-hydroxylase (DβH)		Mouse, Rat [1]
DA	Eel, Trout [3]	Mouse, Rat [1]
Phenylethanolamine N-methyltransferase (PNMT)		Mouse, Rat [1,2]
5HT		Mouse, Rat [2]
GAD	Mouse [4], Rat [5], Eel, Trout [3], Turtle [6]	
GABA$_B$ Receptors	Rat [7]	
Vasoactive intestinal polypeptide (VIP)	Cat, Monkey [8], Rat [9], Guinea Pig [10]	
Methionine-enkephalin-Arg6-Gly7-Leu8	Rat [11]	
ACh		Eel, Trout [3], Mouse, Rat [4]
P2X$_2$	Mouse [4], Rat [12]	
Polycystic kidney disease-2-like 1 (PKD2L1)	Mouse [13], Rat [4]	

differences. Whether these differences could have impacted on the loss of regenerative capacity of mammalian spinal cords is of great importance.One of the greatest differences observed between mammalian and non-mammalian CSFcCs is their expression of monoamines. Non-mammalian CSFcCs, such as those of the eel and trout, express tyrosine hydroxylase (TH), the enzyme that is needed for the production of DA, and express DA itself (Roberts et al., 1995). On the other hand mammalian CSFcCs are devoid of DA, TH, 5HT and dopamine-β-hydroxylase (DβH) and phenylethanolamine N-methyltransferase (PNMT), the enzymes required for the conversion of DA to noradrenaline and noradrenaline to adrenaline, respectively (Jaeger et al., 1983; Nagatsu et al., 1988). It is interesting to note, however, that despite the lack of expression of all these monoamines and the enzymes required for their synthesis, the CSFcCs of both mice and rats express L-aromatic acid decarboxylase (AADC), the enzyme that converts L-3,4-dihydroxyphenylalanine (L-DOPA) to DA and 5-Hydroxytryptophan to 5HT (Jaeger et al., 1983; Nagatsu et al., 1988). Another cell type, known as monoenzymatic-AADC neurones have been discovered throughout the brain, including in the suprachiasmatic nucleus (Ishida et al., 2002; Ugrumov, 2009). Also within the suprachiasmatic nucleus, *in-situ* hybridisation, has found mRNA for a membrane transporter of large neutral amino acids that can capture L-DOPA from the extracellular fluid (Fernandez et al., 2005). Loading the extracellular fluid of the suprachiasmatic nucleus with L-DOPA resulted in the appearance of DAergic neurones whose distribution correlated with that of AADC neurones (Ishida et al., 2002), implying that these AADC-neurones can take up L-DOPA from the extracellular fluid and subsequently convert it to DA. As CSFcCs are in contact with the CSF, it is possible that they could be performing a similar function. The expression of DA within CSFcCs could have been missed as L-DOPA may only be available at certain times of day or following certain perturbations. Alternatively the expression of AADC could be an evolutionary remnant that is no longer functional.

The one consistency between all species investigated to date is their expression of the enzyme GAD, the enzyme required to produce the neurotransmitter GABA (Barber et al., 1982; Roberts et al., 1995; Fernandez et al., 2002). This conservation throughout evolution suggests that the expression of GABA within CSFcCs is one of functional significance. In mammals GABAergic CSFcCs are found surrounding the CC in dorsal, ventral and lateral locations (Barber et al., 1982). In non-mammalian vertebrates, such as the eel and trout, there is a location specific expression of GABAergic CSFcCs as they are predominantly found lateral

to the CC, with DAergic CSFcCs located surrounding the ventral pole of the CC (Roberts et al., 1995). It would appear that throughout evolution the expression of monoamines such as DA has been lost, however, that of GABA has been maintained and these GABAergic CSFcCs could be compensating for the loss of the monoaminergic CSFcCs.

It is possible that it is not only the cell bodies of CSFcCs that are GABAergic, electron microscopy studies in the rat demonstrate that CSFcCs possess small, clear synaptic vesicles in the CSF-contacting terminal bulbs (Unpublished observation Deuchars's Lab). Given the lack of monoamine and ACh expression in mammalian CSFcCs it would be logical to suggest that the small, clear synaptic vesicles are either GABA- or glutamate-containing. In support of the presence of GABA within these vesicles, immunohistochemistry has revealed the presence of the vesicular GABA transporter (VGAT), which is necessary to load synaptic vesicles with GABA, within the CSF-contacting terminal bulbs in rats (Conte, 2009). In addition, large, dense granules were observed within the terminal bulb using electron microscopy in rats. As immunohistochemistry has revealed the presence of the endogenous opioid peptide, methionine-enkephalin-Arg6-Gly7-Leu8, in the rat (Shimosegawa et al., 1986) and vasoactive intestinal polypeptide (VIP) in the monkey within CSFcCs it could be proposed that one of these peptides is present in the large, dense granules, although neither have been confirmed by electron microscopy (Fuji et al., 1983; Gibson et al., 1984; Lamotte, 1987). In addition to these vesicles, this lab has identified that the terminal bulb contains certain molecules involved in the exocytosis of synaptic vesicles, including synaptic vesicle protein 2 (SV2) and synaptophysin (Edelmann et al., 1995; Chang and Sudhof, 2009) . This indicates that mammalian CSFcCs could be capable of releasing GABA or peptide transmitters into the CSF of the CC, suggesting that the CSF-contacting process has a secretory function.

The CSF-contacting process could also perform a sensory function. The presence of cilia suggests that CSFcCs have a mechanosensory function, possibly monitoring the flow of CSF (Vigh et al., 1977), although this has never been supported by any functional studies. In addition, as mammalian CSFcCs possess fewer and less developed cilia than non-mammalian CSFcCs (Vigh et al., 1983) it suggests that mechanosensation would be limited and that it is not the primary function of mammalian CSFcCs.

CSFcCs also express receptors and channels capable of sensing the environment suggesting that CSFcCs could perform a different type of sensory function. These sensory ion channels are expressed on both the cell bodies and CSF-contacting processes of CSFcCs of mice and rats. One of these channels is the purinergic receptor, $P2X_2$ (Figure 1.1), a non-selective cation channel whose natural ligand is ATP (North and Surprenant, 2000; Stoeckel et al., 2003). Despite the ligand being ATP, the function of this receptor is also modulated by pH (King et al., 1997; Stoop et al., 1997). $P2X_2$ receptors expressed by CSFcCs do appear to be functional as the application of ATP elicited a depolarisation, with the channel properties resembling those of $P2X_2$ receptors (Marichal et al., 2009). Another channel observed in CSFcCs is the transient receptor potential polycystin 3 channel, also known as polycystic kidney disease-2-like 1(PKD2L1) channel (Stoeckel et al., 2003; Huang et al., 2006). PKD2L1 is a relatively newly discovered channel therefore its properties are poorly understood. However, when in a complex with polycystic kidney disease-1-like 3 it has been observed to respond to the application of acid with a large inward current (Ishimaru et al., 2006). PKD2L1 is believed to be found within the cytosol, thus it reacts to intracellular acidification as opposed to extracellular acidification (Huang et al., 2008), although intracellular acidification can occur as a consequence of extracellular acidification; on activation PKD2L1 appears to mediate intracellular calcium release (Huang et al., 2008). CSFcCs increase their rate of action potential firing in response to a decrease in pH from 7.4 to 6.9 (Huang et al., 2006), and to produce a large inward current in response to a 100 ms pressure application of pH 6 solution (Marichal et al., 2009), although the channel through which this response was mediated was not determined in either experiment. The CSFcCs considered so far have been spinal CSFcCs, however, there are also CSFcCs present in the dorsal vagal complex of the mouse brainstem that express PKD2L1 (Orts Del'immagine et al., 2012). In these brainstem CSFcCs, spontaneous single channel activity with properties strongly resembling those of PKD2L1 channels have been reported (Orts Del'immagine et al., 2012).

The ability of CSFcCs to respond to changes in pH and ATP implies that they could be sensing the CSF or the extracellular solution in the area surrounding the CC. Alternatively or indeed additionally, the CSFcCs could be receiving synaptic inputs from ATP-releasing terminals on to post-synaptic densities containing $P2X_2$ receptors. Electron microscope studies in the rat and mouse have shown that CSFcCs are contacted by synaptic boutons (Stoeckel et al., 2003; Alfaro-Cervello

et al., 2012) providing evidence that CSFcCs are to some extent integrated into the circuitry of the spinal cord; however, what neurotransmitters are present in these synaptic boutons is yet to be observed at the ultrastructural level. Immunohistochemistry in rats has revealed GABAergic terminals in close apposition to CSFcCs (Mclaughlin et al., 1975) and functional studies, also in rats, suggest that these terminals form synapses onto CSFcCs as whole cell patch clamp recordings reveal that CSFcCs can respond to the pressure application of GABA, although whether this effect was direct was not investigated (Marichal et al., 2009). The GABAergic response in this investigation was mediated by $GABA_A$ receptors as it was fully antagonised by the $GABA_A$ receptor antagonist gabazine (Marichal et al., 2009); however, as this experiment was not performed in a low Ca^{2+} solution or in the presence of compounds that prevent synaptic transmission, unequivocal evidence for the expression of $GABA_A$ receptors by spinal CSFcCs has not been provided. At a membrane potential of -80 mV spontaneous inward current activity that is antagonised by gabazine has been observed in mouse brainstem CSFcCs, indicating the presence of functional GABAergic synapses onto brainstem CSFcCs (Orts Del'immagine et al., 2012). Immunohistochemistry has provided evidence indicating that CSFcCs express $GABA_B$ receptors in the rat (Margeta-Mitrovic et al., 1999), although as yet there is no functional evidence for the presence of $GABA_B$ receptors in CSFcCs. Nevertheless, the combined evidence suggests that CSFcCs could release GABA and respond to GABA, implying that the CSFcCs could communicate with each other and could regulate their own excitability with a negative feedback mechanism.

Finally, with regards to function, it has been proposed that CSFcCs could connect the internal CSF, found within the CC, with the external CSF, found surrounding the entire spinal cord (Vigh et al., 2004). The CSFcCs could become excited through either mechanosensation of the CSF flow within the CC or via changes in pH or neurotransmitter content of the CSF within the CC, and as a result release neurotransmitters into the external CSF. However, although this may be their function in lower vertebrates, the lack of synapse formation observed in the axons of mammalian CSFcCs (Stoeckel et al., 2003) suggests that they are not involved in secreting neurotransmitter or neuropeptides into the external CSF. It appears more likely that their primary role is to sense the environment in their immediate vicinity due to the functional evidence showing their ability to respond to changes in ATP concentrations and pH, and possibly use this information to regulate the local environment surrounding the CC.

1.3.3.2 Phenotype of CSFcCs

One big question regarding CSFcCs is whether they are mature neurones, immature neurones, glial or a mixed population of cells. There are two main methods used to study cell types, immunohistochemistry and electrophysiology. Immunohistochemistry has revealed that CSFcCs in the mouse do not express glial fibrillary acidic protein (GFAP; Hamilton et al., (2009); Sabourin et al., (2009)) a glial marker, indicating that they are not glial cells. However, in the rat they do not express neuronal nuclei (NeuN), a widely used marker of mature neurones, either (Mullen et al., 1992; Marichal et al., 2009). There are a few types of mature neurones that do not express NeuN, including cerebellar purkinje cells (Mullen et al., 1992); therefore a lack of NeuN is not a definitive method for determining whether CSFcCs are neurones. In fact, immunohistochemistry in the rat and mouse has revealed that CSFcCs express doublecortin (Dcx), polysialylated-neural cell adhesion molecule (PSA-NCAM), neuronal specific class III β-tubulin (Tuj1), the neurone specific RNA binding protein (HuC/D) and GAP 43 (Figure 1.1; Stoeckel et al., (2003); Hamilton et al., (2009); Marichal et al., (2009); Conte (2009)). These are proteins predominantly expressed during states of maturation, at times when the neurone is considered immature; however, they can also be expressed by mature neurones undergoing plastic changes (Lee et al., 1990; Theodosis et al., 1991; Benowitz and Routtenberg, 1997; Okano and Darnell, 1997; Brown et al., 2003). Using PSA-NCAM as an example, many areas in the adult CNS contain neurones that regularly undergo morphological alterations, such as dendritic remodelling which leads to alterations in the existing synapses; in these areas there is a high expression of PSA-NCAM, for example in the adult hypothalamo-neurohypophysial system of the rat (Theodosis et al., 1994). It is possible that the area surrounding the CC is one such area whose neurones are regularly undergoing morphological and thus synaptic remodelling.

To better determine whether CSFcCs are mature neurones that undergo plastic changes, immature neurones or a mixture of both, functional studies using whole cell patch clamp electrophysiology were employed. In rats, this has revealed that CSFcCs are a heterogenous population. They have characteristics of immature neurones that are at varying degrees of maturity. Based on the electrophysiological properties of mammalian CSFcCs from the rat they have previously been divided into three different subtypes (Marichal et al., 2009). The first subtype had high input resistances and responded to depolarising current pulses with slow Ca^{2+}-mediated depolarisations that were abolished in the presence of Mn^{2+}. The second subtype

had smaller input resistances and produced what the authors termed as a spike in response to the injection of a positive current pulse. The use of the term spike rather than action potential implies that although this was a significant, fast event with a depolarising and repolarising phase, it did not meet the normal definition of an action potential in that the size was smaller and the half-amplitude duration slower than would be expected; this term spike will be used throughout this work in the same context. The single spikes observed in this subtype had an average amplitude of 38 mV, an average half amplitude duration of 6 ms and were abolished in the presence of TTX, thus indicating that they were mediated by voltage-gated Na^+ channels. The third subtype was able to respond to the positive current pulse with multiple spikes. On average these spikes had a larger amplitude of 56 mV and a shorter half-amplitude duration of 4 ms, than those in the second subtype. Within this subtype there can be further differentiation; some CSFcCs responded with robust repetitive firing, whereas others could not sustain the firing throughout or the half-amplitude duration of the spikes increased throughout the pulse.

CSFcCs also varied in their responses to GABA; from their resting membrane potential some CSFcCs depolarised whilst others hyperpolarised, with reversal potentials ranging from -43 mV to -80 mV (Marichal et al., 2009). The varying reversal potentials were due to differences in intracellular Cl^- concentration, which are determined by the variable expression of the Na^+-K^+-$2Cl^-$ cotransporter (NKCC1) and the K^+-Cl^- cotransporter (KCC2). Immature neurones express high levels of NKCC1 (Clayton et al., 1998) which drives Cl^- into the cell in exchange for the extrusion of Na^+ and K^+, thus maintaining a high intracellular Cl^- concentration. On activation of GABA receptors the Cl^- ions exit the cell due to the concentration gradient, causing a depolarisation. As neurones mature they express less NKCC1, thus the KCC2 transporter has a greater influence over the intracellular Cl^- concentration (Rivera et al., 1999); KCC2 drives Cl^- out of the cell in exchange for K^+ moving into the cell thus the intracellular Cl^- concentration is lower as neurones mature. Thus the lower intracellular Cl^- concentration means that when GABA receptors are activated the Cl^- moves into the cell, causing a hyperpolarisation. Therefore the variable responses of CSFcCs to positive current pulses and GABA appear to support the belief that CSFcCs are immature neurones at varying levels of maturity.

Another question to ask concerning CSFcCs is whether they are born postnatally? To investigate this question, a number of studies have used 5-bromo-2'-

deoxyuridine (BrdU), a marker that can be incorporated into newly synthesised DNA during the S phase of the cell cycle, highlighting newly developed cells (Wojtowicz and Kee, 2006). Under physiological conditions in the rat, CSFcCs were only observed when the BrdU injections were given during the embryonic period, E7-E17, not when the injections were given during the postnatal period, P0-P5, providing evidence that CSFcCs are born in the embryo and not postnatally (Marichal et al., 2009). Furthermore, other studies have been unable to observe co-localisation of BrdU with the mature neuronal marker, NeuN, or the immature marker, Dcx, either under physiological conditions or following perturbations (Johansson et al., 1999; Horner et al., 2000; Martens et al., 2002; Mothe and Tator, 2005). A small number of studies have observed newborn neurones in the adult spinal cord and these will be discussed later, however, those newborn neurones observed do not have the morphology of CSFcCs (see section 1.5.4.2; Danilov et al., (2006); Shechter et al., (2007); Vessal et al., (2007); Shechter et al., (2011)).

1.3.4 Ependymal Cells

Other than the CSFcCs, the most well defined cell type within the substantia gelatinosa centralis is the ependymal cell. This is the cell type that directly surrounds the CC forming the barrier between the CSF and the rest of the grey matter. It is becoming increasingly clear that there are different subtypes of ependymal cells as well as other poorly defined cell types within the ependymal layer.

Ependymal cells in the postnatal spinal cord of the mouse are derived from Nkx6.1 homeodomain progenitor gene-expressing ventral neuroepithelial cells (Fu et al., 2003). In the rat, they line the CC with a single layer in most areas of the CC; however, in certain regions there can be up to four layers of ependymal cells (Bruni and Reddy, 1987). The thickness of the ependymal layer is generally dependent on the spinal region, with the thoracic region having the thinnest ependymal layer, followed by the cervical region, then the lumbar region and finally the sacral region generally has the thickest ependymal layer in the rat (Bruni and Reddy, 1987).

The ependymal cells themselves are a pseudostratified cuboidal to columnar shape with a round nucleus located in the mid to basal aspect of the cell (Bruni and

Reddy, 1987). Microvilli cover the apical cell surface, with a cluster of long cilia in the centre projecting into the CC. Neighbouring ependymal cells have closely apposed lateral margins that are joined by zonula adherins junctions near the apical surface (Del Bigio, 2010). In the rat, the basal surface of the ependymal cells is separated from the underlying grey matter by a basement membrane that consists of collagens and fibronectin (Azzi et al., 1989). Ependymal cells are also connected to each other by gap junctions, allowing intercellular communication and aiding in ion homeostasis and volume regulation. Both connexin 43 (Belliveau and Naus, 1995; Ochalski et al., 1997; Marichal et al., 2012) and connexin 45 (Chapman et al., 2012) are present in ependymal cells of the rat spinal cord. Connexin 30 is expressed in ependymal cells lining the ventricles (Kunzelmann et al., 1999); however, it is not known whether it is expressed in those lining the CC.

Immunohistochemistry in the mouse has revealed that ependymal cells express both the intermediate filament protein, vimentin, and the calcium binding protein, S100β (Hamilton et al., 2009). Sox2, another marker of undifferentiated stem and progenitor cells in the forebrain subventricular zone (SVZ) is expressed by all ependymal cells surrounding the CC in the mouse (Hamilton et al., 2009). Ependymal cells in the rat express the transporter NKCC1 (Kanaka et al., 2001), suggesting that they accumulate intracellular Cl$^-$, as described previously for immature neurones.

Few electrophysiological studies of ependymal cells have been made; however, a recent study by Marichal et al., (2012) has provided the first electrophysiological characterisation of ependymal cells at the lateral aspects of the CC of the mammalian spinal cord in P0-P5 rats. The cells recorded had a low input resistance of 124 ± 24 MΩ, a hyperpolarised resting membrane potential of -84 ± 2 mV and passive responses to depolarising current pulses, with a linear voltage-current relationship. The study demonstrated gap junction coupling between ependymal cells, through dye-coupling observed by Alexa 488 which was present in the intracellular solution of the patch pipette. The functional presence of gap junctions was demonstrated by an increase in input resistance observed following the application of the gap junction blocker, carbenoxelone. This study did not investigate whether the ependymal cells could respond to neurotransmitters.

1.3.4.1 Ependymal cell subpopulations

Studies have analysed the ultrastructure of cells in the ependymal layer using electron microscopy and as a result have identified a plethora of subpopulations of ependymal cells in the murine spinal cord (Meletis et al., 2008; Alfaro-Cervello et al., 2012). The classical cuboidal ependymal cell was identified using the marker FoxJ1, which specifically identifies cells with motile cilia (Meletis et al., 2008). Studying the ciliary structure of these ependymal cells revealed that the most common ependymal cell type had two long motile (9+2 microtubule axoneme structure) cilia; this was named as a biciliated ependymal cell (Alfaro-Cervello et al., 2012). There were also ependymal cells with one, three and four cilia; the cells with four cilia were binucleated, containing two distinct nuclei (Alfaro-Cervello et al., 2012). All of these cells expressed the intermediate filament protein, vimentin, which is typically used to identify ependymal cells (Alfaro-Cervello et al., 2012). A subpopulation of these cells express the cannabinoid receptor, CB1, in the mouse (Garcia-Ovejero et al., 2012).

In addition to the cuboidal ependymal cells described above, a number of studies in the murine spinal cord have determined cells that have varied structural or molecular properties from the cuboidal ependymal cell (Meletis et al., 2008; Hamilton et al., 2009; Sabourin et al., 2009; Alfaro-Cervello et al., 2012; Marichal et al., 2012). Unfortunately, there is currently no consensus as to what these cell types should be called, with each study using different names; the following paragraphs, figure 2 and table 2 aim to clarify this issue by uniting the findings.

Using scanning and transmission electron microscopy a population of CC-contacting astrocytes (Acc) were observed within the ependymal layer in cervical, thoracic and lumbar regions surrounding of the spinal cord; these cells contacted the CC through a thin process, had a primary cilium and were defined as astrocytes due to their expression of GFAP (Alfaro-Cervello et al., 2012). These Accs were distributed in the lateral and ventral regions around the CC and also expressed vimentin and nestin.

All of the other subpopulations of ependymal cells had a preferential expression at either the dorsal or ventral poles (Meletis et al., 2008; Hamilton et al., 2009; Sabourin et al., 2009). The FoxJ1 marker identified a cell type whose cell body was

Table 1.2: Summary of the cell types in the ependymal layer of the spinal cord of postnatal mice.

[1] (Alfaro-Cervello et al., 2012), [2] (Hamilton et al., 2009), [3] (Sabourin et al., 2009), [4] (Meletis et al., 2008), [5] (Marichal et al., 2012), [6] (Marichal et al., 2009).

Cell type		Markers					Location surrounding CC
		Vimentin	GFAP	Nestin	BLBP	Dcx	
Cubiodal ependymal cell		+	-	-	-	-	All regions
Acc [1]		+	+	+	-	-	Lateral, ventral
Radial ependymal cell [4]	Nestin-expressing [2]	+	?	+	?	-	Dorsal, ventral, few lateral
	GFAP-expressing [2]	+	+	?	?	-	Dorsal, ventral
	BLBP-expressing [3]	-	+	?	+	-	Dorsal
Radial glia [5]		-	-	+	?	-	Dorsal, ventral
CSFcC [6]		-	-	-	-	+	All regions

similar to that of cuboidal ependymal cells but had a long basal process that extended from the cell bodies found at the dorsal and ventral poles of the CC along the dorsoventral axis; these cells were termed radial ependymal cells (Meletis et al., 2008). Using immunohistochemistry, three markers were identified predominantly at the dorsal pole but also at the ventral pole of the CC in the mouse and rat: GFAP, nestin and brain lipid binding protein (BLBP; Hamilton et al., (2009); Sabourin et al., (2009); Alfar-Cervello et al., (2012); Marichal et al., (2012)). All of these markers identified the cell bodies plus the radially projecting fibres. The GFAP-expressing cells located at the dorsal and ventral poles appear to differ from those of Accs as some studies observed that they did not co-localise with vimentin (Alfaro-Cervello et al., 2012), although other studies have observed a co-localisation of the two proteins (Hamilton et al., 2009); this could be due to the use of different antibodies. GFAP-expressing cells at the dorsal pole only co-localise with the less frequently observed BLBP-expressing cells (Sabourin et al., 2009; Alfaro-Cervello et al., 2012). Nestin-expressing cells are also observed at the dorsal pole, with fewer seen at the ventral pole and a very small amount found in lateral regions of the CC in the rat (Hamilton et al., 2009). The nestin expressing cells co-localise with vimentin but it is unclear whether they co-localise with either GFAP or BLBP (Hamilton et al., 2009). The cells defined as radial ependymal cells by Meletis et al., (2008) could encompass all of the cells types observed at the dorsal and ventral poles with different protein expressions, therefore, until further clarification is made these cells will be referred to as radial ependymal cells.

In the turtle, a lower vertebrate, neural progenitor cells known as radial glia are expressed in high numbers around the CC throughout adulthood (Russo et al., 2008). These radial glia express BLBP and have a long process that extends away from the CC; on this classification the BLBP expressing radial ependymal cells observed in rats and mice could be radial glia (Meletis et al., 2008; Russo et al., 2008; Hamilton et al., 2009; Sabourin et al., 2009). Interestingly, some of the nestin expressing processes extending along the dorsal and ventral midline in the rat spinal cord have been found to originate from cell bodies further away from the CC, it has also been proposed that these cells could be the equivalent mammalian radial glia (Marichal et al., 2012). Unlike the cuboidal ependymal cells found at the lateral aspects of the CC, these nestin-expressing cells that have been proposed as radial glia were found to have a higher input resistance (361 ± 56 MΩ), a lack of dye-coupling, outward currents with the properties of delayed rectifier K^+ currents and A-type K^+ currents and inward currents with properties of low voltage-activated

Ca^{2+} currents (Marichal et al., 2012). The radial glia in the turtle depolarise in response to GABA, a response which is mediated via the GABA transporter (GAT)-3 and through GABA$_A$ receptors and induces an increase in intracellular Ca^{2+} (Reali et al., 2011). It remains to be seen whether radial ependymal cells or radial glia in mammals are capable of a similar response.
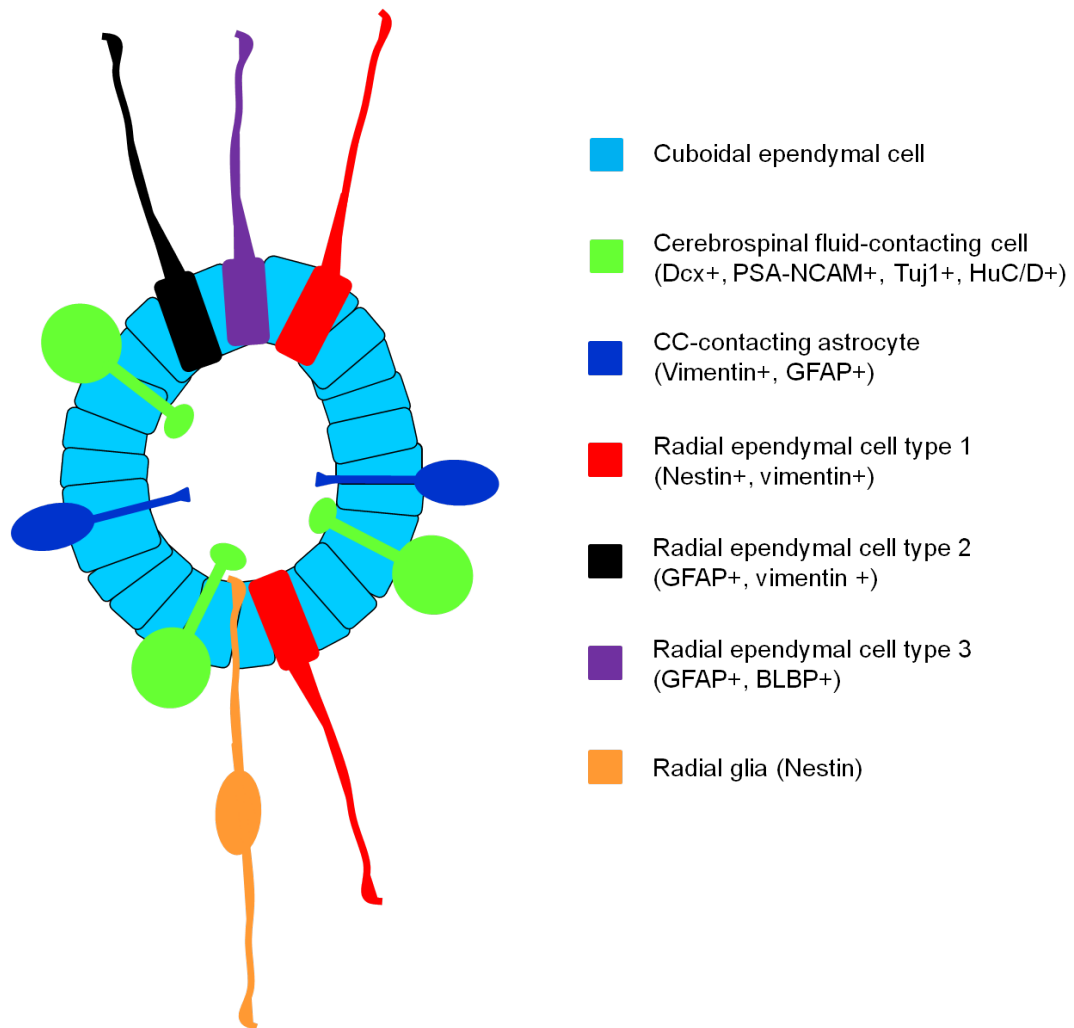
Figure 1.2: Cell subtypes surrounding the CC of the postnatal spinal cord in mammals.

1.3.4.2 Neurogenic potential of ependymal cells

As stated some subpopulations of ependymal cells within the mammalian postnatal spinal cord express nestin and GFAP; these are both expressed by neural

progenitor cells and neural stem cells in other postnatal neurogenic niches, although GFAP is also used widely as a marker of astrocytes. Ki67, which is expressed by actively proliferating cells at all stages of their cell cycle (Gerdes et al., 1984), and BrdU, a marker of newborn cells, are also expressed by ependymal cells. The following section will examine these points further, discussing the neurogenic potential of ependymal cells and using other postnatal neurogenic niches for comparison.

The SVZ is a well established and characterised mammalian postnatal neurogenic niche located near the walls of the lateral ventricles in the brain (Ihrie and Alvarez-Buylla, 2011). It consists of a quiescent population of ependymal cells that line the lateral ventricles and a heterogeneous subependymal cell population that consists of astrocytes, transit amplifying progenitors, neuroblasts, tanycytes, microglia and blood vessels (Doetsch et al., 1997; Tavazoie et al., 2008). The neural stem cells are believed to be the subependymal astrocytes, which express GFAP, retain an apical contact with the lateral ventricle and produce the transit amplifying progenitor cells that in turn produce the neuroblasts which mature and migrate to become olfactory bulb neurones (Lois and Alvarezbuylla, 1994; Doetsch et al., 1999; Mirzadeh et al., 2008). There are parallels that can be drawn between the SVZ and the CC region, namely the presence of cells expressing GFAP and the neural stem and precursor marker, nestin (Doetsch et al., 1997; Hamilton et al., 2009). To distinguish whether GFAP- and nestin- expressing cells are capable of proliferation in the CC region as well as the SVZ, immunohistochemistry for Ki67 was combined with immunohistochemistry for GFAP or nestin in the rat (Hamilton et al., 2009). Ki67 immunohistochemistry in the rat and mouse revealed that there was proliferation in the ependymal layer and that it was predominantly found at the dorsal pole of the CC (Hamilton et al., 2009; Sabourin et al., 2009). Ki67 was commonly found co-labelled with nestin at the dorsal pole, indicating that the population of nestin expressing cells within the CC are important in proliferation (Hamilton et al., 2009). In contrast to the involvement of nestin expressing cells in proliferation in the CC region and the role of GFAP expressing astrocytes in the SVZ, Ki67 was never seen to co-localised with GFAP (Hamilton et al., 2009), suggesting that GFAP expressing cells of the ependymal layer are not involved in proliferation. It is possible, however, that proliferating GFAP expressing cells could have been missed for two reasons. Firstly, the GFAP expressing ependymal cells are fewer in number than the nestin expressing ependymal cells. Secondly, the GFAP expressing astrocytes in the SVZ are a slowly proliferating cell type unlike

some of the nestin expressing cells in the SVZ (Doetsch et al., 1997), therefore if the same is true for the CC region, the slower proliferation rate could have been missed by the Ki67 immunohistochemistry.

In addition to the use of Ki67 immunohistochemistry, BrdU (Wojtowicz and Kee, 2006) has been used to investigate the proliferation of cells surrounding the CC (Johansson et al., 1999; Hamilton et al., 2009). These methods showed that, *in-vivo* under physiological conditions in rodents, ependymal cells proliferate but that this appears to be in the form of symmetrical ependymal division, with the purpose to maintain ependymal cell numbers, and not to produce any non-ependymal progeny (Johansson et al., 1999; Hamilton et al., 2009). However, grey matter from cervical, thoracic, lumbar and sacral adult mouse spinal cord tissue can be cultured *in-vitro* to form spheres of undifferentiated cells, known as neurospheres, which can be separated into individual cells that self renew (Weiss et al., 1996). These cells can also be stimulated by epidermal growth factor and basic fibroblast growth factor to differentiate into neurones, astrocytes and oligodendrocytes (Weiss et al., 1996), providing evidence that the cells are multipotent. The ability of cells to self renew and produce cells of multiple lineages are the two key criteria required for a cell to be classed as a neural stem cell, thus neural stem cells are present in the spinal cord. Importantly, if the CC region is not present within the cultured mouse tissue there is a distinct lack of neurosphere formation even when both epidermal growth factor and basic fibroblast growth factor are present within the culture media (Martens et al., 2002); this implies that cells within the area surrounding the CC are neural stem cells. Injection of the dye, 1,1'-dioctadecyl-6,6'-di(4sulphopentyl)-3,3,3',3'tetramethylindocarbocyanin (DiI), into the ventricles of rats labelled cells lining the CC, allowed tracking of these cells and their progeny and demonstrated that following spinal cord injury cells lining the CC differentiated into astrocytes (Mothe and Tator, 2005). To confirm that it is ependymal cells specifically that are the neural stem cells, a genetically modified FoxJ1 mouse was made that had an inducible, permanent and heritable reporter gene, β-galactosidase (Meletis et al., 2008). FoxJ1 is restricted to cells with motile cilia, for example ependymal cells, thus in FoxJ1 mice, any new born cells produced from ependymal cells will be identified by their β-galactosidase expression. In these mice, all of the ependymal cell division was symmetrical under physiological conditions, however, following spinal cord injury ependymal cells differentiated into both astrocytes, which subsequently migrated towards the site of injury and oligodendrocytes (Meletis et al., 2008; Barnabe-Heider et al., 2010). Therefore, it appears that ependymal cells

need specific environmental conditions and cues to differentiate as opposed to merely proliferate.

One example of a factor that could be influencing the neural stem cell potential of ependymal cells is the oxygen levels, for example hypoxia prevents neural stem cell differentiation and promotes proliferation (Gustafsson et al., 2005). The notch pathway has been shown to be essential to allow this hypoxia driven control of neural stem cell proliferation and differentiation (Gustafsson et al., 2005). In fact, notch signalling has been shown to heavily influence neurogenesis in the adult zebrafish, with inhibition of the notch pathway increasing the generation of new motor neurones following a spinal cord injury (Dias et al., 2012). Furthermore, the ability of ependymal cells to differentiate into different populations of interneurones is being studied in the zebrafish spinal cord (Kuscha et al., 2012). The ability of this organism to generate new neurones in the spinal cord is in contrast to the restricted generation of new neurones in the mammalian system, as will be subsequently discussed, and means that zebrafish are a great model to study spinal cord regeneration.

There are currently only a few studies that have observed the formation of new neurones in the adult mammalian spinal cord (Danilov et al., 2006; Shechter et al., 2007; Vessal et al., 2007; Shechter et al., 2011), and of these studies only one could define the cells surrounding the CC as the source of this neurogenesis (Danilov et al., 2006). The first case was in a model of multiple sclerosis, known as experimental autoimmune encephalomyelitis, in rats (Danilov et al., 2006). This study used the same technique as Mothe & Tator (2005), injecting DiI into the ventricles to label cells surrounding the CC. These cells proliferated and in 10/15 animals they differentiated into cells which expressed the neuronal markers NeuN and Tuj1, and the newborn cell marker, BrdU. These newborn neurones could produce action potentials in response to the injection of a positive current pulse, indicating that they are also functional. The second case observed newborn neurones expressing both the marker of immature neurones, Dcx, and BrdU predominantly in the dorsal horn under physiological conditions in the mouse (Shechter et al., 2007). It is not clear why this study would observe such a phenomenon when others using the same technique have failed to make such findings, however, it could be due to the administration of a higher dose of BrdU compared to studies which failed to find newborn neurones, or a difference in the antibodies used to detect the neuronal nature of the newborn cells. The third case

related to the second and revealed that an increased number of newborn neurones were produced two-four weeks following the repeated exposure to novel tactile stimuli; this study also used a higher dose of BrdU and the same neuronal marker (Shechter et al., 2011). Finally, the fourth case observed newborn neurones in the dorsal horn in both primates and rats following a dorsal root lesion but not following a dorsal column transection (Vessal et al., 2007). The cells were identified as newborn using BrdU and identified as neuronal using the neurone markers, NeuN, Dcx and GAD67. In addition to these studies, when neural stem cells originating in the rat spinal cord are implanted into the hippocampus they can differentiate into neurones (Shihabuddin et al., 2000). These studies, with the exception of Shechter et al., (2007) indicate that newborn neurones can be produced in the adult spinal cord but under specific conditions. They also indicate that ependymal cells are one of the sources of newborn neurones (Danilov et al., 2006) but there could be other sources, for example a neural progenitor population in the dorsal horn (Vessal et al., 2007; Shechter et al., 2011).

1.3.4.3 Other proposed functions of ependymal cells

For many years ependymal cells had been considered to perform little more than a barrier function between the CSF in the ventricles and CC and the grey matter of the brain and spinal cord. In addition to the role they appear to have in neurogenesis, it is becoming clear that they are a multifunctional cell type that perform a wide range of tasks. To date, most of the studies investigating ependymal cells are relevant to those lining the ventricles of the brain, with few studies investigating ependymal cells lining the CC; therefore unless stated the following applies to ependymal cells of the ventricles but it is likely that some properties will be conserved in ependymal cells of the CC. It must be noted that many of the following studies consider ependymal cells as a single cell type and thus do not consider any variation between cuboidal and radial ependymal cells.

The barrier function assigned to ependymal cells is an important one, as they produce proteins that are capable of preventing harmful metabolites in the CSF from re-entering into the grey matter (Del Bigio, 2010). For example, ependymal cells in rats and humans express catechol-O-methyltransferase, an enzyme involved in the inactivation of catecholamines (Matsumoto et al., 2003) and mice

express monoamine oxidase B, an enzyme involved in the inactivation of biogenic amines (Vitalis et al., 2002). These enzymes could protect the grey matter from trace amines that are found in the CSF (Vitalis et al., 2002). In line with this, ependymal cells can also regulate the amount of energy substrates present in the CSF; evidence for this come from the rat and mouse and includes their possession of facilitative glucose transporters (Yu et al., 1995; Kobayashi et al., 1996; Silva-Alvarez et al., 2005), which can remove glucose from the CSF, glucokinase, which can act as a glucose sensor, and monocarboxylase transporters, which are involved in the uptake and release of lactate, pyruvate and ketone bodies (Pierre et al., 2000). This ability could ensure that energy substrates within the CSF are maintained at the necessary levels.

Ependymal cells can also release substances, including growth factors and thus perform a trophic function both in the developing and adult CNS (Del Bigio, 2010). These growth factors include fibroblast growth factor 2 (Cuevas and Gimenez-Gallego, 2000), which is important for brain development but is also expressed in the adult rat, vascular endothelial growth factor, which is expressed embryonically in humans (Arai et al., 1998) and appears to be important for the stability of ependymal cells themselves (Maharaj et al., 2008), and S100β, which is a Ca^{2+} binding protein that is expressed embryonically and throughout adulthood and has both neurotrophic and gliotrophic properties, amongst many other growth factors (Del Bigio, 2010).

The function of ependymal cell cilia has been a source of much debate. Recently, the (9+2) cilia of mammalian ependymal cells surrounding the CC have been observed to move back-and-forth, in a motion consistent with that seen for other (9+2) cilia (Alfaro-Cervello et al., 2012); this is in contrast to the rotary motion observed by the (9+0) cilia that are present on the ependymal cells surrounding the zebrafish CC (Kramer-Zucker et al., 2005). Cilia on ependymal cells can beat in a coordinated way (Roth et al., 1985); this beating can be increased by the application of 5HT and adenosine, with the effect of ATP being variable as both increases and decreases in ciliary beating have been observed following its application in rats and mice (Nguyen et al., 2001; Genzen et al., 2009b). The receptor mediating the 5HT regulation is unknown and it can only be postulated that the P2X7 receptor mediates the ATP response, due to the presence of P2X7 mRNA in rat ependymal cells throughout the ventricular system and CC (Yu et al., 2008; Genzen et al., 2009a). Selective A_{2B} receptor antagonists confirmed that it is

this receptor mediating the adenosine induced ciliary beating in rats (Genzen et al., 2009b). The variation in ciliary beat frequency along the ventricular system of hamsters suggests that ciliary beating does not contribute to the bulk flow of CSF, however, it could still aid in the movement of cellular debris along with the bulk flow, ensuring that the CC, which is a narrow cavity, remains unobstructed (Roth et al., 1985). It has also been postulated that this ciliary beating could stir the local CSF to facilitate diffusion of its contents, optimising the dispersal of neuronal messengers (Roth et al., 1985; Nguyen et al., 2001). Indeed it has been suggested that these cilia could aid in the formation of concentration gradients of guidance molecules in the CSF that direct the migration of neuroblasts from the SVZ to the olfactory bulb (Sawamoto et al., 2006).

As demonstrated, ependymal cells are a multifunctional cell type, performing a protective barrier from harmful CSF metabolites, facilitating diffusion of messengers within the CSF and acting as neural stem/progenitor cells. It is only recently that the importance of ependymal cells has been recognised and there is still a lot to discover about this cell type.

1.4 Cerebrospinal fluid

Given the close proximity of cells within the substantia gelatinosa centralis to the CSF it is important to understand a little about CSF, including its flow, composition and proposed functions.

1.4.1 Flow of CSF

The adult human CNS has a constant volume of roughly 140 mls of CSF, with approximately 30 mls within the ventricles and CC, and 110 mls in the subarachnoid spaces found on the outside of the brain and spinal cord (see review Veening and Barendregt (2010)). CSF is produced by areas of specialised epithelial cells called the choroid plexus; these are located in parts of the lateral, third and fourth ventricles. The bulk flow of CSF is in a caudal direction, from the lateral ventricles, through the third ventricle to the fourth ventricle. At the base of the fourth ventricle, CSF can either flow into the subarachnoid space to bathe the outside of the brain or it can flow down into the CC where it will eventually reach the filum

terminale and access the subarachnoid space. CSF in the subarachnoid space eventually passes through membrane structures called arachnoid granulations to drain into the venous blood. CSF has been observed to flow at a rate of 1 ml/minute within the CC of the rat. This bulk flow throughout the ventricular system and CC appears to be driven by the arterio-venous pressure gradient and CSF secretion in the choroid plexus. In addition to the bulk flow, there is also laminar flow of CSF; this type of flow occurs close to the ependyma and appears to be driven by the ciliary beating of ependymal cells, as a result the flow is not necessarily in a caudal direction and it achieves mixing of the constituents of CSF (see reviews Johanson et al., (2008); Skipor and Thiery (2008); Veening and Barendregt (2010)).

1.4.2 Composition of CSF

CSF is a clear fluid as it is 99 % water. It also contains numerous ions, Na^+, K^+, Ca^{2+}, Mg^{2+}, Cl^- and HCO_3^-, and micronutrients such as vitamin C, folates, deoxyribonucleic acids, vitamin B6 and glucose (Spector and Johanson, 1989). The concentration of K^+, Ca^{2+}, HCO_3^- and glucose are all lower in CSF than in plasma and the pH, usually 7.33, is slightly more acidic. Although the amount of proteins found in CSF is only 0.5 % of that found in blood plasma (Spector and Johanson, 1989), there is still a wide range of proteins found within the CSF. Detailed proteonomic analysis of human embryonic CSF revealed the presence of numerous peptides, with 27.8 % being involved in protein metabolism and modification, 25 % being involved in signal transduction, 16.1 % being involved in developmental processes and 4.4 % being involved in cell proliferation and differentiation (Zappaterra et al., 2007). Finally, there are a host of supra- and sub-ependymal structures containing different neuroactive substances that are differentially distributed over specific regions (see review Veening and Barendregt (2010)). For example, in rats and monkeys terminals originating in the raphe nuclei and containing 5HT have been located along the walls of the ventricular system but were particularly dense along the third ventricle where they are well placed to release 5HT into the CSF (Chan-Palay, 1976). Other neuroactive substances observed in terminals in the CSF include luteinising hormone releasing hormone, corticotrophin releasing factor, adreno-corticotropic hormone, melatonin, neuropeptide tyrosine and oxytocin (see reviews Skipor and Thiery (2008) ;

Veening and Barendregt (2010)). These terminals could release these substances into the CSF and enable their widespread and long distance distribution.

1.4.3 Function of CSF

One of the first noted functions of the CSF was that it provides buoyancy to the brain, which aids in protecting the brain from any damage that would otherwise result from any sudden movements of the head (Spector and Johanson, 1989). Another function is to remove waste products; these products diffuse into the CSF from interstitial fluid and are carried in the bulk flow to be removed into the venous circulation. More recently it has become apparent that the CSF contains many molecules that are important in cellular signalling and can influence cellular proliferation. Combined with the fact that the apical surfaces of neural stem cells border with the CSF, this has led to the hypothesis that CSF can influence neurogenesis (see review Lehtinen and Walsh (2010)). In support of this, cultures of neurospheres formed from human neural stem cells can be maintained when CSF alone is used as the culture medium (Lehtinen et al., 2011). Molecules including insulin-like growth factor 2, Slit1/2 and sonic hedgehog are found within the CSF and studies where their expression has been altered demonstrates their ability to influence neurogenesis (Sawamoto et al., 2006; Huang et al., 2010; Lehtinen et al., 2011). Thus, CSF is a complex fluid that works in unison with ependymal cells to ensure the health of the grey matter.

1.5 Inputs to lamina X

As well as the possible neuroactive substances found in the CSF, lamina X receives many neuronal inputs from the periphery, from supraspinal nuclei and from local interneurones found with the spinal cord itself. These inputs vary in the neurotransmitters that they release and the functional relevance of such inputs is predominantly unknown.

Terminals expressing VGluT1 have been observed in lamina X of the rat; terminals expressing VGluT1 are generally considered to arise from neurones in the

periphery, supporting the presence of inputs from the periphery to lamina X (Kaneko et al., 2002). The inputs from the periphery have been identified as nociceptive primary afferents in the cat and monkey (Light and Perl, 1979). Terminals expressing endogenous opioid met-enkephalin (Hokfelt et al., 1977; Gibson et al., 1981) and substance P (Hokfelt et al., 1975; Gibson et al., 1981) have been identified in lamina X of the rat. In addition to the widespread distribution of substance P expressing terminals within lamina X, immunohistochemistry revealed a dense plexus of substance P fibres ventral to the CC in the rat (Barber et al., 1979). Although whether these substance P fibres are from the periphery, supraspinal regions or substance P-immunoreactive interneurones that have been identified in the dorsal horn of the cat (Arvidsson et al., 1990) is unknown.

Known supraspinal inputs include noradrenergic terminals, revealed by DβH, which are found in close apposition to both partition neurones and CC cluster cells inn the rat (Takeoka et al., 2010). There are also inputs from the hypothalamus, with orexin-, vasopressin- and oxytocin- expressing terminals observed within lamina X of a number of different mammals, predominantly within the CAA where the SPNs reside (Swanson and Mckellar, 1979; Sawchenko and Swanson, 1982; van den Pol, 1999). There are many 5HT-immunoreactive terminals in lamina X with 5HTergic axon varicosities observed close to the CC, in close apposition to ChAT positive SPNs, partition cells and CC cluster cells in the rat (Takeoka et al., 2009). Anterograde and retrograde tracing in the rat have revealed that the majority of these terminals originate from supraspinal sources, particularly the raphe nuclei in the brainstem (Bowker et al., 1981; Bacon et al., 1990). Some axons, however, have been identified from thoracic (T10) to sacral (S1) spinal cord that is caudal to a spinal cord transection at T9, indicating that at least some of the axons arise from rarely observed 5HT interneurones in the rat (Takeoka et al., 2009).

As well as the VGluT1-immunoreactive terminals observed in lamina X, VGluT2-immunoreactive terminals have been observed in the rat (Kaneko et al., 2002), indicating the presence of glutamatergic inputs from within the CNS. These VGlut2-containing terminals could originate from the glutamatergic interneurons, observed in the mouse, in lamina X and lamina VII that influence the motor output from the spinal cord (Wilson et al., 2005; Hinckley et al., 2005). There are many ChAT positive fibres in lamina X with some terminal-like structures observed in close apposition to ChAT negative cells in the ependymal layer of rats (Barber et al., 1984; Phelps et al., 1984). It is likely that these cholinergic terminals originate from

cholinergic interneurones, including the partition neurones and the CC-cluster cells. There are also many GABAergic terminals observed within lamina X of the rat (Mclaughlin et al., 1975) with electron microscopy revealing that some of these GABAergic terminals form synapses with ependymal cells (Magoul et al., 1987). The source of these GABAergic terminals could be the local GABAergic interneurones that are found lateral to the CC in the rat (Barber et al., 1982).

Given the variety of inputs to lamina X, it is important to consider the receptors that are present within lamina X that could be mediating the postsynaptic responses to the release of neurotransmitters or neuromodulators from these inputs. The following sections 1.6-1.9 will focus on the receptors that are present within lamina X that could be mediating responses to cholinergic inputs (section 1.6), GABAergic inputs (section 1.7), 5HTergic inputs (section 1.8) and substance P inputs (section 1.9). These chapters will consider the structure, composition, distribution and function of the relevant receptors as well as the role that these receptors are known to play in postnatal neurogenesis. The focus is on these four neurotransmitter systems as there are a large amount of ACh-, GABA-, 5HT- and substance P- containing terminals within lamina X, in particular in the area directly surrounding the CC, suggesting that all of these neurotransmitters/neuromodulators are well placed to influence CSFcCs and ependymal cells. In addition, there is evidence that each of these neurotransmitters can influence neurogenesis which is pertinent given the neurogenic potential of this area. More specifically, the GABAergic system is considered due to previous reports of GABAergic responses in CSFcCs and the influence of GABA on neurogenesis in other areas. The 5HTergic and substance P systems are considered as they can be assigned more specific roles than GABA and thus give an indication of the function of CSFcCs if they were to respond to these neurotransmitters. Finally, the cholinergic system is considered due to the great influence that is has on the other postnatal neurogenic niches, the DG and the SVZ.

1.6 Cholinergic receptors

There are a vast array of cholinergic receptors located throughout the body whose properties and functions are highly varied. Cholinergic receptors can be divided into two subtypes: muscarinic ACh receptors (mAChRs) which are metabotropic

receptors that are coupled to heterotrimeric guanine nucleotide-binding proteins (G-proteins) and nicotinic ACh receptors (nAChRs) which are ligand-gated ion channels.

1.6.1 Structure, distribution and function of mAChRs

mAChRs are class I, seven transmembrane, G-protein coupled receptors; they are encoded by five mammalian genes (M1-M5), and are also known as receptor subtypes M1-M5 (Caulfield and Birdsall, 1998). mAChR subtypes are coupled to different G-proteins (see reviews Caulfield (1993); Caulfield and Birdsall (1998)). M1, M3 and M5 receptors preferentially couple to the *Pertussis* toxin-insensitive $G_{\alpha q/11}$ family of G-proteins (Caulfield, 1993). ACh binding to these receptors results in the inhibition of K^+ channels which causes a depolarisation at the postsynaptic density. M2 and M4 are preferentially coupled to the *Pertussis* toxin-sensitive $G_{\alpha i}$ family of G-proteins (Caulfield, 1993). ACh binding to postsynaptic M2 receptors results in $G_{\alpha i}$ activation which subsequently activates inwardly rectifying K^+ channels causing a hyperpolarisation at the postsynaptic membrane. ACh binding to presynaptic M2 and M4 receptors results in $G_{\alpha i}$ activation which subsequently inhibits voltage-gated Ca^{2+} channels, causing a hyperpolarisation at the presynaptic membrane which decreases the likelihood of neurotransmitter release (Caulfield, 1993).

The mAChR subtypes have different distribution patterns within the CNS. M1 mAChRs have an abundant expression in all major forebrain areas, for example, in the hippocampus, the cerebral cortex and the striatum, but do not appear to be expressed in the spinal cord of mice (Oki et al., 2005). Autoradiography using the non-selective muscarinic ligand, ^{3}[H]-*N*-methylscopolamine (^{3}[H]NMS) in wild-type and M2 mAChR knock out mice, revealed that M2 mAChRs have a widespread distribution and are the predominant subtype of mAChR found in the thalamus, hypothalamus, midbrain, medulla, pons, cerebellum, and spinal cord (Oki et al., 2005). Pre-incubating sections from the thoracic spinal cord with pirenzepine, to occlude M1, M3 and M4 mAChRs, followed by autoradiography using the ligand ^{3}[H]NMS revealed the presence of M2 mAChRs in most areas of the spinal cord including lamina X in the rat (Hoglund and Baghdoyan, 1997). Mice lacking functional M2 mAChRs show a markedly reduced analgesic response to a centrally administered muscarinic agonist (Gomeza et al., 1999); this effect is likely mediated by M2 mAChRs located in both the spinal cord and at the supraspinal level.

Autoradiography using the ligand ^{3}[H]NMS in wild-type and M3 mAChR knock out mice, revealed that M3 mAChRs have a wide distribution and are expressed in the hippocampus, hypothalamus, midbrain, pons, medulla and spinal cord (Oki et al., 2005). More in depth investigation of the spinal cord using ^{3}[H]NMS following the occlusion of M1, M2 and M4 mAChRs revealed expression of M3 mAChRs in laminae I and II of superficial dorsal horn but not in lamina X of the rat (Hoglund and Baghdoyan, 1997). M4 mAChRs are expressed in the cerebral cortex, striatum, thalamus and spinal cord of mice (Oki et al., 2005), however, the distribution of M4 mAChRs within the laminae of spinal cord is unknown. The distribution and function of M5 mAChRs are not as well understood as the other mAChR subtypes and have not been observed in the spinal cord (see review Eglen (2006)). In summary, only M2 mAChRs have been positively identified in lamina X, however, M4 mAChRs may also be present. Both of these receptors cause hyperpolarisations (Caulfield, 1993), therefore, any muscarinic mediated ACh effects in lamina X would be expected to be inhibitory.

1.6.2 Structure and composition of nAChRs

nAChRs are part of the cys-loop family of ligand-gated ion channels that contains GABA$_A$ receptors, GABA$_C$ receptors, glycine receptors and 5HT$_3$ receptors, amongst others (see review Sine and Engel (2006)). The receptors are transmembrane oligomeric proteins composed of five subunits (Figure 1.3; Karlin et al., (1983)). Each subunit has four transmembrane segments, with the ion channel itself being lined by the second transmembrane segment (Unwin, 1993, 2005). The ACh binding site is found on the relatively hydrophilic extracellular amino acid segment of the subunit (Karlin et al., 1983; Chiara et al., 1999; Brejc et al., 2001). The conformational change from the closed, resting state to the open state occurs on agonist binding (Watanabe et al., 1998), allowing the movement of Na$^+$ and Ca^{2+} into the cell and K$^+$ out of the cell (Mulle and Changeux, 1990); this is subsequently halted as the channel closes to enter a desensitised state.
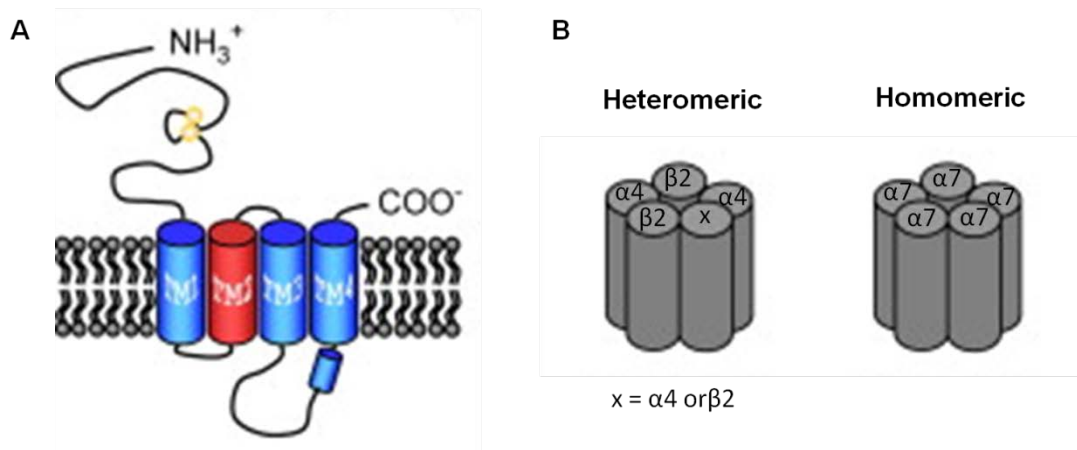
Figure 1.3: Structure of ligand gated ion channels of the cys-loop family.

A) Schematic representation of a single subunit with four transmembrane segments. B) Schematic representation of the pentameric structure of cys-loop family ion channels. Examples of nAChRs with either heteromeric or homomeric structures are shown (Modified from Collingridge et al., (2009)).

There are five different types of subunits that contribute to muscle nAChRs, α, β, γ, δ and ε (Raftery et al., 1980; Takai et al., 1985), however, there are only two subunit groups in neuronal nAChRs, α2-α10 and β2-β4 (for identification of different subtypes in different species see review Sargent (1993)). The receptors are predominantly heteromeric, consisting of α and β subunits; these include the subunits α2-α6 and β2-β4, and are defined pharmacologically by their ability to bind to nicotine and other related agonists with nano molar affinity (Romano and Goldstein, 1980; Clarke et al., 1985). Conversely, α7, α8 and α9 subunits can form homomeric receptors, independent of β subunits; these are defined pharmacologically by their nano molar affinity for α-Bungarotoxin (α-BgT), with only a micro molar affinity for nicotine (Clarke et al., 1985; Couturier et al., 1990). There are a large number of possible subunit combinations that are present in nAChRs, therefore it is common to use the term 'containing' when referring to specific nAChRs, where containing is denoted by an asterix (*). For example α7-containing nAChRs are referred to as α7*nAChRs. The homomeric α7*nAChRs have quite different properties to the other nAChRs; they have a higher Ca^{2+} permeability and

a higher rate of desensitisation than any other nAChR currently known (Bertrand et al., 1993; Wooltorton et al., 2003). Their pharmacological profile is also quite unique: choline, the breakdown product of ACh, is a weak yet selective α7*nAChR agonist (Papke et al., 1996), methyllycaconitine (MLA) is a specific α7*nAChR antagonist at concentrations ≤ 20 nM (Alkondon et al., 1992; Wonnacott, 1993), and finally many synthetic compounds are being produced to act as α7*nAChR-selective agonists and modulators, for example 1-(5-chloro-2,4-dimethoxy-phenyl)-3-(5-methyl-isoxazol-3-yl)-urea, known as PNU-120596, selectively potentiates cholinergic responses mediated by α7*nAChRs (Hurst et al., 2005).

1.6.3 Distribution and function of nAChRs

The function of nAChRs in the mammalian CNS is not straightforward as they are found at numerous subcellular locations, including presynaptic terminals, postsynaptic terminals, extrasynaptic sites, dendrites, soma and axons (Dani and Bertrand, 2007). A high proportion of nAChRs are found on presynaptic terminals modulating neurotransmitter release (see review Wonnacott (1997)). nAChRs modulate neurotransmitter release by two methods: firstly, in a TTX-sensitive manner, preterminal nAChRs facilitate propagation of the action potential (Lena et al., 1993) and secondly in a TTX-insensitive manner, terminal presynaptic nAChRs cause a local depolarisation that activates voltage-sensitive Ca^{2+} channels, resulting in an increase in local Ca^{2+} concentration and the stimulation of synaptic vesicle release (McMahon et al., 1994; Tredway et al., 1999).

Some nAChRs are found in postsynaptic somatodendritic regions, although this is relatively rare (Alkondon et al., 1998; Frazier et al., 1998). There are also nAChRs found at perisynaptic and extrasynaptic regions, where they are believed to modulate neuronal activity in response to the volume transmission of ACh, which is also referred to as non-synaptic or paracrine transmission (Umbriaco et al., 1994; Descarries et al., 1997). Finally, nAChRs are also expressed on many non-neuronal cells, including astrocytes, macrophages, endothelial cells of the vascular system and epithelial cells that line the respiratory airways (see review Wessler and Kirkpatrick (2008)).

nAChRs are distributed widely throughout the CNS, however, this study will only consider their distribution throughout the spinal cord. *In-situ* hybridisation in the rat revealed the presence of low levels of α4 and β2 subunits throughout the spinal cord, and low levels of α2 and α3 in more specific regions, including lamina X (Wada et al., 1989). A stronger signal was observed for the α7 subunit in the superficial dorsal horn, the ventral horn and lamina X, following *in-situ* hybridisation in the rat (Seguela et al., 1993). Looking at lamina X in more detail, studies using whole cell patch clamp electrophysiology in the rat have determined the functional expression of nAChRs in specific neuronal cell populations. At numerous levels of the spinal cord, in the ventral half of the dorsal commissure, interneurones are capable of responding to ACh; the responses were not affected by the α7*nAChR specific antagonists, MLA and α-BgT, thus this provides evidence of functional non α7*nAChRs in the CAA (Bordey et al., 1996b). In response to the application of the nicotinic agonist, 1,1-dimethyl-4-phenylpiperazinium iodide (DMPP), SPNs in the CAA were found to have two separate responses (Bradaia and Trouslard, 2002b). The first response was a fast decaying α-BgT-sensitive current that indicated the presence of α7*nAChRs (Bradaia and Trouslard, 2002b), evoked excitatory postsynaptic potentials (EPSP) could also be antagonised by α-BgT, demonstrating that the α7*nAChRs are located at postsynaptic densities on SPNs (Bradaia et al., 2005). The second response was a non-desensitising, α-BgT-insensitive current that indicated the presence of non α7*nAChRs; these receptors were suggested to be located at extrasynaptic locations due to the non-desensitising nature of the response over the 20 second agonist application (Bradaia and Trouslard, 2002b). It was suggested that the non α7*nAChR could contain α4 and β2 subunits; this is because β2*nAChRs are less sensitive to cytosine compared to DMPP and ACh, and α4β2*nAChRs are very sensitive to ACh compared to DMPP, correlating with the agonist potencies observed in this study (Luetje and Patrick, 1991; Bradaia and Trouslard, 2002b).

nAChRs have also been found on presynaptic terminals within lamina X (Bradaia and Trouslard, 2002a; Seddik et al., 2006). Glycinergic mediated mIPSPs were recorded in SPNs of the CAA; an increase in mIPSP frequency but not in mIPSP amplitude was observed following the application of DMPP. This suggests an increase in the number of vesicles released rather than an increased post-synaptic response indicating the presence of presynaptic nAChRs on glycinergic terminals (Bradaia and Trouslard, 2002a). Other nAChR agonists could mimic the DMPP effect on glycinergic mIPSPs, however, ACh was the most potent whereas cytosine

was the least potent; this suggests the involvement of α4β2*nAChRs (Luetje and Patrick, 1991; Bradaia and Trouslard, 2002a). In addition, the DMPP effect on glycinergic mIPSPs could be partially antagonised by MLA, indicating the involvement of α7*nAChRs. GABAergic mIPSPs can also be recorded from SPNs in the CAA; the frequency but not the amplitude of these mIPSPs can be increased by ACh indicating the presence of nAChRs on the presynaptic terminals of GABAergic interneurones (Seddik et al., 2006). Choline, the preferential α7*nAChR agonist (Papke et al., 1996), could not mimic the ACh-induced effect on GABAergic IPSPs suggesting that non α7*nAChRs are mediating this response. This was confirmed as DHβE, a non α7*nAChR antagonist at the concentration of 1 μM, that was used by Seddik et al., (2006), antagonised the ACh-induced GABAergic mIPSPs in SPNs (Seddik et al., 2006). This receptor is suggested to be an α4β2*nAChR because DHβE is a preferential antagonist at β2*nAChRs, compared to β4*nAChRs (Harvey and Luetje, 1996), and at α4*nAChRs, compared to α3*nAChRs (Harvey et al., 1996). Thus there are a number of nAChRs expressed at different subcellular locations on different neuronal populations within lamina X, however, their presence and function within the area directly surrounding the CC has not been investigated.

1.6.4 Role of ACh in postnatal neurogenesis

In the developing CNS and in established areas of postnatal neurogenesis, neurotransmitters are important in regulating neuronal maturation. In cell lines such as the small cell lung carcinoma cell line, in which α7*nAChRs are expressed, nicotine can induce cellular proliferation (Quik et al., 1994). In cultures of spinal neurones, growth cones turn and neurites extend towards ACh; this turning is abolished in the presence of a nicotinic antagonist, D-turbocararine, and in Ca^{2+} free extracellular solutions (Zheng et al., 1994). ACh does not, however, have any direct influence over the neurogenic niche in the SVZ. Nevertheless, ablating cholinergic neurones of the basal forebrain by injecting 192IgG-saporin into the lateral ventricles, reduces cholinergic inputs to the olfactory bulb and decreases the number of newly born neurones in rats (Cooper-Kuhn et al., 2004). In addition, enhancing cholinergic signalling by the intraperitoneal administration of the acetylcholinesterase inhibitor, donezepil, increased the survival of BrdU-labelled newborn neurones in the olfactory bulb and the dentate gyrus (DG) of the mouse

hippocampus (Kaneko et al., 2006). In the DG of rats and mice, newborn neurones receive cholinergic inputs, as evidenced by the presence of vesicular ACh transporter (VAChT) or ChAT in close apposition to BrdU- or PSA-NCAM-expressing cells, respectively (Kaneko et al., 2006; Kotani et al., 2006). PSA-NCAM expressing immature neurones of the mouse DG express α7*nAChRs, β2*nAChRs, M1 mAChRs and M4 mAChRs, indicating that both nicotinic and muscarinic ACh receptors could influence these immature neurones (Kaneko et al., 2006). For both the nicotinic receptors, there is functional evidence that they influence postnatal neurogenesis. There is a decrease in the number of BrdU-expressing newborn cells in the DG in β2*nAChR knockout mice (Harrist et al., 2004). In postnatal wild-type mice, ACh promotes the switch from excitatory GABAergic signalling to inhibitory GABAergic signalling in DG neurones, however, in α7*nAChR knockout mice the switch is delayed and the DG neurones show abnormally high levels of NKCC1 (Liu et al., 2006b; Liu et al., 2007). Furthermore, the normal survival, maturation and integration of adult-born neurones is reliant on the presence of functional α7*nAChRs (Campbell et al., 2010). For example, in one to three month old mice, less BrdU-expressing newborn neurones are found in α7*nAChR knockout mice four weeks but not two weeks post-BrdU injection compared to in wild type mice; this indicates that more newborn neurones die in the two to four week period after being produced in α7*nAChR knockout mice (Campbell et al., 2010). Labelling newborn cells with a GFP-tagged virus revealed that the dendritic arbours are less complex and truncated as evidenced by the fewer branch points and the shorter dendritic length, in α7*nAChR knockout mice compared to wild-type mice (Campbell et al., 2010). These studies demonstrate the importance of nAChRs in postnatal neurogenesis; however, they have yet to be studied in the neurogenic niche of the spinal cord.

1.7 GABAergic receptors

There are two categories of GABAergic receptors: ionotropic receptors, which include $GABA_A$ receptors and $GABA_C$ receptors, and metabotropic receptors, which include $GABA_B$ receptors. $GABA_C$ has now officially been subsumed into the $GABA_A$ receptor class and will be considered as such in this study (Olsen and Sieghart, 2008).

1.7.1 Structure, composition and function of GABA$_A$ receptors

GABA$_A$ receptors are part of the cys-loop family of ligand-gated ion channels that also includes nAChRs, and thus the receptors are made up of five subunits, each of which contains four transmembrane domains, with the second transmembrane domain forming the ion channel lining, as described for nAChRs (see chapter 1.6.2; see review Sine and Engel (2006)). There are 19 different GABA$_A$ receptor subunits that have been identified in humans, including α1-6, β1-3, γ1-3, ρ1-3, δ, ε, π and θ (Simon et al., 2004). Despite this wide variety of subtypes the majority of GABAergic receptors within the mammalian CNS consist of α-, β- and γ-subunits, with the most common receptor subtype consisting of α1, β2 and γ2 isoforms (see review Barnard et al., (1998)). It is believed that this subtype comprises of two α1- and two β2-subunits with one γ2-subunit, although there is little evidence for this yet *in-situ* (see review Olsen and Sieghart (2008)).

On ligand binding GABA$_A$ receptors undergo a conformational change that allows the movement of Cl$^-$ ions and to a lesser extent bicarbonate ions (HCO$_3^-$; Bormann et al., (1987)) through the pore. In mature neurones, the intracellular Cl$^-$ concentration is low in comparison to the extracellular Cl$^-$ concentration, thus when the GABA$_A$ receptors open the Cl$^-$ ions move into the cell along the electrochemical gradient making the cell more negative i.e. hyperpolarising the cell. In immature neurones, the intracellular Cl$^-$ concentration is higher than in mature neurones, so even though it is not a greater concentration than the extracellular Cl$^-$ concentration, the negative membrane potential of the cell leads to the movement of Cl$^-$ ions out of the cell, making the cell more positive i.e. depolarising the cell. The difference in intracellular Cl$^-$ concentration is predominantly due to the differential expression of the two cation exchangers: NKCC1 and KCC2 (as discussed in section 1.3.3.2; Clayton et al., (1998); Rivera et al., (1999)).

There are two types of transmission mediated by GABA$_A$ receptors, these are synaptic, which can also be known as phasic transmission, and extrasynaptic, which can also be known as tonic or paracrine transmission (see review Farrant and Nusser (2005)). Phasic transmission is the more classically known action of GABA, which results in rapid and direct transmission of signals from one neurone to another, with GABA-containing vesicles released from the pre-synaptic terminal to bind to GABA receptors at the post-synaptic density of the post-synaptic terminal (see reviews Edwards et al., (1990); Mody et al., (1994)). Phasic transmission can

also include the activation of perisynaptic receptors that are activated by synaptic spillover of GABA (Telgkamp et al., 2004); this mode of transmission could be considered a mix of phasic and tonic GABAergic transmission. Tonic transmission is a more recent concept (see review Brickley and Mody (2012)); it has more long-term, modulatory effects on neurones. GABA transporters can release GABA from neurones or astrocytes in a way that does not correlate with the activity of the cell from which it is released, this GABA can activate extrasynaptic $GABA_A$ receptors (Kaneda et al., 1995; Brickley et al., 1996). The two types of transmission are mediated by $GABA_A$ receptors composed of different subunits, for example, the most abundant $GABA_A$ receptor composition $\alpha1(2)\beta2(2)\gamma2$ is located at the post-synaptic density, as are most $\gamma2$-subunit containing $GABA_A$ receptors (Essrich et al., 1998; Schweizer et al., 2003). The exception to this rule is the $\alpha5\beta\gamma2$-containing $GABA_A$ receptor, with immunohistochemistry revealing that $\alpha5$-containing $GABA_A$ receptors in pyramidal-like cells in the hippocampus are located extrasynaptically and electrophysiological studies in the IML of the spinal cord revealing that $\alpha5$-containing $GABA_A$ receptors mediate a tonic conductance (Brunig et al., 2002; Wang et al., 2008). Finally, the δ-subunit, which often replaces the $\gamma2$-subunit, is present in extrasynaptic $GABA_A$ receptors which mediate a tonic conductance (Nusser et al., 1998). For example, tonic conductances have been observed in cerebellar granule cells, mediated by $GABA_A$ receptors containing $\alpha6\beta\delta$ subunits (Brickley et al., 2001) and in hippocampal dentate granule cells, mediated by $GABA_A$ receptors containing $\alpha4\beta\delta$ subunits (Stell et al., 2003).

1.7.2 Distribution of $GABA_A$ receptors

$GABA_A$ receptors are distributed widely throughout the CNS, therefore, only their expression within the spinal cord will be considered. In the superficial layers of the dorsal horn, laminae I-III, expression of $\alpha2$, $\alpha3$, $\beta2/\beta3$ and $\gamma2$ subunits has been observed following immunohistochemistry in a number of different mammals, whereas $\alpha1$ and $\alpha5$ subunits were expressed in only lamina III of the superficial dorsal horn (Alvarez et al., 1996; Bohlhalter et al., 1996). Throughout laminae IV-VIII an abundant expression of $\alpha1$, $\alpha2$, $\alpha3$, $\alpha5$, $\beta2/\beta3$ and $\gamma2$ subunits has been observed by immunohistochemistry, although these subunits were expressed by distinct areas and populations of neurones (Bohlhalter et al., 1996). For example, in the rat reverse transcription-PCR (RT-PCR) within the IML found expression of the

α5 subunit (Wang et al., 2008). Immunohistochemistry also demonstrated that motorneurones of lamina IX showed a high expression of α2 and γ2 subunits, a low expression of the α5 subunit and no expression of α1, α3 and β2/β3 subunits (Bohlhalter et al., 1996). In lamina X, immunohistochemistry found that α1, α3, β2/β3 and γ2 subunits are highly expressed, although there is also some expression of α2 and α5 subunits (Bohlhalter et al., 1996). Both α6 and δ subunits could not be detected by immunohistochemistry, *in-situ* hybridisation or RT-PCR in the spinal cord (Wisden et al., 1991; Bohlhalter et al., 1996; Wang et al., 2008). Immunohistochemistry for the ρ1 and ρ2 subunits, previously defined as GABA$_C$ receptor subunits, revealed that they were distributed throughout the adult rat spinal cord, including lamina X (Rozzo et al., 2002). Strong evidence suggests the presence of functional GABA$_A$ receptors on CSFcCs (see section 1.3.3.1), however, the evidence is not unequivocal and the receptor composition has not been investigated.

1.7.3 GABA$_B$ receptors

GABA$_B$ receptors belong to the same class as metabotropic glutamate receptors, and form a functional heterodimer consisting of two subunits, GABA$_{B1}$ and GABA$_{B2}$, both of which contain seven transmembrane domains (Kaupmann et al., 1997; Kaupmann et al., 1998). GABA$_B$ receptors are coupled to *Pertussis* toxin sensitive G-proteins (Andrade et al., 1986). Through these G-proteins, the activation of GABA$_B$ receptors can mediate the inhibition of voltage-activated presynaptic Ca^{2+} channels which decreases transmitter release (Holz et al., 1986; Dolphin and Scott, 1987), and activates a postsynaptic inwardly rectifying K$^+$ current which hyperpolarises the postsynaptic cell (Newberry and Nicoll, 1984; Gahwiler and Brown, 1985; Inoue et al., 1985; Andrade et al., 1986). Work defining the function and distribution of GABA$_B$ receptors has been greatly advanced by the specific agonist, baclofen (Bowery et al., 1980).

Autoradiography revealed the presence of GABA$_B$ receptors throughout the spinal cord, with the greatest amount of binding sites present in lamina II (Price et al., 1987). In the mammalian spinal cord, binding sites were observed in the dorsal region of lamina X and appeared to associate with the distribution of SPNs (Price et al., 1987); this correlates with electrophysiological recordings from SPNs of the IML

where baclofen induced a hyperpolarisation (Wang et al., 2010). Immunohistochemistry in the rat has revealed that CSFcCs express $GABA_B$ receptors (Margeta-Mitrovic et al., 1999), although there is no functional evidence of such expression to date. *In-situ* hybridisation and immunohistochemistry in the rat revealed that $GABA_{B1}$ receptors were differentially distributed throughout the cord, predominantly in laminae II and IX, whereas $GABA_{B2}$ receptors were evenly distributed throughout the spinal cord, including lamina X (Towers et al., 2000).

To summarise, functional $GABA_A$ receptors are present on CSFcCs in rats (Marichal et al., 2009), however, subunit distribution data show that α1, α2, α3, α5, β2/β3, γ2, ρ1 and ρ2 $GABA_A$ receptor subunits are all expressed in lamina X, therefore the composition of the $GABA_A$ receptor on CSFcCs is unknown. $GABA_B$ receptors have also been observed on CSFcCs; however, there is no functional confirmation of such expression.

1.7.4 Role of GABA receptors in postnatal neurogenesis

There is a great deal of evidence proving that GABA plays an important role in mammalian postnatal neurogenesis; this evidence is greatest for the SVZ (Carleton et al., 2003) and the DG (Tozuka et al., 2005). In the rodent SVZ, neuronal precursor and stem cells express $GABA_A$ receptors and can respond to GABA with an increase in intracellular Ca^{2+}; resulting in the inhibition of progression through the cell cycle (Nguyen et al., 2003; Wang et al., 2003; Liu et al., 2005). RT-PCR demonstrated that the precursor cells themselves could be producing GABA as they expressed the enzymes GAD65 and GAD67 that are required to synthesise GABA (Nguyen et al., 2003). Furthermore, the addition of $GABA_A$ antagonists to cultured spheres of precursor cells increased the number of BrdU-expressing newborn cells, indicating that GABA is acting as an autocrine modulator, being tonically released from the spheres to regulate their own rate of proliferation (Nguyen et al., 2003). Electrical stimulation of neuroblasts in the SVZ also induced depolarisation in neuronal precursor cells that could be antagonised by $GABA_A$ antagonists and enhanced by GAT blockers (Liu et al., 2005). The release of GABA could act as a feedback mechanism from newborn neurones to neural precursor/stem cells in the SVZ. A decrease in the speed of migration of newborn neurones from the SVZ to the olfactory bulb was observed in the presence of GABA

as viewed by time-lapse video microscopy from acute brain slices in rodents, indicating that newborn neurones also express GABA receptors (Bolteus and Bordey, 2004). Addition of the GABA$_A$ receptor antagonist, bicuculline, increased the rate of migration of these neurones suggesting the presence of endogenous GABA acting in a tonic manner, reducing migration (Bolteus and Bordey, 2004). Although the ambient GABA reduces migration, observing the neurones using time-lapse microscopy both in culture and in acute brain slices from rodents revealed that GABA is necessary for the proper initiation, elongation and stabilisation of dendrites (Gascon et al., 2006); thus the levels of ambient GABA must be finely tuned to allow dendritic formation without inhibiting migration.

In the mouse DG, spontaneous, transient, TTX-sensitive currents were observed in neural progenitor cells; these transients could be inhibited by bicuculline indicating that neural progenitor cells of the DG, like those of the SVZ, express GABA$_A$ receptors (Wang et al., 2005). Application of GABA elicits a depolarisation of the neural progenitor cells which initiates an increase in intracellular Ca^{2+} and the expression of NeuroD, a positive regulator of neuronal differentiation (Tozuka et al., 2005), implying that GABA induced depolarisations can promote neuronal differentiation in the mouse. As with newborn neurones in the SVZ, those in the DG can also respond to GABA, in fact there is a sequence in ability to respond to neurotransmitters which newborn neurones progress through that was determined in the mouse by retroviral labelling of proliferating cells and their progeny with GFP to follow their maturation (Ge et al., 2006). Firstly, three days following birth of the newborn neurones, a tonic GABAergic current was revealed in the presence of bicuculline, then at seven days a bicuculline-sensitive post-synaptic current was observed and finally at 14 days a glutamate antagonist-sensitive current was seen (Ge et al., 2006). Knock down of NKCC1 expression in newborn DG neurones resulted in tonic hyperpolarisations by GABA, delayed the time point at which postsynaptic GABAergic and glutamatergic currents were observed and drastically reduced the number of spontaneous synaptic currents (Ge et al., 2006). This suggests that tonic GABA-mediated depolarisations are essential for the correct formation of the GABAergic and glutamatergic synapses.

In the CC region of the adult turtle, a lower vertebrate with a substantial regenerative capacity (Dervan and Roberts, 2003), there are numerous modes of GABAergic signalling (Reali et al., 2011). Neural progenitors are depolarised by GABA; this response is mediated through both GAT3 and GABA$_A$ receptors,

although whether this depolarisation mediates neurogenesis is yet to be investigated (Reali et al., 2011).

This section has demonstrated how essential GABAergic signalling is for the appropriate proliferation and differentiation of neural progenitor cells and for the correct migration and synapse formation of newborn neurones in the postnatal neurogenic niches of the mammalian brain. GABAergic signalling has already been shown in the neurogenic niche of the postnatal turtle CC and in CSFcCs of the mammalian spinal cord; however, there is no evidence to date about how GABA affects the neurogenic capability of the mammalian CC.

1.8 5HT receptors

There are seven subfamilies of 5HT receptors, $5HT_1$-$5HT_7$ with 14 receptor subtypes including $5HT_{1A}$, $5HT_{1B}$, $5HT_{1D}$, $5HT_{1E}$, $5HT_{1F}$, $5HT_{2A}$, $5HT_{2B}$, $5HT_{2C}$, $5HT_3$, $5HT_4$, $5HT_{5A}$, $5HT_{5B}$, $5HT_6$, $5HT_7$ (Hoyer et al., 1994; Barnes and Sharp, 1999). All of the receptors, with the exception of the $5HT_3$ receptor, are G-protein coupled receptors.

1.8.1 Structure and function of 5HT receptors

The metabotropic 5HT receptors vary in functional properties due in part to the different G-proteins that they are coupled to and the subsequent downstream effects that occur (See review Raymond et al., (2001)). For example, $5HT_{1A}$ receptors couple negatively to adenylate cyclase via G-proteins to mediate downstream signalling (Schoeffter and Hoyer, 1988; Bertin et al., 1992) and also induce a neuronal hyperpolarisation through the opening of K^+ channels that are directly coupled to G-proteins (Andrade et al., 1986). On the other hand, $5HT_2$ receptors couple positively to phospholipase C via G-proteins and induce intracellular Ca^{2+} release (Conn and Sanders-Bush, 1986). $5HT_3$ receptors are unique to the 5HT receptor subfamilies in that they are ligand-gated ion channels that do not mediate their effects through G-proteins (Derkach et al., 1989). The activation of $5HT_3$ receptors results in a rapid cellular depolarisation as it is a cation selective ion channel (Derkach et al., 1989; Malone et al., 1991). The great variety

of 5HT receptors and the downstream effects that they mediate are vast and will be covered no further in this study.

1.8.2 Distribution of 5HT receptors

Autoradiography revealed the presence of both $5HT_{1A}$ receptors and/or $5HT_7$ receptors, as identified by 8-OH-[^{3}H]DPAT, in the dorsal region of lamina X in the thoracic and lumbar spinal cord of the rat (Marlier et al., 1991). The same study identified $5HT_{1B}$ receptors in lamina X, surrounding the CC, using [^{125}I]iodocyanopindolol; the density of these receptors increased along the rostro-caudal gradient, with the most $5HT_{1B}$ receptors identified in the sacral spinal cord (Marlier et al., 1991). Autoradiography using [^{3}H]ketanserin revealed $5HT_2$ receptors in the area surrounding the CC, these were predominant at the thoracic level of the spinal cord (Marlier et al., 1991). *In-situ* hybridisation in the rat determined that it is the $5HT_{2C}$ receptor subtype, and not the $5HT_{2A}$ receptor, that is expressed around the CC; with a higher density dorsal and lateral to the CC, compared with ventral to the CC (Fonseca et al., 2001). The $5HT_3$ receptor mRNA has also been identified at low levels in lamina X at all spinal cord levels (Fonseca et al., 2001). Immunohistochemistry in the rat revealed the presence of the $5HT_{5A}$ receptor subtype dorsal to the CC in the CAA (Doly et al., 2004). The gene expression nervous system atlas (GENSAT) that generates bacterial artificial chromosome (BAC) reporter mice demonstrates that cells directly surrounding the CC express $5HT_{5B}$ and $5HT_6$ receptors. These cells have a morphology resembling CSFcCs; however, it is not conclusive that they are CSFcCs. The presence of such a wide variety of 5HT receptors along with the high density of 5HT-immunoreactive terminals in lamina X (Takeoka et al., 2009), suggests that the 5HTergic system is important in regulating cells within lamina X and is capable of mediating a diverse range of responses within these cells. Given the presence of both 5HTergic interneurones in lamina X (Takeoka et al., 2009) and supraspinal inputs from the raphe nuclei of the brainstem (Bowker et al., 1981) the 5HTergic system appears to be an essential part of the circuitry that connects lamina X to the rest of the CNS.

1.8.3 Role of 5HT receptors in postnatal neurogenesis

5HT has been demonstrated to influence neurogenesis in the postnatal mammalian CNS, in both the DG and the SVZ (see review Young et al., (2011)). For example, the number of adult mouse SVZ derived primary neurospheres cultured *in-vitro* was increased following the direct application of 5HT and following the infusion of 5HT into the lateral ventricles prior to culturing (Hitoshi et al., 2007). In the rat DG, the number of BrdU expressing cells was decreased following a lesion to the raphe nuclei, where most 5HTergic neurones reside; this decrease can be reversed following a foetal raphe graft (Brezun and Daszuta, 2000). In addition, chronic treatment with antidepressant drugs such as fluoxetine, which is a 5HT selective reuptake inhibitor (Wong et al., 1975), increased the number of BrdU-expressing cells within the rat DG (Malberg et al., 2000), indicating that 5HT influences neurogenesis in the rodent DG.

5HT appears to exert this influence over postnatal neurogenesis through a number of 5HT receptors (see review Young et al., (2011)). To investigate the role of 5HT receptors in cell proliferation, neurogenesis and newborn cell survival three different BrdU protocols were used in the rat. For cell proliferation, animals were terminated immediately following the injection of BrdU which was given at the end of specific 5HT receptor agonist or antagonist treatments (Banasr et al., 2004; Soumier et al., 2009). For neurogenesis, animals were terminated four weeks following the injection of BrdU which was given at the end of specific 5HT receptor agonist or antagonist treatments and newborn neurones were identified by performing dual immunohistochemistry for BrdU and NeuN in fixed tissue (Banasr et al., 2004; Soumier et al., 2009; Soumier et al., 2010). Finally, newborn cell survival was investigated by injecting BrdU on the first experimental day, then applying the specific 5HT receptor agonists or antagonists before terminating the animals (Soumier et al., 2009; Soumier et al., 2010). Using these protocols it was determined that in the DG, activation of $5HT_{1A}$ receptors by ($\pm$)-8-Hydroxy-2-dipropylaminotetralin (8-OH-DPAT) increases the number of proliferating cells, the number of BrdU-expressing newborn neurones and the survival of these BrdU-expressing newborn neurones (Banasr et al., 2004; Soumier et al., 2010). In the SVZ, activation of $5HT_{1A}$ receptors by 8-OH-DPAT increases the number of proliferating cells and the number of BrdU-expressing newborn neurones; however, it does not increase the survival of these newborn neurones in the olfactory bulb (Banasr et al., 2004; Soumier et al., 2010). It has been suggested that the chronic activation of $5HT_{1A}$ receptors could reduce the migration of newborn neurones from

the SVZ to the olfactory bulb (Soumier et al., 2010). In the DG, antagonism of $5HT_{2A}$ receptors decreases cell proliferation (Banasr et al., 2004) whereas antagonism of $5HT_{2C}$ receptors by agomelatine increases cell proliferation (Soumier et al., 2009). The $5HT_{2C}$ receptor agonist, RO600,175 has no effect on the number or survival of newborn neurones (Soumier et al., 2010). In contrast, activation of $5HT_{2C}$ receptors in the SVZ increases the number of proliferating cells and the number of newborn neurones in the olfactory bulb (Banasr et al., 2004; Soumier et al., 2010). $5HT_{2C}$ receptors are not expressed on proliferating cells within the SVZ but are expressed by ependymal cells of the choroid plexus (Palacios et al., 1990), therefore the effect of the $5HT_{2C}$ agonist on SVZ proliferation appears to be indirect. The differential effects of $5HT_{2C}$ agonists and antagonists within various regions serves to highlight how difficult it is to determine the role of 5HT receptors in adult neurogenesis, considering how the role of receptors varies from one neurogenic niche to another and from one aspect of neurogenesis to another, such as cell proliferation to migration of newborn neurones.

1.9 Substance P receptors

Substance P is a peptide neuromodulator that is a member of the tachykinin family, which was previously known as the neurokinin family (Chang et al., 1971). The other members of this family include neurokinin A, neurokinin B, and the more recently discovered neuropeptide K, neuropeptide γ and hemokinin-1(Kangawa et al., 1983; Kage et al., 1988; Carter and Krause, 1990; Burcher et al., 1991; Zhang et al., 2000; Pennefather et al., 2004). Three tachykinin receptors have been discovered, NK_1, NK_2 and NK_3. These are G-protein coupled receptors with seven transmembrane spanning domains (see review Nakanishi (1991)). Substance P can activate all three receptors; however, it has a far greater potency at NK_1 receptors (Regoli et al., 1994), therefore these receptors will receive the main focus.

1.9.1 Structure of substance P receptors

Evidence from pharmacology studies had suggested that NK_1 receptors were G-protein coupled receptors (Macdonald and Boyd, 1989); this was confirmed by the cloning of this receptor which determined the seven transmembrane domain structure of the NK_1 receptor (Masu et al., 1987; Yokota et al., 1989). The activation of NK_1 receptors by substance P results in the initiation of a number of downstream

pathways through the interaction with $G_{\alpha q/11}$, $G_{\alpha s}$ and $G_{\alpha i}$ proteins, and thus has numerous outcomes (see review Quartara and Maggi (1997)). Coupling to $G_{\alpha q/11}$ protein results in the accumulation of inositol phosphate, the release of intracellular Ca^{2+} and mediates an inward current (Nakajima et al., 1992; Kwatra et al., 1993; Mochizuki-Oda et al., 1994). Coupling to $G_{\alpha s}$ protein results in an increase in cAMP and an inhibition of K^+ channels (Nakajima et al., 1988; Mitsuhashi et al., 1992; Nakajima et al., 1992; Takeda et al., 1992). Coupling to the $G_{\alpha i}$ protein results in the opening of large conductance Cl^- channels (Sun et al., 1993).

1.9.2 Distribution of substance P receptors

In-situ hydridisation in the rat revealed the presence of cells expressing NK_1 receptor mRNA in the dorsal horn, the IML and the area surrounding the CC (Elde et al., 1990). Immunohistochemistry in the rat revealed that the most intense labelling of NK_1 receptors within the spinal cord was at thoracic levels in the IML, followed by lamina I, part of the substantia gelatinosa (Nakaya et al., 1994). Moderate levels of NK_1 receptor expression have been observed in laminae III, IV and X with immunohistochemistry (Nakaya et al., 1994). The subcellular expression of the NK_1 receptor has varied in studies, with some in the rat observing mainly dendritic labelling in the superficial layers of the dorsal horn (Moussaoui et al., 1992), whereas others in humans observed numerous cell bodies expressing the NK_1 receptor (Ding et al., 1999). Cell bodies expressing the NK_1 receptor were observed in laminae IV, V, X and in the IML, however, no specific cell types have been observed to express NK_1 receptors in lamina X (Moussaoui et al., 1992; Ding et al., 1999). The presence of NK_1 receptors and substance P immunoreactive terminals in lamina X in the rat (Hokfelt et al., 1975; Gibson et al., 1981) indicates that cells within lamina X receive inputs from substance P expressing terminals and have the machinery to mediate a response. The relevance of these terminals to the function of cells within lamina X is unknown but would depend greatly on whether the terminals are from cells located in the periphery, nuclei of the brain or intraspinally.

1.9.3 Role of substance P receptors in postnatal neurogenesis

The role of substance P in postnatal neurogenesis is currently poorly understood. The number of SVZ-derived neurospheres cultured *in-vitro* increased in the presence of substance P in the rat; this increase was reversed in the presence of the NK_1 receptor antagonist, L-703,606 (Park et al., 2007). This indicates that substance P promoted cell proliferation of neural progenitor cells through NK_1 receptor activation. Infusion of substance P into the lateral ventricles for five days whilst giving injections of BrdU resulted in an increase in the number of BrdU- and Dcx-expressing cells within both the SVZ and DG (Park et al., 2007). In contrast, a decrease in the number of BrdU- and Dcx-expressing cells was observed in both the SVZ and DG following the infusion of L-703,606 (Park et al., 2007). These experiments suggest that substance P promotes neurogenesis *in-vivo* in both the SVZ and DG. The above experiments were all carried out following the induction of transient focal ischaemia, however, using the same experimental paradigm but following a traumatic brain injury there was no significant increase in the number of BrdU- and Dcx-expressing cells (Carthew et al., 2012). Instead, a large increase in BrdU- and IBA1-expressing microglia was observed along with a decrease in functional motor recovery that was assessed by the rotarod test (Carthew et al., 2012). Thus the role of substance P in neurogenesis is obviously a complex one.

NK_1 receptor knock out studies have also been used to investigate the role of substance P in neurogenesis. Mice deficient in the NK_1 receptor and wild-type littermates were both injected with BrdU and terminated at a number of time points. An increase in BrdU expressing cells was observed in the DG but not in the SVZ in NK_1 receptor knockout mice when animals were terminated one day after BrdU injection (Morcuende et al., 2003). When animals were terminated 28 days after BrdU injection there was no longer an increased number of BrdU expressing cells in the NK_1 receptor knockout mice (Morcuende et al., 2003). This indicates that NK_1 receptor knockout mice have an elevated amount of neurogenesis but not of newborn neuronal survival compared to their wild-type littermates. Although there are complicated effects of substance P on neurogenesis, it is clearly influential and deserves further investigation. Given the presence of substance P and NK_1 receptors in lamina X and the neurogenic potential of the area surrounding the CC, it is possible that substance P could be influencing neurogenesis within this area.

1.10 Hypothesis and Aims

There is currently very little understanding of how cells in the area surrounding the CC of the spinal cord are affected by neurotransmitters and neuromodulators and how they are integrated into the circuitry of the spinal cord. Sections 1.6-1.9 have demonstrated the presence of ACh, GABA, 5HT, substance P and some of their respective receptors within this area. It has also provided evidence that each of the neurotransmitters/neuromodulators can influence cells within other neurogenic niches.

There are two overarching aims of this study. The first is to determine whether ependymal cells and CSFcCs are integrated into the spinal cord and to begin to assign a functional role to CSFcCs. The second is to investigate whether any parallels can be established between the cells in this area and those of other postnatal neurogenic niches. Hypotheses have been developed which relate to either the first aim, second aim or both aims; these specific hypotheses and the reasoning behind them are as follows:

1. It is hypothesised that CSFcCs from rats aged P9-P21 have properties resembling those observed in rats aged P0-P5 and represent a similar heterogenous population. This will aid in determining whether CSFcCs are in the process of maturation or have reached their terminal phenotype.

2. It is hypothesised that CSFcCs in rats and mice aged P9-P21 respond to GABA, given the ability of CSFcCs in rats aged P0-P5 to respond to GABA and the ability of immature neurones in other postnatal neurogenic niches to respond to GABA.

3. It is hypothesised that CSFcCs are capable of responding to 5HT and substance P given the large amount of 5HT- and substance P-immunoreactive terminals in close proximity to the CC. Although a number of neurotransmitters and neuromodulators are found in close proximity to the CC, 5HT and substance P will be investigated as they have more specific functional roles which, if CSFcCs are responsive, could illuminate a functional role for CSFcCs.

4. It is hypothesised that ependymal cells in rats and mice aged P9-P21 have passive response properties and a high degree of gap junction coupling, as observed in rats aged P0-P5 and neural stem/progenitor cells in other postnatal neurogenic niches.

5. It is hypothesised that ependymal cells in rats aged P9-P21 are capable of responding to GABA given the ability of neural stem/progenitor cells in other postnatal neurogenic niches to respons to GABA.

6. It is hypothesised that both CSFcCs and ependymal cells in rats aged P9-P21 are capable of responding to ACh as there is an abundance of cholinergic terminals surrounding the CC and ACh is known to influence other postnatal neurogenic niches.

These hypotheses will be tested using a combination of whole cell patch clamp electrophysiology, intracellular dye-loading and immunohistochemistry.

Chapter 2 - General Methods

All experiments were carried out in line with the Animals Scientific Act (1986) and the ethical standards set out by the University of Leeds Ethical Review Committee by individuals with Home Office approval. Every effort was made to minimise the number of animals used and their suffering.

2.1 Animals

The predominant breed of animal used within this study was the Wistar rat. These rats were acquired from the in-house breeding facility at the Central Biomedical Services unit here at the University of Leeds. At this facility the rats lived in a 12 hour light-dark cycle and were provided with water and food *ad libitum*.

To show that the results are not solely relevant to this breed, some experiments have also been performed using C57bl6 mice. Both wild-type C57bl6 mice and GAD67-GFP mice with a C57bl6 background were used. The GAD67-GFP mice expressed GFP under the control of the endogenous GAD67 promotor as a result of the insertion of GFP cDNA into the GAD67 locus (Tamamaki et al., 2003). These mice have been validated since GFP-expressing cells were found in the same regions as those in which GAD cells have been reported by both immunohistochemistry and *in-situ* hybridization (Barber et al., 1982; Feldblum et al., 1995; Tamamaki et al., 2003). Thus GAD67 expressing CSFcCs expressed GFP in these mice, aiding the visualisation of these cells when viewed under an epifluorescent microscope (Olympus BX50W1; Olympus U-RFL-T).

2.2 Spinal cord slice preparation

Two different methods of slice preparation were used depending on the age of the animal. The first method was used for animals aged 9-20 days old and has been used previously in this laboratory (Deuchars et al., 2001). In slices from older animals, however, it has proved more difficult to obtain stable neuronal recordings. Therefore, the original spinal cord preparation protocol was modified for animals aged 21 days or over to maximise the number of healthy cells in such slices (Husch et al., 2011).

For both types of preparation, Wistar rats (9-21 days old) and C57bl6 mice (9-26 days old) were anaesthetised by administration of urethane (2 g/kg of body weight) or pentabarbitone (60 mg/kg) I.P., respectively. Animals were deemed sufficiently anaesthetised when the pedal withdrawal reflex was abolished in response to a noxious pinch.

2.2.1 Slice preparation for animals aged 9-20 days

Using blunted scissors an incision was made through the skin from the caudal aspect of the sternum to the distal aspect of the clavicle on either side of the animal to allow access to the rib cage. The rib cage was then removed to expose the heart, clearing away any membranes that may be obstructing access to the heart. A transcardiac perfusion was then performed; this involved creating an incision in the right atrium, then injecting approximately 10 mls (mouse) or approximately 20 mls (rat) of gassed (95 % O_2: 5 % CO_2), ice cold sucrose artificial cerebrospinal fluid (sucrose aCSF; for composition see table 2.1) into the left ventricle using a shortened, blunted 19 gauge needle. Animals were considered sufficiently perfused when blanching of the liver, tail, paws and nose became apparent. The transcardiac perfusion was important as it cooled the spinal cord tissue and reduced the amount of Na^+ ions present thus reducing the amount of cell death occurring in the spinal cord by excitotoxicity. Animals were then killed by decapitation using scissors. A dorsal laminectomy was performed which involved using blunted scissors to remove the skin above the vertebral column, then using spring scissors to cut through the vertebrae surrounding the spinal cord starting at the top as access was already available due to the decapitation. The nerve rootlets that are attached to the spinal cord were then severed allowing the whole spinal cord to be removed and transferred to a petri dish containing ice cold, gassed (95 % O_2: 5 % CO_2) sucrose aCSF. Under a dissecting microscope (SM2 2B, Nikon, Japan), fine forceps were used to removed both the dura and pia mater. The lower thoracic or upper lumber areas of the spinal cord were chosen to slice; from these areas a section of spinal cord roughly 1 cm in length was cut for slicing.

To improve slicing of the spinal cord it was embedded in a 3 % solution of warm agar in sucrose aCSF which was allowed to cool before cutting into a block. The block of agar containing the spinal cord was then attached to a larger supporting block of 4 % agar (in 0.9 % saline) before gluing onto the cutting platform of a vibrating microtome (Leica VT1200s, Leica Microsystems, UK). Submerging the

block in ice cold, gassed (95 % O_2: 5 % CO_2) sucrose aCSF in the cutting chamber allowed 300 μm thick transverse slices to be cut using a stainless steel vibratome blade with the speed set at 0.3 mm/s and the amplitude at 1.5 mm. Slices were transferred to a holding chamber containing gassed (95 % O_2: 5 % CO_2) aCSF (for composition see table 2.1), and left to equilibrate in this solution at room temperature for 30-60 minutes.

2.2.2 Slice preparation for animals aged 21 days or above

Following the initial administration of anaesthetic (see section 2.2 for details), animals were maintained at a deep level of anaesthesia by placing on ice and were oxygenated to keep tissue alive by placing a small funnel over the nose and mouth supplying 95 %O_2: 5 % CO_2. A dorsal laminectomy was performed, which included first removing the skin from the back with blunted scissors, then using spring scissors to cut the vertebral column and spinal cord at T1 level, then cutting away the vertebrae and nerve rootlets from T1 to the sacral levels. Gassed (95 % O_2: 5 % CO_2), ice cold glycerol aCSF (for composition see table 2.1) was superfused over the spinal cord to aid visibility during this procedure. Glycerol aCSF has previously been utilised in procedures that have obtained stable recordings from cells within spinal cord slices from older animals (Husch et al., 2011) and as such replaced the norml use of sucrose aCSF in this method. The spinal cord from T1 to S1 was then removed and transferred to a petri dish containing ice cold, gassed (95 % O_2: 5 % CO_2) glycerol aCSF. Under a dissecting microscope, fine forceps were used to remove both the dura and pia mater. As before, a section of spinal cord 1 cm long was cut from the lower thoracic or upper lumber areas of the spinal cord.

The spinal cord was embedded in a 3 % solution of warm agar in glycerol aCSF and cooled before a block was cut. The block of agar containing the spinal cord was attached to a larger supporting block of 4 % agar (in 0.9 % saline) before gluing onto the cutting platform of a vibrating microtome. Submerging the block in ice cold, gassed (95 % O_2: 5 % CO_2) glycerol aCSF in the cutting chamber allowed 300 μm thick transverse slices to be cut using a stainless steel vibratome blade with the speed set at 0.3 mm/s and the amplitude at 1.5 mm. Slices were transferred to a holding chamber containing gassed (95 % O_2: 5 % CO_2) aCSF at 37°C. Once all the slices were cut, the solution was allowed to cool to room temperature and the

slices were left to equilibrate in this solution for 30-60 minutes before recordings were made.

Table 2.1: Compositions of extracellular solutions.

The components and their final concentration in the solutions are given for the two solutions used for spinal cord slice preparation, sucrose aCSF and glycerol aCSF, and for the extracellular solution used for recording from cells within the spinal cord slices, aCSF.

Component	Final concentration (mM)		
	Slice preparation		Recording
	Sucrose aCSF	Glycerol aCSF	aCSF
Sucrose	217		
Glycerol		222	
NaCl			124
$NaHCO_3$	26	25	26
KCl	3	3.1	3
$MgSO_4.7H_2O$	2	1.25	2
NaH_2PO_4	2.5		2.5
KH_2PO_4		1.2	
Glucose	10	11	10
$CaCl_2$	1	2.5	2

2.3 Electrophysiology

2.3.1 Whole cell patch electrode preparation

A Sutter P-97 micropipette puller (Sutter Instruments, USA) was used to pull micropipettes (resistance 5-8 MΩ, tip diameter approximately 1-3 µm) from borosilicate glass capillary tubing (inside diameter 0.94 mm, outside diameter 1.2

mm, Warner Instruments, USA). Micropipettes were filled with intracellular solution (mM): K gluconate (110), EGTA (11), $MgCl_2$ (2), $CaCl_2$ (0.1), HEPES (10), Na_2ATP (2), NaGTP (0.3). Additionally the intracellular solution contained 0.5 % Neurobiotin (Vector Laboratories, USA) and 0.02 % dextran tetramethylrodamine (rhodamine; Invitrogen, USA) to allow visualisation of the neurone post-recording.

2.3.2 Perforated patch electrode preparation

A stock solution of 1-2 mg amphotericin B / 50 µl of DMSO was prepared and stored in the dark. For recordings, 6 µl of stock was dissolved in 500 µl intracellular pipette solution and thoroughly vortexed. Microelectrodes with a smaller resistance (4-6 MΩ) were initially tip dipped in intracellular solution, prior to back filling with the amphotericin B-containing intracellular solution.

2.3.3 Experimental set-up

Spinal cord slices were immersed in a custom made recording chamber and secured under tightly stretched crossed threads. From a storage flask, a steady flow (~4-6 ml/min) of oxygenated (95 % O_2: 5 % CO_2) aCSF was gravity fed to flow across the recording chamber and was subsequently removed by suction and discarded. The solutions were not heated to maximise slice viability and minimise electrical noise; therefore the recordings were taken at room temperature. The bath application of oxygenated (95 % O_2: 5 % CO_2) drug solutions was achieved by switching a 3-way tap to allow the gravity feed of drug solutions in place of the aCSF from the storage chamber.

A micropipette filled with intracellular solution was placed over a silver chloride wire and secured by the electrode holder (QSW A12P, Warner Instruments, USA); it was ensured that just enough intracellular solution was present in the micropipette so that the wire was in contact with the intracellular solution but that this was as small an amount as possible (approximately ¼ of the micropipette was filled with intracellular solution). The electrode holder possessed a side arm that allowed the application of positive and negative pressure to the electrode tip. A silver chloride

pellet was placed in the recording chamber to act as a reference electrode. Both the recording electrode and the reference electrode were connected to the CV-4 1/100U headstage (Axon Instruments, USA) as detailed in figure 2.1; therefore a full electrical circuit was achieved when the electrode was lowered into the aCSF within the recording chamber. A micromanipulator (PatchStar, Scientifica, UK) was attached to the headstage to allow the course and fine control of the microelectrode as it was positioned in the recording chamber. Signals from the recording electrode were preamplified by the headstage, filtered by a Bessel low pass filter set at 2-5kHz, passed through the Axopatch 1D amplifier (Axon Instruments, USA) and filtered for mains noise by a HumBug (Quest Scientific via Digitimer, UK). The signal was then converted from an analogue signal to a digital signal by the Digidata 1322A analogue to digital converter unit (Axon Instruments, USA) before being captured by the pClamp 9 software (Axon Instruments, USA) on a PC. The acquisition frequencies were 20kHz for the intial recordings to identify cell type (see section 2.3.5) and 5kHz for the continuous recordings to identify drug responses.

A Master-8 stimulator (A.M.P.I., Israel) was used to control the timing and duration of current and voltage pulses. Channel 1 of the Master-8 triggered the start of a sweep in the pClamp software via the Digidata 1322A, whilst also triggering channel 2 of the Master-8. Channel 2 of the Master-8 then initiated a current or voltage pulse from the Axopatch 1D amplifier.

At the opposite side of the recording chamber another micromanipulator (PatchStar, Scientifica, UK) held a blunted micropipette (resistance 3-5 MΩ, tip diameter 3-4 μm) that was filled with drug solutions. The micropipette was connected to a PV800 pneumatic pico pump (World Precision Instruments Ltd, UK) which was connected to a pressurised gas cylinder; this allowed the rapid, focal extrusion of drug solutions onto the recorded cell. The PV800 pneumatic pico pump was also connected to the Digidata 1322A which was in turn connected to the pClamp 9 software on the PC; this allowed the visualisation of exactly when the pressure ejection of the drug occurred, enabling the time to onset of response to be measured.
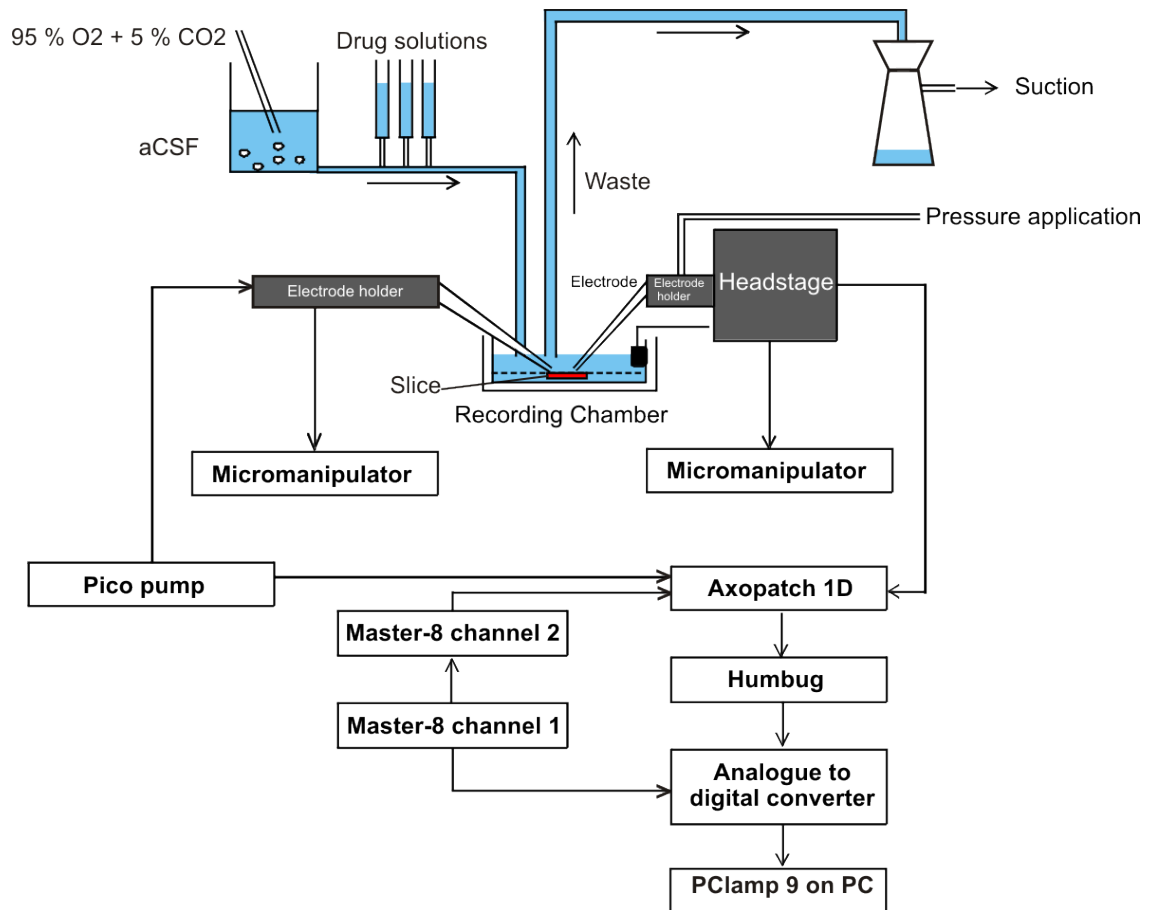
Figure 2.1: Experimental set-up for whole cell patch clamp electrophysiology recordings.

See experimental set-up section for details.

2.3.4 Whole cell and perforated patch clamp recordings

An upright microscope (Olympus BX50W1) was used to identify the CC at x10 magnification. Viable CSFcCs, ependymal cells and nearby interneurones were viewed at x60 magnification first using the upright microscope then using differential interference contrast (DIC) imaging on a computer monitor using QCapture Pro software via a camera (QImaging Rolera-XR, Q imaging, Canada) attached to the microscope. Ependymal cells were easily identified by their location surrounding the CC, their cuboidal shape and their lack of CC-contacting process. CSFcCs were

identified by their subependymal location, a more spherical cell body in comparison to the ependymal cells and the presence of a CC-contacting process. In GAD67-GFP mice CSFcCs were visualised using epifluorescence.

Positive pressure was applied to the electrode before lowering it into the solution. In current clamp mode the pipette offset was compensated using the amplifier's offset dial, and the pipette resistance, due to a -250 pA current pulse, was compensated using the amplifier's series resistance dial to give a voltage of 0 mV. Viewed by the x10 objective, the tip of the electrode was positioned above the CC using the coarse controls of the micromanipulator. The amplifier was then switched to voltage clamp mode and the track function utilised. Changing to the x60 magnification and the fine piezoelectric controls of the micromanipulator, the tip of the electrode was lowered towards a cell of interest until the positive pressure caused a dimple to appear in the cell membrane. The positive pressure was released and the seal formation was observed by monitoring the current response to a voltage pulse of 25 mV. Sometimes a small amount of gentle suction was required to form a seal of sufficient resistance. A seal was considered strong enough when the current response equated to a ≥3 GΩ resistance. The amplifier was switched back to current clamp, the current pulse reduced to -50 pA and a small negative current applied to maintain the cell at -60 mV to -80 mV. To achieve the whole cell patch clamp configuration a short, sharp suction was applied. To achieve the perforated patch clamp configuration the cell was left following seal formation until the resistance began to increase.

2.3.5 Neuronal characterisation

To characterise voltage responses in current clamp, positive and negative current (ranging from -120 pA to +120 pA) was injected into the cells in the form of 1 s pulses that were triggered by the Master-8 stimulator, with the amplitude adjusted by the amplifier. The injection of positive current brought some cells to the threshold for firing an action potential, induced rapid depolarisations in some cells and resulted in rectangular depolarisations in other cells. The injection of negative current resulted in hyperpolarisations which allowed the input resistance of cells to be calculated using Ohm's law. Together these challenges gave an indication of the cell type.

2.3.6 Preparation and application of drugs

To characterise the responses of cells to drug solutions/compounds, hyperpolarising pulses of -2 to -50 pA were applied, with the size of current dependant on cell type; usually -2 to -10 pA for CSFcCs, -5 to -20 pA for interneurones and -10 to -50 pA for ependymal cells. The majority of compounds were superfused at a flow rate of ~4-6 mls / min. However to allow direct, fast application of ACh and GABA, a blunted micropipette that was attached to the pico pump was filled with the drug and lowered close to the recorded cell prior to whole cell patch clamp configuration being achieved. Intervals of 5 minutes were allowed between pressure applications of ACh and GABA to ensure that receptors would not be in a desensitised state. In some cases antagonists or allosteric modulators were superfused in conjunction with the pressure ejection of ACh. The compounds applied, their known functions and the final concentrations in the recording chamber are given (Table 2.2). The reasoning for using the given concentrations is also stated and is based on either the EC_{50} or IC_{50} values of the compounds or the previous effective use of the compound at this concentration. All compounds were stored at 10^3 their working concentrations, with the exceptions of ACh and 5HT, that were weighed and dissolved fresh on the day of use, and DHβE and MLA that were stored at 10^4 their working concentration. All drugs were dissolved in water with the exceptions of diazepam and 18β-Glycyrrhetinic acid that were dissolved in ethanol and PNU-120596 that was dissolved in DMSO.

2.3.7 Analysis

Data was captured using the Clampex programme and data was analysed in the Clampfit programme, both part of the pClamp 9 software. The input resistance of a cell was calculated using Ohm's law (input resistance = voltage response / current injected), and was taken using the average voltage response from two separate negative current injections. Cell types (i.e. ependymal, CSFcC and interneurone) and cell subtypes (i.e. CSFcC subtypes 1-3) were determined based on the voltage responses to the injection of positive current with regards to the shape of the response and the ability to produce an action potential, and on the size of their input resistance, calculated from the injection of negative current pulses. The average data for each cell type and subtype is expressed as mean ± S.E.

Table 2.2: Drugs used in this study.

Common and chemical names, known functions, final bath concentrations, the reasoning for these concentrations and the suppliers are given.

Common drug name Chemical name	Known function	Final concentration	Reasoning for concentration	Supplier
5-Hydroxytryptamine, 5HT, serotonin 3-(2-Aminoethyl)-1H-indol-5-ol	5HT receptor agonist	10 µM	EC_{50} 9.56 µM (Rick et al., 1995), 10 µM used previously (Wang and Dun, 1990; Pickering et al., 1994).	Sigma
Substance P RPKPQQFFGLM	NK_1 receptor agonist	1 µM	EC_{50} can vary from 19 nM to 12 µM (Nalivaiko et al., 1997).	Tocris
GABA γ-Aminobutyric acid	GABA receptor agonist	200 µM (bath), 500 µM (pipette)	The GABA concentration applied was used to induce maximal responses (Uchida et al., 1996).	Sigma
Bicuculline [R-(*R**,*S**)]-5-(6,8-Dihydro-8-oxofuro[3,4-*e*]-1,3-benzodioxol-6-yl)-5,6,7,8-tetrahydro-6,6-dimethyl-1,3-dioxolo[4,5-*g*]isoquinolinium	$GABA_A$ receptor antagonist, α7*nAChR antagonist	10-100 µM	10 µM used previously (Bradaia & Trouslard, 2002; Deuchars et al., 2005). 100 µM ensures effect at extrasynaptic receptors (Wang et al., 2008).	Ascent

Common drug name Chemical name	Known function	Final concentration	Reasoning for concentration	Supplier
Gabazine, SR-95531 6-Imino-3-(4-methoxyphenyl)-1(6*H*)-pyridazinebutanoic acid	GABA$_A$ receptor antagonist	2.5 -50 µM	Previously used effectively (Wang et al., 2008).	Sigma
Baclofen (R)-4-Amino-3-(4-chlorophenyl)butanoic acid	GABA$_B$ receptor agonist	5-10 µM	IC$_{50}$ 2.5 µM at rat SPNs (Wu and Dun, 1992).	Tocris
Acetylcholine, ACh 2-(Acetyloxy)-N,N,N-trimethylethanaminium	AChR agonist	3-10 mM (pipette)	Previously used effectively in rodent hippocampus (Henderson et al., 2005; John, 2010).	Sigma
Atropine α-(Hydroxymethyl)benzeneacetic acid 8-methyl-8-azabicyclo[3.2.1]oct-3-yl ester	mAChR antagonist	5 µM	Previously used effectively (Henderson et al., 2005; John, 2010).	Sigma
Mecamylamine, MCA N,2,3,3-Tetramethylbicyclo[2.2.1]heptan-2-amine	nAChR antagonist	50 µM	Previously used effectively at 25 µM (Henderson et al., 2005).	Tocris

Common drug name Chemical name	Known function	Final concentration	Reasoning for concentration	Supplier
Dihydro-β-erythroidinne, DHβE (2S,13bS)-2-Methoxy-2,3,5,6,8,9,10,13-octahydro-1H,12H-benzo[i]pyrano[3,4-g]indolizin-12-one	Non α7*nAChR antagonist	1 µM	1 µM determined effective but 10 µM unspecific (Bradaia & Trouslard, 2002).	Tocris
Methyllycaconitine, MLA [1α,4(S),6β,14α,16β]-20-Ethyl-1,6,14,16-tetramethoxy-4-[[[2-(3-methyl-2,5-dioxo-1-pyrrolidinyl)benzoyl]oxy]methyl]aconitane-7,8-diol	α7*nAChR antagonist	20 nM	20 nM is specific for α7*nAChRs, higher concentrations are unspecific (Wonnacott, 1993). Previously used effectively (Henderson et al., 2005; John, 2010).	Tocris
PNU-120596 N-(5-Chloro-2,4-dimethoxyphenyl)-N′-(5-methyl-3-isoxazolyl)-urea	α7*nAChR positive allosteric modulator	10 µM	Previously used effectively (Dickinson et al., 2007; John, 2010).	Ascent
Tetrodotoxin, TTX Octahydro-12-(hydroxymethyl)-2-imino-5,9:7,10a-dimethano-10aH-[1,3]dioxocino[6,5-d]pyrimidine-4,7,10,11,12-pentol	Voltage-gated Na^+ channel blocker	1 µM	Commonly used effectively (Bordey et al., 1996a; Wang et al., 2008).	Sigma

Common drug name Chemical name	Known function	Final concentration	Reasoning for concentration	Supplier
AP-5 D-(-)-2-Amino-5-phosphonopentanoic acid	NMDA receptor antagonist	50 µM	Previously used effectively (Henderson et al., 2005; John, 2010).	Tocris
NBQX 2,3-Dioxo-6-nitro-1,2,3,4-tetrahydrobenzo[f]quinoxaline-7-sulfonamide	AMPAR and kainate receptor antagonist	20 µM	Previously used effectively (Henderson et al., 2005; John, 2010).	Tocris
18β-Glycyrrhetinic acid 3β-Hydroxy-11-oxo-18β,20β-olean-12-en-29-oic acid	Gap junction blocker	100 µM	Previously used effectively (Pierce et al., 2010).	Sigma

To determine the effects of superfused drugs, the input resistance and membrane potential were measured before, during and after the drug application, and for each condition, an average was determined from three measurements. Data is expressed as mean ± S.E. Current was not injected during the pressure application of drugs as this would distort the fast voltage responses observed, therefore, for these applications only the change in membrane potential/voltage was used to determine the size of the drug effect. The time to onset of response and time to peak response were also measured following the pressure application of drugs. The data for each cell type in response to the pressure ejection of drugs was expressed as mean ± S.E. To determine whether a superfused drug had affected the response of the cell to the pressure ejected drug, the size of the voltage change in response to the pressure ejected drug was measured before, during and after the superfusion of the additional drug.

2.3.8 Statistics

Data were tested to ensure that they were normally distributed. If data was normally distributed a parametric test was used to determine whether there was any significant difference between subtypes or following drug applications. If data was not normally distributed the equivalent non-parametric test was used to determine any significant differences between subtypes or following drug applications. The specific tests used to determine significant differences between groups are detailed in table 2.3.

Post-hoc Bonferroni tests were used following one-way ANOVAs, repeated measures ANOVAs and two-way ANOVAs to determine the differences between specific groups. Where a Kruskall-Wallis H test or a Friedman test were used to determine whether there was a significant difference, a Mann-Whitney U test or a Wilcoxon Signed Rank test, respectively, were used to determine the differences between specific groups. Statistical results were reported with the test statistic, the degrees of freedom and the p value. Data was considered significant when $p < 0.05$ (denoted by *), however, to highlight results with higher degrees of significance $p < 0.01$ (denoted by **) and $p < 0.001$ (denoted by ***) were used.

Table 2.3: Statistical tests used in this study.

Displayed are the parametric tests and the equivalent non-parametric tests used to determine whether there were statistically significant differences between groups of data for specific circumstances.

What difference is being tested for?	Parametric test and associated test statistic	Non-parametric test and associated test statistic
Between subtypes (2 groups) or species	Independent samples t-test (t)	Mann-Whitney U test (U)
Between subtypes (3 or more groups)	One-way ANOVA (F)	Kruskal-Wallis H test (H)
Before and during drug application	Paired samples t-test (t)	Wilcoxon Signed Rank test (Z)
Before, during and after drug application	Repeated measures ANOVA (F)	Friedman test (X^2)
Between subtypes and drug application	Two-way ANOVA (F)	n/a
Correlation	n/a	Spearman's Rank-Order Correlation (r_s)

2.4 Histological identification of recorded cells

As detailed in section 2.3.1, the intracellular solution contained Neurobiotin and rhodamine which diffused into the cells during recording to allow the morphology of the cell to be determined.

2.4.1 Identification of recorded cells using rhodamine

The rhodamine could be visualised immediately post-recording whilst the electrode was still attached, the rhodamine was visualised when excited by a wavelength of 550 nm using an epifluorescence microscope (Olympus BX50W1; Olympus U-RFL-

T). The image of a rhodamine-filled cell was captured using QCapture Pro software via a camera (QImaging Rolera-XR, Q imaging, Canada) that is attached to the microscope. Following the image capture of rhodamine the recording electrodes were carefully removed from cells by applying a small amount of positive pressure.

2.4.2 Identification of recorded cells using Neurobiotin

Neurobiotin is a gap junction permeable tracer (Kita and Armstrong, 1991; Vaney, 1991), unlike rhodamine (Heyman and Burt, 2008), therefore it can reveal whether the recorded cell was coupled by gap junctions to neighbouring cells; it also enables a more detailed cell morphology to be visualised. The visualisation of Neurobiotin requires multiple steps. Firstly, the recovered slices were fixed in 0.1 M phosphate buffer (PB) containing 4 % paraformaldehyde (PFA) and 0.25 % glutaraldehyde for < 24 hours at 4°C. Following 3 x 10 minute washes in 0.1 M PB, slices were removed from the agar in which they were originally cut and embedded in gelatine (10 % solution in distilled water). The gelatin embedded slices were fixed for 1 hour in 0.1 M PB containing 4 % PFA and 0.25 % glutaraldehyde before washing for 3 x 10 minutes in 0.1 M PB and cutting serial sections of 50-80 µm using a vibrating microtome (VT1000S, Leica Microsystems, UK). Sections were collected and washed for 3 x 10 minutes in 0.1 M PBS. At this stage some cells were incubated in 0.1 M PBS containing 0.1 % Triton X100 and streptavidin conjugated to AlexaFluor 555 (Invitrogen) at a concentration of 1:1000 which directly binds to Neurobiotin. Sections were washed 3 x 10 minutes in 0.1 M PBS, mounted on glass coverslips and air dried. Sections were then mounted in Vectasheild (Vector Laboratories) and covered with a glass coverslip before being visualised using a Zeiss LSM510 Meta laser scanning confocal microscope. Using the confocal microscope z-stacks were taken of the sections to allow the processes to be followed throughout the slice. Projections of the whole cell were created from the z-stacks using Carl Zeiss LSM software. Most cells, however, were visualised by 3, 3'-diaminobenzidine (DAB). To allow visualisation of cells with DAB, sections were incubated in 0.1 M PBS containing 0.1 % Triton X100 and 1 % H_2O_2, to permeabilise the cell membranes and block endogenous peroxidise activity, respectively. Sections were then washed for 3 x 10 minutes in 0.1 M PBS and incubated in extravidin peroxidise (EAP; Sigma-Aldrich, Poole, 1:250 in 0.1 M PBS) for 36-78 hours at 4°C to detect the Neurobiotin. Sections were washed for 3 x 10

minutes in 0.1 M PBS, then 10 minutes in tris buffer (pH 7.6) to remove any unbound EAP. Sections were incubated in DAB (0.5 mg/ml in tris buffer) for 10 minutes before adding H_2O_2 to give a resulting concentration of 0.01 % H_2O_2. The progress of the reaction was then monitored every minute until the cell could be visualised. The reaction was stopped by washing in tris, followed by 3 x 10 minute washes in 0.1 M PB. Sections were mounted temporarily for imaging and drawing using the Nikon Eclipse E600 microscope in 0.1 M PB under glass coverslips. For permanent mounting, sections were washed in distilled H_2O for 10 minutes before dehydrating in increasing concentration of alcohol 30 %, 50 %, 70 % and 95 % for 5 minutes each and in 100 % for 10 minutes. Sections were incubated in Xylene for 2 x 5 minutes before mounting on a glass coverslip and leaving to air dry. DPX was used to cover the sections, a coverslip added and left to harden overnight before further viewing if necessary.

2.5 Immunohistochemistry

2.5.1 Fixed spinal cord section preparation

As previously stated, all experiments were carried out in line with the Animals Scientific Act (1986) by individuals with Home Office approval. Wistar rats and GAD67-GFP mice (9-12 days old or adult) were anaesthetised by administration of pentabarbitone (60 mg/kg) I.P. Animals were deemed sufficiently anaesthetised when the pedal withdrawal reflex was abolished in response to a noxious pinch. Using blunted scissors an incision was made through the skin from the caudal aspect of the sternum to the distal aspect of the clavicle on either side of the animal to allow access to the rib cage. The rib cage was then removed to expose the heart, clearing away any membranes that may be obstructing access to the heart. A transcardiac perfusion was then performed; this involved creating an incision in the right atrium, then injecting approximately 10 mls (mouse) or approximately 20 mls (rat) of 4 % PFA into the left ventricle using a shortened, blunted 19 gauge needle. Using blunted scissors the whole vertebral column was dissected out, from which the whole spinal cord was dissected out using spring scissors and post-fixed in 4 % PFA overnight. The spinal cord was washed in 0.1 M PB and the dura and pia mater were removed. Roughly 3 mm of lower thoracic or upper lumbar spinal cord was cut, the same area as that used in the preparation of slices for

electrophysiology recordings, and sectioned at 50 μm in 0.1 M PB on a vibrating microtome (VT1000S, Leica Microsystems, UK).

2.5.2 Immunohistochemistry on fixed sections

Sections were collected in 0.1 M PBS and washed for 3 x 10 minutes in 0.1 M PBS. Sections were incubated in pepsin (2 mg/ml in 0.2 M hydrochloric acid) for 5 minutes (Watanabe et al., 1998); pepsin digests both bound and unbound proteins enabling the primary antibody to better penetrate the tissue. Sections were washed for 3 x 10 minutes in 0.1 M PBS, before incubating in primary antibodies overnight in 0.1 M PBS containing 0.3 % Triton X100, 3 % donkey serum, 0.8 % bovine serum albumin at the concentrations given in table 2.4. Triton X100 is a detergent that permeabilises the cell membranes allowing access to intracellular antigens. Donkey serum and bovine serum albumin are used to reduce the amount of unspecific binding of the antibodies used to the tissue. An anti-PKD2L1 antibody (for details see table 2.4) was used to identify CSFcCs; the antibody used produced the same distribution pattern for PKD2L1 as that seen in PKD2L1-GFP recombinant mice (Huang et al., 2006). Alternatively, to identify CSFcCs in GAD67-GFP mice, an anti-GFP antibody (for details see table 2.4) was used. An anti-calbindin antibody (for details see table 2.4) was used to identify ependymal cells, this antibody has been demonstrated to reliably identify calbindin as there was no labelling in calbindin knock-out mice (Airaksinen et al., 1997). An anti-ChAT antibody (for details see table 2.4) was used to identify cholinergic terminals; the antibody used has reliably identified ChAT-expression in the rat spinal cord previously and produced the same distribution pattern for ChAT as that seen with other anti-ChAT antibodies (Barber et al., 1984; Phelps et al., 1984) and that seen in mice expressing Cre under control of the ChAT promotor (GENSAT). An anti-5HT antibody (for details see table 2.4) was used to identify 5HT-containing terminals; the antibody used was specific for 5HT-expressing neurones (Milstein et al., 1983) and produced an identical distribution pattern of 5HT-expressing terminals to that previously observed (Newton et al., 1986). An anti-substance P antibody (for details see table 2.4) was used to identify substance P-containing terminals; this antibody has been shown to be specific for substance P (Cuello et al., 1979) and produced an identical distribution pattern of substance P expressing terminals to that previously observed (Barber et al., 1979). Sections were washed in

0.1 M PBS for 3 x 10 minutes before incubating in the appropriate secondary antibodies at 1:1000 (Table 2.5) for 2 hours. Sections were then washed in 0.1 M PBS for 3 x 10 minutes before leaving to air dry onto glass slides. Once dry, sections were mounted in Vectasheild (Vector Laboratories) and covered with a glass coverslip. To eliminate the possibility of unspecific staining occurring with the secondary antibodies, sections that had not been incubated in primary antibodies were incubated in both secondary antibodies.

2.5.3 Image capture and analysis

Initial images were taken on the Nikon Eclipse E600 microscope, and then z-stacks were taken of the CC area using a scanning confocal microscope. Images were viewed using Carl Zeiss LSM software before importing to CorelDRAW X4 software where images were adjusted for brightness, contrast and intensity, and to assemble the figures.

Table 2.4: List of primary antibodies.

Primary antibodies used, detailing the species the antibody was produced in, the concentration at which it was used and where it was sourced from.

Antibody	Species	Concentration	Source
Anti-5HT	Rat	1:200	AbD Serotec
Anti-calbindin	Mouse	1:500	Swant CB300
Anti-ChAT	Goat	1:500	Millipore
Anti-GFP	Rabbit	1:1000	Invitrogen
Anti-PKD2L1	Rabbit	1:1000	Abcam
Anti-substance P	Rat	1:1000	Medimabs

Table 2.5: List of secondary antibodies.

Secondary antibodies used, detailing the species the antibody was produced in, the concentration at which it was used and where it was sourced from.

Antibody	Species	Concentration	Source
Anti-Goat IgG, Alexa Fluor 488	Donkey	1:1000	Invitrogen
Anti-Mouse IgG Alexa Fluor 555	Donkey	1:1000	Invitrogen
Anti-Rabbit IgG, Alexa Fluor 488	Donkey	1:1000	Invitrogen
Anti-Rabbit IgG, Alexa Fluor 555	Donkey	1:1000	Invitrogen
Anti-Rat IgG, Alexa Fluor 555	Goat	1:1000	Invitrogen

Chapter 3 - Basic characteristics of CSFcCs and their responses to neurotransmitters and neuromodulators

3.1 Introduction

CSFcCs are a unique cell type found surrounding the CC and are defined by their CC-contacting process which ends in a large, bulbous terminal contacting the CSF (Vigh et al., 1977). They also possess an axon which extends from the cell body to terminate on the ventral and ventrolateral surfaces of the spinal cord, although the synaptic terminals on these axons do not contain synaptic machinery (Stoeckel et al., 2003). As discussed in the general introduction, the function of CSFcCs is currently unknown. The intention of this chapter is to investigate the electrophysiological properties of CSFcCs and their ability to respond to neurotransmitters and neuromodulators in order to resolve this deficiency. The one previous study of mammalian CSFcCs categorised the cells into three subtypes: cells that had active response properties but could not spike, single spiking cells and repetitive spiking cells (Marichal et al., 2009). These data indicated that CSFcCs could be immature neurones in varying states of maturity; however BrdU studies suggest that these cells do not appear to be born postnatally. Alternatively, the CSFcCs could be mature cells with varying electrophysiological subtypes that correspond to their varying functions, for example the role of some CSFcCs may not require the ability to produce a spike. Instead they may transmit information through Ca^{2+} signalling or the transport of substances from the CSF to different areas of the spinal cord.

An effective method of determining the function of CSFcCs is to investigate which neurotransmitters and neuromodulators CSFcCs respond to. To date, however, only the effect of GABA on CSFcCs has been investigated (Marichal et al., 2009). GABA was shown to have variable effects on CSFcCs, inducing depolarisations in some CSFcCs and hyperpolarisations in others, this was taken to support the theory that CSFcCs are at different levels of maturity but could also indicate a difference in function of CSFcCs. Although the ability of CSFcCs to respond to GABA could draw parallels to the newborn neurones in the SVZ and DG (Bolteus and Bordey, 2004; Ge et al., 2006), it does not reveal an immediate function for them. This is because there is a widespread distribution of GABAergic neurones throughout the spinal cord and they are not generally associated with a specific function. To help assign a function to CSFcCs it would be useful to study whether neurotransmitters or neuromodulators whose distribution is more specific and whose role is better defined are interacting with CSFcCs. Both 5HT-immunoreactive and substance P-immunoreactive terminals have been identified in the area

surrounding the CC of the spinal cord (Barber et al., 1979; Takeoka et al., 2009). Although the effects of 5HT and substance P are many and complex, their distributions and functions within the spinal cord are more defined than that of GABA. For example, 5HT is known to be involved in autonomic control (Pierce et al., 2010) and motor control (Dunbar et al., 2010), where as substance P is widely associated with nociception (De Koninck and Henry, 1991). Determining whether CSFcCs respond to either of these neurotransmitters/neuromodulators is the first step towards establishing a functional role for CSFcCs.

3.1 Hypothesis and aims

To aid in determining whether CSFcCs are in the process of maturation, the basic electrophysiological properties of CSFcCs in spinal cord slices from rats aged P9-P21 are investigated and compared to previous studies of CSFcCs from rats aged P0-P5. It is hypothesised that there are no differences in the basic properties of CSFcCs or the heterogenity of the population of CSFcCs in rats aged P9-P21 compared to those aged P0-P5. It is also hypothesised that CSFcCs in spinal cord slices from mice aged P9-P21 have similar properties.

To investigate how CSFcCs are integrated into the spinal cord circuitry, their responses to a number of neurotransmitters and neuromodulators that are abundant in lamina X are investigated. The neurotransmitters and neuromodulators could also be capable of influencing any maturation and/or plasticity occurring in CSFcCs. More specifically, given the ability of CSFcCs from rats aged P0-P5 to respond to GABA, it is hypothesised that CSFcCs from rats and mice aged P9-P21 are capable of responding to GABA. Due to the more specific functional roles of 5HT and substance P within the spinal cord, it is useful to determine whether CSFcCs can respond to these neurotransmitters/neuromodulators. As there is an abundance of 5HT- and substance P-immunoreactive terminals surrounding the CC, it is hypothesised that CSFcCs are capable of responding to 5HT and subtance P.

These hypotheses will be tested using whole cell patch clamp electrophysiology, intracellular dye-loading and immunohistochemistry.

3.2 Results

The majority of data in this chapter is from spinal cord slices prepared from Wistar rats, however, there is some data collected in spinal cord slices prepared from C57/bl6 mice. Unless otherwise stated data is from Wistar rats.

3.2.1 CSFcCs can be categorised into three subtypes

Electrophysiology revealed that CSFcCs were a varied population of cells. Their phenotype ranged from one indistinguishable from that of ependymal cells to a phenotype resembling a robust repetitively firing neurone. Due to this varied phenotype, the criterion used to define a cell as a CSFcC was the visualisation of a CSF-contacting process post-recording using either rhodamine or Neurobiotin. To aid analysis, CSFcCs were categorised into three subtypes based on their responses to depolarising current pulses, however, the phenotypes of CSFcCs vary within the subtypes and some of the subtypes could be joined together and viewed as responses ranging along a continuum.

Subtype 1 CSFcCs had a phenotype that was indistinguishable from ependymal cells (see chapter 4.2.1; Figure 3.1A). They had a resting membrane potential of -74.29 ± 0.82 mV (n = 21; Figure 3,1D), a low input resistance of 71.12 ± 8.40 MΩ (n = 21; Figure 3.1E, 3.3C) and a lack of spontaneous or evoked activity such as EPSPs. There was a significant moderate, positive correlation between the resting membrane potential and the input resistance (r_s (19) = 0.440, P = 0.046). This indicated that cells with a more negative resting membrane potential generally had a smaller input resistance. Within subtype 1 CSFcCs, the cells could be further categorised into subtype 1A and 1B by visualisation of Neurobiotin with DAB post-recording. Neurobiotin can pass through gap junctions (Kita and Armstrong, 1991; Vaney, 1991), therefore if cells are coupled to neighbouring cells, these cells may be visualised by DAB. Only 12 out of 21 CSFcCs could be categorised into 1A or 1B as cells were not always successfully visualised by DAB. Subtype 1A CSFcCs were defined as cells which were coupled to neighbouring cells, resembling ependymal cells (see chapter 4.2.1; Figure 3.1B). 7 out of 12 CSFcCs were subtype 1A, this group had a resting membrane potential of -75.71 ± 1.27 mV (Figure 3.1D) and an input resistance of 41.39 ± 3.53 MΩ (Figure 3.1E). Subtype 1B CSFcCs were defined as cells which were visualised alone and not coupled to neighbouring cells (Figure 3.1C). 5 out 12 CSFcCs were subtype 1B, this group had a resting membrane potential of -73.60 ± 0.93 mV (Figure 3.1D) and an input resistance of
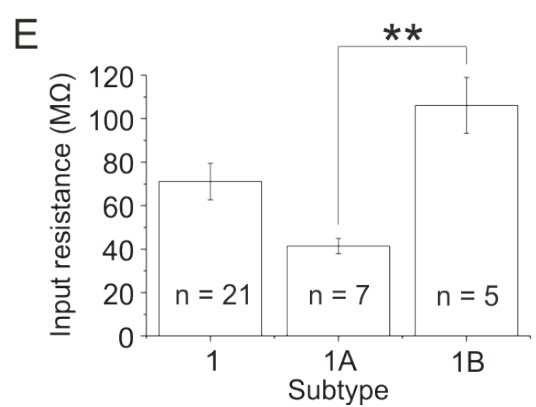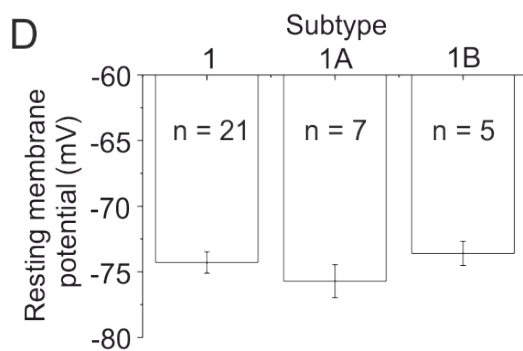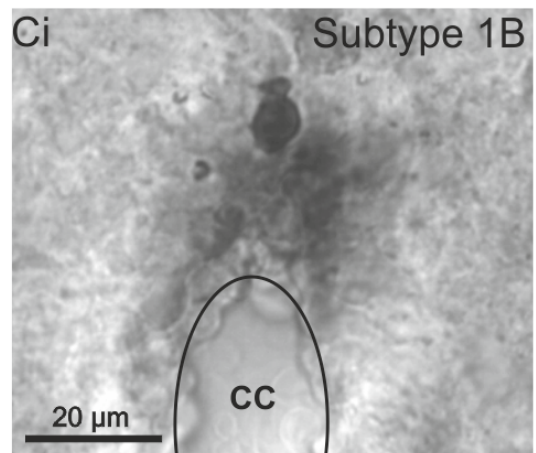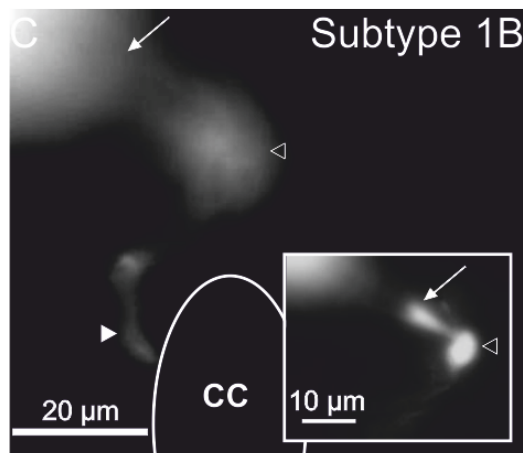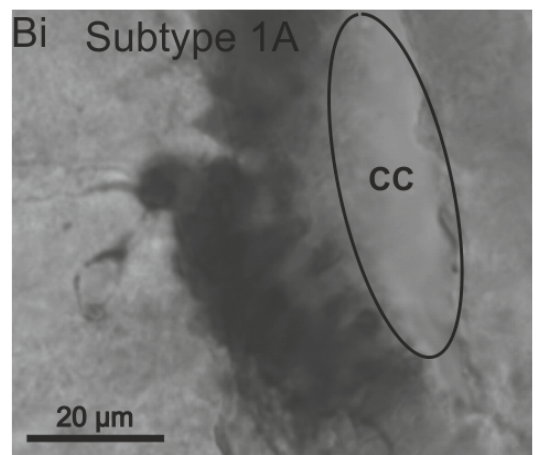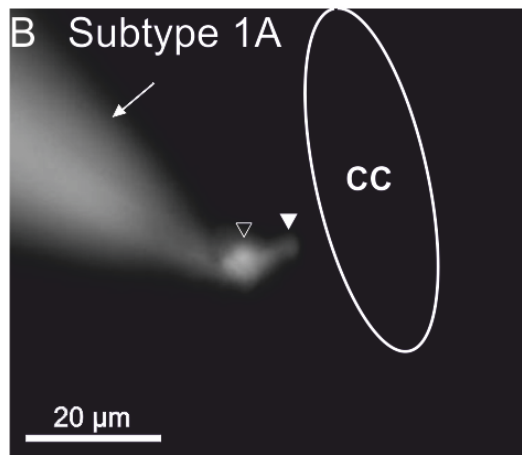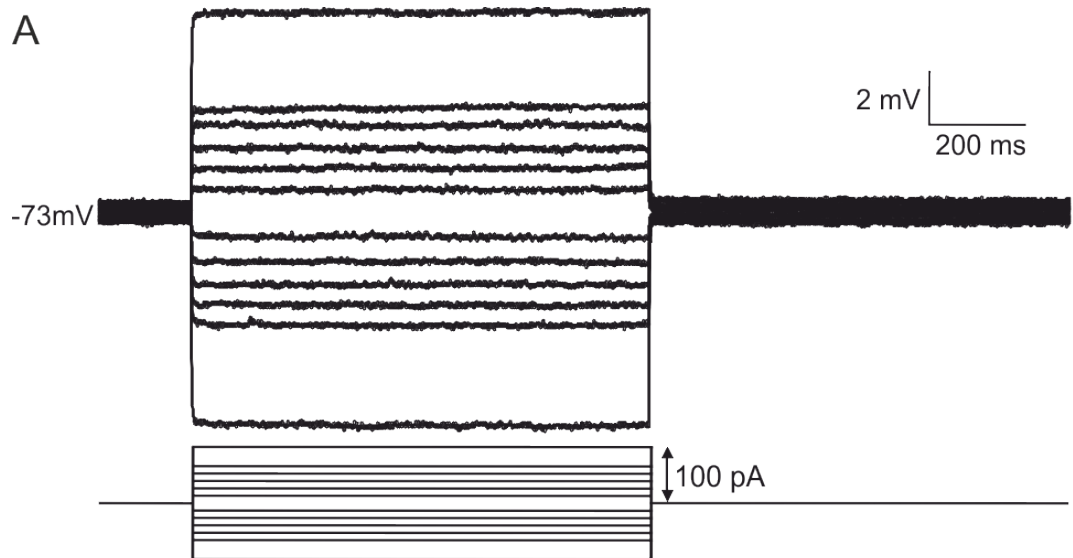
106.15 ± 12.88 MΩ (Figure 3.1E). The input resistance of subtype 1A CSFcCs was significantly lower than that of subtype 1B CSFcCs (U = 0.00, P = 0.004; Figure 3.1E), this was determined using a Mann-Whitney U test as the data was not normally distributed. The smaller input resistance of subtype 1A CSFcCs indicates that there is very little resistance to the movement of ions in and out of these cells through either ion channels or gap junctions. In the case of these cells the small input resistance is indicative of a high degree of gap junction coupling which was highlighted by the dye-coupling. Despite the resting membrane potential of subtype 1A CSFcCs being more negative than that of subtype 1B CSFcCs, there was no significant difference between the two (t (10) = -1.24, P = 0.243; Figure 3.1D).

Subtype 2 CSFcCs were defined by the production of a single fast depolarisation in response to the injection of positive current. The single fast depolarisation ranged on a continuum, from a fast but small depolarisation, then a single spike (Figure 3.2A) and finally to a single action potential (Figure 3.2B). The term spike is used in reference to a fast event that has definable depolarising and repolarising phases but could not be considered an action potential as it does not overshoot 0 mV. Some subtype 2 CSFcCs had membrane potential oscillations that followed the single spike or action potential; these oscillations looked like unsuccessful attempts to produce further spikes. Within the total population of subtype 2 CSFcCs (n = 136), 22 produced a fast depolarisation, 59 generated a spike and 55 generated an action potential. Rebound depolarisations were often observed following a negative current pulse (Figure 3.2A, B). Subtype 2 CSFcCs frequently exhibited spontaneous activity, with EPSPs visible (Figure 3.2A, B). Subtype 2 CSFcCs had a large input resistance of 2679.66 ± 127.00 MΩ (n = 136) that was significantly larger than that of subtype 1 CSFcCs (U = -7.364, P < 0.001; Figure 3.3C), a Mann-Whitney U test was used to determine this difference following a Kruskal-Wallis H test which revealed there was a significant difference between the 3 CSFcC subtypes (H (2) = 56.655, P < 0.001); both tests were used because the data was not normally distributed. Rebound depolarisations were observed following the injection of negative current (Figure 3.2A, B), suggesting the presence of T-type Ca^{2+} channels. Visualisation of subtype 2 CSFcCs post-recording always revealed a single CSFcC indicating that these cells were not coupled to neighbouring cells (Figure 3.2Ai, Bi).

Subtype 3 CSFcCs were defined by their ability to produce multiple spikes or action potentials in response to the injection of positive current (Figure 3.2C). The

Figure 3.1: CSFcCs with passive response properties.

A) Example whole cell patch clamp trace in current clamp of a subtype 1 CSFcC responding to the injection of positive and negative current pulses. B-C) Excitation of rhodamine post-recording revealed cells with CSF-contacting processes. Cell bodies are highlighted by unfilled arrowheads, CSF-contacting processes are highlighted by filled arrowheads and patch pipettes are highlighted by arrows. Inset (C) shows cell body in focus on a different level to the CSF-contacting process. Bi-Ci) Visualisation of Neurobiotin by DAB in the same cells revealed either a cluster of cells in the location of the recorded cell (subtype 1A; Bi) or the same single cell (subtype 1B; Ci). All images are orientated so dorsal is at the top. D-E) Comparison of the mean resting membrane potential ± S.E (D) and the mean input resistance ± S.E (E) for subtype 1 CSFcCs, compared to subtype 1A and subtype 1B CSFcCs. ** = $p < 0.01$.

A

2 mV
200 ms

-73mV

100 pA

B Subtype 1A

CC

20 µm

Bi Subtype 1A

CC

20 µm

C Subtype 1B

CC

20 µm

10 µm

Ci Subtype 1B

CC

20 µm

D

Subtype

Resting membrane potential (mV)

-60

-65

-70

-75

-80

1   1A   1B

n = 21   n = 7   n = 5

E

**

Input resistance (MΩ)

120

100

80

60

40

20

0

1   1A   1B
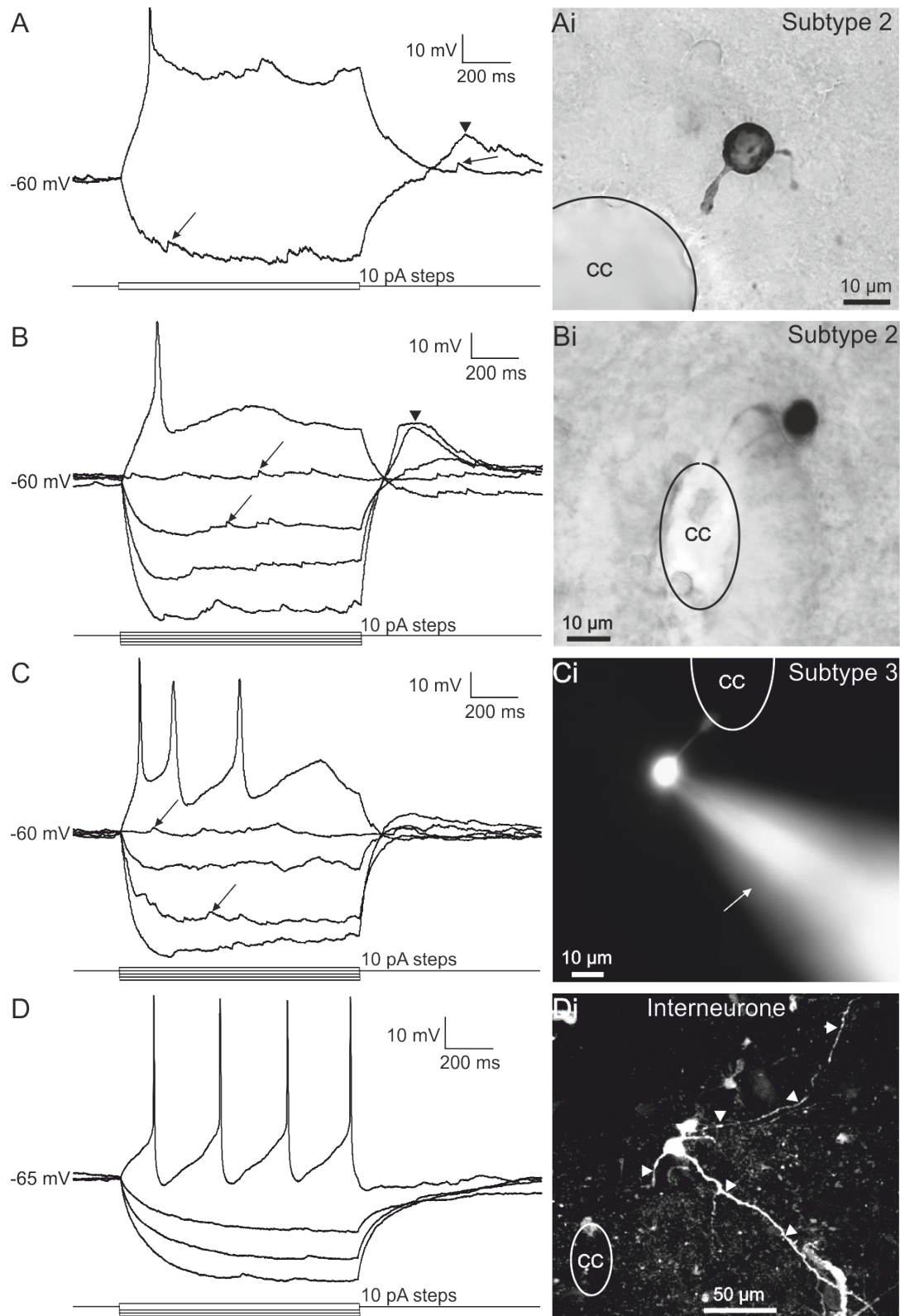
Subtype

n = 21   n = 7   n = 5

phenotypes of cells within this subtype varied on a continuum from those only capable of producing two spikes or action potentials, to others that could produce three or four spikes or action potentials, whilst a rare few cells were capable of firing repetitive action potentials. Subtype 3 CSFcCs exhibited spontaneous activity in the form of EPSPs and sometimes spikes or action potentials (Figure 3.2C). In response to the injection of negative current some subtype 3 CSFcCs displayed a voltage sag which is indicative of an Ih. Subtype 3 CSFcCs had a large input resistance 2565.64 ± 175.72 MΩ (n = 59) that was significantly larger than subtype 1 CSFcCs (U = -6.774, P < 0.001; Figure 3.3C) but was not significantly different from subtype 2 CSFcCs (U = -0.225, P = 0.822; Figure 3.3C); as prior a Mann-Whitney U test was used to determine the differences as the data was not normally distributed. Visualisation of subtype 3 CSFcCs post-recording revealed a single CSFcC with no coupling to neighbouring cells (Figure 3.2Ci).

The proportion of CSFcCs in each subtype was not the same. The majority of CSFcCs, 63 % (n = 136) were classified as subtype 2 CSFcCs, 27 % (n = 59) were classified as subtype 3 CSFcCs and 10% (n = 21) were classified as subtype 1 CSFcCs (Figure 3.3A). The majority of experiments were performed in slices from P11 rats; however, there was an age range from P9-P21. To verify that the proportion of CSFcC subtypes did not vary within this age range, the percentage of CSFcCs categorised in each subtype was investigated in the P21 rats only. Of the 13 CSFcCs recorded from P21 rat slices, 15 % were subtype 1, 69 % were subtype 2 and 15 % were subtype 3 (Figure 3.3B), indicating that there are not more multiple firing CSFcCs in older P21 rats compared to the population of CSFcCs in P9-P21 rats.

Interneurones located close to the CC were occasionally recorded from, these were initially distinguished by their robust, repetitive firing of action potentials and confirmed post-recording by a lack of CSF-contacting process (Figure 3.2D). The interneurones had an input resistance of 1339.32 ± 385.13 MΩ (n = 7), which was significantly different from the input resistance of CSFcCs (H (3) = 62.599, P < 0.001); this was determined by a Kruskall-Wallis H test as data was not normally distributed. Using a Mann-Whitney U test to investigate differences between groups determined that the input resistance of interneurones was significantly larger than that of subtype 1 CSFcCs (U = 0.00, P < 0.001) and significantly smaller than that of subtype 2 CSFcCs (U = 193.5, P = 0.008) and subtype 3 CSFcCs (U = 87, P = 0.013).

Figure 3.2: CSFcCs with active response properties.

A-B) Example whole cell patch clamp traces in current clamp of two subtype 2 CSFcCs, one producing a single spike (A) and one producing a single action potential (B) in response to the injection of positive current. Rebound depolarisations following the injection of negative current were observed in both cells. The visualisation of Neurobiotin by DAB post-recording confirmed the cells as CSFcCs (Ai, Bi). C) Example trace of a subtype 3 CSFcC producing multiple action potentials in response to the injection of positive current. The excitation of rhodamine post-recording confirmed the cell as a CSFcC (i). D) Example trace of an interneurone repetitively firing action potentials in response to the injection of positive current. The visualisation of Neurobiotin by streptavidin 555 post-recording confirmed that the cell was an interneurone (i). All images are orientated so dorsal is at the top. Black arrows indicate spontaneous synaptic activity; black arrowheads indicate rebound depolarisations; white arrows indicate the patch pipette; white arrowheads highlight projections.

A

-60 mV

10 mV
200 ms

10 pA steps

Ai — Subtype 2 — CC — 10 μm

B

-60 mV

10 mV
200 ms

10 pA steps

Bi — Subtype 2 — CC — 10 μm

C

-60 mV

10 mV
200 ms

10 pA steps

Ci — Subtype 3 — CC — 10 μm

D

-65 mV

10 mV
200 ms

10 pA steps

Di — Interneurone — CC — 50 μm

To determine whether CSFcCs with a similar range of properties are conserved in other mammalian species as well as rats, recordings were taken from the CC area of the spinal cord of mice aged P8-P19. Functional responses could be observed in CSFcCs from the spinal cords of mice, with the type and heterogeneity of responses being indistinguishable from those observed in the rat spinal cord (data not shown). From the 13 CSFcCs recorded in mice, 15 % were classified as subtype 1 CSFcCs, 69% were classified as subtype 2 CSFcCs and 15 % were classified as subtype 3 CSFcCs.

As mentioned, some subtype 2 and 3 CSFcCs displayed spontaneous EPSPs (Figure 3.2A-C), suggesting that they receive excitatory synaptic input. Bath application of AP5 and NBQX, antagonists of glutamatergic NMDA and AMPA receptors, respectively, reduced the number of EPSPs produced by CSFcCs (n = 10; data not shown). This suggests the presence of glutamatergic synapses onto subtype 2 and 3 CSFcCs.

3.2.2 CSFcCs possess ventrally or laterally projecting basal processes

The visualisation of rhodamine immediately post-recording allowed the observation of the CSF-contacting process; however, other processes could sometimes be seen. These processes were better identified following the visualisation of Neurobiotin with DAB. Not all cells were successfully visualised post-recording and some processes were lost in the resectioning procedure, therefore no attempt was made to quantify process direction or length, or to correlate it in relation to CSFcC subtype. Generally only one other process was observed from the CSFcCs, these projected from the cell bodies ventrally towards either the ventral horn or the ventral median fissure (Figure 3.4A), or laterally towards the IML and the white matter beyond (Figure 3.4B). Processes did not appear to branch at any point (Figure 3.4). Some of these processes ended in quite large terminals that could be indicative of growth cones or could be the result of the resectioning procedure (Figure 3.4Aii, Bii).
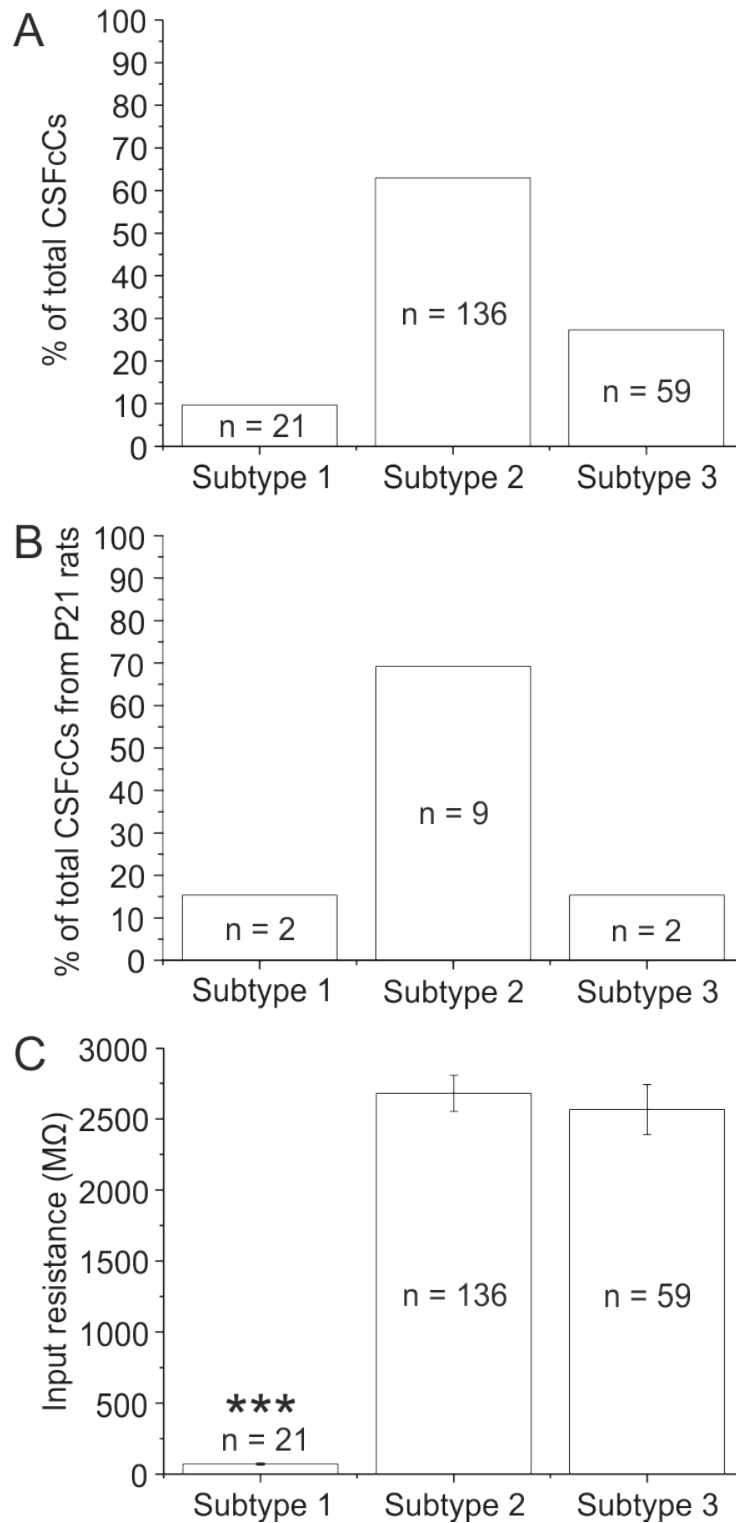
Figure 3.3: Comparisons of CSFcC subtypes.

A, B) Number of CSFcCs in each subtype expressed as a percentage of total CSFcCs, for CSFcCs recorded from rats aged P9-P21 (A) and CSFcCs recorded from rats aged P21 only. C) Comparison of the mean input resistance ± S.E depending on CSFcC subtype, *** = $p < 0.001$.
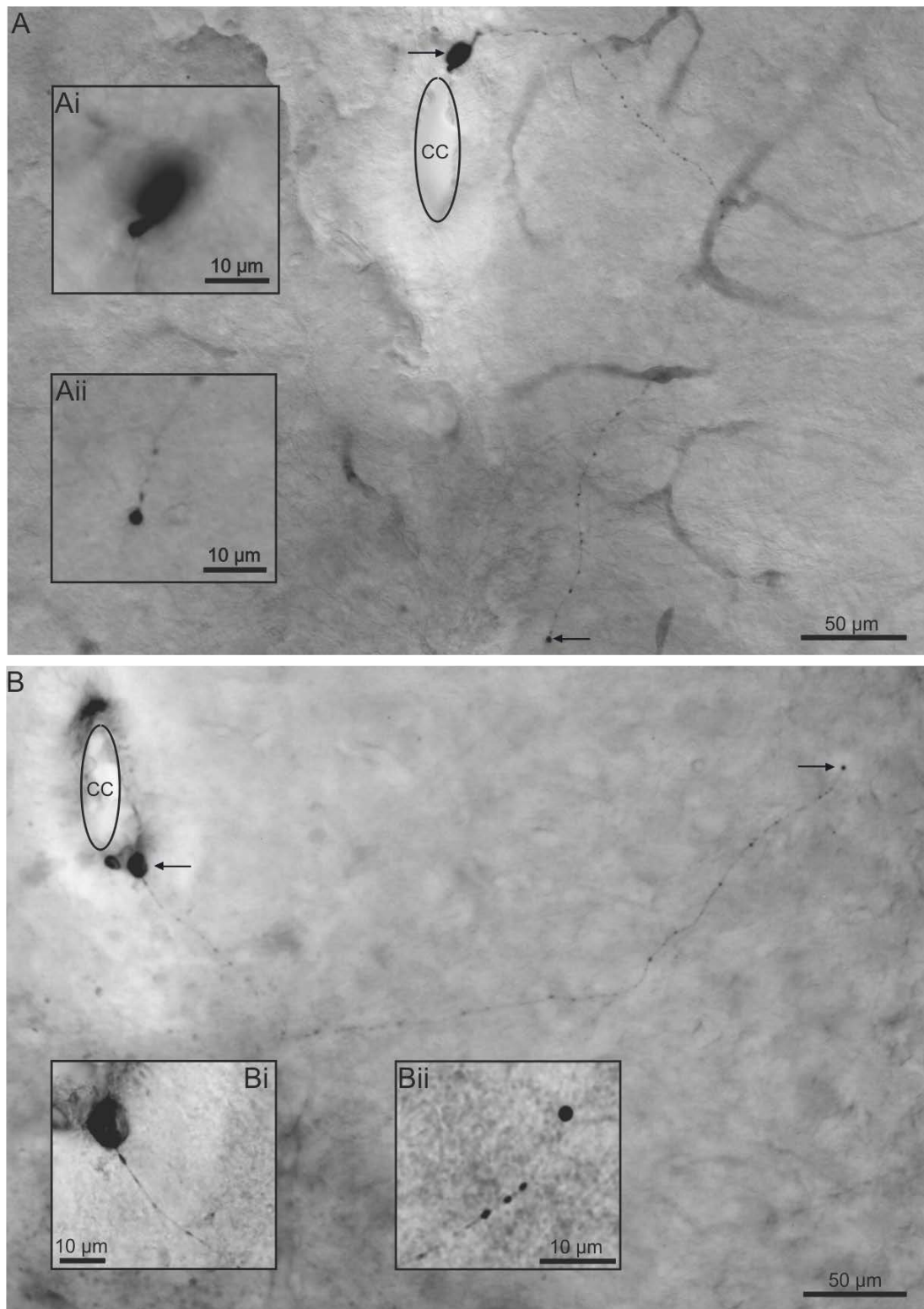
Figure 3.4: Basal processes of CSFcCs.

Visualisation of Neurobiotin with DAB revealed ventrally (A) or laterally (B) projecting basal processes of CSFcCs. Cell bodies (i) and process endings (ii) are highlighted by arrows and expanded in insets. All images are orientated so dorsal is at the top.

3.2.3 CSFcNs respond to GABA

CSFcCs with active response properties have been previously reported under the name of CSF-contacting neurones (CSFcNs; Marichal et al., (2009)). Therefore for the rest of this chapter, the CSFcCs from this study which displayed active response properties, subtype 2 and 3 CSFcCs, will be referred to as CSFcNs. CSFcNs have been shown previously to respond to GABA, this study bath applied GABA (200 µM) to CSFcNs to confirm that they did respond to GABA and thus further confirm that this was the same population of cells as examined by Marichal et al.,(2009). This study observed that all CSFcNs responded to GABA (n = 13), although there was great variation in the responses; 7 out of 13 CSFcNs depolarised (Figure 3.5A) and 6 out of 13 CSFcNs hyperpolarised (Figure 3.5B). With this variation it is not surprising that a Friedman test revealed that there was no significant difference between the membrane potential of CSFcNs before (-43.34 ± 0.61 mV; n = 13), during (-44.95 ± 2.19 mV; n =13) and following (-43.13 ± 0.87; n = 13; X^2 (2) = 0.154, P = 0.926; Figure 3.5C) the bath application of GABA when investigated as a single group. There was, however, a significant difference in the mean input resistance of CSFcNs before (2434.68 ± 323.89 MΩ; n = 13), during (701.44 ± 106.08 MΩ; n = 13) and following (2353.94 ± 341.85; n = 13; F (2, 24) = 36.196, P < 0.001; Figure 3.5D) the bath application of GABA. With post-hoc tests revealing that the input resistance during the application of GABA was significantly smaller than before (P < 0.001) and after (P < 0.001) the GABA application.

Due to the variation in the responses of CSFcNs to GABA, they were sorted into depolarising and hyperpolarising groups. Subsequently, a Friedman test determined that there was a significant difference between the membrane potential of CSFcNs before (-43.63 ± 0.73 mV; n = 7), during (-38.68 ± 0.82 mV; n = 7) and following (-44.30 ± 0.60 mV; n = 7; X^2 (2) = 10.571, P = 0.005; Figure 3.5E) the bath application of GABA in the depolarising CSFcN group. As expected for the depolarising CSFcN group, Wilcoxon Signed Rank tests revealed that the membrane potential during the GABA application was significantly less negative than before (Z = -2.366, P = 0.018) and following (Z = -2.366, P = 0.018) the GABA application. As observed for the whole group data, the input resistance before (2171.36 ± 518.37 MΩ; n = 7), during (664.45 ± 174.85 MΩ; n = 7) and following (2110.21 ± 534.3 MΩ; n = 7) the application of GABA were significantly different from each other in the depolarising CSFcN group (F (2, 12) = 13.990, P = 0.008; data not shown). The membrane potential of the hyperpolarising CSFcN group was also found to be significantly different before (-43.01 ± 1.07; n = 6), during (-52.26 ±

Figure 3.5: CSFcNs respond to GABA with both depolarisations and hyperpolarisations.

A-B) Whole cell patch clamp traces in current clamp of CSFcNs depolarising (A) and hyperpolarising (B) to the bath application of GABA (200 µM). The downward voltage deflections were in response to the regular injection of -10 pA current pulses. C-D) Mean ± S.E membrane potential (C) and input resistance (D) under control conditions, during the bath application of GABA and following wash of GABA. E-F) Mean ± S.E membrane potential of CSFcNs in the depolarising group (E) and in the hyperpolarising group (F) under control conditions, during the bath application of GABA and following wash of GABA. * = p < 0.05, ** = p < 0.01, *** = p < 0.001.
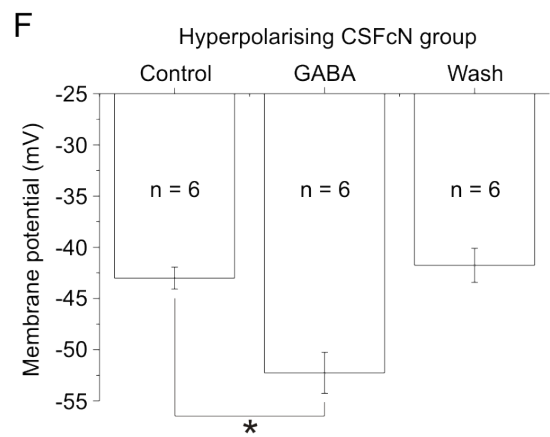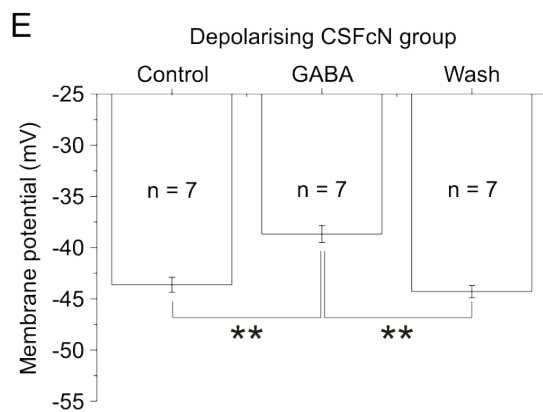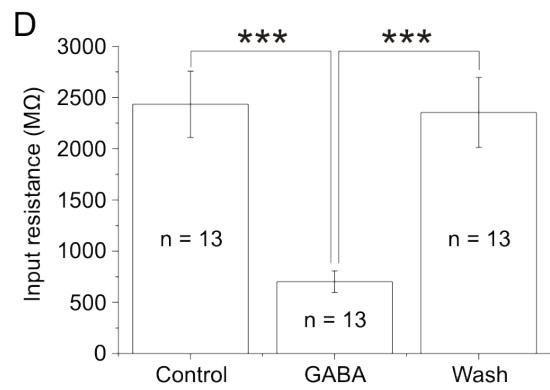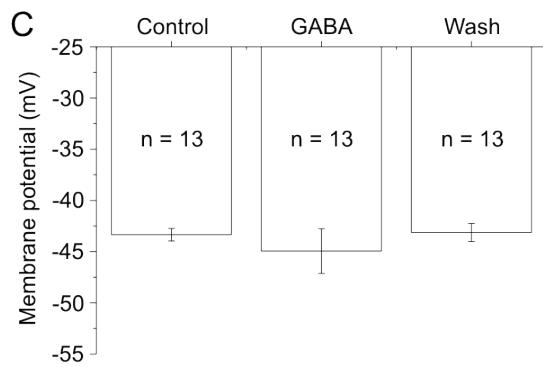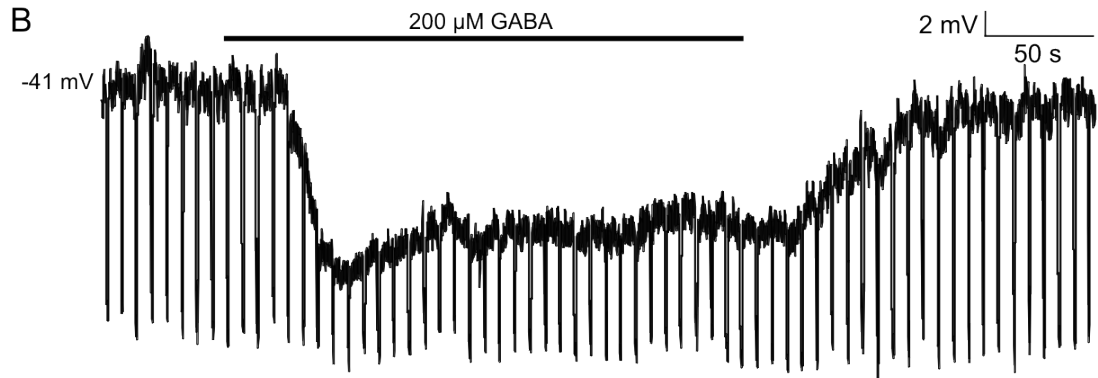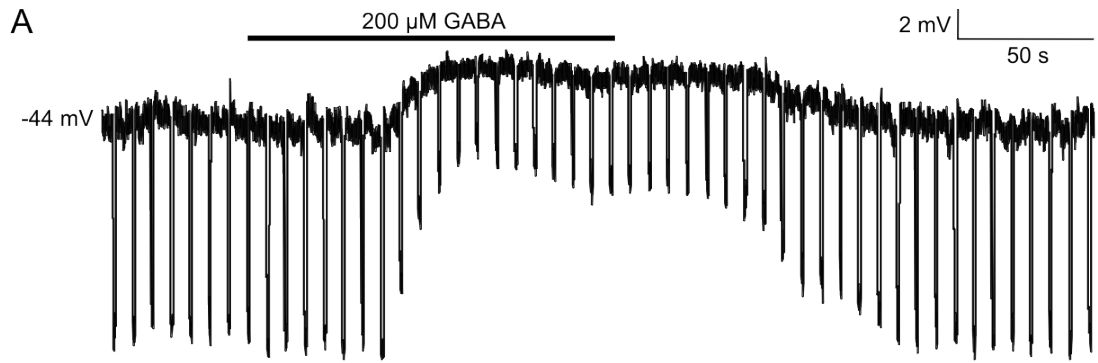
2.01; n = 6) and following (-41.76 ± 1.67; n = 6; F (2, 10) = 11.081, P = 0.003; Figure 3.5F) the bath application of GABA. With post-hoc tests confirming that the membrane potential during the GABA application was significantly more negative than the membrane potential before GABA was applied (P = 0.046). A Friedman test determined that the input resistance before (2741.89 ± 366.41 MΩ; n =6), during (744.58 ± 122.55 MΩ; n = 6) and following (2638.28 ± 421.87 MΩ; n = 6) the application of GABA was also significantly different in the hyperpolarising CSFcN group (X^2 (2) = 9, P = 0.011; data not shown). The change in input resistance on application of GABA was not significantly different between the depolarising (1506.90 ± 376.77 MΩ; n = 7) and hyperpolarising (1997.31 ± 378.63 MΩ; n = 6) CSFcN groups (t (11) = -0.913, P = 0.381; data not shown). This indicates that the difference in the change in membrane potential between the two groups is not a result of differences in input resistance. To ensure that the difference was not due to a difference in the set membrane potentials of the two groups, they were compared. There was no significant difference between the set membrane potential of the depolarising CSFcN group and that of the hyperpolarising CSFcN group (t (11) = -0.491, P = 0.633; Figure 3.5E, F), indicating that this had no influence over the response to GABA. There did not appear to be any association between the CSFcN subtype and whether the CSFcN depolarised or hyperpolarised to GABA. For example, 57 % of depolarising CSFcNs were subtype 2 CSFcCs compared to 67 % of hyperpolarising CSFcNs and 43 % of depolarising CSFcNs were subtype 3 CSFcCs compared to 33 % of hyperpolarising CSFcNs.

GABA was also bath applied to CSFcNs in mouse spinal cord slices to give an indication of whether the ability of CSFcNs to respond to GABA is conserved in more than one mammalian species. The changes in membrane potential of CSFcNs in mice were also varied, with 2 CSFcNs depolarising and 2 CSFcNs hyperpolarising in response to GABA bath application. The mean input resistance of these CSFcNs was significantly different before (1391.92 ± 285.74 MΩ; n = 4), during (400.83 ± 156.92 MΩ; n = 4) and following (1388.42 ± 335.96 MΩ; n = 4; F (2, 6) = 21.723, P = 0.002; data not shown) the bath application of GABA.

To better understand the response of CSFcNs to GABA, the focal pressure application of GABA (500 µM) at different membrane potentials was investigated. At more hyperpolarised membrane potentials (-60 and -80 mV), the pressure application of GABA could elicit a spike followed by a slower, more sustained depolarisation (Figure 3.6A). When the membrane potential of the CSFcNs was

adjusted by changing the amount of current applied to CSFcNs, the reversal from a hyperpolarising response to a depolarising response to GABA occurred between -30 mV to -40 mV (n = 3; Figure 3.6).

To verify the previous report that the GABA response is mediated by $GABA_A$ receptors (Marichal et al., 2009), GABA was bath applied in the presence of the $GABA_A$ antagonists, bicuculline or gabazine. Both depolarising (n = 2) and hyperpolarising (n = 2) GABA responses could be antagonised by bicuculline (10-50 µM; n = 3; Figure 3.7A) or gabazine (50 µM; n = 1; Figure 3.7B). Bicuculline could also antagonise the GABAergic response in CSFcNs recorded from mouse spinal cord slices (n = 2). Neither bicuculline nor gabazine appeared to have an effect on the membrane potential, input resistance or spontaneous activity of CSFcNs when applied alone. Although, bicuculline (50 µM) and gabazine (50 µM) could fully antagonise the GABAergic response, the effect of the $GABA_B$ receptor agonist, baclofen was still investigated to eliminate any possibility that $GABA_B$ receptors contribute to the GABAergic response. CSFcNs did not respond to baclofen (10 µM) in rats (n = 2) or mice (n = 4; Figure 3.7C). There was no significant difference in the input resistance of CSFcNs in mice under control conditions (1709.58 ± 387.14 MΩ; n = 4), during the bath application of baclofen (1728.17 ± 372.16 MΩ; n = 4) and following the bath application of baclofen (1807.33 ± 419.45 MΩ; n = 4; F (2, 6) = 1.561, P = 0.285). Neither was there a significant difference in the membrane potential of CSFcNs in mice under control conditions (-45.53 ± 1.54 mV; n = 4), during the bath application of baclofen (-45.49 ± 1.68 mV; n = 4) and following the bath application of baclofen (-45.28 ± 1.92 mV; n = 4; X^2 (2) = 0.500, P = 0.779).
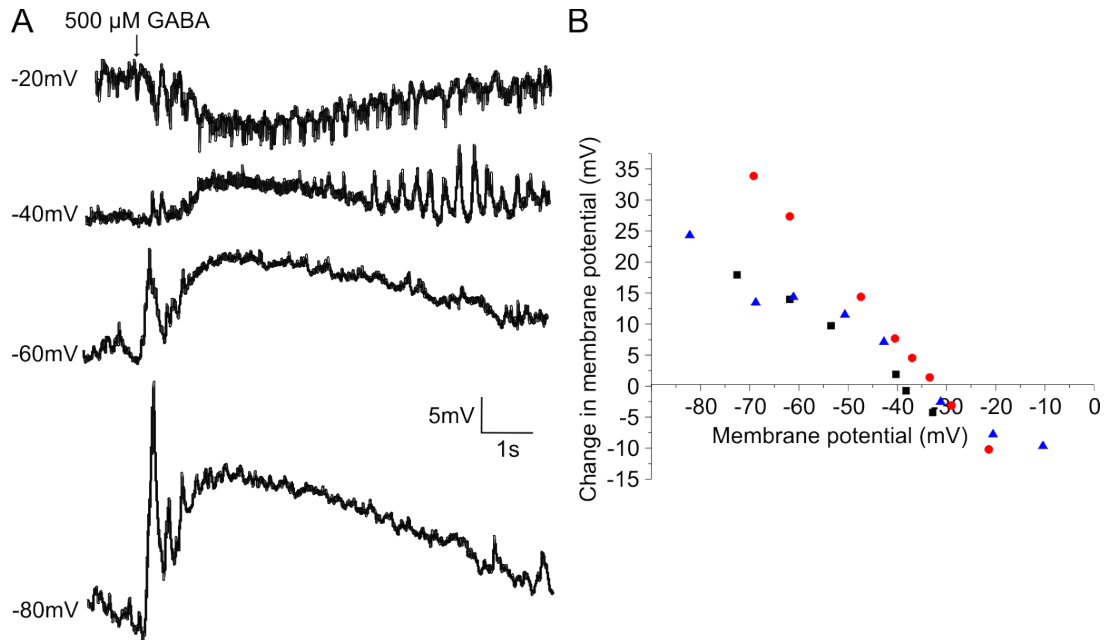
Figure 3.6: Focal pressure application of GABA indicates the reversal potential of GABA in CSFcNs.

A) Whole cell patch clamp traces in current clamp of a CSFcN responding to the focal pressure application of GABA (500 µM) at increasingly negative membrane potentials that were set by adjusting the current injected. B) The change in membrane potential of three CSFcNs (▲ ■ ●) in response to the focal pressure application of GABA at different membrane potentials.

Figure 3.7: GABA responses in CSFcNs are mediated by GABA$_A$ receptors.

A) Whole cell patch clamp traces in current clamp of the same CSFcN during the application of GABA (200 µM) alone (A) and during the application of GABA in the presence of bicuculline (50 µM; Ai). The downward voltage deflections are in response to the regular injection of -5 pA current pulses. B) Whole cell patch clamp traces in current clamp of the same CSFcN during the application of GABA (200 µM) alone (B) and during the application of GABA in the presence of gabazine (50 µM; Bi). The downward voltage deflections are in response to the regular injection of -10 pA current pulses. C) Whole cell patch clamp traces in current clamp of a CSFcN from a mouse spinal cord slice during the bath application of baclofen (10 µM). The downward voltage deflections are in response to the regular injection of -5 pA current pulses.

A

200 μM GABA

5 mV
20 s

-60 mV

Ai

50 μM bicuculline

200 μM GABA

5 mV
20 s

-60 mV

B

200 μM GABA

5 mV
50 s

-40 mV

Bi

50 μM gabazine

200 μM GABA

5 mV
50 s

-42 mV

C

10 μM baclofen

5 mV
20 s

-45 mV
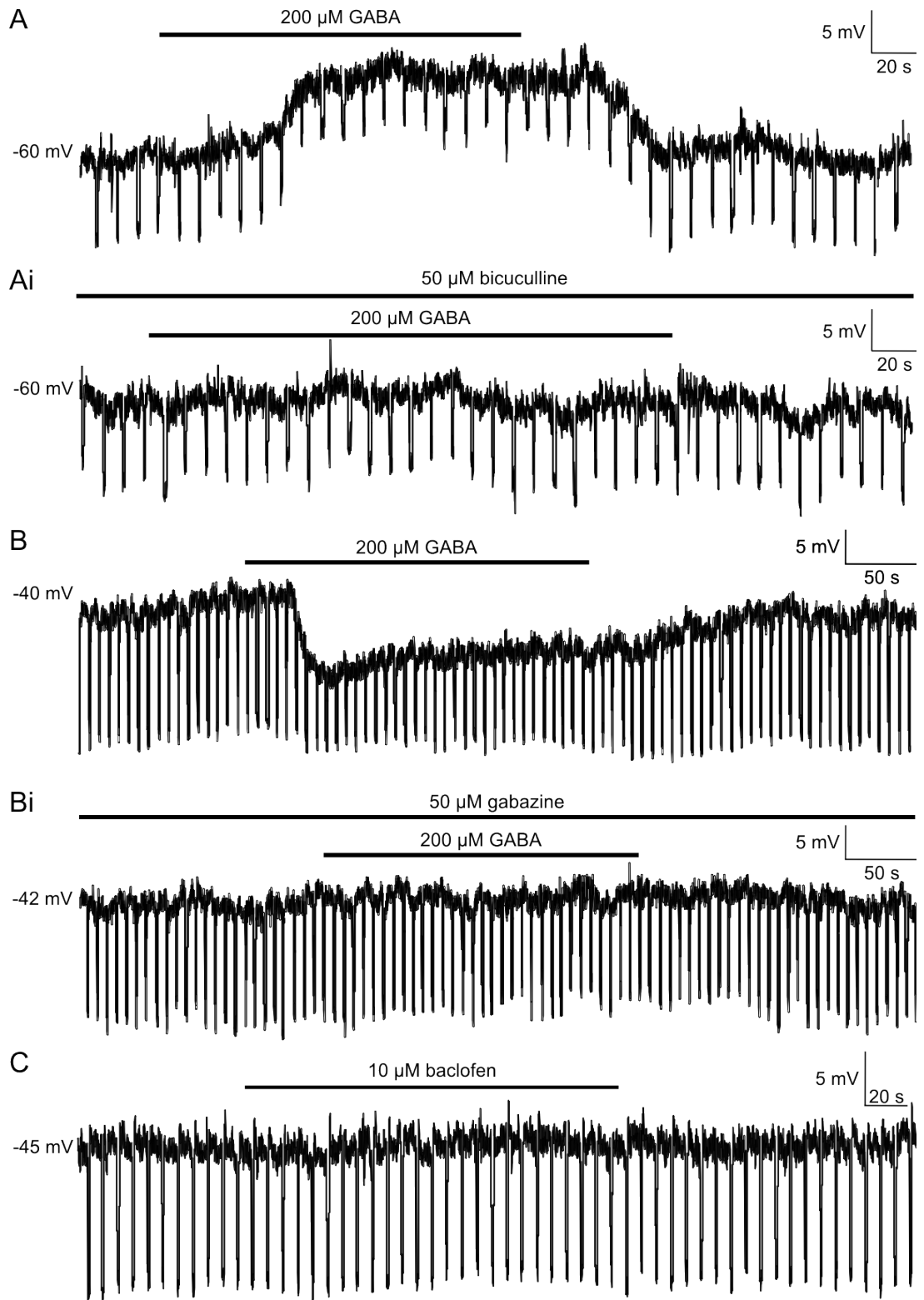
3.2.4 5HT-immunoreactive terminals are found in close apposition to CSFcNs, however, there is no immediate electrophysiological response to 5HT

As CSFcNs have been shown to respond to GABA, their ability to respond to other neurotransmitters was investigated. In particular an interaction between CSFcNs and 5HT was examined due to previous reports of 5HT-containing terminals in the area surrounding the CC (Takeoka et al., 2009). Immunohistochemistry using a specific anti-5HT antibody confirmed the presence of numerous 5HT-immunoreactive terminals in the area surrounding the CC (Figure 3.8A). When spinal cord sections were dual labelled with the anti-5HT antibody and the anti-PKD2L1 antibody, which selectively labels CSFcNs, 5HT-immunoreactive terminals were observed in close apposition to CSFcNs (Figure 3.8B, C; work completed by J.Burgess). The amount of CSFcNs with close appositions from 5HT-immunoreactive terminals was not quantified but it was clear that not every CSFcN received a close apposition. To investigate whether CSFcNs could respond to 5HT, it was bath applied to spinal cord slices. There was no electrophysiological response that could be observed to the bath application of 5HT (10 µM) in rat CSFcNs (Figure 3.8D). Specifically, there was no significant difference between the membrane potential before the 5HT application (-48.86 ± 3.32 mV; n = 8), during the 5HT application (-48.29 ± 3.24 mV; n = 8) and following the 5HT application (-48.83 ± 3.28 mV; n = 8; F (2, 14) = 3.542, P = 0.057; Figure 3.8E). Neither was there a significant difference between the input resistance before the 5HT application (2340.73 ± 417.18 MΩ; n = 9), during the 5HT application (2405.36 ± 454.06 MΩ; n = 9) and following the 5HT application (2403.47 ± 440.02 MΩ; n = 9; X^2 (2) = 2.457 P = 0.293; Figure 3.8F).

Due to the lack of discernable effect of 5HT (10 µM) on CSFcNs in the rat spinal cord, the effect of 5HT was investigated in the mouse spinal cord. Again, however, there were no electrophysiological responses to the bath application of 5HT (10 µM) in mice CSFcNs (n = 4: data not shown). There was no significant difference between the membrane potential before the 5HT application (-46.47 ± 1.68 mV; n = 4), during the 5HT application (-45.55 ± 1.46 mV; n = 4) and following the 5HT application (-46.35 ± 1.38 mV; n = 4; F (2, 6) = 4.680, P = 0.06). Neither was there a significant difference between the input resistance before the 5HT application (1991.83 ± 235.76 MΩ; n = 4), during the 5HT application (2110.00 ± 353.49 MΩ; n = 4) and following the 5HT application (2055.50 ± 255.17 MΩ; n = 4; F (2, 6) = 0.573, P = 0.592).

In contrast, there was a significant difference in the membrane potential of nearby interneurones within the rat spinal cord before (-57.42 ± 0.48 mV; n = 3), during (-53.34 ± 1.5 mV; n = 3) and after (-57.06 ± 0.82 mV; n = 3; F (2, 4) = 7.932, P = 0.041) the bath application of 5HT (10 µM; Figure 3.8G). The depolarisation of interneurones to 5HT was accompanied by an increase in firing (Figure 3.8G). In two separate interneurones, the pressure application of 5HT (10 mM) resulted in either a depolarisation (n = 1; Figure 3.8Gi) or a hyperpolarisation (n = 1; Figure 3.8Gii).

As 5HT receptors are G-protein coupled receptors, with the exception of $5HT_3$, it was possible that a response to 5HT was being missed in CSFcNs because some of the molecules necessary to mediate the response were being washed out by the intracellular solution from the patch pipette. The perforated patch technique was therefore employed, using amphotericin B in the intracellular solution. Although responses to GABA were sometimes observed, responses to 5HT (10 µM; n = 3) were unconvincing and as a result the use of this technique was discontinued.

Figure 3.8: Immunohistochemistry and electrophysiology of 5HT in relation to CSFcNs.

A-C) Immunohistochemistry for 5HT (A) and PKD2L1 (B), with close appositions between 5HT-immunoreactive terminals and PKD2L1-immunoreactive CSFcNs revealed in the merged image (C). Ai-Ci) Insets highlight an example close apposition. D) A whole cell patch clamp trace in current clamp from a CSFcC during the bath application of 5HT (10 µM). Downward voltage deflections are in response to the regular injection of -5 pA current pulses. Grouped data (mean ± S.E) of membrane potential (E) and input resistance (F) for CSFcNs in rats under control conditions compared to the bath application of 5HT (10 µM) and following the wash of 5HT. G) Whole cell patch clamp traces in current clamp from an interneurone during the bath application of 5HT (10 µM) and from two different interneurones during the focal pressure application of 5HT (10 mM; Gi, Gii). Downward voltage deflections in Gii are in response to the regular injection of -5 pA current pulses. Immunohistochemistry in this figure was completed by J.Burgess.

A 5HT
Ai

B PKD2L1
Bi

C
Ci
10 µm
5 µm

D CSFcN

10 µM 5HT

5 mV

100s

-55 mV

E

Control   5HT   Wash

n = 8   n = 8   n = 8

Membrane potential (mV)

F

Input resistance (MΩ)

n = 9   n = 9   n = 9

Control   5HT   Wash

G Interneurone

10 µM 5HT

10 mV
200 s

-60 mV

Gi 10 mM 5HT

5 mV
50 s

-60 mV

Gii 10 mM 5HT

-60 mV

5 mV
5 s
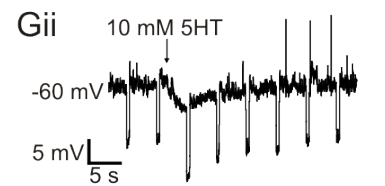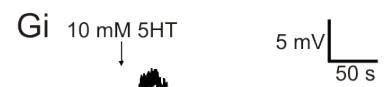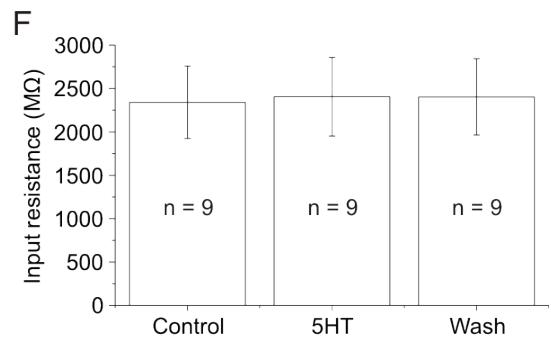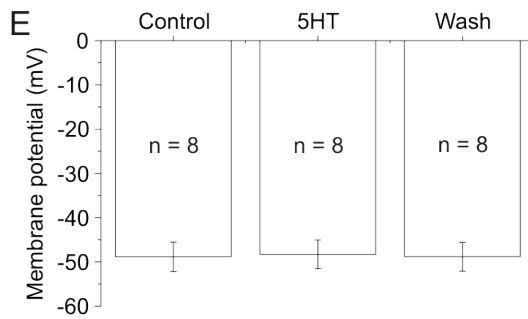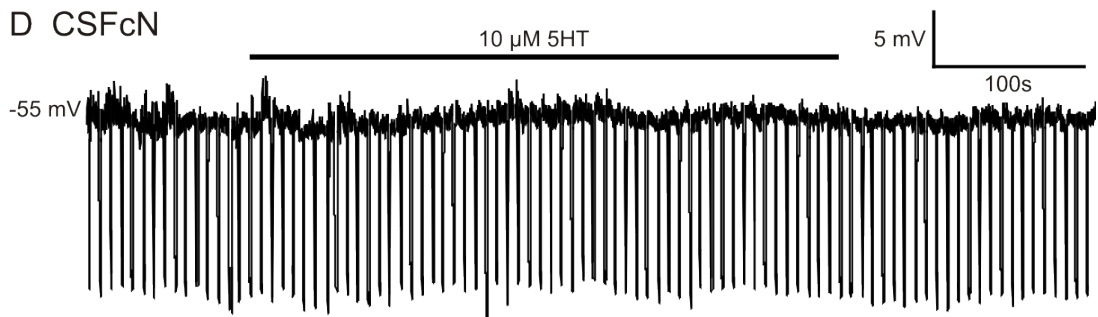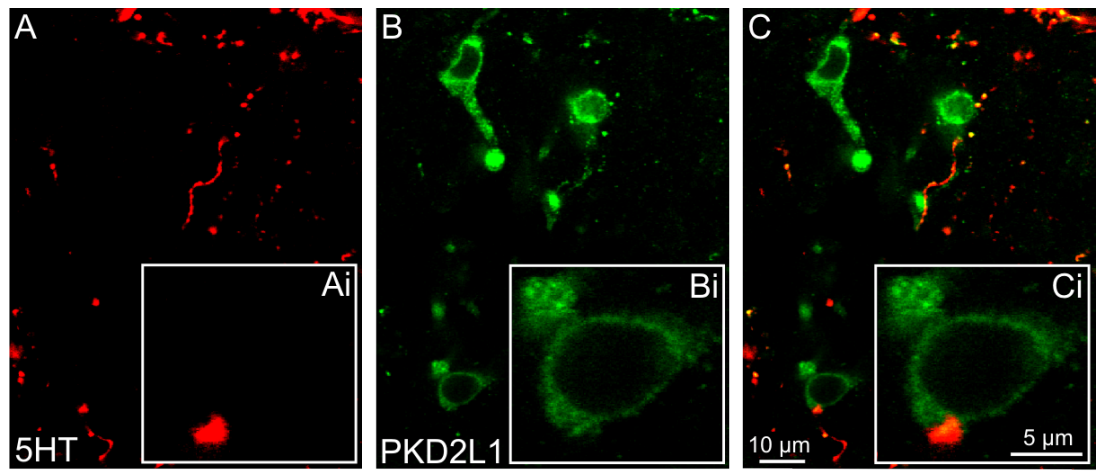
3.2.5 Substance P-immunoreactive terminals are found in close apposition to CSFcNs, however, there is no immediate electrophysiological response to substance P

As with 5HT, substance P-immunoreactive terminals have been observed in the area surrounding the CC (Barber et al., 1979). Substance P-immunoreactive terminals have been observed in close apposition to some PKD2L1-immunoreactive CSFcNs in rats (Unpublished observation Deuchars's lab) and to some GFP-expressing CSFcNs in GAD67-GFP mice (Figure 3.9A-C; work completed by I.Edwards). The possible interaction between substance P and CSFcNs was therefore investigated using electrophysiology, with a view to understanding the function of CSFcNs. In response to the bath application of substance P (1 μM), however, there was no electrophysiological response in CSFcNs of the rat spinal cord (n = 29; Figure 3.9D). The membrane potential of CSFcNs was not significantly different before (-55.12 ± 1.71 mV; n = 29), during (-54.19 ± 1.66 mV; n = 29) and following the application of substance P (-54.69 ± 1.62 mV; n = 29; F (2, 56) = 2.927, P = 0.076; Figure 3.9E). Grouped data for the input resistance of CSFcNs before, during and following the application of substance P was not normally distributed. The Friedman test determined that there was no significant difference between the input resistance of CSFcNs before (2397.49 ± 209.80 MΩ; n = 29), during (2255.88 ± 180.08 MΩ; n = 29) and following the application of substance P (2262.43 ± 202.19 MΩ; n = 29; X^2 (2) = 1.310, P = 0.519; Figure 3.9F). In addition, there appeared to be no difference in the spontaneous activity that was recorded from CSFcNs under control conditions and in the presence of substance P (data not quantified; Figure 3.9Di, Dii). In CSFcNs that were spontaneously firing spikes or action potentials, there was no observable change in the shape of the spikes or action potentials. Due to the uncertain nature of the success of perforated patch clamp recordings of CSFcNs in response to 5HT, perforated patch clamp recordings were not used to investigate the effect of substance P on CSFcNs.

In contrast, there was a significant difference between the membrane potential of nearby interneurones before (-59.50 ± 0.39 mV; n = 4), during (-52.37 ± 1.88; n = 4) and after (-59.86 ± 0.62 mV; n = 3) the bath application of substance P (1 μM; F (2, 4) = 14.723, P = 0.014). The depolarisation of interneurones observed in substance P was accompanied by an increase in action potential firing (Figure 3.9G).

Figure 3.9: Substance P has no effect on the electrophysiology of CSFcNs.

A-C) Immunohistochemistry for substance P (A) and GFP to highlight GAD67-GFP expressing CSFcNs (B). Close appositions between substance P-immunoreactive terminals and GAD67-GFP-expressing CSFcNs are revealed in the merged image (C). Insets highlight a CSFcN with a number of substance P-immunoreactive close appositions. D) Whole cell patch clamp traces in current clamp from a CSFcN during the bath application of substance P (1 µM). Downward voltage deflections are in response to the regular injection of -10 pA. Expanded traces before (Di) and during (Dii) substance P application allow any changes in spontaneous activity to be observed. E-F) Grouped data (mean ± S.E) of membrane potential (E) and input resistance (F) of CSFcNs under control conditions compared to the bath application of substance P (1 µM) and following the wash of substance P. G) Whole cell patch clamp traces in current clamp from an interneurone during the bath application of substance P (1 µM). Downward voltage deflections are in response to the regular injection of -5 pA. Expanded traces before (Gi) and during (Gii) substance P application allow any changes in spontaneous activity to be observed. Immunohistochemsitry in this figure was completed by I.Edwards.
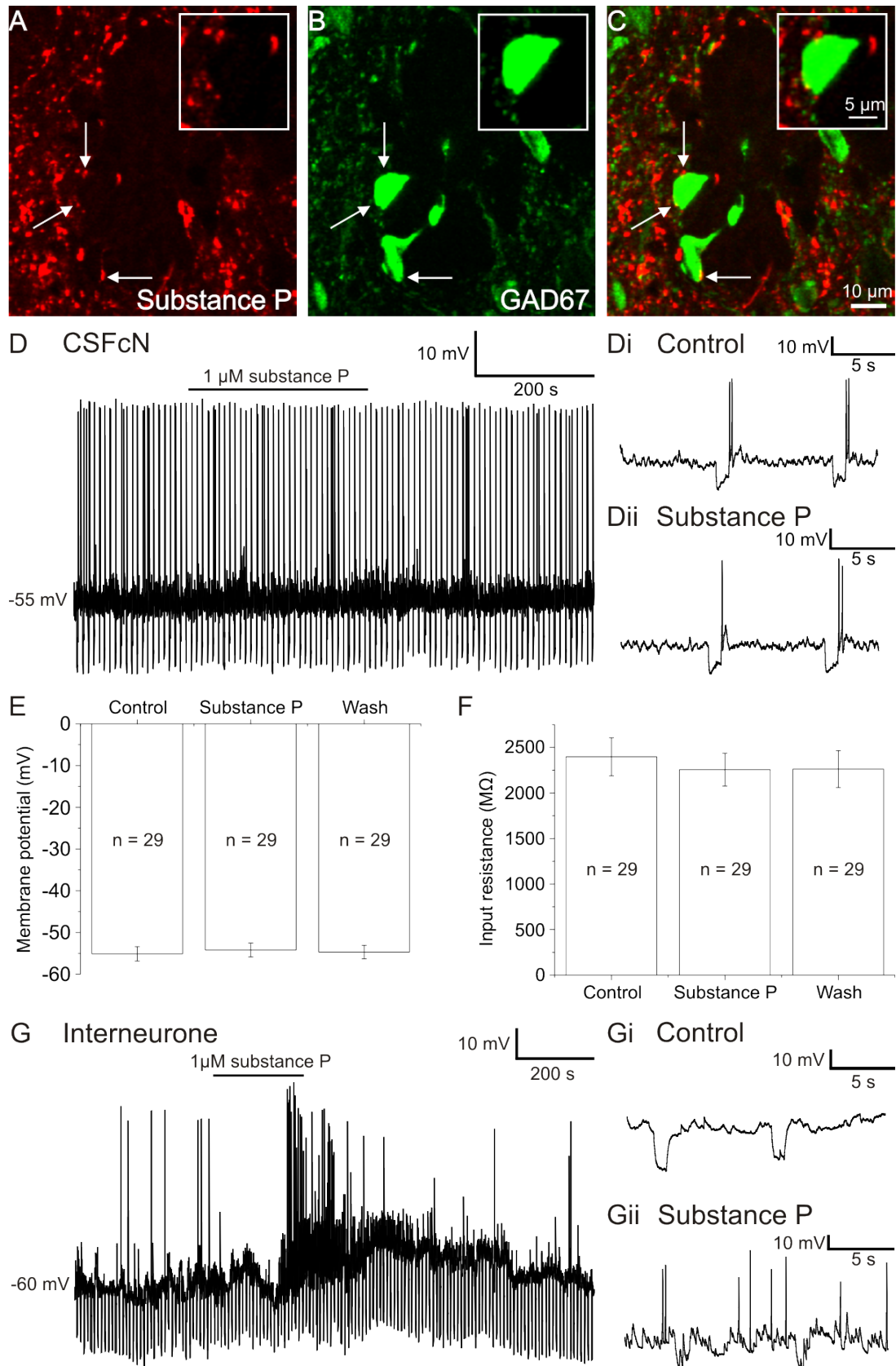
3.3 Discussion

This chapter characterises the basic electrophysiological properties of CSFcCs. It categorises CSFcCs into three subtypes based on their response to the injection of positive current pulses. The first subtype responded passively and is the first report of a glial-like CSFcC, the second subtype produced a single fast depolarisation and the third subtype produced multiple spikes. Due to the active response properties of subtype 2 and 3 they have been subsequently, collectively referred to as CSF-contacting neurones (CSFcNs). Processes from CSFcCs were observed projecting both ventrally and laterally. The study confirmed previous reports that CSFcNs could respond to GABA, with strong evidence indicating that the response was mediated by $GABA_A$ receptors and not $GABA_B$ receptors. This study observed spontaneous EPSPs in CSFcNs and provided evidence that these EPSPs were glutamatergic in nature. This study found that although 5HT-immunoreactive terminals were observed in close apposition to CSFcNs, no immediate electrophysiological response was observed when 5HT was bath applied to CSFcNs. Similarly, although substance P-immunoreactive terminals have previously been observed in close apposition to CSFcNs, there was no electrophysiological response of CSFcNs to substance P.

3.3.1 There appear to be CSFcCs with different phenotypes

Both the electrophysiological data and the post-recording histology demonstrate that there are CSFcCs with different phenotypes. The electrophysiology provides evidence that they have varied responses to current pulses, however, whether they are several populations of cells with varied phenotypes or one population of cells that are at different stages of maturation is not clear. Similar phenotypes to that of the CSFcCs described in this study were observed in the study by Marichal et al., (2009). The exception to this is the subtype 1 CSFcCs; a population of CSFcCs with passive response properties has never been reported before. This subtype of CSFcCs resembled glial cells due to their more negative resting membrane potential, low input resistance and passive responses. These subtype 1 CSFcCs could be very immature CSFcCs that have not yet matured into subtype 2 and 3 CSFcCs. This is quite unlikely, however, as there is such a large disparity between the electrophysiological properties of subtype 1 and subtype 2 CSFcCs; if one was to become the other, more intermediate phenotypes would be observed, as between subtype 2 and 3 CSFcCs. A recent study using electron microscopy to

study the cell types surrounding the CC, identified a population of cells called CC-contacting astrocytes (Accs), that possess CC-contacting processes but express GFAP (Alfaro-Cervello et al., 2012). Given the location, morphology and glial-like electrophysiological properties of subtype 1 CSFcCs, it appears likely that they are in fact these Accs. To confirm this, immunohistochemistry for GFAP could be performed on slices from which subtype 1 CSFcCs have been recorded and filled with rhodamine. As this study found that there were two populations of subtype 1 CSFcCs, one where cells had lower input resistances and were dye coupled and one with cells with higher input resistances that were not dye coupled, it suggests that some Accs could be gap junction coupled. The phenotype of the cells with which these subtype 1A CSFcCs are coupled is unknown but from the large number of dye filled cells in the ependymal layer it is highly probable that subtype 1A CSFcCs are coupled to ependymal cells. Whether subtype 1A CSFcCs are gap junction coupled to ependymal cells because they are at an earlier stage of differentiation than subtype 1B CSFcCs or whether they are simply performing a different function is unclear. The number of subtype 1 CSFcCs recorded in this study could have been underestimated as a percentage of the entire CSFcC population. This is due to an improvement in technology part way through the study which enabled the subtype 1A CSFcCs to be more easily distinguished from ependymal cells.

The cells defined in this study as subtype 2 and 3 CSFcCs had active response properties and appear to correspond to the three subtypes of CSFcNs described by Marichal et al., (2009); therefore it has been proposed that subtype 2 and 3 CSFcCs from this study can be collectively referred to as CSFcNs. The three subtypes of CSFcNs that Marichal et al., (2009) described were depolarising CSFcNs whose responses were predominantly mediated by Ca^{2+} channels rather than voltage-gated Na^+ channels, single spiking CSFcNs and multiple spiking CSFcNs. These same subtypes were observed in this study, however, there appeared to be too few of the depolarising cells present to form their own subtype; therefore for this study those cells were combined with the single spiking cells to form one category, the subtype 2 CSFcCs. Interestingly, if the population of only CSFcNs (subtype 2 and 3 CSFcCs) within this study are considered using the same defining criteria as Marichal et al., (2009), for example, splitting subtype 2 CSFcCs into depolarising and single spiking cells, a very similar proportion of cell types are observed. 11 % of depolarising/non-spiking cells in this study compared to 11.5 % in Marichal et al., (2009), 59 % of single spiking cells in this study compared to 57

% in Marichal et al., (2009) and 30 % of multiple spiking cells compared to 31.5 % in Marichal et al., (2009). This remarkable similarity suggests that there was no bias in either study as to which cells were targeted. As the study by Marichal et al., (2009) was completed in rats P0-P5, the fact that the same proportion of subtypes was observed in the present study which was completed predominantly in P11 rats suggests that the cells are already in their final phenotype by P0. In addition, the fact that there was not a greater proportion of multiple spiking cells in P21 rats in this study indicates that CSFcNs are not undergoing the process of maturation from one subtype to another over this time period. All of this data supports the evidence that CSFcNs are not born in the postnatal spinal cord (Marichal et al., 2009) and supports the hypothesis that there is no difference between the properties of CSFcNs in rats aged P0-P5 and rats aged P9-P21.

The histology performed post-recording also revealed differences within the CSFcC population regarding where the non CSF-contacting process projected. Although it was not confirmed in this study, it is highly likely that these processes are axons rather than dendrites, as a previous study identified similar long basal processes expressing synaptotagmin and GAP 43, a protein expressed highly during axogenesis (Stoeckel et al., 2003). The indirect nature of projections and the fact that the final destination of some projections may not be in the slice from which the cell was recorded makes it difficult to determine where every projection terminates. It is clear, however, that the CSFcCs do not all project to the same spinal cord area or group of cells. Some of the CSFcCs projected ventrally, whereas others projected laterally towards the IML. It has been proposed that CSFcCs communicate information from the internal CSF to the external CSF (Vigh et al., 2004) and some CSFcC projections were observed close to the ventral median fissure, supporting this theory. Some projections, however, seem to terminate within the grey matter, ending in quite large terminals. These terminals could be growth cones, although no lamellipodia and filopodia which are indicative of growth cones could be visualised (see review Landis (1983)), however, this could be due to a lack of sensitivity of the DAB. Alternatively, large endings at the end of processes can indicate that an axon has been damaged in the cutting procedure. These projections could be bound for the external CSF but are in the process of growing. Alternatively there could be a subset of CSFcCs that have a different function and project to cells within the grey matter of the spinal cord. The ventrally projecting CSFcCs could be heading towards motor neurones or neurones involved within the

locomotor circuitry, where as the laterally projecting CSFcCs could be coursing towards the SPNs in the IML.

3.3.2 Understanding the varied GABA responses within the CSFcN population

The ability of CSFcNs to respond to GABA is consistent with the only other functional study of mammalian CSFcNs (Marichal et al., 2009) and supports the hypothesis that CSFcNs from rats aged P9-P21 can respond to GABA as well as those from rats aged P0-P5. The large decrease in input resistance on bath application of GABA is consistent with an opening of channels within the cell membrane. Both depolarising and hyperpolarising responses were observed in response to the bath application of GABA. This is unexpected as even if there are differences in the physiological concentrations of intracellular Cl^-, this should not matter as the Cl^- concentration of all cells should be set by the intracellular pipette solution. The reversal potential of GABA (E_{GABA}) is based predominantly on the Cl^- reversal potential (E_{Cl}), which was -103 mV in this study. It is also affected by the HCO_3^- reversal potential (E_{HCO3}; Bormann et al., (1987)), which was -12 mV in this study; this makes E_{GABA} slightly less negative than -103 mV, however, not enough to explain the depolarisations observed from ~-45 mV. One possible explanation is that the bath application was not in the presence of TTX or low Ca^{2+} solutions, therefore there could be an indirect effect contributing to the depolarisation. For example, GABA could be hyperpolarising inhibitory neurones which tonically inhibit CSFcNs, thus creating a disinhibition of CSFcNs. This is unlikely, however, as bicuculline or GABA did not have any effect on the CSFcNs unless in the presence of bath applied GABA, suggesting that there is not tonic GABAergic input to CSFcNs. To fully confirm that the GABAergic effects are directly onto CSFcNs, GABA should be bath applied in the presence of blockers of synaptic transmission such as TTX or low Ca^{2+} solution.

Another possible explanation for the depolarising action of GABA has been developed and substantiated by Staley et al., (1995) in which they argue that the overstimulation of $GABA_A$ receptors can lead to a shift in E_{GABA} away from E_{Cl} towards E_{HCO3}; the theory is as follows. When $GABA_A$ receptors are initially activated there is a Cl^- influx and a HCO_3^- efflux, resulting in an accumulation of Cl^- in the intracellular solution and an accumulation of HCO_3^- in the extracellular

solution near the cell membrane. These accumulations shift the electrochemical gradients for both ions, reducing their flux. It is this point at which the HCO_3^- gradient can be more swiftly corrected than the Cl^- gradient, leading to a greater efflux of HCO_3^- compared to the influx of Cl^-, thus depolarising the cell. The HCO_3^- gradient is better maintained because the decrease in intracellular HCO_3^- drives the diffusion of membrane permeable CO_2 into the cell. Here CO_2 joins with intracellular H_2O allowing carbonic anhydrase to catalyse the regeneration of HCO_3^-, which subsequently moves out of the cell (Pasternack et al., 1993). This hypothesis is supported by data from Staley et al., (1995) showing that decreasing the regeneration of HCO_3^- (by either removing extracellular CO_2 by buffering aCSF with HEPES and 100 % O_2, inhibiting carbonic anhydrase with acetazolamide and increasing neuronal H^+ using amiloride, an inhibitor of the neuronal Na^+-H^+ exchanger) prevents depolarising responses to GABA. Indirect evidence to support this theory is that GABAergic-mediated IPSPs have been observed in neurones that depolarise in response to the bath application of GABA (Milligan et al., 2004). Unfortunately, as IPSPs have not been observed in CSFcNs this cannot be used as a method to demonstrate that the GABA-mediated depolarisation is due to an overstimulation. It is also not a fully satisfactory explanation as some of the CSFcNs can actually hyperpolarise in response to the bath application of GABA. A possible explanation of why some CSFcNs hyperpolarise and some depolarise could be due to the expression of $GABA_A$ receptors which are composed of different subunits. There are a large number of subunits and subsequent combinations of these subunits that can form $GABA_A$ receptors. Each subunit confers different properties to the $GABA_A$ receptor, resulting in $GABA_A$ receptors with varying biophysical properties, including their affinity for GABA, the efficacy of GABA, mean channel open time and rate of desensitisation (see review Farrant and Nusser (2005)). Given the unknown subunit assembly of the $GABA_A$ receptors mediating the responses in CSFcNs it is difficult to speculate whether there are $GABA_A$ receptors composed of different subunits on certain CSFcNs and exactly how the receptor compositions would affect transmission if there were different $GABA_A$ receptors. It could, however, be proposed that those CSFcNs which hyperpolarised in response to GABA expressed $GABA_A$ receptors at which GABA had a lower affinity and was not very efficacious and thus the receptors were not over stimulated and the balance of Cl^- influx to HCO_{3-} efflux was maintained throughout the GABA application. Conversely, CSFcNs which depolarised in response to GABA could express $GABA_A$ receptors at which GABA had a high affinity and was very efficacious and could induce a long mean channel open time, resulting in rapid

overstimulation by GABA and a fast imbalance between Cl^- influx to HCO_{3-} efflux. This is only speculation and further investigation into the composition of the $GABA_A$ receptors expressed is needed.

To reduce both the issues of indirect GABAergic responses and of overstimulation by the bath application of GABA, GABA was pressure ejected locally onto CSFcNs. Using this method E_{GABA} was found to be between -30 mV and -40 mV, which implies that the intracellular pipette solution is incapable of setting E_{GABA} to a more negative potential. This was not the case in the study by Marichal et al., (2009), where E_{GABA} was found to be close to the expected E_{Cl} imposed by the intracellular pipette solution. Although it is not clear, it is likely that Marichal et al, (2009) used TTX to block voltage gated Na^+ channels and TEA to block voltage gated K^+ channels during their investigation of E_{GABA}, thus preventing any secondary responses. Given the different responses to the bath application of GABA in this study, it would be an interesting future experiment to compare whether the cells that depolarised or hyperpolarised in response to the bath application of GABA had different reversal potentials when calculated from the pressure application of GABA. As the pressure application of GABA can still induce depolarisations in CSFcNs at membrane potentials at which a hyperpolarisation should occur, other possible explanations for the depolarisation other than overstimulation must be considered. One such possible explanation involves the GABA transporter, GAT1. Images from both the Allen Brain Atlas and the brain atlas of gene expression, GENSAT, suggest that CSFcNs express GAT1. The uptake of GABA from the extracellular fluid into cells via GAT1 requires the uptake of two Na^+ ions and one Cl^- ion, indicating that for every GABA molecule taken into a cell, a net positive ion is taken up (Mager et al., 1993). Therefore the application of GABA to CSFcNs would result in the uptake of GABA into CSFcNs with a net positive charge; although it is doubtful that this would be sufficient to result in a depolarisation of CSFcNs. There is another possible yet highly unlikely reason for observing depolarisations in some CSFcNs and this is that the CSFcNs were unhealthy. For example, Dzhala et al., (2012) found that there was an increase in intracellular Cl^- within neurones in the superficial layers of acute hippocampal brain slices, compared to smaller healthier looking cells deeper within the slices. The reason this explanation is unlikely is because the characterisation of CSFcNs in this study demonstrated healthy, robust cells.

Despite the uncertainty with regards to the nature of the GABAergic response, the important point is that this study confirms that CSFcNs are capable of responding to GABA. It must be noted, however, that although CSFcNs could respond to the bath or pressure application of GABA, no evidence of endogenous GABA was found. In particular, IPSPs which would indicate the presence of synaptic GABA release onto CSFcNs were not observed. Neither was there an effect on the membrane potential or input resistance of CSFcNs when bicuculline or gabazine were applied, indicating a lack of endogenous GABA. Nevertheless, given the nature of the preparation the endogenous supply of GABA may have been disrupted. The antagonism of the GABAergic response by the $GABA_A$ antagonist, gabazine, is consistent with the antagonism observed by Marichal et al.,(2009) and substantiates that the GABAergic response of CSFcNs is mediated by $GABA_A$ receptors. Furthermore, despite previous reports of $GABA_B$ receptor expression by CSFcNs (Margeta-Mitrovic et al., 1999), the lack of response to the $GABA_B$ agonist, baclofen, strongly suggests that there is no involvement from $GABA_B$ receptors. As $GABA_B$ receptors are G-protein coupled receptors, there is the possibility that wash out of molecules essential to mediate downstream effects occurred. The complete antagonism of the GABAergic response in the presence of $GABA_A$ antagonists, combined with the lack of effect of baclofen, however, suggests that $GABA_B$ receptors are simply not involved in mediating the CSFcN response to GABA. As stated earlier, the subunit compositions of the $GABA_A$ receptors are unknown. A number of $GABA_A$ receptor subunits have been observed in lamina X using immunohistochemistry, including high levels of α1, α3, β2/3, γ2 subunits and lower levels of α2 and α5 subunits (Bohlhalter et al., 1996). Only α6 and δ subunits have been confirmed as absent within lamina X using *in-situ* hybridisation (Wisden et al., 1991). Therefore, the only assumption that can currently be made as to the composition of the $GABA_A$ receptor is that it contains β2/3 and γ2 combined with one of the α subunits, α1, α2, α3 or α5.

An extremely important point to consider regarding the functional importance of CSFcNs responding to GABA is the source of the GABA. Whether the source is synaptic terminals from other neurones (Mclaughlin et al., 1975), paracrine release from nearby cells, autocrine release from CSFcNs or from the CSF has a great impact on the role of CSFcNs. This will be discussed further in the general discussion as it also applies to other chapters.

3.3.3 CSFcNs do not have any immediate changes in membrane potential or input resistance to 5HT or substance P

As 5HT- and substance P-immunoreactive terminals have been previously observed close to the CC (Hokfelt et al., 1975; Barber et al., 1979; Takeoka et al., 2009) it was hypothesised that there could be interactions between 5HT- and substance P-expressing cells and CSFcNs. Although, CSFcNs have been shown to respond to GABA, GABAergic neurones are located throughout the CNS so this does not provide much evidence as to the functional role of CSFcNs with regards to their integration into the rest of the spinal cord circuitry. As 5HT- and substance P-containing neurones have much more restricted distribution patterns and are attributed to more specific functional roles, the investigation of the interaction between these neurones and CSFcNs was deemed important to understand the functional importance of CSFcNs. Unfortunately, despite immunohistochemistry that was performed in this study or previously, suggesting that there are 5HT- and substance P-containing terminals in close apposition to some CSFcNs, there were no identified responses in the electrophysiological parameters measured to 5HT or substance P in the spinal cord slice preparation. The ability of nearby interneurones within the same spinal cord slices to respond to either 5HT or substance P demonstrates the viability of both the spinal cord slices and the compounds applied, therefore excluding either of these possibilities as reasons for the discrepancy between the immunohistochemistry and the electrophysiology. This lack of response of CSFcNs to 5HT or substance P should lead to the rejection of the hypothesis that CSFcNs can respond to 5HT and substance P, however, as some possible types of cellular effects were not measured, it still leaves this hypothesis open for acceptance or rejection. It is possible that 5HT or substance P could affect electrophysiological parameters not measured in this study; to investigate the effect of 5HT and substance P on a wider range of channels, the responses of cells to the injection of positive or negative current injections could have been investigated. Other possible reasons for the discrepancy between the immunohistochemistry and the electrophysiology include the fact that the close apposition does not actually confirm the presence of direct synaptic contacts on to CSFcNs; this would need to be confirmed by electron microscopy. Another explanation could be that the intracellular contents are being diluted and washed out by the intracellular solution from the patch pipette, removing some of the molecules needed to enable G-protein coupled responses. Although this is obviously not the case for the interneurones, CSFcNs are smaller cells which could make them more susceptible to wash out. Steps were made to reduce the likelihood of this occurrence, for example ATP and

GTP were added to the intracellular solution. To completely rule out this possibility perforated patch clamp recordings were attempted using amphotericin B in the intracellular patch pipette solution. Possible depolarisations were observed in response to the application of 5HT; however, there were a number of discrepancies that questioned the validity of the perforated patch clamp recordings. The final possibility to explain the discrepancy between the immunohistochemistry and the electrophysiology is that 5HT and substance P are activating receptors on the CSFcNs and downstream effects are being initiated but these effects do not result in the opening of any ion channels so there is no immediately detectable electrophysiological response. The downstream effects could be initiating intracellular cascades that are capable of influencing gene expression and cellular processes like growth or migration (see general introduction sections 1.8 and 1.9). This likelihood is supported for 5HT by the possible expression of $5HT_{5B}$ and $5HT_6$ receptors by CSFcNs (GENSAT); if 5HT receptors are expressed by CSFcNs then they must be mediating some response to 5HT. Effects like growth or migration which occurs over a longer time period would be better monitored using techniques like organotypic slice cultures and time lapse imaging, as will be discussed further in the general discussion.

3.3.4 Conclusions

There appear to be numerous subtypes of CSFcCs including a glial CSFcC, subtype 1 and a neuronal CSFcC, subtype 2 and 3. There also appears to be subtypes defined by different criteria, such as whether they are gap junction coupled or not, where the destination of the non CSF-contacting process is and how the cells respond to GABA. These differences highlight the varied nature of the CSFcC population and suggest that there are CSFcCs with specific roles performing different functions within the spinal cord. The lack of responses to both 5HT and substance P is intriguing and highlights the importance of investigating these cells by a wider range of electrophysiological challenges and by means other than electrophysiology. Finally, the presence of EPSPs and the confirmation that CSFcNs respond to GABA through $GABA_A$ receptors suggests that they could be either integrated into the wider spinal cord circuitry or GABA could be used as a method of communication between the different cells of the neurogenic niche surrounding the CC.

Chapter 4 - Basic characteristics of ependymal cells and their response to GABA

4.1 Introduction

Ependymal cells surrounding the CC of the mammalian spinal cord have received very little attention and their functional characteristics are poorly understood. Most of the work on ependymal cells within the spinal cord to date has been concerned with their ultrastructure. This has led to the discovery that there are subtypes of ependymal cells, including the classical cuboidal to columnar shaped cells (Bruni and Reddy, 1987) and the more recently defined radial ependymal cells (see chapter 1.3.4; Meletis et al., (2008)). More recent work has focussed on the role of ependymal cells as neural stem/progenitor cells and their importance in neurogenesis following spinal cord injury or the onset of other pathological conditions, as discussed in the general introduction (Danilov et al., 2006; Barnabe-Heider et al., 2010).

A recent study has provided the first characterisation of the basic electrophysiological properties of ependymal cells surrounding the CC of the mammalian CC (Marichal et al., 2012). This study defined the cells as having a low input resistance (124 ± 24 MΩ), a resting membrane potential of -84 ± 2 mV and passive response properties to current pulses (Marichal et al., 2012). Gap junction proteins connexin 43 and connexin 45 are present on ependymal cells surrounding the CC (Ochalski et al., 1997; Chapman et al., 2012; Marichal et al., 2012) and dye-coupling has been observed (Marichal et al., 2012), however the significance of gap junction coupling between ependymal cells has yet to be considered. This could be of importance as gap junction coupling is known to influence proliferation in the developing CNS and is also observed between neural progenitor cells in the postnatal SVZ (Bittman et al., 1997; Lacar et al., 2011).

There are currently no studies that have investigated the effect of neurotransmitters on ependymal cells surrounding the CC of the mammalian spinal cord. A recent study by Reali et al., (2011) explored the effects of GABA on BLBP immunoreactive progenitor cells that are found surrounding the CC of turtle spinal cord; these cells appear to be similar to the radial ependymal cells or potential radial glia observed surrounding the mammalian CC (Meletis et al., 2008; Marichal et al., 2012). GABA was capable of depolarising these progenitor cells and inducing increases in intracellular Ca^{2+}, suggesting that GABA is capable of stimulating long lasting intracellular effects within these cells (Reali et al., 2011). The response to GABA could be antagonised by either the GABA transporter-3 (GAT3) blocker, SNAP

5114, the GABA$_A$ receptor antagonist, gabazine or both SNAP 5114 and gabazine combined (Reali et al., 2011), highlighting variation within the population of progenitor cells. This variation was even more apparent when GABA was applied in the presence of the gap junction blocker, carbenoxelone, which completely abolished GABA induced depolarisations in some cells, indicating that the initial response originated from a neighbouring, coupled cell. Mammalian ependymal cells could be capable of responding to GABA in a similar manner, especially as there are two potential sources of GABA around the mammalian CC; GABAergic CSFcCs which express VGAT (Conte, 2009) and GABAergic terminals (Mclaughlin et al., 1975).

Given the importance of ependymal cells as a neural stem/progenitor population and our current poor understanding of the electrophysiological properties of ependymal cells, it is pertinent to increase our knowledge about how mammalian ependymal cells communicate between themselves and whether they can respond to external stimuli, such as GABA.

4.1 Hypothesis and aims

This chapter aims to ascertain whether ependymal cells in spinal cords from rats and mice aged P9-P21 have similar properties to those from rats aged P0-P5 and thus determine whether there are any changes in their properties during postnatal development. As such it is hypothesised that ependymal cells from the spinal cords of rats and mice aged P9-P21 have passive electrophysiological properties as observed for ependymal cells from rats aged P0-P5. It is also hypothesised that a high degree of gap junction coupling occurs between ependymal cells as observed in younger animals. This second hypothesis also relates to the second aim of this chapter, which is to determine whether ependymal cells share common properties with neural stem and/or progenitor cells from other postnatal neurogenic niches. To further meet the second aim, it is hypothesised that ependymal cells are capable of responding to GABA, given the many sources of GABA near ependymal cells and the effects of GABA on other neural stem/progenitor cells. This third hypothesis also relates to the final aim of this chapter which is to investigate whether ependymal cells are integrated into the spinal cord circuitry. These hypotheses will

be tested using whole cell patch clamp electrophysiology and intracellular dye loading.

4.2 Results

The majority of data in this chapter is from spinal cord slices prepared from Wistar rats, however, there are some data collected in spinal cord slices prepared from GAD67-GFP mice. Unless otherwise stated, data is from Wistar rats and all figures are produced from data collected in Wistar rats.

4.2.1 Basic electrophysiological characteristics of ependymal cells

Post-recording visualisation of cells using rhodamine allowed confirmation of the cell type; cells were considered ependymal if they were within the ependymal layer and no CC-contacting process could be observed (Figure 4.1C). The ependymal cells recorded in this study had negative resting membrane potentials, small input resistances and displayed no spontaneous or evoked activity (Figure 4.1A-C). There is a linear relationship between the change in voltage in response to a current pulse and the size of the current pulse (Figure 4.1B); this demonstrates that ependymal cells have passive responses indicative of a lack of voltage-gated ion channels. In Wistar rats, a resting membrane potential of -75.67 ± 0.52 mV (n = 79) was observed compared to a resting membrane potential of -73.14 ± 0.88 mV (n = 6) in GAD67 mice; the two resting membrane potentials from different species were not significantly different (t (84) = -1.440, P = 0.154; Figure 4.1D). In rats, the input resistance was calculated as 96.35 ± 12.65 MΩ (n = 79) compared to 80.29 ± 12.83 MΩ (n = 7) in GAD67 mice; again the input resistances from different species were not significantly different (t (84) = 0.375, P = 0.709; Figure 4.1E). A Spearman's rank order correlation test found a significant but weak positive correlation between the resting membrane potential and the input resistance of ependymal cells in rats (r_s (79) = 0.337, P = 0.002; Figure 4.1F), demonstrating that ependymal cells with more negative resting membranes potentials generally have smaller input resistances.

Figure 4.1: Basic electrophysiological characteristics of ependymal cells.

A) Example whole cell patch clamp trace recorded in current clamp of an ependymal cell responding to the injection of positive and negative current pulses. B) The change in voltage (ΔV) with respect to the current injected for the same ependymal cell. C) The recorded cell was confirmed as an ependymal cell post-recording by visualisation of rhodamine, indicated by the arrowhead, the arrow indicates the rhodamine-filled patch electrode. D) Mean resting membrane potential ± S.E in rats and GAD67 mice. E) Mean input resistance ± S.E in rats and GAD67 mice. F) Relationship between resting membrane potential and input resistance of ependymal cells in rats.
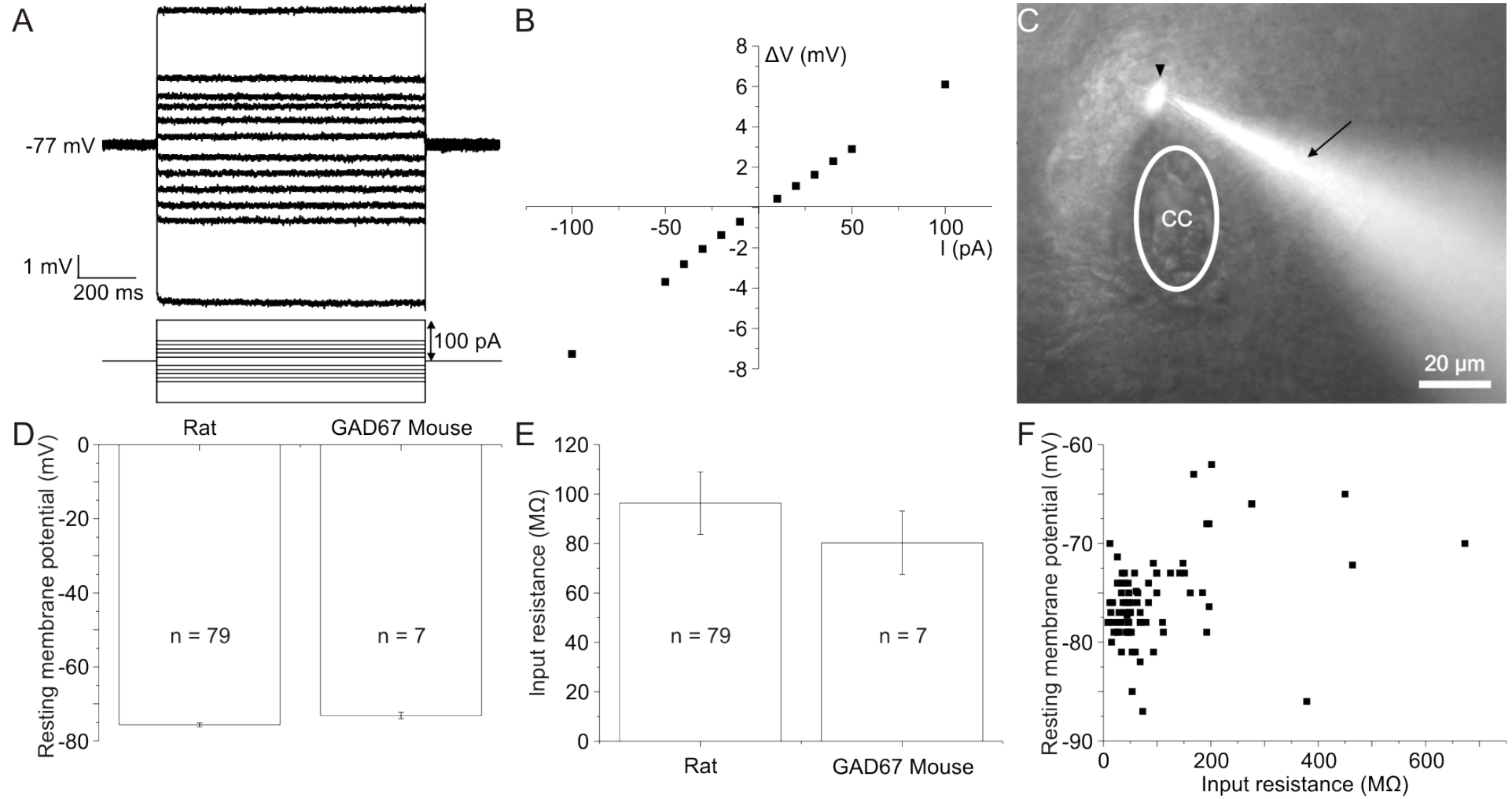
4.2.2 Dye coupling and gap junction blockers reveal that ependymal cells are coupled to each other

Neurobiotin, one of the tracers included in the intracellular solution, is gap junction permeable (Kita and Armstrong, 1991; Vaney, 1991). Therefore, if the recorded ependymal cell is coupled to other ependymal cells by gap junctions, the Neurobiotin will diffuse through the gap junctions to fill some of the connected ependymal cells. In this study, the visualisation of Neurobiotin with DAB revealed that the ependymal cells were highly coupled (n = 28 out of 28 recovered; Figure 4.2). The degree of Neurobiotin labelling demonstrated different levels of coupling between ependymal cells, for example a single layer of ependymal cells in one region of the CC could be observed as dye-filled (n = 18; Figure 4.2A), or a larger group consisting of multiple layers of ependymal cells but still within one region of the CC (n = 7; Figure 4.2B), or very rarely the whole ependymal layer surrounding the CC were dye-filled (n = 3; Figure 4.2C). Post-recording visualisation of cells with rhodamine, which is not gap junction permeable (Heyman and Burt, 2008), showed no coupling of cells, indicating that there was no spillage of tracers.

Visualisation of Neurobiotin and/or rhodamine revealed that some of the ependymal cells had processes (n = 24; Figure 4.2D). Only with the visualisation of rhodamine could it be guaranteed that the processes originated from the ependymal cells recorded; with visualisation of Neurobiotin, the processes could be arising from the dye-coupled cells. Based on both the rhodamine and Neurobiotin visualisation, many processes were found originating at the dorsal pole of the CC, from which they extended dorsally along the midline, often reaching the white matter (n = 12; Figure 4.2D). Slightly fewer processes were observed from the ventral pole, extending ventrally towards the ventral median fissure (n = 10). Finally, a small number of processes were observed from the lateral aspects of the CC (n = 2). Of the processes observed there appeared to be no branching.
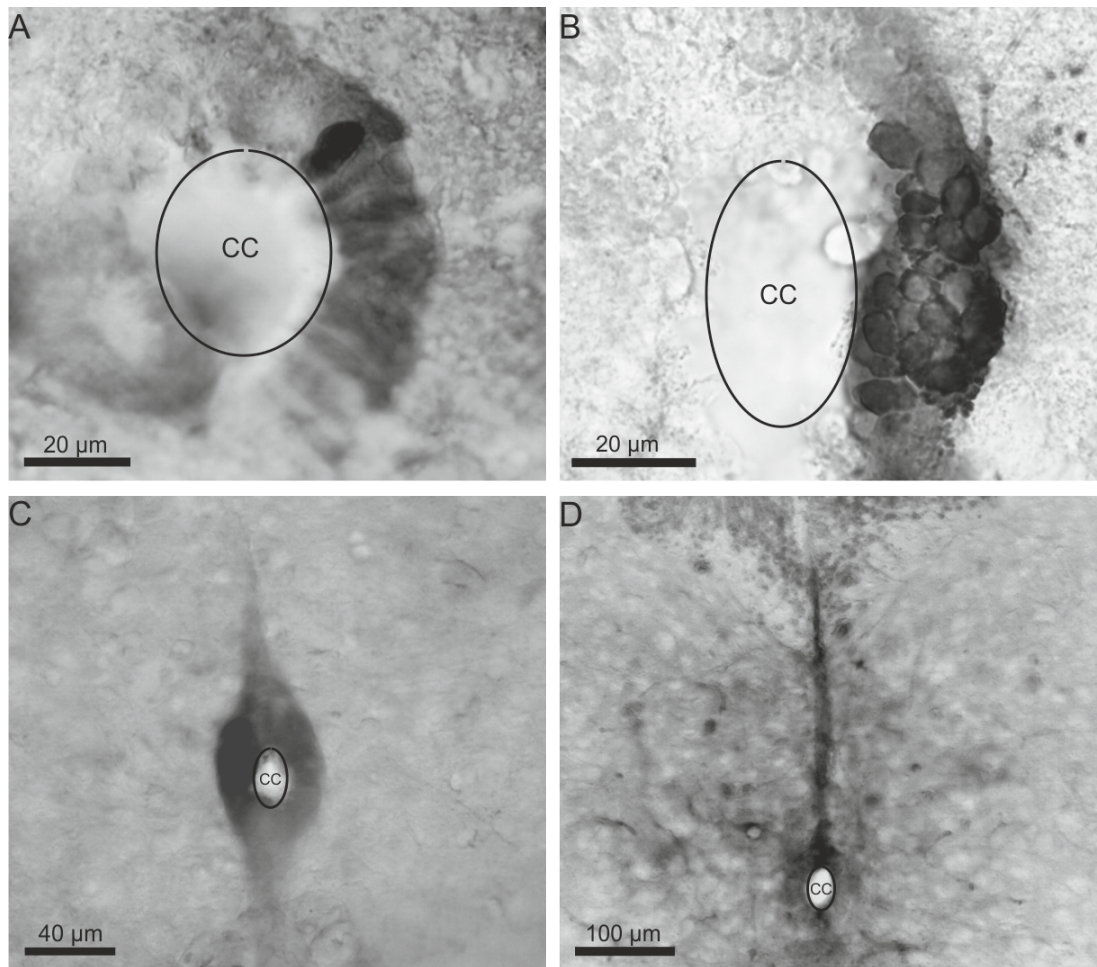
Figure 4.2: Intracellular dye-loading of Neurobiotin revealed coupling between ependymal cells.

Visualisation of Neurobiotin by DAB revealed a single layer of ependymal cells that were dye-coupled around a region of the CC (A), multiple layers of ependymal cells that were dye-coupled around a region of the CC (B), ependymal cells that are dye-coupled around the whole of the CC (C) and dorsal processes extending from some of the cells within a group of dye-coupled ependymal cells located at the dorsal pole of the CC (D). Images are all orientated with dorsal at the top.

To determine the effect that the gap junction coupling was having on the electrophysiological properties of ependymal cells, the non selective gap junction blocker 18β-glycyrrhetinic acid (100 μM; Davidson and Baumgarten (1988)) was bath applied. On application of 18β-glycyrrhetinic acid, the input resistance of every ependymal cell tested increased (n = 6; Figure 4.3A, B, D), with increases ranging from 57 MΩ to 1346 MΩ and an average increase of 360 ± 201 MΩ (n = 6), which translated to a percentage increase of 592 ± 248 % (n = 6). The input resistance was significantly greater following the bath application of 18β-glycyrrhetinic acid (Z = -2.201, P = 0.028; Figure 4.3D); this was determined using a Wilcoxon Signed Rank Test as the data were not normally distributed. The range of changes in input resistance suggest that the ependymal cells are coupled to different degrees, supporting the dye-coupled data. 18β-glycyrrhetinic acid also had an effect on the membrane potential of 4 out of 6 ependymal cells, causing a depolarisation in these 4 cells (Figure 4.3B). The average change in the membrane potential from the responders group was 26 ± 10 mV (n = 4); this change was not found to be significantly different (t (3) = -2.648, P = 0.077; Figure 4.3C) and is likely due to the large range of responses (8.5 mV to 51.6 mV). Interestingly, the average change in input resistance for the cells that did not depolarise in response to 18β-glycyrrhetinic acid (63.43 ± 6.35 MΩ; n = 2) was smaller than that of those that did depolarise in response to 18β-glycyrrhetinic acid (505.19 ± 280.82 MΩ; n = 4), although the number of cells was too low to test for the significance of this difference (Figure 4.3E). Instead, the correlation between the change in input resistance and change in membrane potential was examined. A Spearman's Rank Order correlation found a strong, significant correlation between the change in input resistance and the change in membrane potential (r_s (4) = 1.000, P < 0.01; Figure 4.3F). This suggests that the depolarisation that occurs in response to the application of 18β-glycyrrhetinic acid is related to the blockade of gap junctions and is not a non gap junction specific effect of 18β-glycyrrhetinic acid. Finally, as the slices were not pre-incubated with 18β-glycyrrhetinic acid prior to recording, the effect of 18β-glycyrrhetinic acid on dye coupling could not be investigated.

Figure 4.3: A gap junction blocker, 18β-glycyrrhetinic acid, can uncouple ependymal cells.

A-B) Example whole cell patch clamp traces recorded in current clamp. The downward voltage deflections are in response to the regular injection of a -50 pA current pulse. In some ependymal cells, bath application of 18β-glycyrrhetinic acid (100 μM) increased the input resistance but did not affect their resting membrane potential (A). In other ependymal cells, 18β-glycyrrhetinic acid both increased their input resistance and depolarised the cell (B). Grouped data (mean ± S.E) of membrane potential (C) and input resistance (D) under control conditions compared to the bath application of 18β-glycyrrhetinic acid, * $p < 0.05$. E) Grouped data (mean ± SE) of the change in input resistance for the cells classed as non-depolarising cells compared to those classed as depolarising cells in response to the bath application of 18β-glycyrrhetinic acid. F) Correlation between the change in input resistance and the change in membrane potential in response to the bath application of 18β-glycyrrhetinic acid, r_s = Spearman's Rank Order Correlation Co-efficient.

A

100 μM 18β-glycyrrhetinic acid

5 mV

200 s

-73 mV

B

100 μM 18β-glycyrrhetinic acid

10 mV

100 s

-75 mV

C

Control   18-β glycyrrhetinic acid

Membrane potential (mV)

n = 4   n = 4

D

Input resistance (MΩ)

*

n = 6

n = 6

Control   18-β glycyrrhetinic acid

E

Change in input resistance (MΩ)

n = 2   n = 4

Non-depolarising cells   Depolarising cells

F

Change in membrane potential (mV)

$r_s = 1.000$, $P < 0.01$

Change in input resistance (MΩ)

4.2.3 Ependymal cells respond to GABA

Given the effect of GABA on the neighbouring CSFcCs (see chapter 3.2.3 and Marichal et al., (2009)) and on radial glia surrounding the CC in the turtle (Reali et al., 2011), responses of ependymal cells to GABA were investigated. There was a significant difference in the membrane potential before (-76.14 ± 0.91 mV; n = 11), during (-72.52 ± 1.12 mV; n = 11) and after (-76.47 ± 0.82 mV; n = 11) the bath application of GABA (200 µM; $F_{(2, 20)}$ = 51.914, $P < 0.001$; Figure 4.4A, B). Post-hoc testing revealed that the membrane potential of ependymal cells in GABA was significantly more depolarised than either before or after the GABA application ($P < 0.001$). It also revealed that the effect of GABA was fully reversible as there was no significant difference between the membrane potential of the ependymal cells before and after the GABA application ($P = 0.240$). The changes in membrane potential in response to GABA ranged from 2.03 mV to 6.46 mV, with an average change in membrane potential of 3.62 ± 0.46 mV (n = 11). Despite this depolarisation, the bath application of GABA had no significant effect on the input resistance of ependymal cells ($F_{(2, 18)}$ = 1.936, $P = 0.173$; Figure 4.4A, C) when comparing input resistance before (71.10 ± 12.17 MΩ; n = 10), during (68.81 ± 10.75 MΩ; n =10) and after the application of GABA (76.40 ± 13.25 MΩ; n = 10). It is unlikely that the depolarisation could be masking any GABA-induced changes in input resistance through the opening or closing of voltage gated channels, as ependymal cells do not appear to possess voltage-gated channels and the depolarisation is relatively small. Nevertheless, to confirm that there is no interference, negative current was applied during the bath application of GABA to return the cell to the membrane potential that it was resting at prior to the GABA application. During this protocol, the input resistance of the cell did not change from that observed during the control period or during the application of GABA at the depolarised membrane potential (n = 1).

To better determine the kinetics of the GABA response, GABA (500 µM) was focally pressure ejected (10 psi, 500 ms) on to ependymal cells (Figure 4.4D). This resulted in a depolarisation with an amplitude of 4.40 ± 2.68 mV (n = 3), the time to the onset of the depolarisation was 140.33 ± 27.94 ms (n = 3) and the time to the peak of the depolarisation was 848.33 ± 61.97 ms (n = 3). Since the positioning of the GABA-filled electrode could affect the time to onset and time to peak depolarisation, therefore, these were not extensively examined.
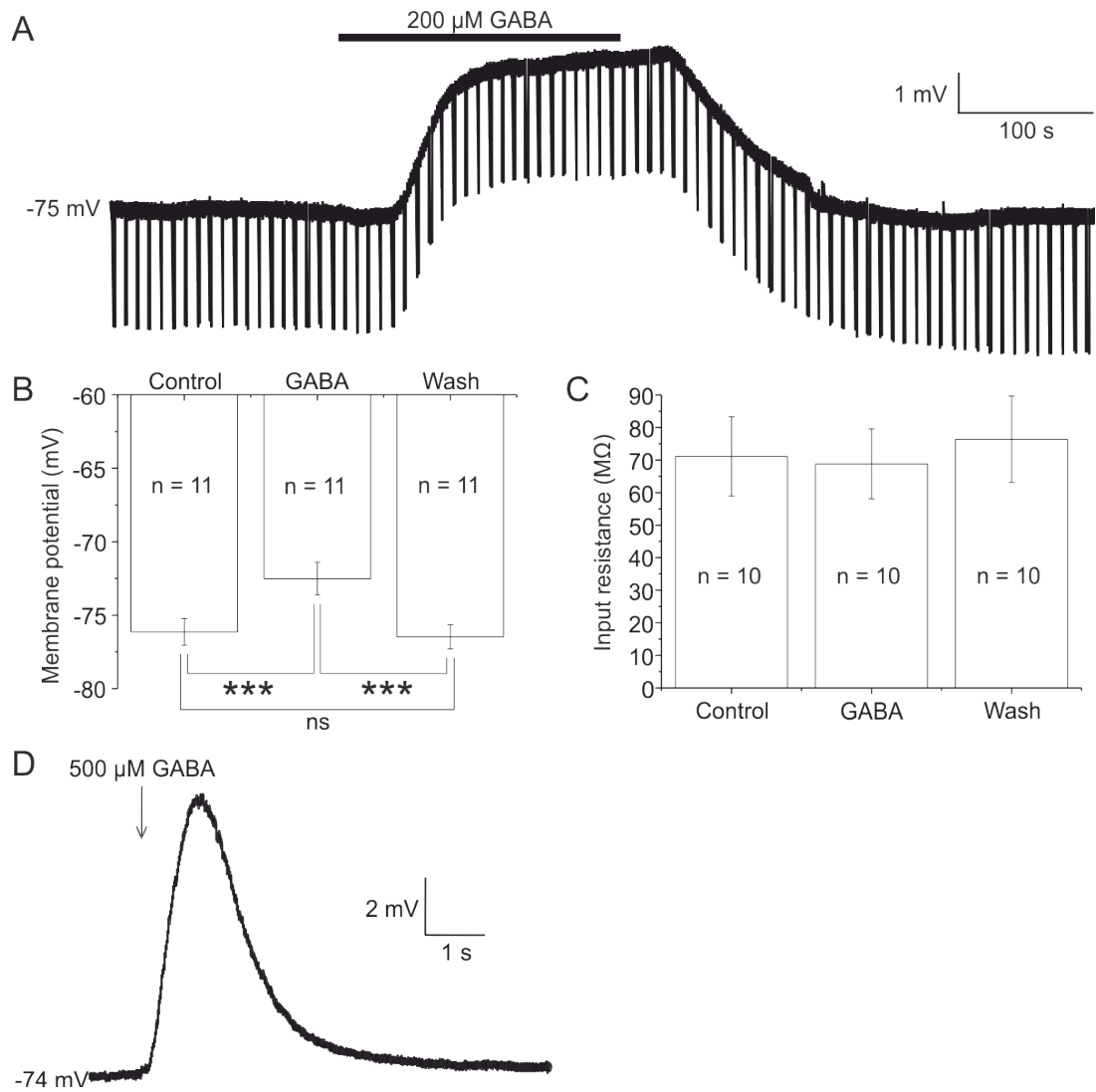
Figure 4.4: Ependymal cells are depolarised by GABA.

A) Whole cell patch clamp trace in current clamp during the bath application of GABA (200 μM) to an ependymal cell. The downward voltage deflections are in response to the injection of -50 pA pulses. B-C) Group data for membrane potential (B) and input resistance (C) during control conditions, the bath application of GABA and recovery, ns = not significant, *** = p < 0.001. D) Focal pressure ejection of GABA (500 μM; 500 ms; 10 psi) rapidly depolarised ependymal cells.

To determine which receptors were mediating the GABA response in ependymal cells, GABA (200 µM) was bath applied in the presence of the $GABA_A$ antagonists, bicuculline (100 µM) and gabazine (2.5 µM), or the $GABA_B$ agonist, baclofen (10 µM) was applied alone. There was no significant difference in the input resistance of the ependymal cells before (78.68 ± 14.08 MΩ; n = 4), during (79.94 ± 14.99 MΩ; n = 4) and after (80.38 ± 15.24 MΩ; n = 4) the co-application of bicuculline and GABA ($F_{(2, 6)}$ = 0.310, P = 0.745). As would be expected, the lack of significant change in input resistance during the co-application of bicuculline and GABA (1.26 ± 1.43 MΩ; n = 4) was not significantly different from that during the application of GABA alone (3.27 ± 1.74 MΩ; n = 4; $t_{(3)}$ = 0.871, P = 0.448; Figure 4.5A, C). As during the application of GABA alone, there was a significant difference in the membrane potential before (76.08 ± 1.41 mV; n = 4), during (-74.70 ± 1.24 mV; n = 4) and after (-76.18 ± 1.39 mV; n = 4) the application of GABA in the presence of bicuculline, with post-hoc tests revealing a significant depolarisation on application of GABA (P = 0.029; Figure 4.5A). This depolarisation by GABA in the presence of bicuculline (1.38 ± 0.24 mV; n = 4) was significantly smaller than the depolarisation observed in GABA alone (3.62 ± 0.46 mV; n = 4; $t_{(3)}$ = 3.685, P = 0.035; Figure 4.5A, B), with the GABAergic response in bicuculline being 41.18 ± 12.14 % (n = 4) of the initial GABA response. The effect of bicuculline on the GABAergic response was reversible (Figure 4.5Aii). The bath application of gabazine (2.5 µM) could also antagonise the GABA response, with a 37 ± 11 % (n = 2) decrease in the size of the depolarisation evoked by GABA (Figure 4.5D). The effect of gabazine on the GABAergic response was also reversible (Figure 4.5Dii). In the majority of cases bicuculline and gabazine had no effect on the membrane potential or input resistance of ependymal cels when applied alone, however, a small depolarisation was observed during the bath application of bicuculline on a small number of occasions (data not shown).

As the $GABA_A$ antagonists could not entirely antagonise the GABAergic response, the effect of baclofen was investigated. There was, however, no significant difference in the membrane potential before (-78.38 ± 1.45 mV; n = 3), during (-78.57 ± 1.59 mV; n = 3) and after (-78.70 ± 1.63 mV; n = 3) the bath application of baclofen ($F_{(2, 4)}$ = 2.601, P = 0.189; Figure 4.6A, B). Neither was there a significant difference in the input resistance before (68.90 ± 13.38 MΩ; n = 3), during (70.55 ± 13.92 MΩ; n = 3) and after (71.98 ± 14.55 MΩ; n = 3) the application of baclofen ($F_{(2, 4)}$ = 1.449, P = 0.366; Figure 4.6A, C).

Figure 4.5: The GABAergic response in ependymal cells is mediated by GABA$_A$ receptors.

Whole cell patch clamp traces in current clamp demonstrate that the depolarisation in response to GABA (200 µM; A, D) is partially antagonised by bicuculline (100 µM; Ai) or gabazine (2.5 µM; Di) in a reversible manner (Aii; Dii). The downward voltage deflections are in response to the regular injection of -50 pA current pulses. Pooled data of the amplitude of the response (B) and of the change in input resistance (C) during the response to the application of GABA compared to the co-application of GABA and bicuculline, * = p < 0.05.

A

200 μM GABA

2 mV

100 s

Ai

100 μM bicuculline

200 μM GABA

Aii

200 μM GABA

B

Amplitude (mV)

n = 4

*

n = 4

GABA   GABA + Bicuculline

C

Change in input resistance (MΩ)

n = 4

GABA   GABA + Bicuculline

D

200 μM GABA

2 mV

100 s

Di

2.5 μM gabazine

200 μM GABA

Dii

200 μM GABA
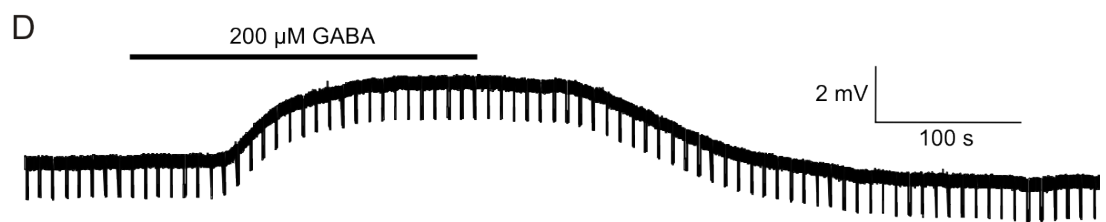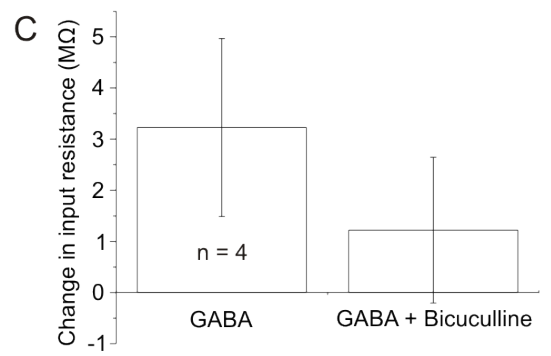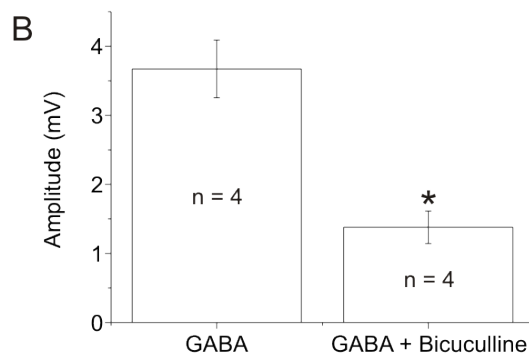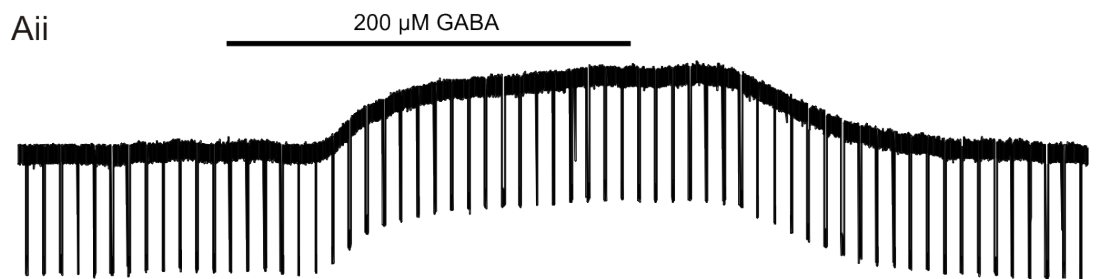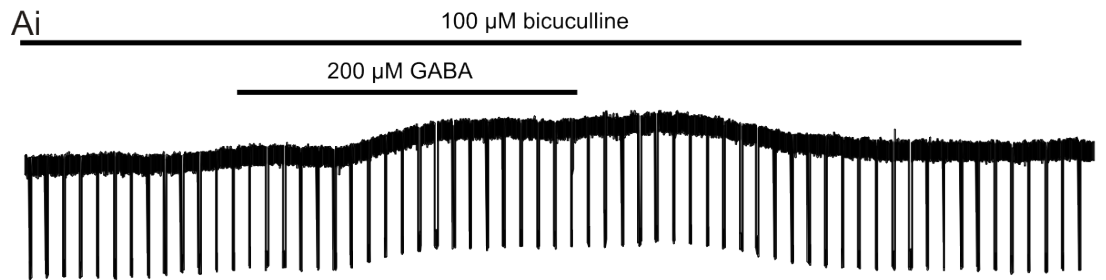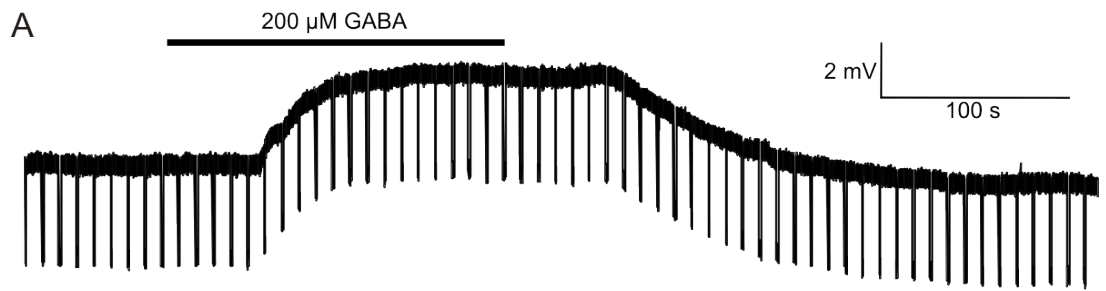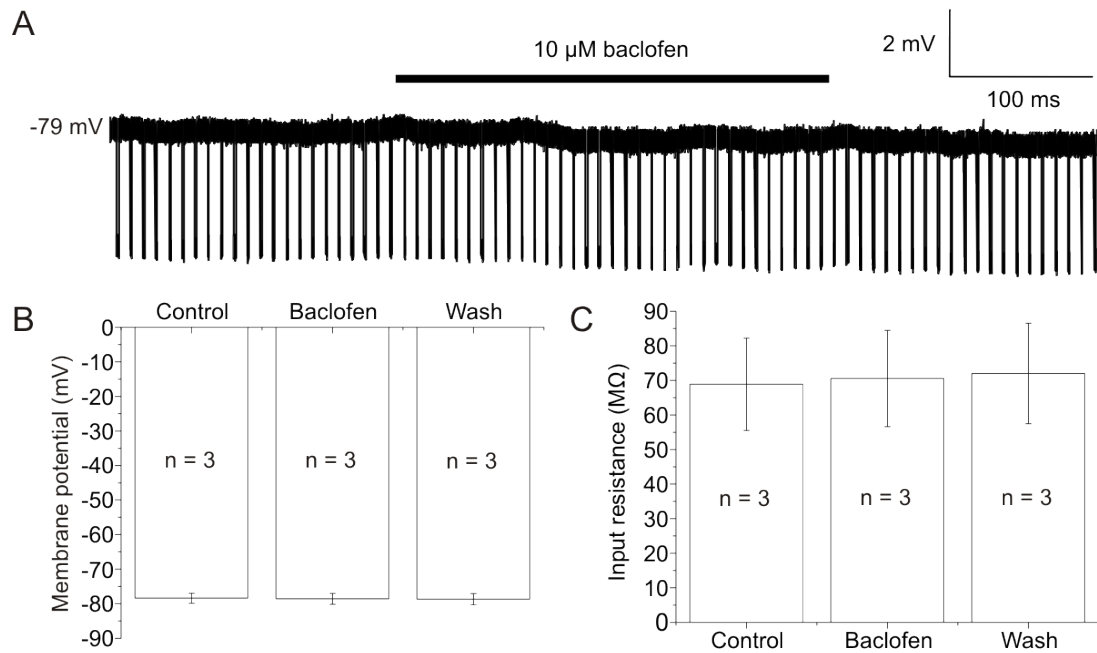
Figure 4.6: Baclofen, a GABA$_B$ agonist, did not elicit a response in ependymal cells.

A) Baclofen (10 µM) had no effect on the membrane potential or input resistance of ependymal cells when bath applied. The downward voltage deflections are in response to the regular injection of -50 pA current pulses. B-C) Mean ± S.E of the membrane potential (B) and input resistance (C) during control conditions, the bath application of baclofen and recovery.

4.3 Discussion

This chapter provides a detailed characterisation of the electrophysiological properties of ependymal cells surrounding the CC and is the first study to demonstrate that ependymal cells in this area within the mammalian spinal cord are capable of responding to neurotransmitters.

Ependymal cells display typical characteristics of glial cells, with negative resting membrane potentials of -74 mV or -76 mV, low input resistances, no spontaneous or electrically evoked activity and passive responses to current pulses which are indicative of a lack of voltage-gated channels. The visualisation of Neurobiotin with DAB following intracellular loading revealed not only that the ependymal cells were coupled but that different degrees of coupling were present. This coupling could be reduced in the presence of the gap junction blocker 18β-glycrrhetinic acid, as evidenced by a large increase in input resistance. Ependymal cells consistently responded to GABA with a depolarisation that could be antagonised by the $GABA_A$ receptor antagonists bicuculline and gabazine, but could not be mimicked by the $GABA_B$ agonist baclofen.

4.3.1 Basic electrophysiological characteristics are consistent with those previously observed

The resting membrane potential of ependymal cells determined in this study in rats, - 76 mV, is relatively similar to those determined previously, -84 mV for ependymal cells in the rat spinal cord (Marichal et al., 2012) and -80 mV for ependymal cells of the rat third ventricle (Jarvis and Andrew, 1988). The resting membrane potentials of ependymal cells in the turtle are higher in both the spinal cord, -87 mV (Russo et al., 2008) and the dorsal cortex, -90 mV (Connors and Ransom, 1987). The resting membrane potential of ependymal cells is highly dependent on the reversal potential of K^+ (E_{K+}; Jarvis and Andrew (1988)), which in this study was -91 mV, therefore in studies with a more negative E_{K+}, due to a higher extracellular K^+ concentration or a lower intracellular K^+ concentration, more K^+ ions will move down the electrochemical gradient into the cell resulting in a less negative membrane potential. Slight variations in the extracellular K^+ concentration within the aCSF or intracellular K^+ concentration within the intracellular patch pipette solution, combined with differences in the region of the ventricle/CC studied and differences in the age of animal studied appear enough to explain the small variation between studies.

The input resistance of ependymal cells determined in this study was 96 MΩ, this is slightly lower than that previously determined for ependymal cells in the rat spinal cord, 124 MΩ (Marichal et al., 2012) and in the turtle spinal cord, 167 MΩ (Russo et al., 2008). The lower input resistance observed in this study compared to others suggests that the cells recorded in this study could be more extensively coupled, or alternatively they could express more channels that are constitutively open. There are two main differences about the ependymal cells in this study compared to that of Marichal et al., (2012) that could explain the variation. Firstly, this study recorded cells from the lower thoracic and upper lumbar levels of the spinal cord compared to the cervical spinal cord; the ependymal population could have slightly different functions at different levels, with the function requiring a different degree of coupling. Secondly, this study recorded from animals P11-P21 compared to P0-P5; the expression of ion channels by other glial cell types within the spinal cord has been shown to change during postnatal development from P1-P19 (Chvatal et al., 1995) and the expression of connexins can vary during development in other regions of the CNS (Leung et al., 2002). In the rat midbrain floor, connexin 43 mRNA expression and protein expression increased steadily from P0 to adulthood (Leung et al., 2002). If the same ontogenic expression pattern occurred in ependymal cells of the spinal cord this could be observed as a smaller degree of coupling and thus an increase in input resistance of ependymal cells at P0 compared to P21; supporting the lower input resistance observed in this study compared to Marichal et al., (2012). Although there are slight differences between the properties of ependymal cells in P9-P21 rats compared to those in P0-P5 rats, the hypothesis that ependymal cells in spinal cords from P9-P21 rats have passive elctrophysiological properties is supported by this data.

The weak correlation between the resting membrane potential and input resistance of ependymal cells in this study suggested that ependymal cells with more negative resting membrane potentials have smaller input resistances. This correlation is supported when observing the effect of the gap junction blocker, carbenoxelone, on the ependymal, progenitor cell population surrounding the CC of the turtle spinal cord. The increase in input resistance that was observed by the application of carbenoxelone was accompanied by a decrease in the resting membrane potential from an average of -88 mV to -78 mV (Russo et al., 2008). Thus together it suggests that more highly coupled cells could have more negative resting membrane potentials.

The lack of spontaneous or evoked activity and the linear voltage-current relationship agreed with previous studies of rat and turtle spinal cord ependymal cells (Russo et al., 2008; Marichal et al., 2009, 2012). This suggests that ependymal cells lack voltage-gated ion channels. When a leak subtraction protocol and carbenoxelone were applied to ependymal, progenitor cells surrounding the turtle CC a small outward current was revealed in some cells (Russo et al., 2008). This current could be reduced by tetraethylammonium (TEA), which suggests the presence of delayed rectifier K^+ channels. It is possible that such a channel could be present in ependymal cells of the rat spinal cord; however, a leak subtraction protocol was used by Marichal et al., (2012) when recording from ependymal cells in the rat and they did not observe any outward current. Other voltage-gated channels such as TTX-sensitive voltage-gated Na^+ channels have also been identified in other glial cell types (Barres et al., 1989) but not in ependymal cells to date. The data in this study suggests that ependymal cells of the postnatal mammalian CC do not express voltage-gated Na^+ channels.

4.3.2 Ependymal cells are coupled by gap junctions to varying degrees

This study confirmed previous reports that dye-coupling occurs between ependymal cells of the rat spinal cord (Marichal et al., 2012) and demonstrated that the coupling occurs in older animals of P9-P21 as well as those aged P0-P5. This data supports the hypothesis that a high degree of coupling occurs between ependymal cells. Additionally it highlighted the different degrees of coupling that occur, with some ependymal cells found in larger groups than others. This variation in the degree of coupling has been found in the ependymal, progenitor population of turtles, where they referred to different sized clusters of cells ranging from clusters covering a whole quadrant to smaller clusters containing a few cells only (Russo et al., 2008). The visualisation of more than one dorsally projecting fibre following recordings indicates that the radial ependymal cells are also capable of dye-coupling.

The increase in input resistance observed in the presence of the gap junction blocker, 18β-glycyrrhetinic acid, is consistent with the dye-coupling and the hypothesis that gap junctions are present between ependymal cells. 18β-glycyrrhetinic acid is a non-selective gap junction blocker, therefore the specific

identity of the connexin subunits forming the gap junctions were not identified. Both connexin 43 (Ochalski et al., 1997; Marichal et al., 2012) and connexin 45 (Chapman et al., 2012) are expressed by ependymal cells of the mammalian spinal cord, and the coupling observed around the turtle CC has been attributed to the connexin 43 subunit as immunohistochemistry revealed its presence there (Russo et al., 2008). Therefore the expression data suggests that connexin 43 and connexin 45 constitute the gap junctions formed between ependymal cells.

The application of 18β-glycyrrhetinic acid depolarised 4 out of 6 cells, with the size of the depolarisation varying greatly between these 4 cells. As stated earlier, depolarisations in cells surrounding the turtle CC have been shown to accompany the increase in input resistance (Russo et al., 2008). The strong correlation between the change in input resistance and the change in membrane potential in response to 18β-glycyrrhetinic acid indicates that the depolarisation is a direct effect of gap junction blockade. The depolarisation could be explained by considering the comparative influences of the *in-vivo* ependymal intracellular Cl^- concentration and the patch pipette intracellular Cl^- concentration, in gap junction coupled and uncoupled states. Ependymal cells lining the ventricles of the rat brain and progenitor cells that surround the CC of the turtle express high levels of NKCC1 which transports Cl^- ions into the cell and thus maintains a high intracellular Cl^- concentration (Kanaka et al., 2001; Reali et al., 2011). It is likely that ependymal cells of the mammalian CC could express high levels of NKCC1 and thus also have high intracellular Cl^- concentrations. Under normal circumstances this *in-vivo* expression of Cl^- transporters would not be relevant as the intracellular solution within the pipette would diffuse into the cell and set a new lower Cl^- concentration. In these cells, however, the highly coupled nature could make it impossible for the intracellular solution within the pipette to set the Cl^- concentration, as Cl^- could pass through the gap junctions connecting the recorded cell to neighbouring cells (Wang and Veenstra, 1997), maintaining a high intracellular Cl^- concentration. Consequently, blocking the gap junctions would prevent any Cl^- entering the recorded cell from neighbouring cells, which would allow the pipette solution to set the Cl^- concentration to a lower concentration. As a result the membrane potential would be less negative, thus the gap junction blocker caused a depolarisation. The variation in the size of the depolarisations could be dependent on how large a cluster of cells the recorded cell is part of and therefore how highly coupled the recorded cell is.

Another factor to consider when using 18β-glycyrrhetinic acid is the non gap junction specific effects. For example, a study recording from cells within a confluent monolayer culture found that 18β-glycyrrhetinic acid not only uncoupled the cells but it also dramatically reduced the Cl^- conductance with little affect on the Na^+ and K^+ conductances (Bohmer et al., 2001). This reduction was attributed to a block of chloride channels not $GABA_A$ receptors, nevertheless, if ependymal cells express chloride channels their blockade by 18β-glycyrrhetinic acid could influence the intracellular Cl^- concentration and the membrane potential of the ependymal cells. In dissociated smooth muscles cells, 18β-glycyrrhetinic acid could induce a depolarisation of the membrane potential which was associated with a decrease in both inward rectifying K^+ channel currents and Ca^{2+}-activated K^+ channel currents (Guan et al., 2007). Although the current-voltage relationship data in this study suggests that ependymal cells do not possess these channels, the depolarisation of ependymal cells in the presence of 18β-glycyrrhetinic acid could suggest that they are in fact present. On the other hand, if these channels are not present in ependymal cells then it is less likely that 18β-glycyrrhetinic acid could be having a non gap junction specific effect. This likelihood is supported by the correlation between the change in input resistance and the change in membrane potential which suggests that the depolarisation is a gap junction related effect and could be a result of the NKCC1 and Cl^- mechanism suggested above.

4.3.3 Understanding the GABAergic response

A depolarisation of ependymal cells was observed following either the bath or focal pressure application of GABA, proving the hypothesis that ependymal cells are capable of responding to GABA. Given that $GABA_A$ receptors are Cl^- channels, and the Cl^- reversal potential (E_{Cl^-}) set by the intracellular solution is -103 mV, a hyperpolarisation would have been expected as Cl^- moved into the cell down the electrochemical gradient. Nevertheless, there are a number of possibilities that could explain the depolarisation seen in ependymal cells in response to GABA. Firstly, ependymal cells express NKCC1; if these channels are expressed in close proximity to the $GABA_A$ receptors in the cell membrane, there could be a local intracellular accumulation of Cl^- near the $GABA_A$ receptors, despite the Cl^- concentration in many areas of the cell being lower due to the lower Cl^- concentration in the intracellular solution from the patch pipette. Thus activation of

the $GABA_A$ receptors by GABA would result in a depolarisation. Secondly, the high degree of gap junction coupling between ependymal cells could result in Cl^- moving from neighbouring cells, which have a high intracellular Cl^- concentration due to the NKCC1 expression, into the recorded cell, which has a low intracellular Cl-concentration due to the intracellular solution in the patch pipette. The influx of Cl^- into the recorded cell could increase the intracellular Cl^- concentration so that it is high enough to cause a depolarisation on the activation of $GABA_A$ receptors. Despite this suggestion, it is unlikely that there would be a sufficient number of gap junctions to overcome the intracellular Cl^- concentration set by the intracellular solution of the patch pipette. Thirdly, GABA could be hyperpolarising the recorded cell but depolarising the neighbouring gap junction coupled cells; in this case the greater number of cells depolarising could mask the hyperpolarisation observed in the recorded cell. Fourthly, it is possible that the depolarisation could be caused by the GABA transporter, GAT3. GAT3 belongs to a family of Na^+-Cl^- dependent GABA transporters; studies on another member of the family, GAT1, have revealed that GABA is transported back into the cells with two Na^+ ions and one Cl^- ion, driven by the electrochemical gradient for Na^+ (Mager et al., 1993). Thus the application of GABA can evoke a depolarisation in cells expressing GABA transporters, as an increase in extracellular GABA results in the uptake of GABA and a net single positive charge. Evidence supporting the presence of GAT3 is that the GABAergic response could not be fully antagonised by $GABA_A$ antagonists, bicuculline and gabazine, even at a high concentration of 100 µM for bicuculline and did not involve $GABA_B$ receptors. In addition, GAT3 has been observed to contribute to the mediation of the GABA response in progenitor cells surrounding the turtle CC (Reali et al., 2011). This was demonstrated by the antagonism of the GABA response by the GAT3 antagonist, SNAP5114. The presence of GABA transporters in ependymal cells was not investigated in this study; however, it is likely that expression of the glial GABA transporter, GAT3 in ependymal cells could contribute to the depolarisation in response to GABA. To verify this, an interesting future experiment would be to apply GABA in the presence of SNAP5114. Finally, as suggested for the GABAergic response in CSFcNs in chapter 3, the $GABA_A$ receptors could be over stimulated leading to an imbalance of the HCO^{3-} efflux and Cl^- influx. Again, as for CSFcNs the likelihood of overstimulation could depend on the subunit composition of the $GABA_A$ receptors (Farrant and Nusser, 2005). It is likely that the depolarisation of ependymal cells to GABA is not a result of one of these possibilities but a combination of some or all of the suggestions.

Ependymal cells in the dorsal cortex of the turtle were previously shown to slowly depolarise during repetitive neural stimulation (Connors and Ransom, 1987). Repetitive neural stimulation involves neurones depolarising and the subsequent opening of voltage-gated K^+ channels and Ca^{2+}-activated K^+ channels, which allows a K^+ efflux and thus increases extracellular K^+ concentrations. It was demonstrated that the increase in local extracellular K^+ concentration fully accounted for the slow depolarisation (Connors and Ransom, 1987). The depolarisation evoked by GABA application could not be mediated by a local increase in extracellular K^+ concentration for a number of reasons. Firstly, although GABA will be acting on neighbouring neurones, for example CSFcNs (see chapter 3), it will mediate an opening of $GABA_A$ receptors which allows the movement of Cl^- ions, thus the response predominantly affects extracellular Cl^- concentrations, not K^+ concentrations. Secondly, the focal pressure application of GABA, which will only affect a small number of cells, still induced a depolarisation in ependymal cells. Finally, the GABAergic response in CSFcNs can be strongly antagonised by $GABA_A$ antagonists (see chapter 3.2.3; Marichal et al., (2009)) but that of ependymal cells can only be partially antagonised by $GABA_A$ antagonists, therefore if the ependymal cells response was due to the CSFcN response, it would be antagonised to the same degree by $GABA_A$ antagonists. Whether the response of ependymal cells to GABA was direct was not specifically investigated, for example, GABA was not applied in the presence of blockade of synaptic transmission, such as TTX or low Ca^{2+} solution. There are, however, synapses between GABAergic terminals and ependymal cells in the rat spinal cord (Magoul et al., 1987) which provides strong evidence that the effect is direct. In addition, the concentration of bicuculline applied would not only fully antagonise the GABAergic response of CSFcCs but would likely fully antagonise the GABAergic response of any other neurones within the spinal cord, which would support the direct nature of the GABAergic response in ependymal cells.

Despite the consistent depolarisation that occurred in response to the bath application of GABA, there was no change in input resistance. A change in input resistance would normally be expected to accompany a response to GABA, as $GABA_A$ receptors would open, allowing the movement of ions and thus decreasing the resistance of the membrane. The input resistance was already very low in these cells due to the extensive coupling; therefore the relative effect of ion channels opening on the size of the input resistance could have been too small to measure. To remove the factor of gap junction coupling, it would be interesting to apply GABA

in the presence of a gap junction blocker; it is possible that a change in input resistance would then be observed. The membrane potential of ependymal cells was repolarised to the resting membrane potential during the application of GABA to ensure that any voltage-gated channels that opened or closed as a result of the depolarisation did not affect the input resistance of the ependymal cell. As there was no difference in input resistance at the repolarised membrane potential and at the depolarised membrane potential during this protocol, this confirmed that the input resistance was not changing during the GABA application and strengthened the argument that ependymal cells do not express any voltage-gated channels.

As the GABAergic response could be antagonised by the $GABA_A$ antagonist, bicuculline, it indicates that the response to GABA is in part being mediated by $GABA_A$ receptors. No cell specific expression of $GABA_A$ receptor subunits has been explored for ependymal cells of the CC, however immunohistochemistry revealed a high expression of α1, α3, β2/β3 and γ2 subunits, a lower expression of α2 and α5 and *in-situ* hybridisation revealed a lack of expression of mRNA for α6 and δ subunits in lamina X (Wisden et al., 1991; Bohlhalter et al., 1996). Therefore, there are a number of possible subunit compositions for the $GABA_A$ receptor mediating the ependymal cell response, with it likely that β2/β3 and γ2 subunits are present combined with α1, α2, α3 or α5 subunits. The composition of the $GABA_A$ receptors could reflect the type of effect that GABA is having on ependymal cells. For example, the subunits confer different properties to the receptors which make them more suited to respond to lower or higher concentrations of GABA and thus more suited to tonic or phasic transmission (Farrant and Nusser, 2005).

As alluded to previously, bicuculline could not completely antagonise the GABAergic response, even at the high concentration of 100 μM. This suggests that there was another receptor or transporter contributing to the mediation of the GABAergic response. The contribution of the $GABA_B$ receptor was investigated using the $GABA_B$ agonist, baclofen. A lack of response to baclofen suggests that ependymal cells do not express $GABA_B$ receptors. This agrees with expression patterns for $GABA_B$ receptors within the spinal cord; with a lack of protein expression and mRNA expression for the GABABR1 subunit and a lack of mRNA expression for the GABABR2 subunit in ependymal cells (Allen Brain Atlas, Margeta-Mitrovic et al., (1999)). The residual GABA response could be a result of GAT3 activity; the presence of GAT3 in mammalian ependymal cells has not been investigated. To investigate whether GAT3 is contributing to the residual GABA

response, the GAT3 blocker SNAP 5114 could be co-applied with bicuculline to see if together they can completely antagonise the GABA response.

The demonstration of ependymal cells responding to GABA is extremely exciting; however, its functional relevance is highly dependent on the source of the GABA. The source could be solely the GABAergic terminals that synapse with ependymal cells (Magoul et al., 1987) or there could also be GABA released in a paracrine manner and found within the CSF; this second suggestion is supported by the small number of cells in which bicuculline alone was observed to have an effect, providing evidence that there could be an endogenous source of tonic GABA. This, along with the possible downstream effects of ependymal cells being excited by GABA and the functional importance of gap junction coupling, will be discussed in the general discussion.

4.3.4 Conclusion

This study demonstrates that ependymal cells surrounding the CC of the postnatal mammalian spinal cord are functionally coupled via gap junctions and is the first study to demonstrate that ependymal cells are capable of responding to the neurotransmitter GABA. The different sizes of gap junction coupled groups of ependymal cells indicate varied degrees of coupling and suggest that ependymal cells function as groups of cells not as lone cells. GABA induces a depolarisation in ependymal cells, which is likely to be a combined result of NKCC1 expression, gap junction coupling and the possible expression of the GABA transporter, GAT3. The GABA response is mediated partially by $GABA_A$ receptors but not $GABA_B$ receptors and could also receive a contribution from GAT3. The ability of ependymal cells to respond to GABA demonstrates that they are capable of responding to changes in the environment and could suggest that they are more integrated into the spinal cord circuitry than previously thought.

Chapter 5 - Responses of CSFcCs and ependymal cells to ACh

5.1 Introduction

There are a large number of cholinergic terminals within lamina X of the mammalian spinal cord (Barber et al., 1984; Phelps et al., 1984). These terminals are likely to originate from the considerable number of cholinergic interneurones that are located within lamina X, including the partition neurones and the CC-cluster cells (Barber et al., 1984; Phelps et al., 1984). Processes originating from CC-cluster cells have been observed to contribute to ChAT-immunopositive processes located near the ependymal layer (Barber et al., 1984; Phelps et al., 1984). A number of ChAT-immunopositive terminal-like structures of unidentified origin have also been identified near ChAT-immunonegative cells in the ependymal layer (Barber et al., 1984). This suggests that cells within the ependymal layer, either ependymal cells and/or CSFcCs could be receiving cholinergic inputs.

Cholinergic receptors or subunits have also been located in lamina X, including M2 mAChRs identified by autoradiography (Hoglund and Baghdoyan, 1997) and the nAChR subunits, α2, α3, α4, α7 and β2, identified by *in-situ* hydridisation (Wada et al., 1989; Seguela et al., 1993). Pharmacology from electrophysiological studies has suggested the presence of both α4β2*nAChRs and α7*nAChRs in lamina X (Bordey et al., 1996a; Bradaia and Trouslard, 2002b). Despite this, the expression of cholinergic receptors by cells directly surrounding the CC is yet to be investigated in either mammals or lower vertebrates.

ACh has been implicated in postnatal neurogenesis in the SVZ (Cooper-Kuhn et al., 2004; Kaneko et al., 2006) and in the DG (Harrist et al., 2004; Campbell et al., 2010). In the DG, there is a decrease in the number of BrdU-expressing newborn cells in β2*nAChR knockout mice (Harrist et al., 2004) and there is a decrease in the survival, maturation and integration of newborn neurones in α7*nAChR knockout mice (Campbell et al., 2010). Given the neural stem cell potential of ependymal cells and the possible immature or plastic nature of CSFcCs, it is feasible that ACh could be influencing the proliferation, survival and plasticity of cells surrounding the CC. Unlike chapter 3, the ability of all CSFcC subtypes to respond to ACh will be investigated, as subtype 1 CSFcCs could be an important cell type within the neurogenic niche. If either ependymal cells or CSFcCs are capable of responding to ACh it is important to distinguish which receptor subtypes are mediating the effects as their activation clearly has different consequences.

There are numerous cholinergic receptor antagonists and modulators that have preferential selectivity for cholinergic receptors containing specific subunits and have thus become useful in determining what cholinergic receptors are expressed by different cell types. Atropine is a well known selective antagonist of mAChRs, whereas MCA is a well known selective antagonist of nAChRs (Rang, 2003). To further determine the subunits which constitute nAChRs, DHβE, MLA and PNU-120596, amongst others, can be utilised. DHβE is a selective non α7*nAChR antagonist at a concentration of 1 µM or lower (Alkondon and Albuquerque, 1993; Bradaia and Trouslard, 2002b) and is a selective α4β2*nAChR antagonist at a concentration of 10 nM or lower (Alkondon and Albuquerque, 1993). MLA is a useful compound to study the involvement of α7*nAChRs, as it is considered to be a selective α7*nAChR antagonist at concentrations of 20 nM or lower (Wonnacott, 1993). An alternative to the use of MLA is to use the more recent discovery, PNU-120596, which is a specific potentiator of α7*nAChR mediated responses (Hurst et al., 2005).

5.1 Hypothesis and aims

Given the close proximity of numerous cholinergic interneurons to the CC and the importance of ACh in other postnatal neurogenic niches, the hypothesis of this chapter is that ependymal cells and CSFcCs of the mammalian spinal cord are capable of responding to ACh. Specifically, this chapter aims to use whole cell patch clamp electrophysiology, intracellular dye-loading and immunohistochemistry to investigate whether ependymal cells and CSFcCs respond to ACh, what type of cholinergic receptors are mediating the response to ACh and whether the receptors mediating the ACh response vary between cell types and cell subtypes.

5.2 Results

All data in this chapter are from cells recorded in spinal cord slices obtained from Wistar rats, P9-P21.

5.2.1 All cell types respond to ACh

All cell types recorded responded to the focal pressure application of ACh (3 mM; 500 ms) with a depolarisation (Figure 5.1). The amplitudes of these responses varied between cell types and cell subtypes (Figure 5.1E, F).

The cholinergic response of ependymal cells ranged from depolarisations of 0.58 mV to 8.09 mV, with an average response of 2.96 ± 0.28 mV (n = 36; Figure 5.1A, F). The time to onset of the response was 145.67 ± 17.04 ms (n = 18; Figure 5.2A) and the time to peak amplitude of the depolarisation was 1463.25 ± 92.00 ms (n = 36) following the onset of the response (Figure 5.2B). The amplitude of the cholinergic response in ependymal cells did not correlate with the input resistance of the cell (r_s (36) = -0.167, P = 0.330), indicating that the degree to which an ependymal cell is coupled does not affect its response to ACh. The cholinergic response of CSFcCs ranged from depolarisations of 0.95 mV to 42.33 mV, with an average response of 17.14 ± 1.24 mV (n = 82; Figure 5.1F), a time to onset of the response of 202.28 ± 24.59 ms (n = 81) and a time from onset to peak amplitude of the depolarisation of 793.25 ± 61.90 ms (n = 82). Due to the wide variety in the amplitude of the cholinergic CSFcC response, the responses of different CSFcCs subtypes (defined in chapter 3.2) to ACh were investigated. Subtype 1 CSFcCs responded with depolarisations ranging from 0.95 to 3.63 mV, with an average amplitude of 2.19 ± 0.22 mV (n = 17; Figure 5.1B, F), a time to onset of the response of 143.71 ± 21.60 ms (n = 17; Figure 5.2A) and a time from onset to peak amplitude of the depolarisation of 1620.00 ± 113.15 ms (n = 17; Figure 5.2B). Subtype 2 CSFcCs responded with depolarisations ranging from 4.82 mV to 33.14 mV, with an average response of 18.92 ± 1.21 mV (n = 46; Figure 5.1C, F), a time to onset of the response of 246.68 ± 41.76 ms (n = 45; Figure 5.2A) and a time from onset to peak amplitude of the depolarisation of 573.86 ± 54.64 ms (n = 46; Figure 5.2B). Subtype 3 CSFcCs responded with depolarisations ranging from 7.02 mV to 42.33 mV, with an average response of 26.19 ± 2.20 mV (n = 19; Figure 5.1D, F), a time to onset of response of 149.53 ± 20.09 ms (n = 19; Figure 5.2A) and a time from onset to peak amplitude of response of 584.68 ± 57.37 ms (n = 19;

Figure 5.2B). The depolarisations evoked by ACh in subtype 2 and 3 CSFcCs were sometimes accompanied by a spike or multiple spikes (Figure 5.1D).

A one-way ANOVA revealed that there was a significant difference in the amplitude of the cholinergic response of ependymal cells, subtype 1 CSFcCs, subtype 2 CSFcCs and subtype 3 CSFcCs ($F_{(3, 113)} = 80.315$, $P < 0.001$). Post-hoc tests revealed there was no significant difference between the amplitude of the cholinergic response in ependymal cells and subtype 1 CSFcCs ($P = 1$), however, the amplitudes of these responses were significantly smaller than those of both subtype 2 and subtype 3 CSFcCs ($P < 0.001$; Figure 5.1E, F). The amplitude of the cholinergic response of subtype 2 CSFcCs was also found to be significantly smaller than that of subtype 3 CSFcCs ($P = 0.001$; Figure 5.1 E, F). There was no significant difference in the time to onset of response between ependymal cells, subtype 1 CSFcCs, subtype 2 CSFcCs and subtype 3 CSFcCs ($H(3) = 0.659$, $P = 0.883$; Figure 5.2A); this was determined using a Kruskal-Wallis H test as the data was not normally distributed. There was a significant difference in the time from onset to peak response between ependymal cells, subtype 1 CSFcCs, subtype 2 CSFcCs and subtype 3 CSFcCs ($H(3) = 66.857$, $P < 0.001$); this was also determined using a Kruskal-Wallis H test as the data was not normally distributed. To further identify between which groups the time to peak response was significantly different, Mann-Whitney U tests were used. These determined that the time to peak response was significantly longer in ependymal cells and subtype 1 CSFcCs than in subtype 2 and 3 CSFcCs ($P < 0.001$; Figure 5.2B). There was no significant difference in the time to peak response between ependymal cells and subtype 1 CSFcCs ($P = 0.350$) or between subtype 2 and 3 CSFcCs ($P = 0.502$).
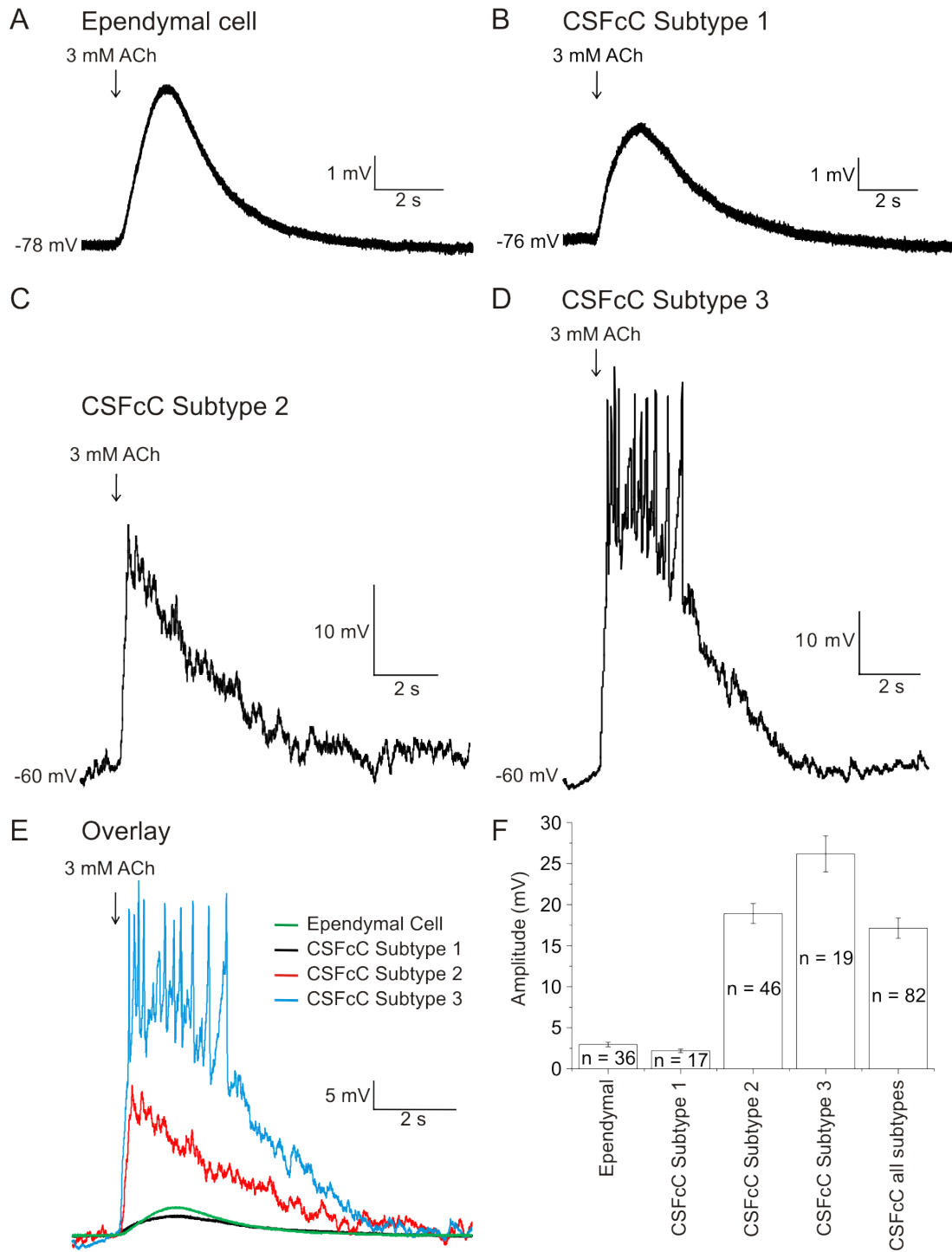
Figure 5.1: Ependymal cells and CSFcCs respond to ACh.

Whole cell patch clamp traces in current clamp from an ependymal cell (A), a subtype 1 CSFcC (B), a subtype 2 CSFcC (C), a subtype 3 CSFcC (D) and all cell types (E) in response to the focal pressure application of ACh (3 mM; 500 ms). F) Amplitude ± S.E of the response to ACh, depending on cell type and cell subtype (see text section 5.2.1 for significance).
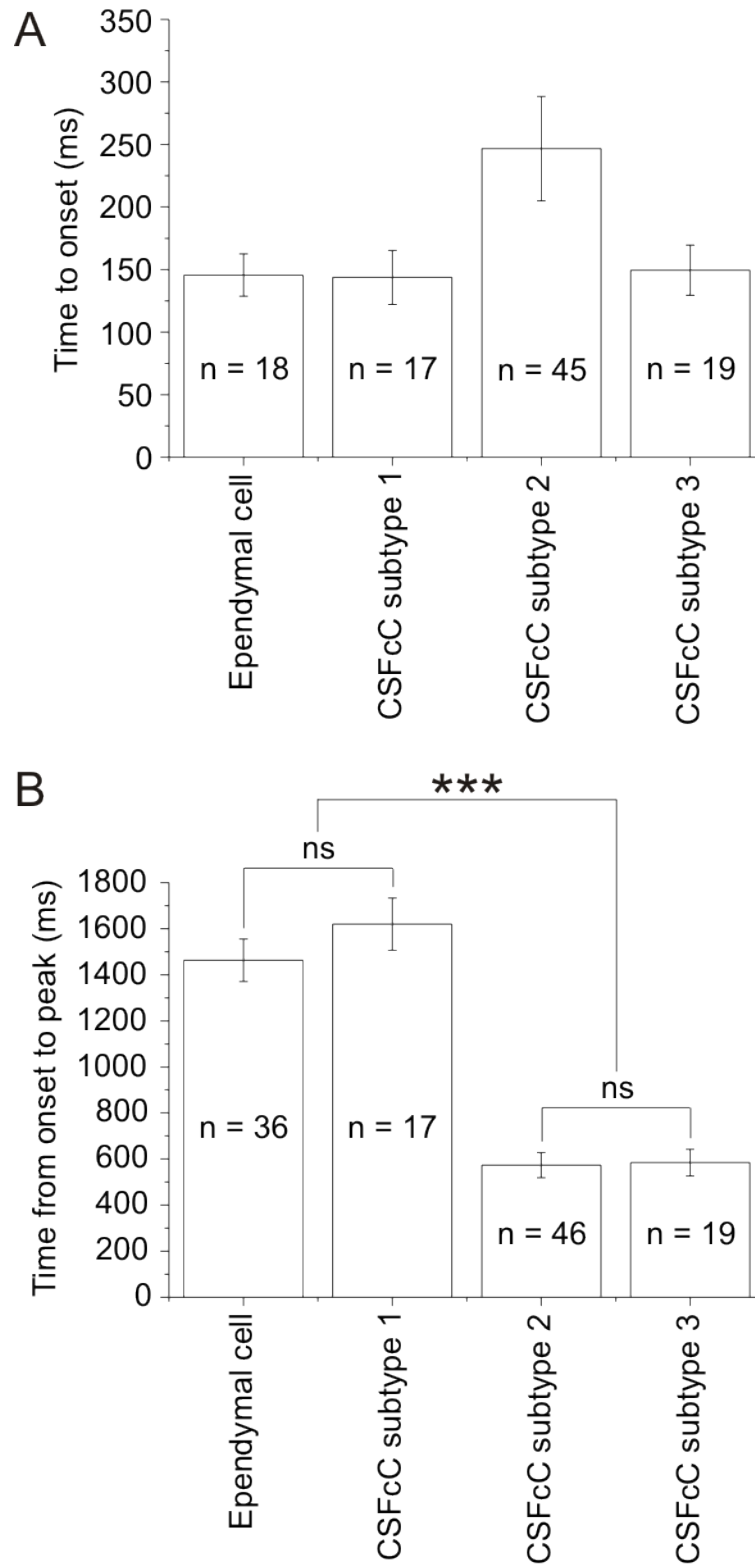
Figure 5.2: The kinetics of the cholinergic response vary between ependymal cells and some CSFcC subtypes.

Time to onset of response (ms; A) and time from onset to peak of response (ms; B) for ependymal cells, subtype 1 CSFcCs, subtype 2 CSFcCs and subtype 3 CSFcCs. *** = p < 0.001, ns = not significant.

5.2.2 The cholinergic response of ependymal cells and CSFcCs is likely due to a direct effect

To give an indication of whether ACh was having a direct effect on ependymal cells and CSFcCs, it was applied in the presence of the voltage-gated Na^+ channel blocker, TTX and in the case of CSFcCs, the glutamate receptor antagonists, AP5 and NBQX. In ependymal cells, there appeared to be a trend towards a small decrease in the amplitude of the response to ACh (3-10 mM; 500 ms; Figure 5.3A), however, a repeated measures ANOVA determined that there was no significant difference between the amplitude of the response during control conditions (2.41 ± 0.75 mV; n = 3), during the bath application of TTX (1.90 ± 0.62 mV; n = 3) and following the wash out of TTX (2.19 ± 0.56 mV; n = 3; Figure 5.3Ai). In CSFcCs, a repeated measures ANOVA determined that there was a significant difference between the amplitude of the response to ACh (3 mM; 500 ms) during control conditions (21.97 ± 5.93 mV; n = 5), during the bath application of TTX (1 µM), AP5 (50 µM) and NBQX (20 µM; 23.82 ± 6.43 mV; n = 5) and following the wash out of drugs (19.27 ± 5.46 mV; n = 5; F (2) = 6.888, P = 0.018; Figure 5.3B). Post-hoc bonferroni tests, however, did not reveal any significant difference between the individual groups of control, drug and wash data. These responses were independent of CSFcC subtype. There was no significant difference in the time to onset of the response from control conditions (183.80 ± 80.64 ms; n = 5), during TTX, AP5 and NBQX (219.40 ± 92.62 ms; n = 5) and following the wash out of drugs (252.00 ± 100.70; n = 5; X^2 (2) = 2.211, P = 0.331) in CSFcCs; this was determined using a Friedman test as the data was not normally distributed. There was also no significant difference in the time to peak response from control conditions (1029.40 ± 157.49 ms; n = 5), during TTX, AP5 and NBQX (1066.80 ± 243.72 ms; n = 5) and following the wash out of drugs (1373.00 ± 352.63 ms; n = 5; X^2 (2) = 2.800, P = 0.247) in CSFcCs.
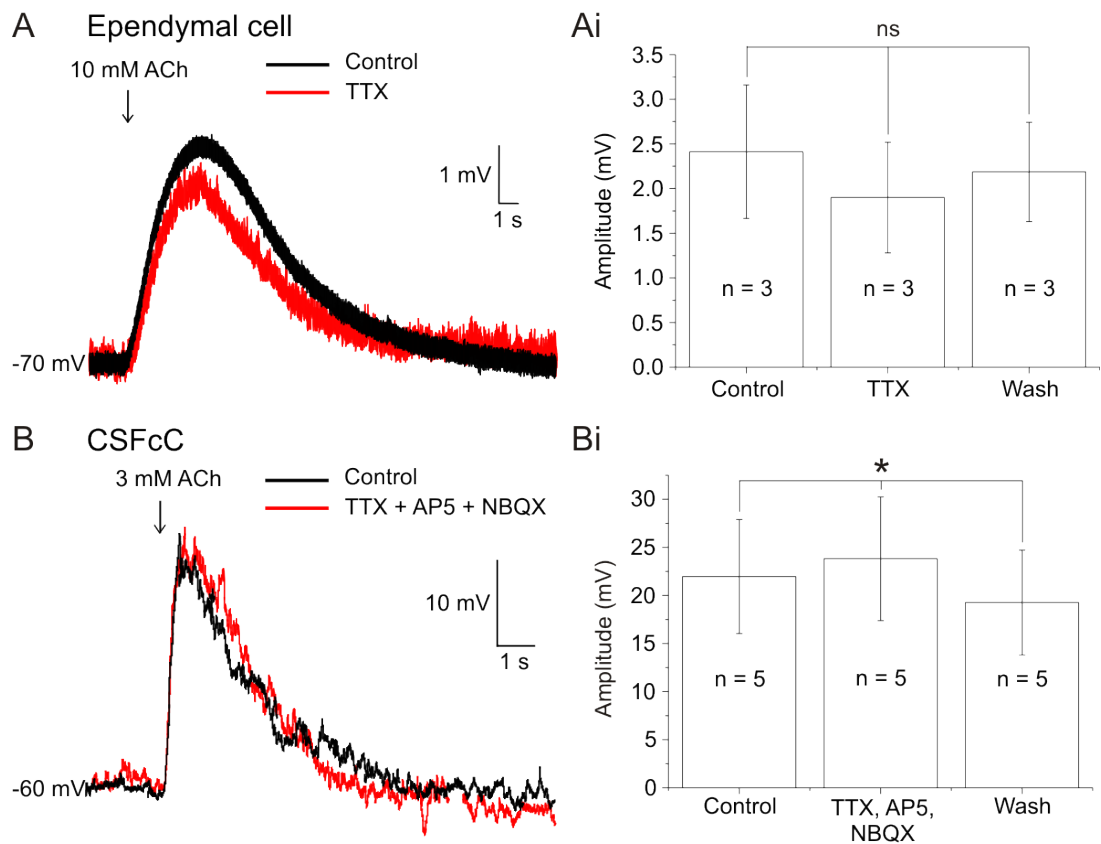
Figure 5.3: The cholinergic response of ependymal cells and CSFcCs is still present during the application of synaptic blockers.

A) Whole cell patch clamp trace in current clamp of an ependymal cell in response to the focal pressure application of ACh (10 mM; 500 ms) during control conditions and during the bath application of TTX (1 µM). Ai) Mean amplitude ± S.E in response to ACh in control conditions, during TTX and following wash out of the compounds, ns = not significant. B) Whole cell patch clamp trace in current clamp of a CSFcC in response to the focal pressure application of ACh (3 mM; 500 ms) during control conditions and during the bath application of TTX (1 µM), AP5 (50 µM) and NBQX (20 µM). Bi) Mean amplitude ± S.E in response to ACh in control conditions, during TTX, AP5 and NBQX and following wash out of the compounds, * = p < 0.05.

5.2.3 The cholinergic responses are mediated by nicotinic receptors

To understand what type of channel was mediating the cholinergic effects the injected current was adjusted to modify the membrane potential; ACh was then applied at different membrane potentials to determine whether the amplitude of the response is dependent on membrane potential and at what membrane potential the current reverses. In CSFcCs, the amplitude of the response to ACh (10 mM; 500 ms) decreased at less negative membrane potentials, with negligible response observed at 0 mV (Figure 5.4A); indicative that the cholinergic response is mediated by non-selective cation channels such as nicotinic rather than muscarinic receptors. In ependymal cells, however, the amplitude of the response to ACh (10 mM; 500 ms) did not vary at different membrane potentials (Figure 5.4B); this could be due to the highly coupled nature observed in chapter 4.
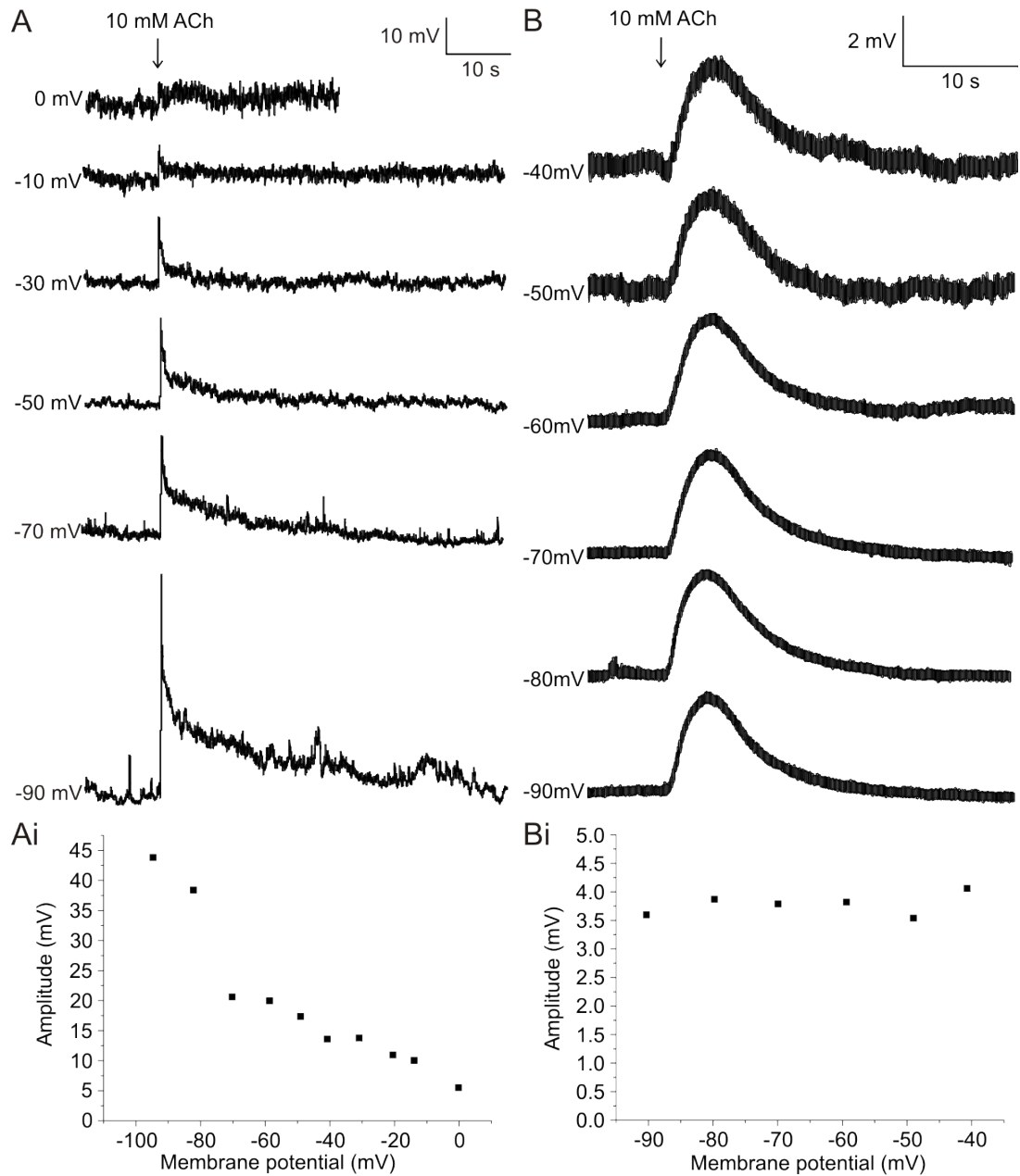
Figure 5.4: Cholinergic responses reverse at 0 mV in CSFcCs but not in ependymal cells.

Whole cell patch clamp traces in current clamp (A, B) and scatter plots (Ai, Bi) of the response to ACh (10 mM) when different amounts of current were applied to adjust the membrane potential for a CSFcC (A) and an ependymal cell (B).

To further investigate which receptors are mediating the cholinergic response, selective antagonists and modulators were utilised; the amplitude of the response to ACh (3 mM; 500 ms) was measured during the bath application of the muscarinic selective antagonist, atropine (5 µM) or the nicotinic selective antagonist, MCA (50 µM). There was no significant difference between the amplitude of the cholinergic response in ependymal cells during control conditions (3.56 ± 0.2 mV; n = 3) and during the bath application of atropine (3.13 ± 0.33 mV; n = 3; $t(2) = 1.867$, $P = 0.203$; Figure 5.5A). Neither was there a significant difference between the time to peak response during control conditions (2161.00 ± 119.92 ms; n =3) and during atropine (2251.00 ± 188.86 ms; n = 3; $t(2) = -0.632$, $P = 0.592$). There was also no significant difference between the amplitude of the cholinergic response in CSFcCs during control conditions (29.58 ± 3.66 mV; n = 4) and during the bath application of atropine (25.83 ± 3.45 mV; n = 4; $t(3) = 2.536$, $P = 0.085$; Figure 5.5B). Again, there was no significant difference between the time to peak response during control conditions (711.25 ± 149.96 ms; n = 4) and during atropine (527.64 ± 92.62 ms; n = 4; $t(3) = 0.742$, $P = 0.512$). The effect of atropine on CSFcCs did not vary with subtype. MCA significantly decreased the amplitude of the response to ACh in ependymal cells from 2.87 ± 0.88 mV (n = 6) to 0.24 ± 0.07 mV (n =6; $t(5) = 3.186$, $P = 0.024$; Figure 5.5C); the ACh response in MCA was only 9 ± 2 % of the initial ACh response. MCA also decreased the amplitude of the ACh response in CSFcCs from 17.9 ± 2.33 mV (n = 6) to 1.13 ± 0.54 mV (n = 6; $t(5) = 7.094$, $P = 0.001$; Figure 5.5D); the ACh response in MCA was only 6 ± 4 % of the initial ACh response. The extent of MCA antagonism in CSFcCs did not vary with subtype. Differences in the time to peak response were not analysed as it could not always be measured in the cases of complete antagonism by MCA. There was sometimes a partial reversal of the MCA antagonism, however, this was only after 30-60 minutes and a return to the original amplitude of the ACh response was never observed (n = 6, ependymal; n = 6, CSFcC). Neither atropine nor MCA had any observable effects on the membrane potential or input resistance of either ependymal cells or CSFcCs when applied alone.

There are many different nAChRs composed of different subunits, therefore to further elucidate the receptors that were mediating the ACh response, drugs selective for non α7*nAChRs and α7*nAChRs were utilised.
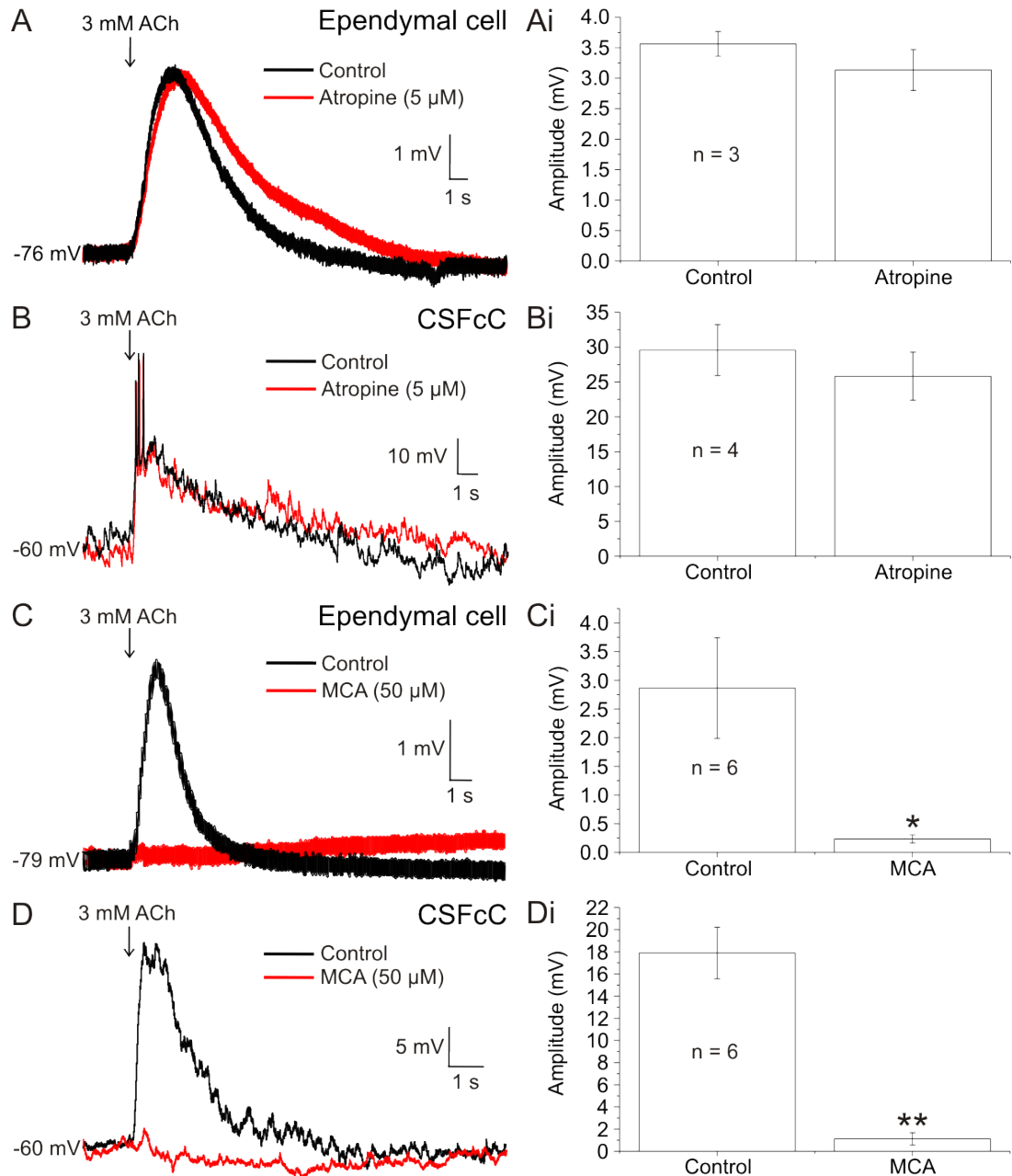
Figure 5.5: Cholinergic responses are mediated by nicotinic ACh receptors.

Whole cell patch clamp traces in current clamp and mean ± S.E of the amplitude of the response to ACh (3 mM; 500 ms) under control conditions and during the bath application of atropine (5 µM) for ependymal cells (A, Ai) and CSFcCs (B, Bi) and during the bath application of MCA (50 µM) for ependymal cells (C, Ci) and CSFcCs (D, Di). * = p < 0.05, ** = p < 0.01. Note the differences in scale and y-axis for cell types.

5.2.4 Contribution of non α7*nAChRs to the cholinergic response is dependent on cell type and cell subtype

To determine whether non α7*nAChRs mediate the cholinergic effect in ependymal cells and CSFcCs, DHβE, was bath applied during the focal pressure application of ACh (3 mM; 500 ms). DHβE is a selective non α7*nAChR antagonist at the concentration used in this study (1 μM).

DHβE significantly decreased the amplitude of the response of ependymal cells to ACh from 3.72 ± 0.66 mV (n = 9) to 1.87 ± 0.38 mV (n = 9; t (8) = 5.208, P = 0.001; Figure 5.6A). DHβE also significantly decreased the amplitude of the response of CSFcCs to ACh from 16.11 ± 1.84 mV (n = 20) to 3.03 ± 0.51 mV (n = 20; t (19) = 7.947, P < 0.001). Despite the effect on amplitude of the response, there was no significant difference between the time to peak response in ependymal cells in control (1810.00 ± 181.01 ms; n = 9) and in DHβE (1779.67 ± 179.33; n =9; t (8) = 0.513, P = 0.622) and in CSFcCs in control (972.61 ± 155.84 ms; n = 18) and in DHβE (1290.28 ± 211.90 ms; n = 18; data not normally distributed; Z = -1.546, P = 0.122). The decrease in amplitude of the cholinergic response in the presence of DHβE was expressed as a percentage of the initial ACh response to allow comparison of the effect of DHβE on the two cell types. The antagonism of the ACh response by DHβE was significantly greater in CSFcCs than in ependymal cells (t (27) = 4.608, P < 0.001; Figure 5.6E), with a cholinergic response of 23 ± 4 % that of the initial ACh response (n = 20) in CSFcCs and 52 ± 4 % in ependymal cells (n = 9). This suggests a greater contribution of non α7*nAChRs to the cholinergic response in CSFcCs.

Separating the CSFcCs into the defined subtypes revealed that there was a differential effect of DHβE on the specific subtypes. DHβE significantly decreased the amplitude of the ACh response of subtype 1 CSFcCs from 2.82 ± 0.44 mV (n = 3) to 1.48 ± 0.31 mV (n = 3; t (2) = 8.916, P = 0.012; Figure 5.6B), subtype 2 CSFcCs from 16.84 ± 1.42 mV (n = 11) to 3.86 ± 0.68 mV (n = 11; t (10) = 11.506; P < 0.001; Figure 5.6C) and subtype 3 CSFcCs from 21.42 ± 2.29 mV (n = 6) to 2.29 ± 1.01 mV (n = 6; t (5) = 6.551, P = 0.001; Figure 5.6D). To allow the comparison of the degree of antagonism of DHβE between the different CSFcC subtypes, the decrease in amplitude of the cholinergic response during the bath application of DHβE was expressed as a percentage of the initial ACh response. In the presence of DHβE the ACh response was 52 ± 4 % (n = 3) of the initial

response in subtype 1 CSFcCs, 22 ± 3 % (n = 11) in subtype 2 CSFcCs and 9 ± 4 % (n = 6) in subtype 3 CSFcCs. A two-way ANOVA determined that there was a significant interaction between the effects of DHβE and CSFcC subtype on the amplitude of the ACh response (F (2, 34) = 16.997, P < 0.001). Post-hoc bonferroni tests revealed that the antagonism by DHβE was significantly greater in subtype 2 and subtype 3 CSFcCs compared to subtype 1 CSFcCs (P < 0.001) and in subtype 3 CSFcCs compared to subtype 2 CSFcCs (P = 0.049; Figure 5.6E). This suggests that the contribution of non α7*nAChRs to the cholinergic response is greatest in subtype 3 CSFcCs, followed by subtype 2 CSFcCs and finally, the contribution is least in subtype 1 CSFcCs.

Although the effect of DHβE on the cholinergic responses was significantly different in ependymal cells compared to CSFcCs as a whole group, when the CSFcCs became divided into subtypes the effect of DHβE on the cholinergic responses of subtype 1 CSFcCs was not significantly different from that of ependymal cells (t (10) = -0.013, P = 0.990).

Despite the effects of DhβE on the ACh-induced response, there was no observable effect of DhβE alone on the membrane potential or input resistance of either ependymal cells or CSFcCs.

5.2.5 α7*nAChRs contribute to the cholinergic response

Although non α7*nAChRs clearly mediate a component of the cholinergic response in all cell types studied, DHβE, did not completely antagonise the cholinergic response. Therefore, the contribution of α7*nAChRs was investigated using MLA, which is a selective α7*nAChR antagonist at the concentration used in this study (20 nM; Wonnacott et al., (1993)).

Bath application of MLA significantly decreased the amplitude of the cholinergic response in ependymal cells from 4.05 ± 0.84 mV (n = 6) to 3.47 ± 0.8 mV (n = 6; t (5) = 4.420, P = 0.007; Figure 5.7A). The amplitude of the cholinergic response in CSFcCs was also significantly decreased in MLA from 24.23 ± 3.55 mV (n = 8) to 19.65 ± 3.39 mV (n = 8; t (7) = 3.877, P = 0.006; Figure 5.7B). There was no significant difference between the time to peak response during control (1952.33 ±

Figure 5.6: Non α7*nAChRs contribute to the cholinergic responses of ependymal cells and CSFcCs.

Whole cell patch clamp traces in current clamp (A-D) and mean amplitude ± S.E of the response (Ai-Di) to ACh (3 mM; 500 ms) under control conditions and during the bath application of DHβE (1 μM) in ependymal cells (A), subtype 1 CSFcCs (B), subtype 2 CSFcCs (C) and subtype 3 CSFcCs (D). E) Mean amplitude ± S.E of the response to ACh during the bath application of DHβE expressed as a percentage of the initial response to ACh, for ependymal cells, CSFcCs and CSFcC subtypes. ns = not significant, * = $p < 0.05$, ** = $p < 0.01$, *** = $p < 0.001$.
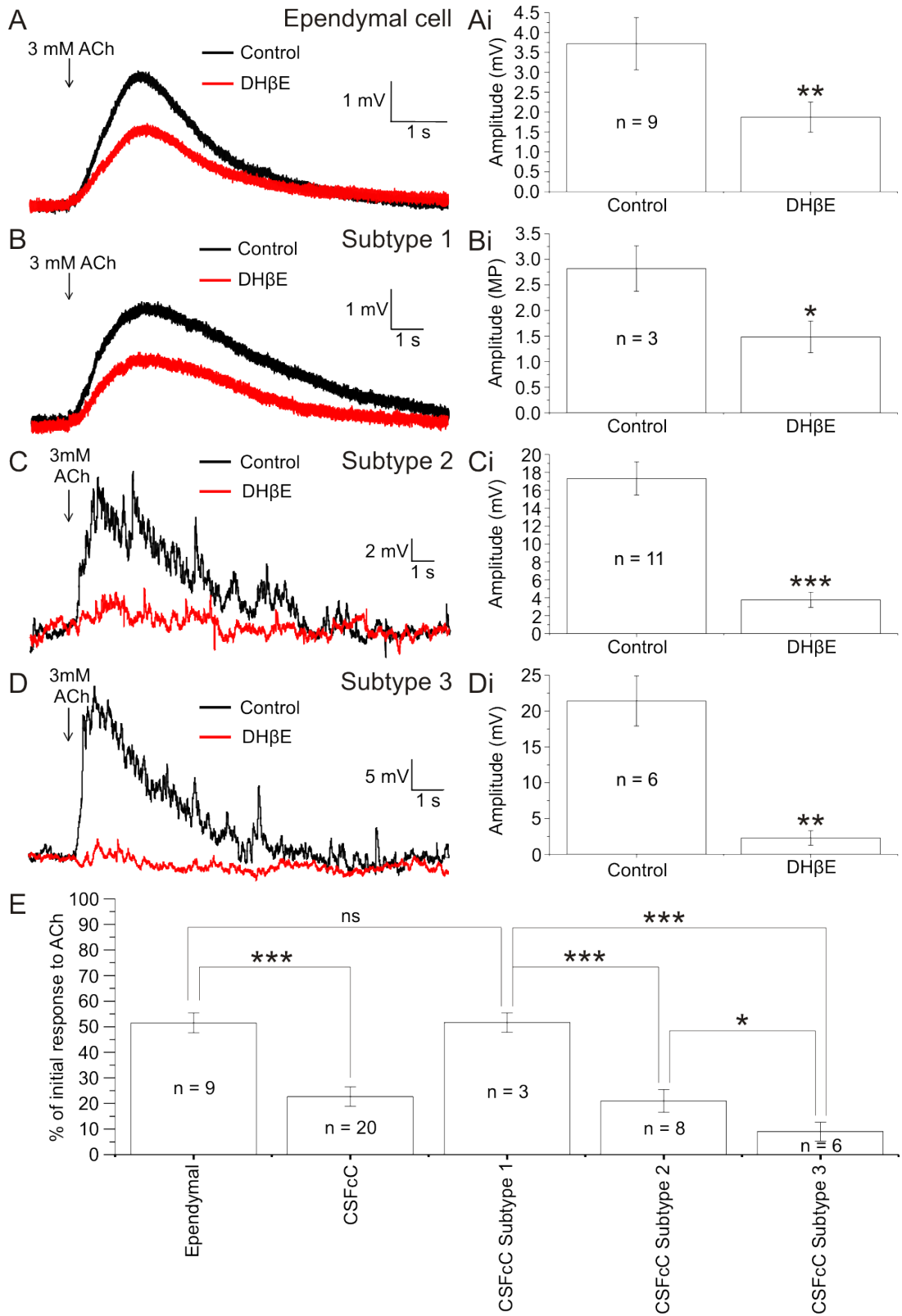
Figure 5.7: Antagonism by MLA demonstrates that α7*nAChRs contribute to the cholinergic response in both ependymal cells and CSFcCs.

Whole cell patch clamp traces in current clamp (A, B) and mean ± S.E of the amplitude of the response to ACh (3 mM; 500 ms; Ai, Bi) under control conditions and during the bath application of MLA (20 nM) for ependymal cells (A, Ai) and CSFcCs (B, Bi). ** = $p < 0.01$.

96.79 ms; n = 6) and during MLA (2046.83 ± 149.68 ms; n =6) for ependymal cells
(t (5) = -1.297, P = 0.251) and during control (600.00 ± 71.96 ms; n = 8) and during
MLA (621.50 ± 76.63 ms; n = 8) for CSFcCs (data not normally distributed; Z =
0.000, P = 1). As for the DHβE results, the decrease in amplitude of the cholinergic
response in the presence of MLA was expressed as a percentage of the initial ACh
response to allow comparison of the effect of MLA on the two cell types. In
ependymal cells, the ACh response in MLA was 84 ± 4 % of the initial ACh
response (n = 6) and in CSFcCs it was 80 ± 5 % (n = 8); the effect in MLA was not
significantly different in the two cell types (t (12) = 0.494, P = 0.630). The effect of
MLA on different CSFcC subtypes was not investigated. Despite the effect of MLA
on the ACh-induced response, there was no observable effect of MLA on the
membrane potential or input resistance of either ependymal cells or CSFcCs when
applied alone.

The selective α7*nAChR potentiator, PNU-120596, was employed to further
investigate the contribution of the α7*nAChRs to the cholinergic responses. Bath
application of PNU-120596 (10 µM) potentiated the cholinergic responses in both
ependymal cells and CSFcCs (Figure 5.8). In ependymal cells there was a
significant increase in the amplitude of the cholinergic response from 1.19 ± 0.17
mV (n = 6) during control to 3.88 ± 1.02 mV (n = 6) during PNU-120596 (t (5) = -
2.879, P = 0.035; Figure 5.8Ai) and in the time to peak response from 954.67 ±
135.15 ms (n = 6) during control to 1847.33 ± 327.92 ms (n = 6) during PNU-
120596 (t (5) = -4.221, P = 0.008; Figure 5.8Aii). In CSFcCs there was a significant
increase in the amplitude of the cholinergic response from 10.48 ± 2.23 mV (n = 9)
during control to 27.84 ± 6.82 mV (n = 9) during PNU-120596 (t (8) = -3.095, P =
0.015; Figure 5.8Bi) and in the time to peak amplitude from 776.33 ± 140.37 ms (n
= 9) during control to 3551.78 ± 1399.18 (n = 9) during PNU-120596 (data not
normally distributed; Z = -2.666, P = 0.008; Figure 5.8Bii). When expressed as
percentages of the initial ACh response, the percentage increase in the amplitude
of the response in PNU-120596 of ependymal cells, 323 ± 78 %, was not
significantly different from that of CSFcCs, 284 ± 45 % (t (13) = 0.469, P = 0.647;
data not shown). Despite the significant effects of PNU-120596 on the ACh-induced
response, it did not have any effects on the membrane potential or input resistance
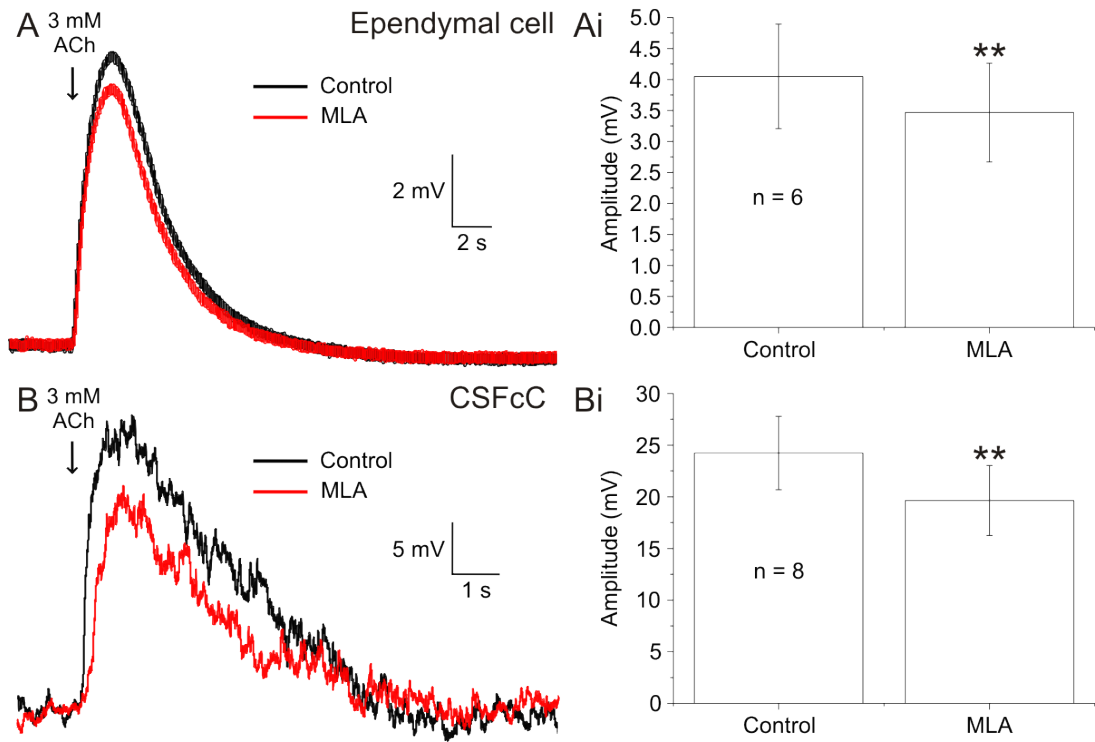of either ependymal cells or CSFcCs when applied alone.
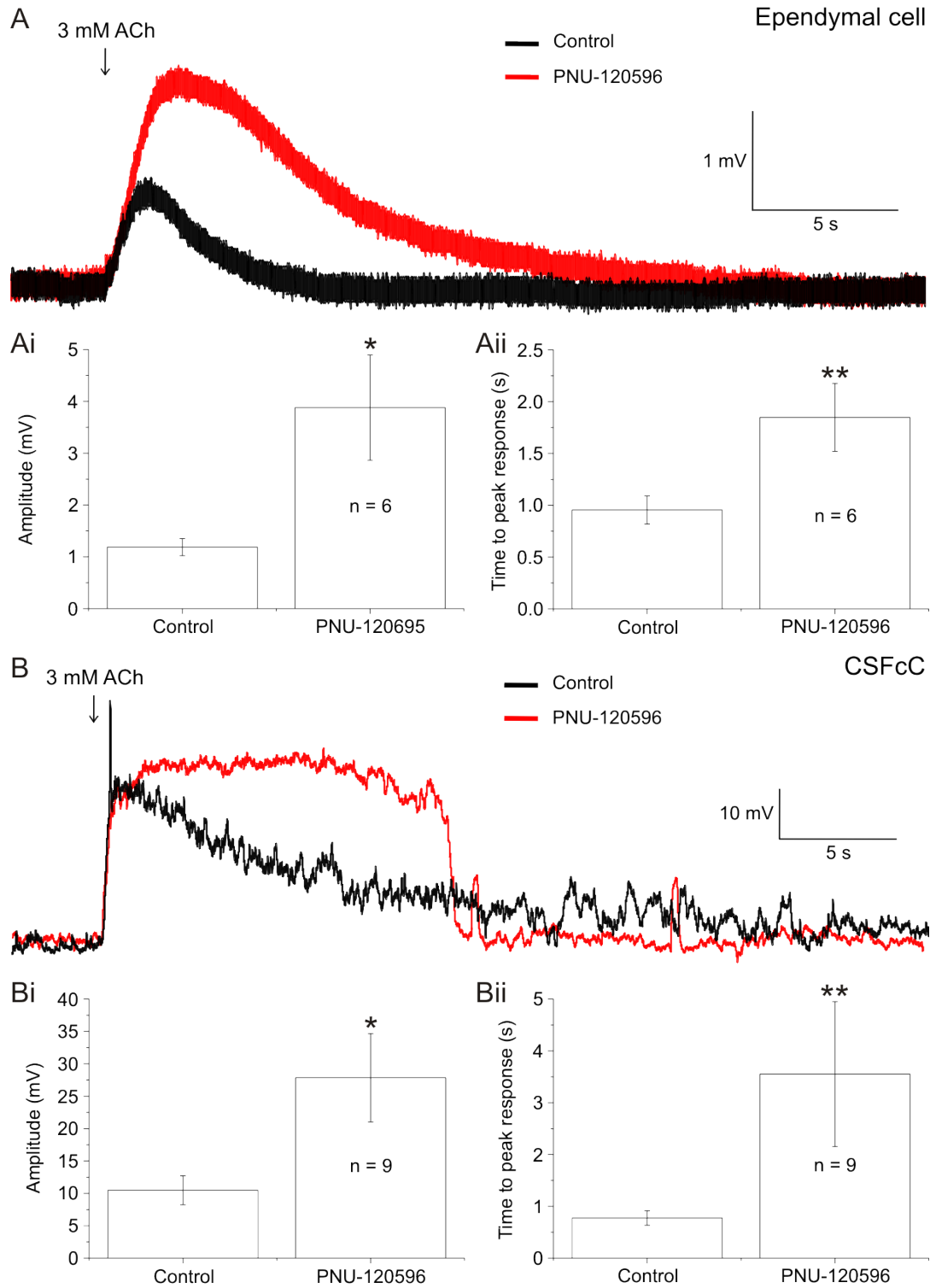
Figure 5.8: Potentiation by PNU-120596 demonstrates that α7*nAChRs contribute to the cholinergic response in both ependymal cells and CSFcCs.

Whole cell patch clamp traces in current clamp (A, B), mean ± S.E of the amplitude of the response to ACh (3 mM; 500 ms; Ai, Bi) and mean ± S.E of the time to peak response (Aii, Bii) during control conditions and during the bath application of PNU-120596 (10 µM) for ependymal cells (A) and CSFcCs (B). * = $p < 0.05$, ** = $p < 0.01$.

The percentage increases observed in the presence of PNU-120596 could be distorted by the different contribution of the non $\alpha7^*$nAChRs in the two cell types. This distortion also makes it difficult to study the effect of PNU-120596 on the different CSFcC subtypes. To remove this distorting factor, the effect of PNU-120596 on the cholinergic response was investigated in the presence of the non $\alpha7^*$nAChR antagonist, DHβE; therefore only the residual $\alpha7^*$nAChR mediated ACh response was potentiated. In ependymal cells there was a significant increase in the amplitude of the cholinergic response from 1.51 ± 0.23 mV (n = 4) during DHβE only to 7.30 ± 1.85 mV (n =4) during DHβE plus PNU-120596 ($t_{(3)}$ = -3.247, P = 0.048; Figure 5.9A) and in the time to peak response from 1546.50 ± 185.69 ms (n = 4) during DHβE only to 3376.00 ± 173.27 ms (n = 4) during DHβE plus PNU-120596 ($t_{(3)}$ = -16.105, P = 0.001). In CSFcCs, there was also a significant increase in the amplitude of the cholinergic response from 3.64 ± 0.69 mV (n = 10) during DHβE only to 27.64 ± 4.03 mV (n = 10) during DHβE plus PNU-120596 ($t_{(9)}$ = -6.201, P < 0.001; Figure 5.9B), however, there was no significant difference in the time to peak response from 1368.50 ± 240.75 ms (n = 10) during DHβE only to 2185.30 ± 597.91 ms (n = 10) during DHβE plus PNU-120596 ($t_{(9)}$ = -1.525, P = 0.162). When expressed as percentages of the initial ACh response, the percentage increase in the amplitude of the response in DHβE plus PNU-120596 of ependymal cells, 496 ± 150 %, was still not significantly different from that of CSFcCs, 948 ± 195 % ($t_{(12)}$ = -1.377, P = 0.194; Figure 5.9C). When divided into subtypes, the percentage increase in the amplitude of the response in DHβE plus PNU-120596 was 496 ± 167 % (n = 2) for subtype 1 CSFcCs, 1010 ± 306 % (n = 5) for subtype 2 CSFcCs and 1147 ± 396 % (n = 3) for subtype 3 CSFcCs (Figure 5.9C). A two-way ANOVA determined that there was no significant interaction between the effects of DHβE plus PNU-120596 and CSFcC subtype ($F_{(2, 14)}$ = 0.664, P = 0.530). To confirm the selectivity of PNU-120596 for $\alpha7^*$nAChRs, PNU-120596 was applied in the presence of MLA in addition to DHβE. In CSFcCs, the potentiation of the cholinergic response by PNU-120596 could be completely antagonised by MLA (20 nM; n = 4; Figure 5.9D). A paired t-test found that there was no significant difference between the amplitude of the cholinergic response in DHβE alone and in DHβE, PNU-120596 and MLA ($t_{(3)}$ = 1.002, P = 0.39; Figure 5.9E), with an amplitude of the response in DHβE, PNU-120596 and MLA of 82 ± 20 % (n = 4) that of those in DHβE alone.

Figure 5.9: Potentiation by PNU-120596 in the presence of DHβE allows the α7*nAChR-mediated component of the cholinergic response in both ependymal cells and CSFcCs to be observed.

Whole cell patch clamp trace in current clamp (A, B) and mean ± S.E of the amplitude of the response to ACh (3 mM; 500 ms; Ai, Bi) during the bath application of DHβE (1 µM) and DHβE plus PNU-120596 (10 µM) for ependymal cells (A, Ai) and CSFcCs (B, Bi). C) Mean amplitude ± S.E of the response in DHβE plus PNU-120596 expressed as a percentage of the initial response to ACh in DHβE, for ependymal cells, CSFcCs and CSFcC subtypes. D) Whole cell patch clamp trace in current clamp to ACh in DHβE only and in DHβE plus PNU-120596 plus MLA. E) Mean amplitude ± S.E in DHβE only, DHβE plus PNU-120596 and DHβE plus PNU-120596 plus MLA. * = $p < 0.05$, *** = $p < 0.001$.
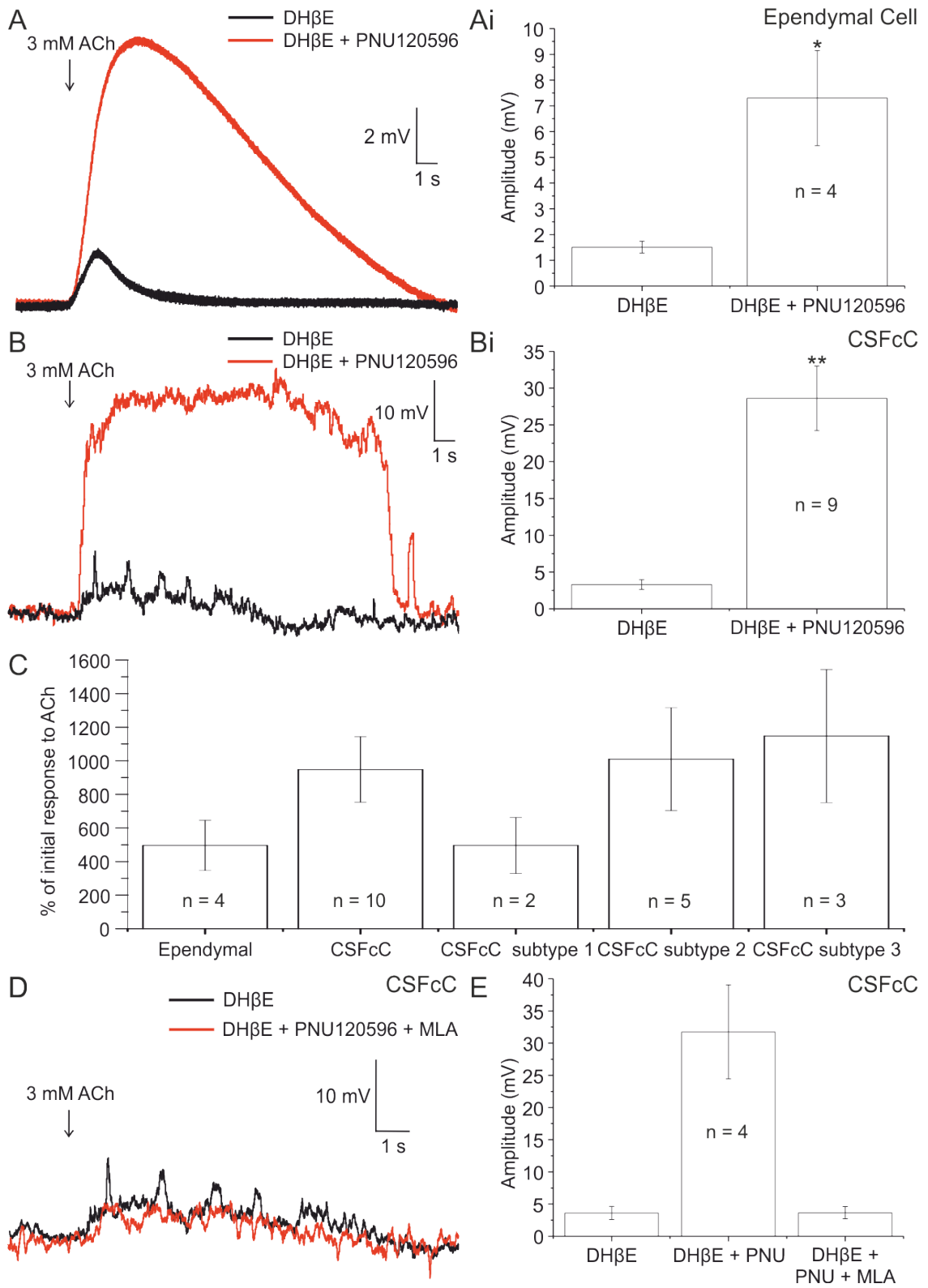
5.2.6 Cholinergic terminals could be the source of the ACh

Given the robust responses of all cell types investigated to ACh, it supports the theory that ACh could be influencing these cells. To aid in understanding the function of ACh on these cell types it is important to determine the source of the ACh. The first step towards this is to determine whether cholinergic terminals are found in close apposition to CSFcCs and ependymal cells. The presence of cholinergic structures in the vicinity of CSFcCs and ependymal cells was demonstrated using immunohistochemistry with an antibody raised against ChAT (Figure 5.10B, E). An antibody raised against PKD2L1 was used to selectively label CSFcCs (Figure 5.10A) and an antibody raised against calbindin was used to identify ependymal cells (Figure 5.10D). ChAT immunopositive structures formed close appositions to some CSFcCs (n = 3 rats; Figure 5.10C) and some ependymal cells (n = 1 rat; Figure 5.10F; immunohistochemistry for calbindin and ChAT was performed by Mukti Singh). The number of ChAT immunopositive structures in close apposition to CSFcCs and ependymal cells was not quantified; however, it was clear that not all of the cells received close appositions.
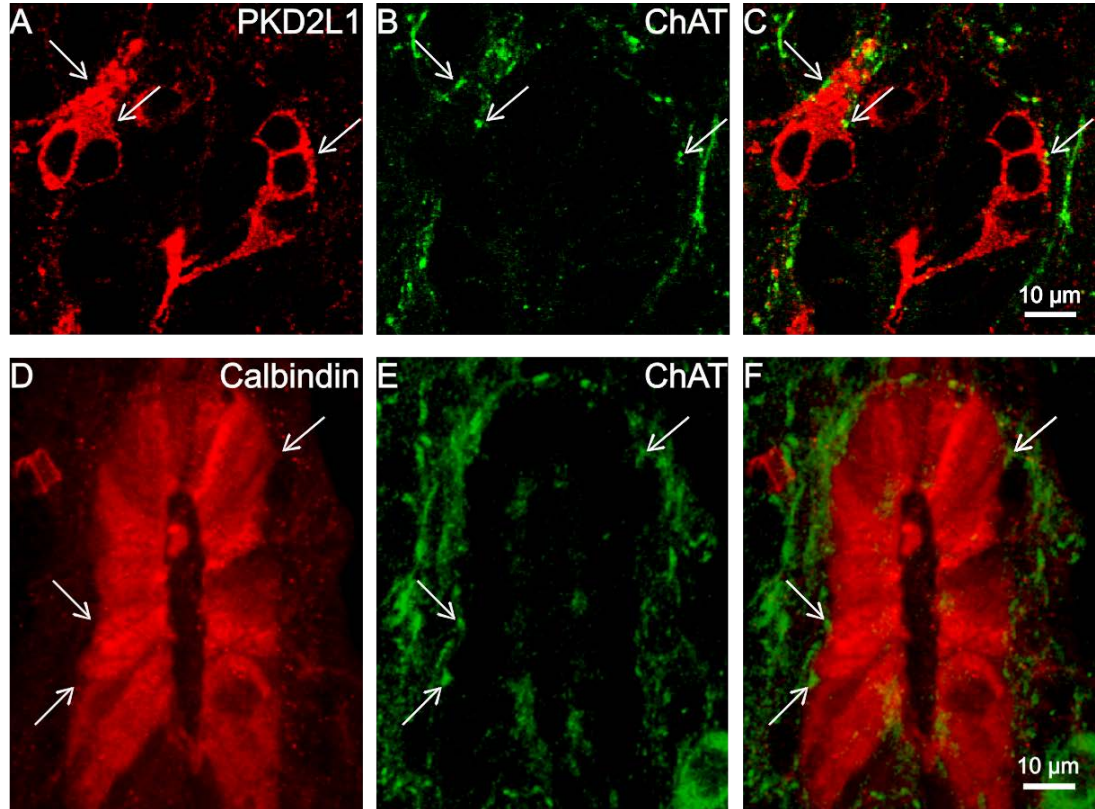
Figure 5.10: Cholinergic structures are found in close apposition to CSFcCs and ependymal cells.

A-C) PKD2L1 immunopositive cell bodies and CC-contacting processes of CSFcCs (A) and ChAT immunopositive structures (B) were observed around the CC of the thoracic spinal cord in P11 rats. Arrows highlight ChAT immunopositive structures that are in close apposition to PKD2L1 immunopositive CSFcCs (C). D-F) ChAT immunopositive structures (E) were also observed in close apposition to calbindin immunopositive ependymal cells (highlighted by arrows; D, F). The scale is the same for images A-C and D-F. Immunohistochemistry for calbindin and ChAT was performed by Mukti Singh.

5.3 Discussion

This chapter provides the first report that both ependymal cells and CSFcCs of the mammalian spinal cord can respond to ACh, thus proving the hypothesis set out at the beginning of this chapter. Moreover, the CSFcC subtypes defined in chapter 3 have responses to ACh of significantly different amplitudes. Evidence supports the idea that the responses are likely to be due to a direct effect of ACh on both the ependymal cells and CSFcCs, given the presence of cholinergic structures in close apposition to these cells and the continued occurrence of a response to ACh in the presence of TTX, NBQX and AP5. Pharmacology indicates that the responses are mediated by nAChRs, predominantly non α7*nAChRs but also by a smaller proportion of α7*nAChRs. The data also suggests that the contribution of non α7*nAChRs to the cholinergic response varies between ependymal cells and CSFcCs, as well as between CSFcC subtypes.

5.3.1 Cholinergic responses of ependymal cells and CSFcCs

The combination of the immunohistochemistry demonstrating the presence of cholinergic structures in close apposition to the CSFcCs and ependymal cells and the electrophysiology demonstrating the continued existence of the ACh response in the presence of TTX, suggests that the ACh responses are direct effects of ACh on receptors expressed by CSFcCs and ependymal cells. The lack of change in time to onset of the response in the presence of TTX also supports the theory that the effect is direct. Nevertheless, although the use of TTX ensures that action potential propagation along the axon cannot occur it does not necessarily prevent synaptic transmission. It is possible that ACh could be activating nAChRs located on a pre-synaptic terminal resulting in the direct influx of Na^+ and importantly Ca^{2+} which is capable of triggering synaptic vesicle release independent of an action potential. To prevent this possibility an extracellular solution with low Ca^{2+} would need to be used; however, this would also reduce the response of post-synaptic nAChRs, therefore low Ca^{2+} solutions were not used in this study. Immunohistochemistry demonstrating the presence of cholinergic structures in close apposition to CSFcCs and ependymal cells supports the idea that the cholinergic effect is direct, however, electron microscopy will need to be performed to confirm the presence of cholinergic synapses onto CSFcCs and ependymal cells. Also, it must be noted that not all CSFcCs and ependymal cells received close appositions from cholinergic structures. This could be the result of using an anti-ChAT antibody to identify cholinergic terminals. ChAT is the enzyme that catalyses

the synthesis of ACh, therefore it is not necessarily always present in cholinergic terminals, as ACh could be synthesised in the cell body and transported to the terminal. An alternative to anti-ChAT would be to use an anti-VAChT antibody. VAChT is the vesicular ACh transporter which must be present in all terminals to transport ACh into the synaptic vesicles; therefore it would identify all cholinergic terminals. This would also ensure that the ChAT immunopositive structures seen in close apposition to ependymal cells and CSFcCs are in fact terminals and not dendrites. It must also be noted that PKD2L1 has been shown to be a specific marker for CSF-contacting neurones (CSFcNs), with all recordings from PKD2L1-expressing cells showing a neuronal phenotype (Huang et al., 2006). It appears likely, therefore, that subtype 1 CSFcCs, which could be CC-contacting astrocytes (Accs; see chapter 3.3.1), do not express PKD2L1. To determine whether subtype 1 CSFcCs have cholinergic terminals in close apposition, it is possible that they could be identified by the expression of GFAP and the presence of a CC-contacting process; the criteria used by Alfaro-Cervello et al., (2012). Alternatively, immunohistochemistry for VAChT could be performed on recovered slices which have rhodamine-containing subtype 1 CSFcCs, although this method can be temperamental and has a low success rate (Deuchars et al., 2001). Finally, even if cholinergic synapses with ependymal cells or CSFcCs could not be demonstrated it would not necessarily mean that ACh is not acting directly on nAChRs expressed by the cells. There is now some evidence demonstrating that cholinergic transmission within the CNS does not always occur at synapses (see review Lendvai and Vizi (2008)). It has been discovered that in many areas of the CNS, cholinergic terminals do not form synapses; this was first demonstrated in the somatosensory cortex of the adult rat, where the synaptic incidence was only 14 % (Umbriaco et al., 1994). In addition, acetylcholinesterase, the enzyme responsible for the breakdown of ACh, has been localised in many areas that are distinct from cholinergic terminals or nAChRs, suggesting that it is monitoring the ambient levels of ACh that are present within the extracellular solution (Descarries et al., 1997). This ambient ACh would be capable of tonically activating nAChRs, which are most commonly found at peri- or extra-synaptic locations (Dani and Bertrand, 2007)). In fact, a constant nicotine exposure has been demonstrated to stabilise α4β2*nAChRs in a high affinity state that is more sensitive to ACh (Vallejo et al., 2005), suggesting that some nAChRs can adapt to respond robustly to low levels of ambient ACh. It is therefore possible that *in-vivo* ependymal cells and CSFcCs are influenced by ambient ACh acting on extrasynaptic nAChRs, either instead of or in addition to synaptic cholinergic transmission.

The variation in the amplitude of the ACh response in ependymal cells and different CSFcC subtypes is unlikely to be due to an inconsistency in the access of the drug to the slice as the different cell types and subtypes were all recorded from similar depths within the slices. They also had a similar time to onset of the response, suggesting that the time it took for the ACh to reach the cells was the same. Of note here is that a high concentration of 3 mM ACh was used for these experiments to ensure that on pressure application into the bathing aCSF solution the concentration would still be high enough to elicit a response; lower concentrations could have been diluted to such a low concentration that responses would not have been observed. The disadvantage of this is that the exact concentration reaching each cell could vary and that concentration is not known. Nevertheless there was an obvious variation in the cholinergic response of subtype 1 CSFcCs compared to that of subtype 2 and 3 CSFcCs which supports the conclusion from chapter 3.3 that subtype 1 CSFcCs are glial cells, likely the Accs described by Alfaro-Cervello et al., (2012). This is reinforced by the similarities observed between the subtype 1 CSFcC cholinergic responses and those of ependymal cells. There was also a more subtle difference in the cholinergic responses of subtype 2 and subtype 3 CSFcCs. This difference is more likely to be due to a different density of receptor expression or a difference in the proportions of receptors mediating the response.

The difference in the time to peak response between ependymal cells and subtype 1 CSFcCs compared to subtype 2 and 3 CSFcCs again suggests variation between the cell types. This corresponds with variations seen between glial cells and neurones within the hippocampus, for example, α7*nAChR-mediated currents in astrocytes have a much longer rise time than those of interneurones (Shen and Yakel, 2012). This difference could be brought about by varying intracellular ion concentrations between the glial and neuronal cells which result in differences in the speed of ion exchange. More likely, it is due to different secondary effects that occur following the initial nAChR activation. For example, in cultured hippocampal neurones, activation of nAChRs results in the activation of voltage-gated Ca^{2+} channels (Barrantes et al., 1995), whereas in cultured hippocampal astrocytes activation of nAChRs does not cause an activation of voltage-gated Ca^{2+} channels but can result in Ca^{2+} induced Ca^{2+} release from intracellular store (Sharma and Vijayaraghavan, 2001). This could be similar for the cells in this study, with subtype 2 and 3 CSFcCs expressing voltage-gated Ca^{2+} channels, while these channels are absent in ependymal cells and subtype 1 CSFcCs where a Ca^{2+} induced Ca^{2+} release mechanism is responsible for effects seen.

5.3.2 Evidence suggests that cholinergic responses are mediated by nAChRs

The variation in the amplitude of the cholinergic response at different membrane potentials and the reversal potential at roughly 0 mV in subtype 2 and 3 CSFcCs strongly suggests that non-selective cation channels are mediating the effect. The non-selective cation channels could be confirmed as nAChRs by the complete antagonism of the cholinergic response in CSFcCs by MCA, a selective nAChR antagonist. MCA also completely antagonised the cholinergic response in ependymal cells, strongly suggesting that this cholinergic response is also mediated by nAChRs. This was not verified by the investigation of the reversal potential. The amplitude of the response to ACh did not vary when the membrane potential of the ependymal cells were set between -40 mV and -90 mV. This is likely due to the large degree of coupling observed amongst ependymal cells (see figures 4.2 and 4.3), which makes it very difficult to control the set potential of an ependymal cell. The reversal potential could be investigated in the presence of a gap junction blocker, for example 18β-glycrrhetinic acid, to enable the membrane potential to be more easily controlled; however, the antagonism by MCA seems sufficient to identify the nAChR as that responsible for mediating the cholinergic response in ependymal cells.

5.3.3 Pharmacological profiles suggest both non α7*nAChRs and α7*nAChRs contribute to the cholinergic responses

The significant degree of antagonism of the ACh response observed in the presence of DHβE suggests that the cholinergic response is mediated in part by non α7*nAChRs in both ependymal cells and CSFcCs. *In-situ* hybridisation studies have revealed the expression of α2, α3, α4 and β2 nAChR subunits within lamina X of the spinal cord (Wada et al., 1989). As DHβE is a preferential antagonist at α4*nAChRs and β2*nAChRs (Harvey and Luetje, 1996; Harvey et al., 1996), and they are present within lamina X it is likely that α4β2*nAChRs are mediating this cholinergic effect on ependymal cells and CSFcCs, however, this needs further confirmation using DHβE at 10 nM which selectively antagonises α4β2*nAChRs (Alkondon and Albuquerque, 1993). The different degrees of antagonism of the cholinergic response by DHβE suggests that the non α7*nAChRs contribute to varying degrees within the cell types investigated. As with the size of the cholinergic response, the degree of antagonism by DHβE observed in subtype 1 CSFcCs was

similar to that of ependymal cells. The antagonism of the cholinergic response by DHβE was greatest in subtype 3 CSFcCs, suggesting that this subtype express the greatest proportion of non α7*nAChRs. Since DHβE is most effective at α4β2*nAChRs, a greater antagonism of the cholinergic response by DHβE could also suggest a greater proportion of α4β2*nAChRs compared to α3*- or β4*-nAChRs within the non α7*nAChRs.

Given that DHβE did not completely antagonise the cholinergic response, combined with the fact that an α7 nAChR subunit reporter mouse made by the GENSAT project showed some GFP expressing CSFcCs, the contribution of α7*nAChRs was examined. This was investigated using MLA which is an α7*nAChR selective antagonist at concentrations of 20 nM or lower (Wonnacott, 1993). The low concentration needed to be selective provides a potential problem when investigating its antagonism of the focal pressure application of a high concentration (3 mM) of ACh. Thus although a small, significant antagonism of the cholinergic response was observed in both ependymal cells and CSFcCs with MLA, it is possible that the proportion of α7*nAChRs mediating the cholinergic effect was being underestimated. In argument against this, the potentiation by PNU-120596 could be completely antagonised with MLA, suggesting that in fact MLA at 20 nM was sufficient to antagonise any α7*nAChR-mediated responses. If the MLA antagonism was entire, it suggests that although there is a difference in the amount of non α7*nAChRs in the cell types, there does not appear to be a difference in the proportion of α7*nAChRs.

The presence of α7*nAChRs was confirmed by the potentiation of the cholinergic response by PNU-120596. PNU-120596 is a type II positive allosteric modulator which increases the peak of the agonist evoked current, prolongs the agonist evoked response in the continued presence of the agonist and increases the mean channel open time of α7*nAChRs (Hurst et al., 2005). In addition, PNU-120596 is capable of reactivating desensitised α7*nAChRs (Gronlien et al., 2007). Importantly for this study, PNU-120596 has no detectable effect on currents mediated by α4β2*-, α3β4*- and α9α10*-nAChRs (Hurst et al., 2005), therefore, the potentiation that was seen in the presence of PNU-120596 is due to the presence of α7*nAChRs in the cells recorded. The type of effects that PNU-120596 is reported to have on α7*nAChR-mediated currents matched up well to the quantified increases in both amplitude and the time it took to reach the peak amplitude and the observation that it increased the duration of the cholinergic response in cells of

this study. Although the average percentage increase in the amplitude of the cholinergic response in ependymal cells was much smaller than that in CSFcCs, the large degree in variation within the cell types meant that there was a lack of significant difference between the two cell types. As the potentiation by PNU-120596 does not reach a maximum until 30-60 minutes of incubation in PNU-120596 (Shen and Yakel, 2012), the potentiation of the cholinergic response could vary depending on how long PNU-120596 has been applied before ACh was applied. In this case, however, ACh was always applied after a given time of incubation in PNU-120596; therefore this should not be contributing to the variation. The different contribution of non $\alpha 7^*$nAChRs could also be complicating the degree of potentiation observed by PNU-120596, which was why it was co-applied with DHβE following a pre-incubation in DHβE. There was still a large amount of variation in the degree of potentiation within the cell types. This is likely due to the inclusion of subtype 1 CSFcCs within the CSFcC cell type; other than their morphology these subtype 1 CSFcCs have characteristics that are indistinguishable from ependymal cells. The problem with variation could perhaps be overcome with an increase in replicates, however, with four different cell types, three of which cannot be morphologically distinguished; obtaining enough recordings to reduce the variation could be a lengthy procedure.

Despite the lack of significant difference between the CSFcC subtypes and ependymal cells with regards to their potentiation by PNU-120596, it looks like there is a trend towards a larger potentiation in subtype 2 and 3 CSFcCs compared to subtype 1 CSFcCs and ependymal cells. Initially this could be thought to suggest that the proportion of $\alpha 7^*$nAChRs contributing to the cholinergic response is greater in subtype 2 and 3 CSFcCs than in subtype 1 CSFcCs and ependymal cells, which would contradict the DHβE data. However, it is more likely that there are simply numerically more $\alpha 7^*$nAChRs on subtype 2 and 3 CSFcCs than on subtype 1 CSFcCs and ependymal cells, thus PNU-120596 has a greater number of receptors that it can affect on subtype 2 and 3 CSFcCs. Despite this larger number, the amount of $\alpha 7^*$nAChRs could still form a relatively low proportion of the nAChRs expressed by subtype 2 and 3 CSFcCs. Conversely, despite the potentiation of the cholinergic response appearing smaller in ependymal cells and subtype 1 CSFcCs, presumably due to a lower number of $\alpha 7^*$nAChRs; the proportion of $\alpha 7^*$nAChRs to non $\alpha 7^*$nAChRs is likely to be higher due to the DHβE data.

5.3.4 Conclusions

This chapter has demonstrated that both ependymal cells and CSFcCs of the mammalian spinal cord are capable of responding to ACh. The responses observed appear to be due to direct effects of ACh on somatodendritic nAChRs. Both non α7*nAChRs and α7*nAChRs appear to contribute to the cholinergic response and the proportions of this contribution appear to differ between cell types. These varied contributions highlight functional differences between the cell types. The demonstration in this study that ependymal cells and CSFcCs can respond to ACh is the first step towards determining whether ACh is affecting these cell types in a physiological system. There is currently no evidence of either cell type responding to endogenous ACh, for example no cholinergic EPSPs were observed nor were there any lone effects of cholinergic antagonists or modulators. Nevertheless, the nature of the preparation could have disrupted the normal source of ACh and the work strongly suggests that both cell types will be influenced by ACh under physiological conditions and thus suggests that they form an integrated part of the spinal cord circuitry.

Chapter 6 - General Discussion

This study has used whole cell patch clamp electrophysiology in an *in-vitro* spinal cord slice preparation, complimented by intracellular dye-loading and immunohistochemistry, to characterise the cells surrounding the CC of the postnatal mammalian spinal cord. This is an area that has received very little attention with regards to its integration into the spinal cord circuitry and the ability of the cells to respond to neurotransmitters and neuromodulators. This study has verified that there are CSFcCs with varying phenotypes, describing for the first time the electrophysiological responses of a glial class of CSFcC. It has demonstrated the large degree of coupling that occurs between ependymal cells and how radial ependymal cells are also part of this coupling. The findings have confirmed reports that CSF-contacting neurones (CSFcNs) respond to GABA and shown that ependymal cells can also respond to GABA. Finally, it has been demonstrated that both CSFcCs and ependymal cells respond to ACh and that this is likely to be a direct effect mediated by differing contributions of non α7*nAChRs and α7*nAChRs. The aims of this study were to investigate whether ependymal cells and CSFcCs are integrated into the spinal circuitry and establish parallels between this area and other postnatal neurogenic niches; the results summarised here provide evidence supporting the integration of these cells into spinal cord circuitry and that there are parallels to other neurogenic niches. Here, the functional implications of the gap junction coupling of ependymal cells and the ability of both ependymal cells and CSFcCs to respond to GABA and ACh will be discussed. Finally, technical considerations and limitations will be discussed before suggesting what future work could be undertaken to further our understanding of this area.

6.1 Functional implications

6.1.1 Are CSFcCs one cell type on a continuum of maturation or a number of cell types whose phenotypes are suited to specific functional roles?

One of the most intriguing debates concerning CSFcCs is whether they belong to one phenotype of cell but cells within that phenotype are at different stages of their functional maturation, or whether in fact CSFcCs have all reached their final phenotype and they are a varied population whose phenotype is most relevant to their function. It appears from this study that subtype 1 CSFcCs are a different phenotype to subtype 2 and 3 CSFcCs. The main evidence for this is that subtype 2 and 3 CSFcCs contain a range of characteristics on which a continuum can be established. From subtype 1 to 2 CSFcCs, however, there is a rather large leap

from completely passive responses and a very low input resistance in subtype 1 CSFcCs, to quite obvious active response properties and a much higher input resistance in subtype 2 CSFcCs. The electrophysiological profile of subtype 1 CSFcCs is consistent with that of a mature glial cell and the morphology corresponds well to the Accs identified by Alfaro-Cervello et al., (2012), although it has not been confirmed by ultrastructural or immunohistochemical studies whether the two cell types are indeed the same. If it is assumed that subtype 1 CSFcCs are Accs, it is interesting to note that Accs possess a primary cilium which contacted the CSF (Alfaro-Cervello et al., 2012); this is similar to the activated SVZ astrocytes, which are proposed to be the neural stem cells of the SVZ (Doetsch et al., 2002). Unfortunately, neither BrdU and [^{3}H]thymidine identified Accs as proliferating cells (Alfaro-Cervello et al., 2012), however, it cannot be ruled out that Accs are a quiescent cell population that could become activated following injury or a spinal cord pathology.

Determining the phenotype of subtype 2 and 3 CSFcCs, which can be collectively referred to as CSFcNs, appears much more complicated. The wide range of electrophysiological responses to the injection of positive current and the fact that they seem to range along a continuum rather than represent distinct subtypes, suggests one phenotype which contains cells that are at different stages of maturation. This is consistent with immunohistochemistry that has demonstrated the expression of numerous markers of immature neurones, such as Dcx, PSA-NCAM and HuC/D (Stoeckel et al., 2003; Hamilton et al., 2009; Marichal et al., 2009). Of note here is that these markers can also be observed in fully mature neurones that are consistently undergoing plastic changes, for example PSA-NCAM is expressed by neurones of the hypothalamo-neurohyphysial system which undergo dendritic remodelling (Theodosis et al., 1994). Therefore, the expression of these markers is not unequivocal evidence that they are immature neurones; they could be fully mature neurones which undergo numerous plastic changes. In support of this, CSFcNs do not express BrdU when injected postnatally; they only express it when it is injected during the embryonic period (Marichal et al., 2009), indicating that CSFcNs are not born postnatally. This is also corroborated by comparing the data in this study which was collected from P11-P21 rats to that of Marichal et al., (2009) which was collected in P0-P5 rats; together the data demonstrates that there is no change in the number of CSFcNs with certain firing patterns from P0 to P21. It was suggested by Marichal et al.,(2009) that the neurones could be in some kind of standby mode, waiting for a cue to continue

maturation. Preliminary evidence supports this suggestion, as CSFcNs appear to migrate following a peripheral nerve insult (Conte, 2009), however, this needs to be further investigated. The basal processes of CSFcNs that have been demonstrated to extend towards the ventral median fissure and ventral horn or laterally, possibly towards the IML, suggest that at least some of the CSFcNs are quite well developed and are not simple immature neurones. The variation in destination of the processes suggests that CSFcNs have different functions. It is possible that the processes are all coursing towards the external CSF; however, this work has demonstrated that they do seem to terminate within the grey matter. The CSFcNs are well placed in a central location of the spinal cord to integrate inputs from the dorsal horn and descending tracts from the brainstem and to subsequently communicate outputs to the lateral and ventral horns. It is possible that some CSFcNs communicate information to the SPNs in the IML that control autonomic output, whilst others communicate information to the motor neurones or premotor interneurones in the ventral horn that influence motor output. Their possible plastic nature could make them amenable to changes induced by sensory input from the periphery, dorsal horn or CSF; for example disruption to peripheral input caused by a peripheral nerve injury induced the migration of CSFcNs (Conte, 2009). Sensory input induced plastic changes in CSFcNs could be translated into a varied output to regions involved in autonomic and motor output. It is unclear to date whether it would be important for CSFcNs to respond to sensory input in physiological situations or whether it is only important during pathological situations. Further investigations need to be made considering the nature of CSFcNs to determine whether they are immature or plastic neurones and whether they are capable of responding to insult or sensory inputs. The future work sections will look at some of the ways in which they can be investigated.

6.1.2 Relevance of gap junction coupling within the CC region

Gap junctions are widely present in neurones to allow the rhythmic firing of groups of neurones (see review Connor & Long (2004)). Ependymal cells and subtype 1A CSFcCs, the gap junction coupled cells observed in this study, only generate passive responses, necessitating the question, what is the function of gap junctions in these cells? It has been proposed that ependymal cells could act as regulators of extracellular K^+, with K^+ moving into the cells at the basal surface from the

extracellular solution of the grey matter and exiting at the apical surface into the CSF, as observed in retinal müller cells (Newman, 1986; Jarvis and Andrew, 1988). The coupling of the ependymal cells could make this process more efficient, as K^+ could be shunted via ependymal cells in areas of high extracellular K^+ to ependymal cells in areas of lower extracellular K^+, as observed in glial syncytiums (see review Kofuji and Newman (2004)). Another possible reason for ependymal cells and subtype 1A CSFcCs to form gap junctions is to allow the control of cellular proliferation. Gap junction coupling occurs in ventricular regions of the embryonic neocortex and in the adult SVZ (Bittman et al., 1997; Liu et al., 2006a). During development, the coupling occurs only between radial glia and neural precursor cells, and is cell cycle phase dependent; uncoupling the cells decreases the number of cells that enter the S (DNA replication phase) of the cell cycle (Bittman et al., 1997). It appears that it is the propagation of Ca^{2+} waves through gap junctions that influences this proliferation; this was demonstrated in the embryonic ventricular zone, as reducing the Ca^{2+} waves between neighbouring radial glia reduces the ventricular zone proliferation (Weissman et al., 2004). More recently, it has been demonstrated that gap junction coupling between neural progenitor cells and another population of astrocyte-like cells within the mouse postnatal SVZ allows the propagation of intercellular Ca^{2+} waves (Lacar et al., 2011). This suggests that the propagation of Ca^{2+} waves through gap junctions is a common mechanism to influence proliferation in both the embryonic and postnatal brain. It is tempting to suggest that this common mechanism could be extended to the postnatal spinal cord, with the propagation of Ca^{2+} waves between ependymal cells and subtype 1 CSFcCs controlling the constant proliferation of ependymal cells that occurs to maintain the ependymal cell population (Johansson et al., 1999).

6.1.3 GABAergic responses in cells surrounding the CC suggest that they are integrated into the spinal cord circuitry and has implications for the neurogenic capacity of the area

There are two possible endogenous sources of GABA that could be influencing ependymal cells and CSFcCs (Figure 6.1). The first source is GABAergic terminals that are known to be present in the area surrounding the CC (Mclaughlin et al., 1975). GABAergic terminals form synapses with ependymal cells (Magoul et al., 1987) and have been observed in close apposition to CSFcNs (Mclaughlin et al.,

1975). Axonal bundles co-expressing GAD, P2X$_2$, PSA-NCAM, GAP 43 and synaptotagmin have been identified both intra- and sub-ependymally (Stoeckel et al., 2003). The co-expression of GAD, P2X$_2$ and PSA-NCAM suggests that these axons originate from CSFcNs, indicating that CSFcNs could be influencing ependymal cells, subtype 1 CSFcCs and possibly other CSFcNs. Alternative sources of GABAergic terminals are the local GABAergic interneurones within lamina X or the dorsal horn (Barber et al., 1982). The functional implication of ependymal cells and CSFcCs receiving GABAergic inputs would be highly dependent on the precise nature of the GABAergic neurones from which the terminals originate. For example, if the terminals originate from GABAergic neurones in the dorsal horn it could further support the possibility that cells surrounding the CC are influenced by sensory inputs.

The second possible source of GABA is from the large terminals that are found at the end of the CSF-contacting processes of CSFcNs. These terminals are immunoreactive for VGAT as well as SV2 and synaptophysin (Conte, 2009), suggesting that they could be capable of releasing GABA into the CSF, onto the apical surfaces of ependymal cells and onto other CSF-contacting processes. If this is the case, excitation of CSFcNs could elicit the release of GABA which subsequently excites ependymal cells and either further excites or inhibits other CSFcNs. Even if CSFcNs are incapable of releasing GABA from their terminals using synaptic machinery, they could be releasing GABA in a non-synaptic, paracrine manner. This has been observed for newborn neurones in the SVZ, where they release GABA in a Ca^{2+} dependent but SNARE independent manner (i.e. non-synaptic) which tonically activates GABA$_A$ receptors on the SVZ astrocytes (Liu et al., 2005). If a similar mechanism is occurring here, GABA released from CSFcNs could be tonically activating GABA$_A$ receptors on ependymal cells, causing an excitation. The release of GABA into the CSF could also cause wider reaching effects than synaptic release from terminals directly onto a postsynaptic site, as GABA could diffuse through the CSF to influence cells within different segments of the spinal cord. This is, however, only a theory as the ability of CSFcCs to release GABA is yet to be tested; the method which could be used to investigate this possibility will be discussed in section 6.3.

The functional consequence of GABA exciting ependymal cells and CSFcCs can only be speculative at present. Firstly, considering ependymal cells, their excitation by GABA could have secondary effects on K$^+$ currents. In numerous astrocytes,

including in the adult hippocampus, activation of $GABA_A$ receptors inhibits outward K^+ currents (Bekar et al., 1999). A similar inhibition could be occurring in ependymal cells; however, the passive nature of the cells recorded in this study suggests that this is not the case (see section 6.2 for further discussion about the possible presence of K^+ currents). A second, greater functional consequence is to consider whether GABA is influencing the proliferative nature of ependymal cells, given that they are the potential neural stem cells of the CC neurogenic niche (Johansson et al., 1999; Barnabe-Heider et al., 2010). In particular, it is helpful to view how GABA influences cells within other neurogenic niches and then translate this to ependymal cells of the CC. GABA excites a number of progenitor cells, including those in the ventricular zone of the developing rat brain (LoTurco et al., 1995), the mammalian postnatal SVZ (Liu et al., 2005), the mammalian postnatal DG (Tozuka et al., 2005) and most recently, the turtle postnatal spinal cord (Reali et al., 2011). The $GABA_A$ mediated excitation can induce increases in intracellular Ca^{2+} (Tozuka et al., 2005; Reali et al., 2011) and influence proliferation and differentiation. In particular, GABA appears to reduce proliferation of neural stem/progenitor cells and induce differentiation to produce more newborn neurones (Liu et al., 2005; Tozuka et al., 2005). Unlike the postnatal neurogenic niches of the mammalian brain and lower vertebrate spinal cord, ependymal cells undergo only symmetrical division to maintain the ependymal cell population under physiological conditions (Johansson et al., 1999). If cells within the CC area respond to GABA in a similar way to the SVZ and DG, the proliferation of ependymal cells rather than differentiation suggests a lack of endogenous GABA under physiological conditions. It is possible that following an injury or the onset of a pathological condition, GABA could be released around this area, limiting proliferation and promoting differentiation. As CSFcNs have been shown to depolarise in response to both a decrease in pH and an increase in ATP (Huang et al., 2006; Marichal et al., 2009), both of which occur during injury, it could be hypothesised that CSFcNs are depolarised following injury eliciting the release of GABA which subsequently excites ependymal cells and promotes their differentiation into astrocytes and oligodendrocytes (Barnabe-Heider et al., 2010). Unfortunately within this study, the effect of GABA on subtype 1 CSFcCs was not investigated; however, if subtype 1 CSFcCs are the equivalent of SVZ astrocytes it is clear that their ability to respond to GABA must also be investigated.

Examining the potential consequences of GABA influencing CSFcNs is difficult given that some CSFcNs appear to depolarise in response to GABA and others

hyperpolarise. Although electrophysiology concerning GABA can be difficult, it can be assumed that the differences in response are not an experimental artefact, given that another study using gramicidin perforated patch recordings, in which the intracellular Cl⁻ is not affected, also saw both depolarising and hyperpolarising responses to GABA (Marichal et al., 2009). The depolarisation of CSFcNs by GABA could be a trigger to release GABA themselves, whether this is by their CSF-contacting terminal or other processes. Alternatively or perhaps additionally, newborn neurones produced within the SVZ are known to depolarise in response to GABA acting via $GABA_A$ receptors which reduces their speed of migration (Bolteus and Bordey, 2004); it is possible that GABA depolarising CSFcNs could inhibit their migration away from the CC region. It is more difficult to determine a functional outcome of CSFcNs responding to GABA with a hyperpolarisation. Firstly, it is possible that CSFcNs could be tonically releasing GABA into the CSF or onto ependymal cells and that a hyperpolarisation by GABA would reduce this tonic release. This is possible as the $GABA_A$ antagonist, bicuculline, applied alone had an effect on a small number of ependymal cells; however, the lack of effect of bicuculline on ependymal cells and the symmetrical proliferation previously discussed argues against the presence of tonic GABA. CSFcNs do also have the basal processes that project laterally and ventrally from which they could be releasing some substance such as GABA; a hyperpolarisation could be affecting this release. A second possibility is concerning migration; a hyperpolarisation of CSFcNs by GABA could allow migration if a stimulus encouraged them. Both of these outcomes are conjecture and the ability of CSFcNs to release GABA and/or migrate must be investigated.

Overall, although little evidence of endogenous GABAergic signalling was observed in these cells, the ability of ependymal cells and CSFcNs to respond to exogenous GABA provides strong evidence that these cells respond to GABA *in-vivo* and suggests that these cells could be integrated into the spinal cord circuitry. It is possible that GABA could enable communication between these different cell types and that these cells could use GABA to translate changes in the spinal cord environment into influencing the neurogenic capacity of this area.

6.1.4 Cholinergic responses of cells surrounding the CC suggest that they are integrated into the spinal cord circuitry and has implications for neurogenesis and plasticity within the area

Ependymal cells and CSFcCs also responded robustly to ACh. This strengthens the argument that both cell types are integrated into the spinal circuitry. The possible source of the ACh has not been identified (Figure 6.1) but it appears to be from cholinergic terminals (Barber et al., 1984). In addition, both ACh and its breakdown product choline are found in the CSF, although only in low concentrations (Tohgi et al., 1994). As choline is a selective agonist at the α7*nAChRs (Papke et al., 1996), its presence within the CSF could result in the activation of α7*nAChRs. The activation of receptors by ACh/choline within the CSF is likely to be in addition to the activation of receptors by ACh released from the cholinergic terminals. The cholinergic neurones from which the cholinergic terminals originate is currently unknown, although it could be reasoned that they are from either the partition cells or the CC-cluster cells which are both cholinergic interneurones located in lamina X, or from the less frequently observed cholinergic interneurones in the dorsal horn (Barber et al., 1984). If the inputs are from cholinergic interneurones within the dorsal horn it could be speculated that ependymal cells and CSFcCs are influenced by sensory information. It is more likely, however, that the cholinergic inputs are originating from the partition neurones or the CC-cluster cells which have been proposed to coordinate the activity of numerous spinal cord segments (Sherriff and Henderson, 1994). Increasing evidence suggests that partition neurones are part of the circuitry controlling locomotion (Huang et al., 2000; Miles et al., 2007), therefore if the cholinergic inputs to ependymal cells or CSFcCs are from partition neurones it is possible that their activation could be coordinated with locomotor events. The purpose of CSFcNs being coordinated with such events could be to induce a global release of GABA into the CSF which could enable communication between different spinal cord segments. Alternatively, the activation of CSFcNs by partition neurones could result in those CSFcNs with laterally projecting processes communicating with neurones involved in autonomic output, thus facilitating the synchronisation of motor and autonomic output.

The function of ACh depolarising ependymal cells and subtype 1 CSFcCs is unknown, however, the expression of nAChRs on these cell types should come as no surprise given the number of other non-neuronal cells with functional nAChRs (see review Sharma and Vijaraghavan (2002)). Both non α7*nAChRs and

α7*nAChRs have been identified in non-neuronal cells. For example, in cultured oligodendrocyte precursor cells from the postnatal corpus callosum, nicotine could induce increases in intracellular Ca^{2+} that were inhibited by DHβE (10 nM) but not by MLA, indicating the presence of α4β2*nAChRs (Rogers et al., 2001). In addition, ACh-induced currents within NG2 expressing oligodendrocyte precursor cells of the postnatal hippocampus could be antagonised by MLA and potentiated by PNU-120596, indicating the presence of α7*nAChRs (Velez-Fort et al., 2009). Interestingly, in both cases the activation of nAChRs resulted in an increase in intracellular Ca^{2+}, suggesting that this is functionally important to non-neuronal cholinergic responses (Velez-Fort et al., 2009). Whether the cholinergic responses induced in ependymal cells and subtype 1 CSFcCs result in an increase in intracellular Ca^{2+} was not investigated in this study but it is undoubtedly an important future experiment. It is possible that the activation of nAChRs on these cell types could induce increases in intracellular Ca^{2+} which could initiate numerous effects, including modulating gene expression and influencing plasticity; although these downstream effects have been predominantly investigated in neurones (see review Dajas-Baildor and Wonnacott (2004)), they could also occur in non-neuronal cells. In addition, it could initiate the propagation of Ca^{2+} waves through gap junctions, as seen in radial glial cells during embryonic neurogenesis and neural progenitor cells in the postnatal SVZ (Weissman et al., 2004; Lacar et al., 2011) which could influence ependymal cell and possibly subtype 1 CSFcC proliferation. In the postnatal DG of the hippocampus, a decrease in the number of BrdU expressing newborn cells indicated that there was a decrease in the rate of proliferation in β2*nAChR knockout mice (Harrist et al., 2004). This suggests that neural progenitor cells of the DG express β2*nAChRs and that their activation influences the rate of proliferation. The data in this study suggest the presence of β2*nAChRs in two possible neural stem/progenitor cell populations, ependymal cells and subtype 1 CSFcCs, indicating that ACh could influence proliferation in the area surrounding the CC by activating β2*nAChRs. Alternatively or indeed additionally, proliferation could also be influenced by α7*nAChRs.

A number of functions of ACh depolarising CSFcNs could be speculated. If CSFcNs are considered to be immature neurones, ACh could be influencing their survival and/or maturation as observed in the DG (Campbell et al., 2010). Newborn dentate granule cells express functional α7*nAChRs but as they mature and integrate into the hippocampal circuitry, that expression is lost (John, 2010). Even though the majority of the cholinergic response of CSFcNs is mediated by non α7*nAChRs in

this study, there is still a part of the response that is mediated by α7*nAChRs. As discussed in chapter 5.3, the greater antagonism of the ACh response by DHβE in subtype 3 CSFcCs compared to subtype 2 CSFcCs, suggests that the proportion of non α7*nAChRs is greater in subtype 3 CSFcCs. Although the evidence is indirect this could indicate that subtype 3 CSFcCs have a smaller proportion of α7*nAChRs than subtype 2 CSFcCs. As subtype 3 CSFcCs could be a more mature phenotype than subtype 2 CSFcCs, the smaller proportion of α7*nAChRs in subtype 3 CSFcCs, is consistent with the reduction in α7*nAChR expression as neurones mature in the DG. It could suggest that as CSFcNs mature, they need fewer α7*nAChR-mediated cholinergic responses to function correctly. Again in the DG, α7*nAChRs have been demonstrated to be essential for the survival and proper integration of adult-born neurones into the existing hippocampal circuitry (Campbell et al., 2010). It is possible that as with the newborn neurones in the DG, cholinergic responses mediated by α7*nAChRs could be important for the survival of CSFcNs. If CSFcNs are immature neurones or mature neurones that are involved in plasticity, their ability to respond to ACh could also be important for neurite growth and path-finding. Experiments have demonstrated that chronic *in-vivo* nicotine exposure increases dendritic length (Brown and Kolb, 2001), however, focal pressure application of nicotine induces neurite retraction of cultured chick ciliary ganglion neurones in an α-BgT and thus α7*nAChR sensitive manner (Pugh and Berg, 1994). In addition, ACh has been shown to induce the turning of nerve growth cones through the activation nAChRs during development (Zheng et al., 1994). The previous data demonstrate how ACh is capable of influencing neurite growth and path-finding, however, it also highlights that the exact role is unclear which makes it difficult to determine how it could be affecting such processes in CSFcNs. The ability of ACh to influence all of these cellular processes is a result of the Ca^{2+} permeable nature of nAChRs which results in an increase in intracellular Ca^{2+} (see review Fucile (2004)). In particular, the high Ca^{2+} permeability of α7*nAChRs results in the initiation of a number of intracellular effects (Dajas-Bailador and Wonnacott, 2004). In view of this, an important next step would be to measure the changes in intracellular Ca^{2+} in CSFcNs.

On the whole, although no evidence of endogenous cholinergic signalling was observed, the ability of ependymal cells and CSFcCs to respond to exogenous ACh is the first indication that these cells are integrated into the spinal cord circuitry through cholinergic signalling. It also suggests that ACh is capable of influencing the proliferative capacity of this area and the survival and integration of CSFcNs

and finally, indicates that the varying proportions of nAChRs expressed could result in differential responses.
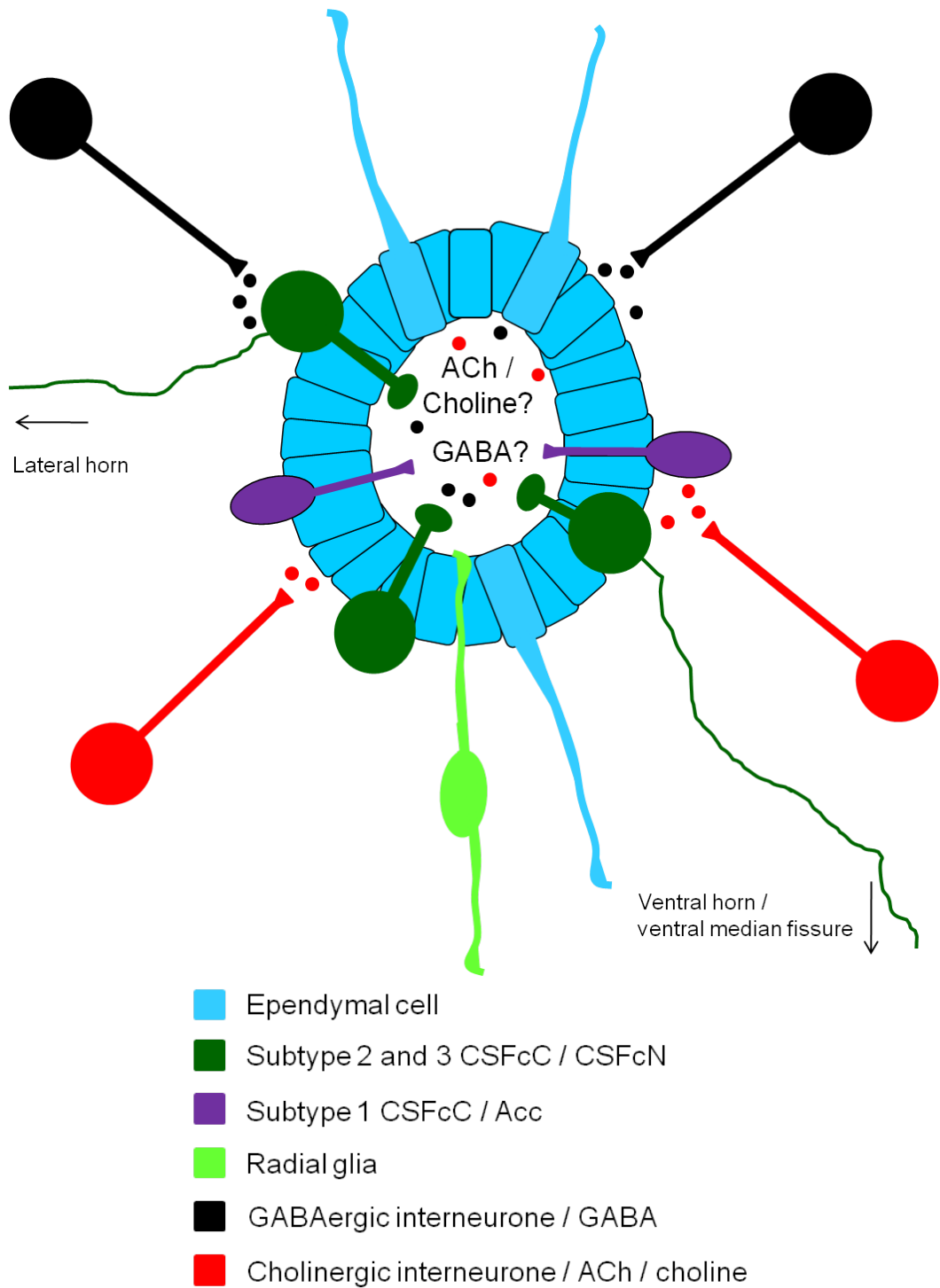

Figure 6.1: Possible sources of GABA and ACh. GABA could be released from the terminals of GABAergic interneurones, CSFcNs or found within the CSF. ACh could be released from cholinergic interneurones or ACh or its breakdown product, choline, could be found within the CSF.

6.2 Technical considerations and limitations

Although the upmost care was taken to ensure that the most appropriate techniques were utilised to examine the cells in this study, all experimental techniques have their pros and cons and these must be addressed. Firstly, the use of the spinal cord slice preparation will be considered. The prime advantage of this preparation is that many of the neuronal circuits are maintained, unlike in cell cultures, however, the cells of interest are still highly accessible, unlike during *in-vivo* experiments. The disadvantages are that some axons are severed which causes the affected cells to become unhealthy and die and it can also result in a loss of synaptic inputs onto the cells of interest. Given the complete lack of spontaneous activity observed in the ependymal cells, it appears likely that the loss of synaptic inputs will have a less significant impact on the phenotype of the ependymal cells compared to the impact on other cell types. Nevertheless, inputs releasing neurotransmitters in a non-synaptic manner could normally be present resulting in different levels of tonic neurotransmitters around ependymal cells and the slicing could disrupt some of the gap junction coupled clusters. As CSFcCs have fewer processes than many neurones or astrocytes it is likely that they would survive the slicing procedure better than many cell types, however, the synaptic inputs that they receive could still be interrupted. Even if the cells of interest are not damaged, local changes in the environment could induce changes within the cells. These changes could occur within minutes, thus affecting the recordings, or they could take hours, having a minimal impact on recordings. For example the number of receptors present at the cell membrane could be changed within minutes, where as changes involving gene transcription would take much longer and are less likely to affect the results obtained. A number of modifications have been utilised during the spinal cord slice preparation to reduce damage, the spread of cell death and thus changes in the environment. For example, the preparation is performed in a chilled sucrose based, Na^+ free aCSF to reduce cell death by excitotoxicity. Another disadvantage of the spinal cord slice preparation is that it restricts the age of the animals that can be investigated, as it becomes more difficult to obtain stable recordings in slices from older animals. The spinal cord slices used in this study were obtained from juvenile animals, P9-P21; therefore they are not fully equivalent to an adult spinal cord. The lack of difference in the percentage of CSFcCs in each subtype in P21 animals compared to the data from younger animals suggests that the study can be tentatively extrapolated to the adult spinal cord. It could be suggested that the spinal cord slice procedure results in slices that are more representative of a pathological state as opposed to a physiological state. Although

this is not intentional, the ultimate interest in this area is to investigate how the cells respond to pathological states and how they could be manipulated to promote injury during these pathological states. In this light, perhaps the damage created during slicing should not be considered as a disadvantage.

A possible consideration of this study is that the cells were investigated in current clamp; this choice was made as the study was primarily interested in the functional voltage responses that could be elicited by the cells. For the most part, working in current clamp was sufficient to obtain reliable and interesting results. There are certain specific questions, however, that could perhaps be more clearly examined using voltage clamp. One example is when exploring the passive responses of both ependymal cells and subtype 1 CSFcCs. Working in voltage clamp, a study of astrocytes throughout the CNS demonstrated that no astrocytes had passive responses (Bordey and Sontheimer, 2000). A few astrocytes that initially appeared to have a linear current-voltage relationship were shown to possess voltage activated currents upon application of a leak subtraction protocol. It is therefore possible that the existence of voltage activated currents in ependymal cells and subtype 1 CSFcCs could have been overlooked. Other studies have observed astrocytes with linear profiles (D'Ambrosio et al., 1998) and the recent study of CC ependymal cells observed linear profiles even when using a leak subtraction protocol. The rates of onset and desensitisation vary between different nAChRs (see review Giniatullin et al., (2005)) and investigating these parameters could have been used to reinforce the pharmacological data. Although these parameters could be investigated in current clamp they have been more extensively characterised in voltage clamp and it could have been an advantage to use this mode.

The pressure application of ACh was used in this study as it allows immediate rapid responses to be observed and reduces the probablility of ACh being broken down. It does, however, have the disadvantage that the exact agonist concentration at the level of the cell is unknown, as it will become diluted as it interacts with the recording aCSF. This is not generally a problem for observing which cells respond to ACh but can create difficulties when examining the relative effects of different antagonists. As some antagonists will be effective against higher agonist concentrations than others, not knowing the agonist concentration could lead to an underestimation of the contribution of some receptor subtypes. Despite this, the ability of DhβE to almost fully antagonise the cholinergic response in subtype 3 CSFcCs demonstrates that the concentration of DhβE used can effectively

antagonise the cholinergic response, and should be capable of antagonising the cholinergic response to similar levels in all cells if the same receptors are present. In addition, the ability of MLA to antagonise the PNU-120596 potentiated cholinergic response suggests that this concentration of MLA is highly effective even at high agonist concentrations. Nevertheless the interpretation of the data regarding the contribution of certain nicotinic subtypes to the cholinergic responses in different cell subtypes should be viewed solely as interpretations and needs further defining, as will be discussed in the future works section.

The majority of the work concerning cells found within the area surrounding the CC has been using turtles and other non-mammalian species (Dervan and Roberts, 2003; Reali et al., 2011). As mammals, the use of rats and mice within this study means that the data can be more confidently related to humans which is the ultimate aim of this research and is therefore a great positive of this study. On the whole, the most appropriate techniques have been used to study the ependymal cells and CSFcCs and they have generated results which provide a solid platform from which future studies can be performed.

6.3 Future work

There are a wide range of future experiments that could be performed, with some of the most pertinent already being remarked upon throughout discussion of this work. These future experiments could be divided into three main areas: firstly, a direct continuation of this work further defining the receptors involved in the cholinergic responses, secondly, using culturing techniques or *in-vivo* protocols to monitor how both GABA and ACh influence cell proliferation, differentiation, growth and migration and whether 5HT and substance P can affect these processes and thirdly, investigating the relationships between the cells within the CC region using dual patch clamp electrophysiology. The ultimate aim of all of these future works would be to understand the functional importance of this area under physiological conditions and to understand how this area could be manipulated following spinal cord pathologies to replace damaged cells and enhance functional recovery.

To further the understanding of the receptors involved in the cholinergic responses a combination of performing experiments in gap junction blockers, completing

voltage clamp experiments and using genetically modified mice could be employed. The gap junction coupled nature of ependymal cells and some subtype 1 CSFcCs could be affecting their cholinergic responses, therefore, the experiments could be performed in the presence of a gap junction blocker such as 18β-glycyrrhetinic acid. This would enable the reversal potential of the cholinergic response to be better investigated and would highlight whether all of the cells respond to ACh or whether some responses are due to neighbouring cells responding to ACh. Voltage clamp experiments would allow the type of current evoked by ACh application to be better understood. Both α7*nAChR and β2*nAChR knockout mice are available (as demonstrated by Harrist et al., (2004) and Campbell et al.,(2010)); comparison of the amplitude and kinetics between wild-type and knockout mice would strengthen the evidence of which receptor subunits are involved in the cholinergic responses and could give a more reliable estimation of their contribution to the response. To further the understanding of the influence of receptor activation on the cells, Ca^{2+} imaging in combination with voltage-gated Ca^{2+} channel blockers and blockers of Ca^{2+} induced Ca^{2+} release could be used. Ca^{2+} imaging would establish whether intracellular Ca^{2+} concentrations are significantly elevated following nAChR activation and whether this varies between cell types, with the different blockers establishing the source of the Ca^{2+}.

The influence of GABA and ACh on proliferation of cells within the spinal cord could be investigated by using organotypic spinal cord slice cultures. In particular the use of PNU-120596 on spinal cord cultures would be informative as this would enhance endogenous ACh rather than adding exogenous ACh. PNU-120596 could be applied in the presence of MLA as a control, and effects on cell proliferation could be monitored by the application of EdU. The effect on specific cell types could be evaluated by performing immunohistochemistry with ependymal cell, CSFcC subtype 1 and CSFcN specific markers. Given the large proportion of the cholinergic response mediated by non α7*nAChR, another experiment in the cultures would be to apply DHβE and monitor the effects on proliferation and CSFcN numbers. This work could then be translated *in-vivo*, with injections of PNU-120596 and EdU given I.P to mice for a week alongside control mice which just receive EdU injections. The mice could then be fixed and the spinal cords processed to look at the number of EdU-expressing newborn cells and the number of PKD2L1-immunoreactive CSFcNs. An alternative to I.P would be to implant osmotic minipumps subcutaneously to deliver PNU-120596 over a longer time period, at a more consistent level. The effects of GABA and associated antagonists

on cell proliferation and numbers of CSFcNs could also be investigated using the organotypic spinal cord slice culture. In particular the use of specific GABA modulators, such as diazepam, within the cultures would be interesting. Given the lack of immediate effects of 5HT and substance P observed in this study, the organotypic slice preparation would be a very useful technique to use to investigate whether 5HT and substance P are having any long term effects on CSFcNs, such as effects on their growth or migration; although further more extensive electrophysiological experiments measuring more parameters such as capacitance could also be undertaken for 5HT and substance P. A final experiment to be considered using the organotypic spinal cord slice culture would be to injure an area of the cord and investigate whether this causes changes in proliferation or whether it induces migration of CSFcNs. If this does induce changes, the effect of GABAergic and cholinergic modulators on the changes could be investigated.

The relationships between the cells in the area surrounding the CC would be very interesting to examine. Dual patch clamp electrophysiology could be used to investigate the relationship between ependymal cells and CSFcNs, ependymal cells and subtype 1 CSFcCs, subtype 1 CSFcCs and CSFcNs, two ependymal cells or two CSFcNs. It would be interesting to stimulate a CSFcN and record from any other cell in order to determine whether CSFcNs are capable of releasing GABA into the CSF. If a response was observed in the other cell, for example an ependymal cell, different $GABA_A$ receptor antagonists or modulators could be applied to see whether the response could be antagonised or enhanced. An alternative way to investigate the relationship between CSFcNs and ependymal cells would be to specifically knock-out the CSFcNs and then study the subsequent effect on ependymal cell survival and proliferation. The most thorough method of specifically removing CSFcNs would be to selectively express diphtheria toxin in CSFcNs; this could be achieved by targeting diphtheria toxin to PKD2L1 expressing cells, as CSFcNs are the only cells within the spinal cord to express PKD2L1. Such mice have been used previously to study the effect of removing PKD2L1 expressing taste cells in the tongue (Huang et al., 2006). To investigate the lineage of cells surrounding the CC and determine whether any CSFcCs originate from ependymal cells the FoxJ1-CreER-RFP mouse could be used; similar mice have been used to great effect before by Meletis et al., (2008) and Barnabe-Heider et al., (2010). FoxJ1 is expressed solely in cells with motile cilia, therefore in the spinal cord, only ependymal cells express FoxJ1. The Cre reporter background of the FoxJ1-CreER mice means that the administration of tamoxifen allows inducible, permanent and

heritable genetic labelling by the expression of red fluorescent protein (RFP). As a result, long term studies of the progeny of ependymal cells can be conducted, with the identity of the progeny being distinguished by dual labelling for specific markers such as PKD2L1.

Given the relatively few studies that have been undertaken regarding this area of the CC, it is not surprising that the list of future experiments could be far more extensive. The experiments suggested are those that are considered to be the most relevant to this current study, the most pertinent to discover functional importance of ependymal cells and CSFcNs and finally, the most realistic and viable.

6.4 The functional relevance of studying the area surrounding the CC

There are many situations in which the spinal cord can no longer function to its full capacity. These include following a spinal cord injury, during a degenerative illness such as multiple sclerosis or simply during ageing. The decline in function can often be attributed to a loss of cells, whether it is a dramatic loss of numerous cell types including neurones following a spinal cord injury, a slower decline in cell numbers with age (Terao et al., 1996) or the specific loss of oligodendrocytes during multiple sclerosis. Some of these pathological states are being treated by the use of stem cell grafts; however, there is still debate about the practicality of this treatment method and there are of course ethical debates over the use of certain types of stem cells (Karussis and Kassis, 2008; Thomas and Moon, 2011). In addition, the slow loss of cell numbers with age would not be suited to treatment by a stem cell graft but would be better suited by a therapy which increases the survival of cells or produces new cells at a slower, steady rate. The presence of a population of endogenous neural stem cells within the spinal cord is therefore of great importance. Following a complete spinal cord transection in lower vertebrates, the ependymal cells proliferate and the area surrounding the CC bridges the transection, enabling the rest of the spinal cord to reform (Dervan and Roberts, 2003). The spinal cord of mammals have not retained this regenerative capability, however, ependymal cells have still retained the characteristics of neural stem cells (Weiss et al., 1996). Under physiological conditions, ependymal cell proliferation is symmetrical and appears to simply maintain the ependymal cell population (Johansson et al., 1999). Following a spinal cord injury, however, ependymal cells

can produce astrocytes and oligodendrocytes (Barnabe-Heider et al., 2010) and in a model of multiple sclerosis ependymal cells have been observed to produce new neurones (Danilov et al., 2006). The environmental changes that occur in these pathological situations must be inducing the transformation from self-renewal to differentiation, although what these environmental changes are is not known. It is therefore important to determine what stimuli ependymal cells and their neighbouring cells respond to and how changes in these stimuli alter the behaviour of ependymal cells, as well as determining what stimuli are important for the survival of these cells. If this can be understood it could be possible to manipulate the proliferation and differentiation of ependymal cells to replace the specific cell type that has been affected by a particular pathology.

6.5 Conclusions

This study has provided an in-depth functional characterisation of the phenotypes of cells surrounding the CC of the postnatal mammalian spinal cord and their ability to respond to neurotransmitters. The variation of phenotypes demonstrates the complexity of the area and the need for further investigation. The ability of ependymal cells and CSFcCs to respond to both GABA and ACh suggests that this potential neurogenic niche could be influenced by these two neurotransmitters, drawing parallels to other postnatal neurogenic niches. It is possible that the manipulation of one or both of these neurotransmitter systems could allow a greater control over the proliferation and differentiation of cells within this area, with beneficial implications for the treatment of spinal cord injury or spinal cord pathologies, such as multiple sclerosis. The fundamental physiological responses revealed in this study are essential to provide a solid platform on which to build towards future clinically relevant studies.

References

Airaksinen MS, Eilers J, Thoenen H, Konnerth A, Meyer, M (1997). Ataxia and altered dendritic calcium signalling in mice carrying a targeted null mutation of the calbindin D28k gene. Proc Natl Acad Sci U S A 94:1488-1493.

Alfaro-Cervello C, Soriano-Navarro M, Mirzadeh Z, Alvarez-Buylla A, Garcia-Verdugo JM (2012) Biciliated ependymal cell proliferation contributes to spinal cord growth. J Comp Neurol.

Alkondon M, Albuquerque EX (1993) Diversity of nicotinic acetylcholine receptors in rat hippocampal neurons. I. Pharmacological and functional evidence for distinct structural subtypes. J Pharmacol Exp Ther 265:1455-1473.

Alkondon M, Pereira EF, Albuquerque EX (1998) alpha-bungarotoxin- and methyllycaconitine-sensitive nicotinic receptors mediate fast synaptic transmission in interneurons of rat hippocampal slices. Brain Res 810:257-263.

Alkondon M, Pereira EF, Wonnacott S, Albuquerque EX (1992) Blockade of nicotinic currents in hippocampal neurons defines methyllycaconitine as a potent and specific receptor antagonist. Mol Pharmacol 41:802-808.

Alvarez FJ, Taylor-Blake B, Fyffe RE, De Blas AL, Light AR (1996) Distribution of immunoreactivity for the beta 2 and beta 3 subunits of the GABAA receptor in the mammalian spinal cord. J Comp Neurol 365:392-412.

Ambalavanar R, Morris R (1989) Fluoro-Gold Injected Either Subcutaneously or Intravascularly Results in Extensive Retrograde Labeling of Cns Neurons Having Axons Terminating Outside the Blood-Brain-Barrier. Brain Research 505:171-175.

Andrade R, Malenka RC, Nicoll RA (1986) A G protein couples serotonin and GABAB receptors to the same channels in hippocampus. Science 234:1261-1265.

Arai Y, Deguchi K, Takashima S (1998) Vascular endothelial growth factor in brains with periventricular leukomalacia. Pediatr Neurol 19:45-49.

Arvidsson U, Cullheim S, Ulfhake B, Bennett GW, Fone KC, Cuello AC, Verhofstad AA, Visser TJ, Hokfelt T (1990) 5-Hydroxytryptamine, substance P, and thyrotropin-

releasing hormone in the adult cat spinal cord segment L7: immunohistochemical and chemical studies. Synapse 6:237-270.

Azzi G, Jouis V, Godeau G, Groult N, Robert AM (1989) Immunolocalisation of extracellular matrix macromolecules in the rat spinal cord. Matrix 9:479-485.

Backman SB, Henry JL (1984) Effects of Oxytocin and Vasopressin on Thoracic Sympathetic Preganglionic Neurons in the Cat. Brain Research Bulletin 13:679-684.

Bacon SJ, Smith AD (1988) Preganglionic Sympathetic Neurons Innervating the Rat Adrenal-Medulla - Immunocytochemical Evidence of Synaptic Input from Nerve-Terminals Containing Substance-P, Gaba or 5-Hydroxytryptamine. J Autonom Nerv Syst 24:97-122.

Bacon SJ, Zagon A, Smith AD (1990) Electron-Microscopic Evidence of a Monosynaptic Pathway between Cells in the Caudal Raphe Nuclei and Sympathetic Preganglionic Neurons in the Rat Spinal-Cord. Exp Brain Res 79:589-602.

Banasr M, Hery M, Printemps R, Daszuta A (2004) Serotonin-induced increases in adult cell proliferation and neurogenesis are mediated through different and common 5-HT receptor subtypes in the dentate gyrus and the subventricular zone. Neuropsychopharmacology 29:450-460.

Barber RP, Vaughn JE, Roberts E (1982) The cytoarchitecture of GABAergic neurons in rat spinal cord. Brain Res 238:305-328.

Barber RP, Vaughn JE, Slemmon JR, Salvaterra PM, Roberts E, Leeman SE (1979) The origin, distribution and synaptic relationships of substance P axons in rat spinal cord. J Comp Neurol 184:331-351.

Barber RP, Phelps PE, Houser CR, Crawford GD, Salvaterra PM, Vaughn JE (1984) The Morphology and Distribution of Neurons Containing Choline-Acetyltransferase in the Adult-Rat Spinal-Cord - an Immunocytochemical Study. Journal of Comparative Neurology 229:329-346.

Barnabe-Heider F, Goritz C, Sabelstrom H, Takebayashi H, Pfrieger FW, Meletis K, Frisen J (2010) Origin of New Glial Cells in Intact and Injured Adult Spinal Cord. Cell Stem Cell 7:470-482.

Barnard EA, Skolnick P, Olsen RW, Mohler H, Sieghart W, Biggio G, Braestrup C, Bateson AN, Langer SZ (1998) International Union of Pharmacology. XV. Subtypes of gamma-aminobutyric acidA receptors: classification on the basis of subunit structure and receptor function. Pharmacol Rev 50:291-313.

Barnes NM, Sharp T (1999) A review of central 5-HT receptors and their function. Neuropharmacology 38:1083-1152.

Barrantes GE, Murphy CT, Westwick J, Wonnacott S (1995) Nicotine increases intracellular calcium in rat hippocampal neurons via voltage-gated calcium channels. Neurosci Lett 196:101-104.

Barres BA, Chun LL, Corey DP (1989) Glial and neuronal forms of the voltage-dependent sodium channel: characteristics and cell-type distribution. Neuron 2:1375-1388.

Bekar LK, Jabs R, Walz W (1999) GABAA receptor agonists modulate K+ currents in adult hippocampal glial cells in situ. Glia 26:129-138.

Belliveau DJ, Naus CC (1995) Cellular localization of gap junction mRNAs in developing rat brain. Dev Neurosci 17:81-96.

Benowitz LI, Routtenberg A (1997) GAP-43: An intrinsic determinant of neuronal development and plasticity. Trends Neurosci 20:84-91.

Bertin B, Freissmuth M, Breyer RM, Schutz W, Strosberg AD, Marullo S (1992) Functional expression of the human serotonin 5-HT1A receptor in Escherichia coli. Ligand binding properties and interaction with recombinant G protein alpha-subunits. J Biol Chem 267:8200-8206.

Bertrand D, Galzi JL, Devillers-Thiery A, Bertrand S, Changeux JP (1993) Mutations at two distinct sites within the channel domain M2 alter calcium permeability of neuronal alpha 7 nicotinic receptor. Proc Natl Acad Sci U S A 90:6971-6975.

Bittman K, Owens DF, Kriegstein AR, LoTurco JJ (1997) Cell coupling and uncoupling in the ventricular zone of developing neocortex. J Neurosci 17:7037-7044.

Bohlhalter S, Weinmann O, Mohler H, Fritschy JM (1996) Laminar compartmentalization of GABAA-receptor subtypes in the spinal cord: an immunohistochemical study. J Neurosci 16:283-297.

Bohmer C, Kirschner U, Wehner F (2001) 18-beta-Glycyrrhetinic acid (BGA) as an electrical uncoupler for intracellular recordings in confluent monolayer cultures. Pflugers Archiv : European journal of physiology 442:688-692.

Bolteus AJ, Bordey A (2004) GABA release and uptake regulate neuronal precursor migration in the postnatal subventricular zone. Journal of Neuroscience 24:7623-7631.

Bordey A, Sontheimer H (2000) Ion channel expression by astrocytes in situ: comparison of different CNS regions. Glia 30:27-38.

Bordey A, Feltz P, Trouslard J (1996a) Nicotinic actions on neurones of the central autonomic area in rat spinal cord slices. J Physiol 497 (Pt 1):175-187.

Bordey A, Feltz P, Trouslard J (1996b) Patch-clamp characterization of nicotinic receptors in a subpopulation of lamina X neurones in rat spinal cord slices. J Physiol 490 (Pt 3):673-678.

Borges LF, Iversen SD (1986) Topography of Choline-Acetyltransferase Immunoreactive Neurons and Fibers in the Rat Spinal-Cord. Brain Research 362:140-148.

Bormann J, Hamill OP, Sakmann B (1987) Mechanism of anion permeation through channels gated by glycine and gamma-aminobutyric acid in mouse cultured spinal neurones. Journal of Physiology 385:243-286.

Bowery NG, Hill DR, Hudson AL, Doble A, Middlemiss DN, Shaw J, Turnbull M (1980) (-)Baclofen decreases neurotransmitter release in the mammalian CNS by an action at a novel GABA receptor. Nature 283:92-94.

Bowker RM, Westlund KN, Coulter JD (1981) Origins of Serotonergic Projections to the Spinal-Cord in Rat - an Immunocytochemical-Retrograde Transport Study. Brain Research 226:187-199.

Bradaia A, Trouslard J (2002a) Nicotinic receptors regulate the release of glycine onto lamina X neurones of the rat spinal cord. Neuropharmacology 43:1044-1054.

Bradaia A, Trouslard J (2002b) Fast synaptic transmission mediated by alpha-bungarotoxin-sensitive nicotinic acetylcholine receptors in lamina X neurones of neonatal rat spinal cord. J Physiol 544:727-739.

Bradaia A, Seddik R, Schlichter R, Trouslard J (2005) The rat spinal cord slice: Its use in generating pharmacological evidence for cholinergic transmission using the alpha7 subtype of nicotinic receptors in the central autonomic nucleus. J Pharmacol Toxicol Methods 51:243-252.

Brejc K, van Dijk WJ, Klaassen RV, Schuurmans M, van Der Oost J, Smit AB, Sixma TK (2001) Crystal structure of an ACh-binding protein reveals the ligand-binding domain of nicotinic receptors. Nature 411:269-276.

Brezun JM, Daszuta A (2000) Serotonin may stimulate granule cell proliferation in the adult hippocampus, as observed in rats grafted with foetal raphe neurons. Eur J Neurosci 12:391-396.

Brickley SG, Mody I (2012) Extrasynaptic GABA(A) receptors: their function in the CNS and implications for disease. Neuron 73:23-34.

Brickley SG, Cull-Candy SG, Farrant M (1996) Development of a tonic form of synaptic inhibition in rat cerebellar granule cells resulting from persistent activation of GABAA receptors. J Physiol 497 (Pt 3):753-759.

Brickley SG, Revilla V, Cull-Candy SG, Wisden W, Farrant M (2001) Adaptive regulation of neuronal excitability by a voltage-independent potassium conductance. Nature 409:88-92.

Brown JP, Couillard-Despres S, Cooper-Kuhn CM, Winkler J, Aigner L, Kuhn HG (2003) Transient expression of doublecortin during adult neurogenesis. Journal of Comparative Neurology 467:1-10.

Brown RW, Kolb B (2001) Nicotine sensitization increases dendritic length and spine density in the nucleus accumbens and cingulate cortex. Brain Res 899:94-100.

Bruni JE, Reddy K (1987) Ependyma of the Central Canal of the Rat Spinal-Cord - a Light and Transmission Electron-Microscopic Study. Journal of Anatomy 152:55-70.

Brunig I, Scotti E, Sidler C, Fritschy JM (2002) Intact sorting, targeting, and clustering of gamma-aminobutyric acid A receptor subtypes in hippocampal neurons in vitro. J Comp Neurol 443:43-55.

Burcher E, Alouan LA, Johnson PR, Black JL (1991) Neuropeptide gamma, the most potent contractile tachykinin in human isolated bronchus, acts via a 'non-classical' NK2 receptor. Neuropeptides 20:79-82.

Campbell NR, Fernandes CC, Halff AW, Berg DK (2010) Endogenous signaling through alpha7-containing nicotinic receptors promotes maturation and integration of adult-born neurons in the hippocampus. J Neurosci 30:8734-8744.

Carleton A, Petreanu LT, Lansford R, Alvarez-Buylla A, Lledo PM (2003) Becoming a new neuron in the adult olfactory bulb. Nat Neurosci 6:507-518.

Carter MS, Krause JE (1990) Structure, expression, and some regulatory mechanisms of the rat preprotachykinin gene encoding substance P, neurokinin A, neuropeptide K, and neuropeptide gamma. J Neurosci 10:2203-2214.

Carthew HL, Ziebell JM, Vink R (2012) Substance P-induced changes in cell genesis following diffuse traumatic brain injury. Neuroscience.

Caulfield MP (1993) Muscarinic receptors--characterization, coupling and function. Pharmacol Ther 58:319-379.

Caulfield MP, Birdsall NJM (1998) International Union of Pharmacology. XVII. Classification of muscarinic acetylcholine receptors. Pharmacol Rev 50:279-290.

Chan-Palay V (1976) Serotonin axons in the supra- and subependymal plexuses and in the leptomeninges; their roles in local alterations of cerebrospinal fluid and vasomotor activity. Brain Res 102:103-130.

Chang MM, Leeman SE, Niall HD (1971) Amino-acid sequence of substance P. Nat New Biol 232:86-87.

Chang WP, Sudhof TC (2009) SV2 Renders Primed Synaptic Vesicles Competent for Ca2+-Induced Exocytosis. Journal of Neuroscience 29:883-897.

Chapman RJ, Lall VK, Maxeiner S, Willecke K, Deuchars J, King AE (2012) Localization of neurones expressing the gap junction protein Connexin45 within the adult spinal dorsal horn: a study using Cx45-eGFP reporter mice. Brain Struct Funct.

Chiara DC, Xie Y, Cohen JB (1999) Structure of the agonist-binding sites of the Torpedo nicotinic acetylcholine receptor: affinity-labeling and mutational analyses identify gamma Tyr-111/delta Arg-113 as antagonist affinity determinants. Biochemistry 38:6689-6698.

Chung JM, Chung K, Wurster RD (1975) Sympathetic preganglionic neurons of the cat spinal cord: horseradish peroxidase study. Brain Res 91:126-131.

Chvatal A, Pastor A, Mauch M, Sykova E, Kettenmann H (1995) Distinct populations of identified glial cells in the developing rat spinal cord slice: ion channel properties and cell morphology. Eur J Neurosci 7:129-142.

Clarke PB, Schwartz RD, Paul SM, Pert CB, Pert A (1985) Nicotinic binding in rat brain: autoradiographic comparison of [3H]acetylcholine, [3H]nicotine, and [125I]-alpha-bungarotoxin. J Neurosci 5:1307-1315.

Clayton GH, Owens GC, Wolff JS, Smith RL (1998) Ontogeny of cation-Cl-cotransporter expression in rat neocortex. Dev Brain Res 109:281-292.

Collingridge GL, Olsen RW, Peters J, Spedding M (2009) A nomenclature for ligand-gated ion channels. Neuropharmacology 56:2-5.

Conn PJ, Sanders-Bush E (1986) Regulation of serotonin-stimulated phosphoinositide hydrolysis: relation to the serotonin 5-HT-2 binding site. J Neurosci 6:3669-3675.

Connors BW, Ransom BR (1987) Electrophysiological properties of ependymal cells (radial glia) in dorsal cortex of the turtle, Pseudemys scripta. J Physiol 385:287-306.

Connors BW, Long MA (2004) Electrical synapses in the mammalian brain. Annu Rev Neurosci 27:393-418.

Conte D (2009). Neuroanatomical properties and connections of GABAergic neurones in Lamina X of the spinal cord of the rat and mouse. In: Institute of Membrane and Systems Biology. University of Leeds: Leeds.

Cooper-Kuhn CM, Winkler J, Kuhn HG (2004) Decreased neurogenesis after cholinergic forebrain lesion in the adult rat. J Neurosci Res 77:155-165.

Couturier S, Bertrand D, Matter JM, Hernandez MC, Bertrand S, Millar N, Valera S, Barkas T, Ballivet M (1990) A neuronal nicotinic acetylcholine receptor subunit (alpha 7) is developmentally regulated and forms a homo-oligomeric channel blocked by alpha-BTX. Neuron 5:847-856.

Cuello AC, Galfre G, Milstein, C (1979) Detection of substance P in the central nervous system by a monoclonal antibody. Proc Natl Acad Sci U S A 76: 3532-3536.

Cuevas P, Gimenez-Gallego G (2000) Fibroblast growth factor and hydrocephalus. Neurol Res 22:102-104.

D'Ambrosio R, Wenzel J, Schwartzkroin PA, McKhann GM, 2nd, Janigro D (1998) Functional specialization and topographic segregation of hippocampal astrocytes. J Neurosci 18:4425-4438.

Dajas-Bailador F, Wonnacott S (2004) Nicotinic acetylcholine receptors and the regulation of neuronal signalling. Trends in pharmacological sciences 25:317-324.

Dani JA, Bertrand D (2007) Nicotinic acetylcholine receptors and nicotinic cholinergic mechanisms of the central nervous system. Annu Rev Pharmacol Toxicol 47:699-729.

Danilov AI, Covacu R, Moe MC, Langmoen IA, Johansson CB, Olsson T, Brundin L (2006) Neurogenesis in the adult spinal cord in an experimental model of multiple sclerosis. Eur J Neurosci 23:394-400.

Davidson JS, Baumgarten IM (1988) Glycyrrhetinic acid derivatives: a novel class of inhibitors of gap-junctional intercellular communication. Structure-activity relationships. J Pharmacol Exp Ther 246:1104-1107.

De Koninck Y, Henry JL (1991) Substance P-mediated slow excitatory postsynaptic potential elicited in dorsal horn neurons in vivo by noxious stimulation. Proc Natl Acad Sci U S A 88:11344-11348.

Del Bigio MR (2010) Ependymal cells: biology and pathology. Acta Neuropathol 119:55-73.

Derkach V, Surprenant A, North RA (1989) 5-HT3 receptors are membrane ion channels. Nature 339:706-709.

Dervan AG, Roberts BL (2003) Reaction of spinal cord central canal cells to cord transection and their contribution to cord regeneration. Journal of Comparative Neurology 458:293-306.

Descarries L, Gisiger V, Steriade M (1997) Diffuse transmission by acetylcholine in the CNS. Prog Neurobiol 53:603-625.

Deuchars SA (2007) Multi-tasking in the spinal cord - do 'sympathetic' interneurones work harder than we give them credit for? J Physiol-London 580:723-729.

Deuchars SA, Morrison SF, Gilbey MP (1995) Medullary-Evoked Epsps in Neonatal Rat Sympathetic Preganglionic Neurons in-Vitro. J Physiol-London 487:453-463.

Deuchars SA, Spyer KM, Gilbey MP (1997) Stimulation within the rostral ventrolateral medulla can evoke monosynaptic GABAergic IPSPs in sympathetic preganglionic neurons in vitro. J Neurophysiol 77:229-235.

Deuchars SA, Brooke RE, Frater B, Deuchars J (2001) Properties of interneurones in the intermediolateral cell column of the rat spinal cord: Role of the potassium channel subunit Kv3.1. Neuroscience 106:433-446.

Deuchars SA, Milligan CJ, Stornetta RL, Deuchars J (2005) GABAergic neurons in the central region of the spinal cord: A novel substrate for sympathetic inhibition. Journal of Neuroscience 25:1063-1070.

Dias TB, Yang YJ, Ogai K, Becker T, Becker CG (2012) Notch Signaling Controls Generation of Motor Neurons in the Lesioned Spinal Cord of Adult Zebrafish. Journal of Neuroscience 32:3245-3252.

Dickinson JA, Hanrott KE, Mok MHS, Kew JNC, Wonnacott S (2007) Differential coupling of alpha 7 and non-alpha 7 nicotinic acetylcholine receptors to calcium-induced calcium release and voltage-operated calcium channels in PC12 cells. J Neurochem 100:1089-1096.

Ding YQ, Zheng HX, Wang DS, Xu JQ, Gong LW, Lu Y, Qin BZ, Shi J, Li HL, Li JS, Shigemoto R, Kaneko T, Mizuno N (1999) The distribution of substance P receptor (NK1)-like immunoreactive neurons in the newborn and adult human spinal cord. Neurosci Lett 266:133-136.

Doetsch F, GarciaVerdugo JM, AlvarezBuylla A (1997) Cellular composition and three-dimensional organization of the subventricular germinal zone in the adult mammalian brain. Journal of Neuroscience 17:5046-5061.

Doetsch F, Caille I, Lim DA, Garcia-Verdugo JM, Alvarez-Buylla A (1999) Subventricular zone astrocytes are neural stem cells in the adult mammalian brain. Cell 97:703-716.

Doetsch F, Petreanu L, Caille I, Garcia-Verdugo JM, Alvarez-Buylla A (2002) EGF converts transit-amplifying neurogenic precursors in the adult brain into multipotent stem cells. Neuron 36:1021-1034.

Dolphin AC, Scott RH (1987) Calcium channel currents and their inhibition by (-)-baclofen in rat sensory neurones: modulation by guanine nucleotides. J Physiol 386:1-17.

Doly S, Fischer J, Brisorgueil MJ, Verge D, Conrath M (2004) 5-HT5A receptor localization in the rat spinal cord suggests a role in nociception and control of pelvic floor musculature. J Comp Neurol 476:316-329.

Dun NJ, Mo N (1988) Invitro Effects of Substance-P on Neonatal Rat Sympathetic Preganglionic Neurons. J Physiol-London 399:321-333.

Dunbar MJ, Tran MA, Whelan PJ (2010) Endogenous extracellular serotonin modulates the spinal locomotor network of the neonatal mouse. J Physiol 588:139-156.

Dzhala V, Valeeva G, Glykys J, Khazipov R, Staley K (2012) Traumatic alterations in GABA signaling disrupt hippocampal network activity in the developing brain. J Neurosci 32:4017-4031.

Edelmann L, Hanson PI, Chapman ER, Jahn R (1995) Synaptobrevin Binding to Synaptophysin - a Potential Mechanism for Controlling the Exocytotic Fusion Machine. Embo J 14:224-231.

Edwards FA, Konnerth A, Sakmann B (1990) Quantal analysis of inhibitory synaptic transmission in the dentate gyrus of rat hippocampal slices: a patch-clamp study. J Physiol 430:213-249.

Eglen RM (2006) Muscarinic receptor subtypes in neuronal and non-neuronal cholinergic function. Auton Autacoid Pharmacol 26:219-233.

Elde R, Schalling M, Ceccatelli S, Nakanishi S, Hokfelt T (1990) Localization of neuropeptide receptor mRNA in rat brain: initial observations using probes for neurotensin and substance P receptors. Neurosci Lett 120:134-138.

Essrich C, Lorez M, Benson JA, Fritschy JM, Luscher B (1998) Postsynaptic clustering of major GABAA receptor subtypes requires the gamma 2 subunit and gephyrin. Nat Neurosci 1:563-571.

Farrant M, Nusser Z (2005) Variations on an inhibitory theme: phasic and tonic activation of GABA(A) receptors. Nat Rev Neurosci 6:215-229.

Feldblum S, Dumoulin A, Anoal M, Sandillon F, Privat A (1995) Comparative distribution of GAD(65) and GAD(67) mRNAs and proteins in the rat spinal cord supports a differential regulation of these two glutamate decarboxylases in vivo. Journal of Neuroscience Research 42:742-757.

Fernandez A, Radmilovich M, Trujillo-Cenoz O (2002) Neurogenesis and gliogenesis in the spinal cord of turtles. Journal of Comparative Neurology 453:131-144.

Fernandez E, Torrents D, Zorzano A, Palacin M, Chillaron J (2005) Identification and functional characterization of a novel low affinity aromatic-preferring amino acid transporter (arpAT) - One of the few proteins silenced during primate evolution. J Biol Chem 280:19364-19372.

Fonseca MI, Ni YG, Dunning DD, Miledi R (2001) Distribution of serotonin 2A, 2C and 3 receptor mRNA in spinal cord and medulla oblongata. Brain Res Mol Brain Res 89:11-19.

Frazier CJ, Buhler AV, Weiner JL, Dunwiddie TV (1998) Synaptic potentials mediated via alpha-bungarotoxin-sensitive nicotinic acetylcholine receptors in rat hippocampal interneurons. J Neurosci 18:8228-8235.

Fu H, Qi YC, Tan M, Cai J, Hu XM, Liu ZJ, Jensen J, Qiu MS (2003) Molecular mapping of the origin of postnatal spinal cord ependymal cells: Evidence that adult ependymal cells are derived from Nkx6.1+ventral neural progenitor cells. Journal of Comparative Neurology 456:237-244.

Fucile S (2004) Ca2+ permeability of nicotinic acetylcholine receptors. Cell calcium 35:1-8.

Fuji K, Senba E, Ueda Y, Tohyama M (1983) Vasoactive Intestinal Polypeptide (Vip)-Containing Neurons in the Spinal-Cord of the Rat and Their Projections. Neurosci Lett 37:51-55.

Gahwiler BH, Brown DA (1985) GABAB-receptor-activated K+ current in voltage-clamped CA3 pyramidal cells in hippocampal cultures. Proc Natl Acad Sci U S A 82:1558-1562.

Garcia-Ovejero D, Arevalo-Martin A, Paniagua-Torija B, Sierra-Palomares Y, Molina-Holgado E (2012) A cell population that strongly expresses the CB1 cannabinoid receptor in the central canal of the rat spinal cord. J Comp Neurol.

Gascon E, Dayer AG, Sauvain MO, Potter G, Jenny B, De Roo M, Zgraggen E, Demaurex N, Muller D, Kiss JZ (2006) GABA regulates dendritic growth by stabilizing lamellipodia in newly generated interneurons of the olfactory bulb. J Neurosci 26:12956-12966.

Ge S, Goh EL, Sailor KA, Kitabatake Y, Ming GL, Song H (2006) GABA regulates synaptic integration of newly generated neurons in the adult brain. Nature 439:589-593.

Genzen JR, Platel JC, Rubio ME, Bordey A (2009a) Ependymal cells along the lateral ventricle express functional P2X(7) receptors. Purinergic signalling 5:299-307.

Genzen JR, Yang D, Ravid K, Bordey A (2009b) Activation of adenosine A2B receptors enhances ciliary beat frequency in mouse lateral ventricle ependymal cells. Cerebrospinal Fluid Res 6:15.

Gerdes J, Lemke H, Baisch H, Wacker HH, Schwab U, Stein H (1984) Cell-Cycle Analysis of a Cell Proliferation-Associated Human Nuclear Antigen Defined by the Monoclonal-Antibody Ki-67. J Immunol 133:1710-1715.

Gibson SJ, Polak JM, Bloom SR, Wall PD (1981) The Distribution of 9 Peptides in Rat Spinal-Cord with Special Emphasis on the Substantia Gelatinosa and on the Area around the Central Canal (Lamina-Xbar). Journal of Comparative Neurology 201:65-79.

Gibson SJ, Polak JM, Anand P, Blank MA, Morrison JFB, Kelly JS, Bloom SR (1984) The Distribution and Origin of Vip in the Spinal-Cord of 6 Mammalian-Species. Peptides 5:201-207.

Giniatullin R, Nistri A, Yakel JL (2005) Desensitization of nicotinic ACh receptors: shaping cholinergic signaling. Trends Neurosci 28:371-378.

Gomeza J, Shannon H, Kostenis E, Felder C, Zhang L, Brodkin J, Grinberg A, Sheng H, Wess J (1999) Pronounced pharmacologic deficits in M2 muscarinic acetylcholine receptor knockout mice. Proc Natl Acad Sci U S A 96:1692-1697.

Gronlien JH, Hakerud M, Ween H, Thorin-Hagene K, Briggs CA, Gopalakrishnan M, Malysz J (2007) Distinct profiles of alpha7 nAChR positive allosteric modulation revealed by structurally diverse chemotypes. Mol Pharmacol 72:715-724.

Guan BC, Si JQ, Jiang ZG (2007) Blockade of gap junction coupling by glycyrrhetinic acids in guinea pig cochlear artery: a whole-cell voltage- and current-clamp study. Br J Pharmacol 151:1049-1060.

Gustafsson MV, Zheng XW, Pereira T, Gradin K, Jin SB, Lundkvist J, Ruas JL, Poellinger L, Lendahl U, Bondesson M (2005) Hypoxia requires Notch signaling to maintain the undifferentiated cell state. Dev Cell 9:617-628.

Hamilton LK, Truong MKV, Bednarczyk MR, Aumont A, Fernandes KJL (2009) Cellular Organization of the Central Canal Ependymal Zone, a Niche of Latent Neural Stem Cells in the Adult Mammalian Spinal Cord. Neuroscience 164:1044-1056.

Harrist A, Beech RD, King SL, Zanardi A, Cleary MA, Caldarone BJ, Eisch A, Zoli M, Picciotto MR (2004) Alteration of hippocampal cell proliferation in mice lacking the beta 2 subunit of the neuronal nicotinic acetylcholine receptor. Synapse 54:200-206.

Harvey SC, Luetje CW (1996) Determinants of competitive antagonist sensitivity on neuronal nicotinic receptor beta subunits. J Neurosci 16:3798-3806.

Harvey SC, Maddox FN, Luetje CW (1996) Multiple determinants of dihydro-beta-erythroidine sensitivity on rat neuronal nicotinic receptor alpha subunits. J Neurochem 67:1953-1959.

Henderson Z, Boros A, Janzso GE, Westwood AJ, Monyer H, Halasy K (2005) Somato-dendritic nicotinic receptor responses recorded in vitro from the medial septal diagonal band complex of the rodent. J Physiol-London 562:165-182.

Heyman NS, Burt JM (2008) Hindered diffusion through an aqueous pore describes invariant dye selectivity of Cx43 junctions. Biophysical journal 94:840-854.

Hinckley CA, Hartley R, Wu L, Todd A, Ziskind-Conhaim L (2005) Locomotor-like rhythms in a genetically distinct cluster of interneurons in the mammalian spinal cord. J Neurophysiol 93:1439-1449.

Hinckley CA, Wiesner EP, Mentis GZ, Titus DJ, Ziskind-Conhaim L (2010) Sensory Modulation of Locomotor-Like Membrane Oscillations in Hb9-Expressing Interneurons. J Neurophysiol 103:3407-3423.

Hitoshi S, Maruta N, Higashi M, Kumar A, Kato N, Ikenaka K (2007) Antidepressant drugs reverse the loss of adult neural stem cells following chronic stress. J Neurosci Res 85:3574-3585.

Hoglund AU, Baghdoyan HA (1997) M2, M3 and M4, but not M1, muscarinic receptor subtypes are present in rat spinal cord. J Pharmacol Exp Ther 281:470-477.

Hokfelt T, Kellerth JO, Nilsson G, Pernow B (1975) Experimental Immunohistochemical Studies on Localization and Distribution of Substance-P in Cat Primary Sensory Neurons. Brain Research 100:235-252.

Hokfelt T, Elde R, Johansson O, Terenius L, Stein L (1977) Distribution of Encephalin-Immunoreactive Cell Bodies in Rat Central Nervous-System. Neurosci Lett 5:25-31.

Holz GGt, Rane SG, Dunlap K (1986) GTP-binding proteins mediate transmitter inhibition of voltage-dependent calcium channels. Nature 319:670-672.

Horner PJ, Power AE, Kempermann G, Kuhn HG, Palmer TD, Winkler J, Thal LJ, Gage FH (2000) Proliferation and differentiation of progenitor cells throughout the intact adult rat spinal cord. Journal of Neuroscience 20:2218-2228.

Hosoya Y, Matsukawa M, Okado N, Sugiura Y, Kohno K (1995) Oxytocinergic Innervation to the Upper Thoracic Sympathetic Preganglionic Neurons in the Rat - a Light and Electron-Microscopic Study Using a Combined Retrograde Transport and Immunocytochemical Technique. Exp Brain Res 107:9-16.

Houser CR, Crawford GD, Barber RP, Salvaterra PM, Vaughn JE (1983) Organization and Morphological-Characteristics of Cholinergic Neurons - an

Immunocytochemical Study with a Monoclonal-Antibody to Choline-Acetyltransferase. Brain Research 266:97-119.

Hoyer D, Clarke DE, Fozard JR, Hartig PR, Martin GR, Mylecharane EJ, Saxena PR, Humphrey PP (1994) International Union of Pharmacology classification of receptors for 5-hydroxytryptamine (Serotonin). Pharmacol Rev 46:157-203.

Huang A, Noga BR, Carr PA, Fedirchuk B, Jordan LM (2000) Spinal cholinergic neurons activated during locomotion: Localization and electrophysiological characterization. J Neurophysiol 83:3537-3547.

Huang AL, Chen XK, Hoon MA, Chandrashekar J, Guo W, Trankner D, Ryba NJP, Zuker CS (2006) The cells and logic for mammalian sour taste detection. Nature 442:934-938.

Huang X, Liu J, Ketova T, Fleming JT, Grover VK, Cooper MK, Litingtung Y, Chiang C (2010) Transventricular delivery of Sonic hedgehog is essential to cerebellar ventricular zone development. Proc Natl Acad Sci U S A 107:8422-8427.

Huang YA, Maruyama Y, Stimac R, Roper SD (2008) Presynaptic (Type III) cells in mouse taste buds sense sour (acid) taste. J Physiol-London 586:2903-2912.

Hurst RS, Hajos M, Raggenbass M, Wall TM, Higdon NR, Lawson JA, Rutherford-Root KL, Berkenpas MB, Hoffmann WE, Piotrowski DW, Groppi VE, Allaman G, Ogier R, Bertrand S, Bertrand D, Arneric SP (2005) A novel positive allosteric modulator of the alpha7 neuronal nicotinic acetylcholine receptor: in vitro and in vivo characterization. J Neurosci 25:4396-4405.

Husch A, Cramer N, Harris-Warrick RM (2011) Long-duration perforated patch recordings from spinal interneurons of adult mice. J Neurophysiol 106:2783-2789.

Ihrie RA, Alvarez-Buylla A (2011) Lake-Front Property: A Unique Germinal Niche by the Lateral Ventricles of the Adult Brain. Neuron 70:674-686.

Inoue M, Matsuo T, Ogata N (1985) Baclofen activates voltage-dependent and 4-aminopyridine sensitive K+ conductance in guinea-pig hippocampal pyramidal cells maintained in vitro. Br J Pharmacol 84:833-841.

Ishida Y, Yokoyama C, Inatomi T, Yagita K, Dong X, Yan LL, Yamaguchi S, Nagatsu I, Komori T, Kitahama K, Okamura H (2002) Circadian rhythm of aromatic L-amino acid decarboxylase in the rat suprachiasmatic nucleus: gene expression and decarboxylating activity in clock oscillating cells. Genes Cells 7:447-459.

Ishimaru Y, Inada H, Kubota M, Zhuang H, Tominaga M, Matsunami H (2006) Transient receptor potential family members PKD1L3 and PKD2L1 form a candidate sour taste receptor. P Natl Acad Sci USA 103:12569-12574.

Jaeger CB, Teitelman G, Joh TH, Albert VR, Park DH, Reis DJ (1983) Some Neurons of the Rat Central Nervous-System Contain Aromatic-L-Amino-Acid Decarboxylase but Not Monoamines. Science 219:1233-1235.

Jarvis CR, Andrew RD (1988) Correlated electrophysiology and morphology of the ependyma in rat hypothalamus. J Neurosci 8:3691-3702.

Johanson CE, Duncan JA, 3rd, Klinge PM, Brinker T, Stopa EG, Silverberg GD (2008) Multiplicity of cerebrospinal fluid functions: New challenges in health and disease. Cerebrospinal Fluid Res 5:10.

Johansson CB, Momma S, Clarke DL, Risling M, Lendahl U, Frisen J (1999) Identification of a neural stem cell in the adult mammalian central nervous system. Cell 96:25-34.

John D (2010) Immunocytochemical and electrophysiological properties of alpha 7 nicotinic acetylcholine receptors in rodent dentate gyrus and a murine cholinergic cell line. In: Institute of Membrane and Systems Biology. University of Leeds: Leeds.

Kage R, McGregor GP, Thim L, Conlon JM (1988) Neuropeptide-gamma: a peptide isolated from rabbit intestine that is derived from gamma-preprotachykinin. J Neurochem 50:1412-1417.

Kanaka C, Ohno K, Okabe A, Kuriyama K, Itoh T, Fukuda A, Sato K (2001) The differential expression patterns of messenger RNAs encoding K-Cl cotransporters (KCC1,2) and Na-K-2Cl cotransporter (NKCC1) in the rat nervous system. Neuroscience 104:933-946.

Kaneda M, Farrant M, Cull-Candy SG (1995) Whole-cell and single-channel currents activated by GABA and glycine in granule cells of the rat cerebellum. J Physiol 485 (Pt 2):419-435.

Kaneko N, Okano H, Sawamoto K (2006) Role of the cholinergic system in regulating survival of newborn neurons in the adult mouse dentate gyrus and olfactory bulb. Genes Cells 11:1145-1159.

Kaneko T, Fujiyama F, Hioki H (2002) Immunohistochemical localization of candidates for vesicular glutamate transporters in the rat brain. Journal of Comparative Neurology 444:39-62.

Kangawa K, Minamino N, Fukuda A, Matsuo H (1983) Neuromedin K: a novel mammalian tachykinin identified in porcine spinal cord. Biochem Biophys Res Commun 114:533-540.

Karlin A, Holtzman E, Yodh N, Lobel P, Wall J, Hainfeld J (1983) The arrangement of the subunits of the acetylcholine receptor of Torpedo californica. J Biol Chem 258:6678-6681.

Karussis D, Kassis I (2008) The potential use of stem cells in multiple sclerosis: an overview of the preclinical experience. Clinical neurology and neurosurgery 110:889-896.

Kaupmann K, Huggel K, Heid J, Flor PJ, Bischoff S, Mickel SJ, McMaster G, Angst C, Bittiger H, Froestl W, Bettler B (1997) Expression cloning of GABA(B) receptors uncovers similarity to metabotropic glutamate receptors. Nature 386:239-246.

Kaupmann K, Malitschek B, Schuler V, Heid J, Froestl W, Beck P, Mosbacher J, Bischoff S, Kulik A, Shigemoto R, Karschin A, Bettler B (1998) GABA(B)-receptor subtypes assemble into functional heteromeric complexes. Nature 396:683-687.

Kiehn O (2006) Locomotor circuits in the mammalian spinal cord. Annu Rev Neurosci 29:279-306.

King BF, Wildman SS, Ziganshina LE, Pintor J, Burnstock G (1997) Effects of extracellular pH on agonism and antagonism at a recombinant P2X(2) receptor. Brit J Pharmacol 121:1445-1453.

Kita H, Armstrong W (1991) A biotin-containing compound N-(2-aminoethyl)biotinamide for intracellular labeling and neuronal tracing studies: comparison with biocytin. J Neurosci Methods 37:141-150.

Kobayashi M, Nikami H, Morimatsu M, Saito M (1996) Expression and localization of insulin-regulatable glucose transporter (GLUT4) in rat brain. Neurosci Lett 213:103-106.

Kofuji P, Newman EA (2004) Potassium buffering in the central nervous system. Neuroscience 129:1045-1056.

Kotani S, Yamauchi T, Teramoto T, Ogura H (2006) Pharmacological evidence of cholinergic involvement in adult hippocampal neurogenesis in rats. Neuroscience 142:505-514.

Kramer-Zucker AG, Olale F, Haycraft CJ, Yoder BK, Schier AF, Drummond IA (2005) Cilia-driven fluid flow in the zebrafish pronephros, brain and Kupffer's vesicle is required for normal organogenesis. Development 132:1907-1921.

Kunzelmann P, Schroder W, Traub O, Steinhauser C, Dermietzel R, Willecke K (1999) Late onset and increasing expression of the gap junction protein connexin30 in adult murine brain and long-term cultured astrocytes. Glia 25:111-119.

Kuscha V, Frazer SL, Dias TB, Hibi M, Becker T, Becker CG (2012) Lesion-induced generation of interneuron cell types in specific dorsoventral domains in the spinal cord of adult zebrafish. Journal of Comparative Neurology 520:3604-3616.

Kwatra MM, Schwinn DA, Schreurs J, Blank JL, Kim CM, Benovic JL, Krause JE, Caron MG, Lefkowitz RJ (1993) The substance P receptor, which couples to Gq/11, is a substrate of beta-adrenergic receptor kinase 1 and 2. J Biol Chem 268:9161-9164.

Lacar B, Young SZ, Platel JC, Bordey A (2011) Gap junction-mediated calcium waves define communication networks among murine postnatal neural progenitor cells. Eur J Neurosci 34:1895-1905.

Lamotte CC (1987) Vasoactive Intestinal Polypeptide Cerebrospinal Fluid-Contacting Neurons of the Monkey and Cat Spinal Central Canal. Journal of Comparative Neurology 258:527-541.

Lamotte CC, Johns DR, Delanerolle NC (1982) Immunohistochemical Evidence of Indoleamine Neurons in Monkey Spinal-Cord. Journal of Comparative Neurology 206:359-370.

Landis SC (1983) Neuronal growth cones. Annual review of physiology 45:567-580.

Lee MK, Tuttle JB, Rebhun LI, Cleveland DW, Frankfurter A (1990) The Expression and Posttranslational Modification of a Neuron-Specific Beta-Tubulin Isotype during Chick Embryogenesis. Cell Motil Cytoskel 17:118-132.

Lehtinen MK, Walsh CA (2010) Neurogenesis at the Brain-Cerebrospinal Fluid Interface. Annu Rev Cell Dev Biol.

Lehtinen MK, Zappaterra MW, Chen X, Yang YJ, Hill AD, Lun M, Maynard T, Gonzalez D, Kim S, Ye P, D'Ercole AJ, Wong ET, LaMantia AS, Walsh CA (2011) The cerebrospinal fluid provides a proliferative niche for neural progenitor cells. Neuron 69:893-905.

Lena C, Changeux JP, Mulle C (1993) Evidence for "preterminal" nicotinic receptors on GABAergic axons in the rat interpeduncular nucleus. J Neurosci 13:2680-2688.

Lendvai B, Vizi ES (2008) Nonsynaptic chemical transmission through nicotinic acetylcholine receptors. Physiol Rev 88:333-349.

Leung DS, Unsicker K, Reuss B (2002) Expression and developmental regulation of gap junction connexins cx26, cx32, cx43 and cx45 in the rat midbrain-floor. Int J Dev Neurosci 20:63-75.

Lewis DI, Coote JH (1990) Excitation and Inhibition of Rat Sympathetic Preganglionic Neurons by Catecholamines. Brain Research 530:229-234.

Light AR, Perl ER (1979) Spinal Termination of Functionally Identified Primary Afferent Neurons with Slowly Conducting Myelinated Fibers. Journal of Comparative Neurology 186:133-150.

Liu X, Bolteus AJ, Balkin DM, Henschel O, Bordey A (2006a) GFAP-expressing cells in the postnatal subventricular zone display a unique glial phenotype intermediate between radial glia and astrocytes. Glia 54:394-410.

Liu XX, Wang Q, Haydar TF, Bordey A (2005) Nonsynaptic GABA signaling in postnatal subventricular zone controls proliferation of GFAP-expressing progenitors. Nature Neuroscience 8:1179-1187.

Liu Z, Neff RA, Berg DK (2006b) Sequential interplay of nicotinic and GABAergic signaling guides neuronal development. Science 314:1610-1613.

Liu Z, Zhang J, Berg DK (2007) Role of endogenous nicotinic signaling in guiding neuronal development. Biochem Pharmacol 74:1112-1119.

Llewellyn-Smith IJ, Weaver LC, Keast JR (2006) Effects of spinal cord injury on synaptic inputs to sympathetic preganglionic neurons. Autonomic Dysfunction after Spinal Cord Injury 152:11-26.

Lois C, Alvarezbuylla A (1994) Long-Distance Neuronal Migration in the Adult Mammalian Brain. Science 264:1145-1148.

Lopez-Bendito G, Sturgess K, Erdelyi F, Szabo G, Molnar Z, Paulsen O (2004) Preferential origin and layer destination of GAD65-GFP cortical interneurons. Cereb Cortex 14:1122-1133.

LoTurco JJ, Owens DF, Heath MJ, Davis MB, Kriegstein AR (1995) GABA and glutamate depolarize cortical progenitor cells and inhibit DNA synthesis. Neuron 15:1287-1298.

Luetje CW, Patrick J (1991) Both alpha- and beta-subunits contribute to the agonist sensitivity of neuronal nicotinic acetylcholine receptors. J Neurosci 11:837-845.

Ma RC, Dun NJ (1986) Excitation of Lateral Horn Neurons of the Neonatal Rat Spinal-Cord by 5-Hydroxytryptamine. Dev Brain Res 24:89-98.

Macdonald SG, Boyd ND (1989) Regulation of substance P receptor affinity by guanine nucleotide-binding proteins. J Neurochem 53:264-272.

Mager S, Naeve J, Quick M, Labarca C, Davidson N, Lester HA (1993) Steady states, charge movements, and rates for a cloned GABA transporter expressed in Xenopus oocytes. Neuron 10:177-188.

Magoul R, Onteniente B, Geffard M, Calas A (1987) Anatomical distribution and ultrastructural organization of the GABAergic system in the rat spinal cord. An immunocytochemical study using anti-GABA antibodies. Neuroscience 20:1001-1009.

Maharaj ASR, Walshe TE, Saint-Geniez M, Venkatesha S, Maldonado AE, Himes NC, Matharu KS, Karumanchi SA, D'Amore PA (2008) VEGF and TGF-beta are required for the maintenance of the choroid plexus and ependyma. J Exp Med 205:491-501.

Malberg JE, Eisch AJ, Nestler EJ, Duman RS (2000) Chronic antidepressant treatment increases neurogenesis in adult rat hippocampus. J Neurosci 20:9104-9110.

Malone HM, Peters JA, Lambert JJ (1991) Physiological and pharmacological properties of 5-HT3 receptors--a patch clamp-study. Neuropeptides 19 Suppl:25-30.

Margeta-Mitrovic M, Mitrovic I, Riley RC, Jan LY, Basbaum AI (1999) Immunohistochemical localization of GABA(B) receptors in the rat central nervous system. Journal of Comparative Neurology 405:299-321.

Marichal N, Garcia G, Radmilovich M, Trujillo-Cenoz O, Russo RE (2009) Enigmatic Central Canal Contacting Cells: Immature Neurons in "Standby Mode"? Journal of Neuroscience 29:10010-10024.

Marichal N, Garcia G, Radmilovich M, Trujillo-Cenoz O, Russo RE (2012) Spatial domains of progenitor-like cells and functional complexity of a stem cell niche in the neonatal rat spinal cord. Stem Cells 30:2020-2031.

Marlier L, Teilhac JR, Cerruti C, Privat A (1991) Autoradiographic mapping of 5-HT1, 5-HT1A, 5-HT1B and 5-HT2 receptors in the rat spinal cord. Brain Res 550:15-23.

Martens DJ, Seaberg RM, van der Kooy D (2002) In vivo infusions of exogenous growth factors into the fourth ventricle of the adult mouse brain increase the proliferation of neural progenitors around the fourth ventricle and the central canal of the spinal cord. Eur J Neurosci 16:1045-1057.

Masu Y, Nakayama K, Tamaki H, Harada Y, Kuno M, Nakanishi S (1987) cDNA cloning of bovine substance-K receptor through oocyte expression system. Nature 329:836-838.

Matsumoto M, Weickert CS, Akil M, Lipska BK, Hyde TM, Herman MM, Kleinman JE, Weinberger DR (2003) Catechol O-methyltransferase mRNA expression in human and rat brain: evidence for a role in cortical neuronal function. Neuroscience 116:127-137.

Mclaughlin BJ, Barber R, Saito K, Roberts E, Wu JY (1975) Immunocytochemical Localization of Glutamate Decarboxylase in Rat Spinal-Cord. Journal of Comparative Neurology 164:305-321.

McMahon LL, Yoon KW, Chiappinelli VA (1994) Electrophysiological evidence for presynaptic nicotinic receptors in the avian ventral lateral geniculate nucleus. J Neurophysiol 71:826-829.

Meletis K, Barnabe-Heider F, Carlen M, Evergren E, Tomilin N, Shupliakov O, Frisen J (2008) Spinal cord injury reveals multilineage differentiation of ependymal cells. Plos Biology 6:1494-1507.

Miles GB, Hartley R, Todd AJ, Brownstone RM (2007) Spinal cholinergic interneurons regulate the excitability of motoneurons during locomotion. P Natl Acad Sci USA 104:2448-2453.

Milstein C, Wright B, Cuello AC (1983) The discrepancy between the cross-reactivity of a monoclonal antibody to serotonin and its immunohistochemical specificity. Molecular immunology 20:113-123.

Mirzadeh Z, Merkle FT, Soriano-Navarro M, Garcia-Verdugo JM, Alvarez-Buylla A (2008) Neural stem cells confer unique pinwheel architecture to the ventricular surface in neurogenic regions of the adult brain. Cell Stem Cell 3:265-278.

Mitsuhashi M, Ohashi Y, Shichijo S, Christian C, Sudduth-Klinger J, Harrowe G, Payan DG (1992) Multiple intracellular signaling pathways of the neuropeptide substance P receptor. J Neurosci Res 32:437-443.

Mochizuki-Oda N, Nakajima Y, Nakanishi S, Ito S (1994) Characterization of the substance P receptor-mediated calcium influx in cDNA transfected Chinese hamster ovary cells. A possible role of inositol 1,4,5-trisphosphate in calcium influx. J Biol Chem 269:9651-9658.

Mody I, De Koninck Y, Otis TS, Soltesz I (1994) Bridging the cleft at GABA synapses in the brain. Trends Neurosci 17:517-525.

Morcuende S, Gadd CA, Peters M, Moss A, Harris EA, Sheasby A, Fisher AS, De Felipe C, Mantyh PW, Rupniak NM, Giese KP, Hunt SP (2003) Increased neurogenesis and brain-derived neurotrophic factor in neurokinin-1 receptor gene knockout mice. Eur J Neurosci 18:1828-1836.

Mothe AJ, Tator CH (2005) Proliferation, migration, and differentiation of endogenous ependymal region stem/progenitor cells following minimal spinal cord injury in the adult rat. Neuroscience 131:177-187.

Moussaoui SM, Hermans E, Mathieu AM, Bonici B, Clerc F, Guinet F, Garret C, Laduron PM (1992) Polyclonal antibodies against the rat NK1 receptor: characterization and localization in the spinal cord. Neuroreport 3:1073-1076.

Mulle C, Changeux JP (1990) A novel type of nicotinic receptor in the rat central nervous system characterized by patch-clamp techniques. J Neurosci 10:169-175.

Mullen RJ, Buck CR, Smith AM (1992) Neun, a Neuronal Specific Nuclear-Protein in Vertebrates. Development 116:201-211.

Nagatsu I, Sakai M, Yoshida M, Nagatsu T (1988) Aromatic L-Amino-Acid Decarboxylase-Immunoreactive Neurons in and around the Cerebrospinal Fluid-Contacting Neurons of the Central Canal Do Not Contain Dopamine or Serotonin in the Mouse and Rat Spinal-Cord. Brain Research 475:91-102.

Nakajima Y, Nakajima S, Inoue M (1988) Pertussis toxin-insensitive G protein mediates substance P-induced inhibition of potassium channels in brain neurons. Proc Natl Acad Sci U S A 85:3643-3647.

Nakajima Y, Tsuchida K, Negishi M, Ito S, Nakanishi S (1992) Direct linkage of three tachykinin receptors to stimulation of both phosphatidylinositol hydrolysis and cyclic AMP cascades in transfected Chinese hamster ovary cells. J Biol Chem 267:2437-2442.

Nakanishi S (1991) Mammalian tachykinin receptors. Annu Rev Neurosci 14:123-136.

Nakaya Y, Kaneko T, Shigemoto R, Nakanishi S, Mizuno N (1994) Immunohistochemical localization of substance P receptor in the central nervous system of the adult rat. J Comp Neurol 347:249-274.

Nalivaiko E, Michaud JC, Soubrie P, LeFur G, Feltz P (1997) Tachykinin neurokinin-1 and neurokinin-3 receptor-mediated responses in guinea-pig substantia nigra: An in vitro electrophysiological study. Neuroscience 78:745-757.

Newberry NR, Nicoll RA (1984) A bicuculline-resistant inhibitory post-synaptic potential in rat hippocampal pyramidal cells in vitro. J Physiol 348:239-254.

Newman EA (1986) Regional specialization of the membrane of retinal glial cells and its importance to K+ spatial buffering. Ann N Y Acad Sci 481:273-286.

Newton BW, Maley BE, Hamill RW (1986) Immunohistochemical Demonstration of Serotonin Neurons in Autonomic Regions of the Rat Spinal-Cord. Brain Research 376:155-163.

Nguyen L, Malgrange B, Breuskin I, Bettendorff L, Moonen G, Belachew S, Rigo JM (2003) Autocrine/paracrine activation of the GABA(A) receptor inhibits the proliferation of neurogenic polysialylated neural cell adhesion molecule-positive (PSA-NCAM+) precursor cells from postnatal striatum. J Neurosci 23:3278-3294.

Nguyen T, Chin WC, O'Brien JA, Verdugo P, Berger AJ (2001) Intracellular pathways regulating ciliary beating of rat brain ependymal cells. J Physiol 531:131-140.

North RA, Surprenant A (2000) Pharmacology of cloned P2X receptors. Annual review of pharmacology and toxicology 40:563-580.

Nusser Z, Sieghart W, Somogyi P (1998) Segregation of different GABAA receptors to synaptic and extrasynaptic membranes of cerebellar granule cells. J Neurosci 18:1693-1703.

Ochalski PA, Frankenstein UN, Hertzberg EL, Nagy JI (1997) Connexin-43 in rat spinal cord: localization in astrocytes and identification of heterotypic astro-oligodendrocytic gap junctions. Neuroscience 76:931-945.

Okano HJ, Darnell RB (1997) A hierarchy of Hu RNA binding proteins in developing and adult neurons. Journal of Neuroscience 17:3024-3037.

Oki T, Takagi Y, Inagaki S, Taketo MM, Manabe T, Matsui M, Yamada S (2005) Quantitative analysis of binding parameters of [3H]N-methylscopolamine in central nervous system of muscarinic acetylcholine receptor knockout mice. Brain Res Mol Brain Res 133:6-11.

Olsen RW, Sieghart W (2008) International Union of Pharmacology. LXX. Subtypes of gamma-aminobutyric acid(A) receptors: classification on the basis of subunit composition, pharmacology, and function. Update. Pharmacol Rev 60:243-260.

Orts Del'immagine A, Wanaverbecq N, Tardivel C, Tillement V, Dallaporta M, Trouslard J (2012) Properties of subependymal cerebrospinal fluid contacting neurones in the dorsal vagal complex of the mouse brainstem. J Physiol.

Palacios JM, Waeber C, Hoyer D, Mengod G (1990) Distribution of serotonin receptors. Ann N Y Acad Sci 600:36-52.

Papke RL, Bencherif M, Lippiello P (1996) An evaluation of neuronal nicotinic acetylcholine receptor activation by quaternary nitrogen compounds indicates that choline is selective for the alpha 7 subtype. Neurosci Lett 213:201-204.

Park SW, Yan YP, Satriotomo I, Vemuganti R, Dempsey RJ (2007) Substance P is a promoter of adult neural progenitor cell proliferation under normal and ischemic conditions. J Neurosurg 107:593-599.

Pasternack M, Voipio J, Kaila K (1993) Intracellular carbonic anhydrase activity and its role in GABA-induced acidosis in isolated rat hippocampal pyramidal neurones. Acta Physiol Scand 148:229-231.

Pennefather JN, Lecci A, Candenas ML, Patak E, Pinto FM, Maggi CA (2004) Tachykinins and tachykinin receptors: a growing family. Life Sci 74:1445-1463.

Phelps PE, Barber RP, Houser CR, Crawford GD, Salvaterra PM, Vaughn JE (1984) Postnatal-Development of Neurons Containing Choline-Acetyltransferase in Rat Spinal-Cord - an Immunocytochemical Study. Journal of Comparative Neurology 229:347-361.

Pickering AE, Spanswick D, Logan SD (1994) 5-Hydroxytryptamine Evokes Depolarizations and Membrane-Potential Oscillations in Rat Sympathetic Preganglionic Neurones. J Physiol-London 480:109-121.

Pierce ML, Deuchars J, Deuchars SA (2010) Spontaneous rhythmogenic capabilities of sympathetic neuronal assemblies in the rat spinal cord slice. Neuroscience 170:827-838.

Pierre K, Pellerin L, Debernardi R, Riederer BM, Magistretti PJ (2000) Cell-specific localization of monocarboxylate transporters, MCT1 and MCT2, in the adult mouse brain revealed by double immunohistochemical labeling and confocal microscopy. Neuroscience 100:617-627.

Price GW, Kelly JS, Bowery NG (1987) The location of GABAB receptor binding sites in mammalian spinal cord. Synapse 1:530-538.

Pugh PC, Berg DK (1994) Neuronal acetylcholine receptors that bind alpha-bungarotoxin mediate neurite retraction in a calcium-dependent manner. J Neurosci 14:889-896.

Quartara L, Maggi CA (1997) The tachykinin NK1 receptor. Part I: ligands and mechanisms of cellular activation. Neuropeptides 31:537-563.

Quik M, Chan J, Patrick J (1994) alpha-Bungarotoxin blocks the nicotinic receptor mediated increase in cell number in a neuroendocrine cell line. Brain Res 655:161-167.

Raftery MA, Hunkapiller MW, Strader CD, Hood LE (1980) Acetylcholine receptor: complex of homologous subunits. Science 208:1454-1456.

Rang HPD, M.M.; Ritter, J.M.; Moore, P.K. (2003) Chapter 10: Cholinergic Transmission. Pharmacology.

Raymond JR, Mukhin YV, Gelasco A, Turner J, Collinsworth G, Gettys TW, Grewal JS, Garnovskaya MN (2001) Multiplicity of mechanisms of serotonin receptor signal transduction. Pharmacol Ther 92:179-212.

Reali C, Fernandez A, Radmilovich M, Trujillo-Cenoz O, Russo RE (2011) GABAergic signalling in a neurogenic niche of the turtle spinal cord. J Physiol-London 589:5633-5647.

Regoli D, Nguyen QT, Jukic D (1994) Neurokinin receptor subtypes characterized by biological assays. Life Sci 54:2035-2047.

Rexed B (1952) The cytoarchitectonic organization of the spinal cord in the cat. J Comp Neurol 96:414-495.

Rick CE, Stanford IM, Lacey MG (1995) Excitation of Rat Substantia-Nigra Pars Reticulata Neurons by 5-Hydroxytryptamine in-Vitro - Evidence for a Direct Action Mediated by 5-Hydroxytryptamine(2c) Receptors. Neuroscience 69:903-913.

Rivera C, Voipio J, Payne JA, Ruusuvuori E, Lahtinen H, Lamsa K, Pirvola U, Saarma M, Kaila K (1999) The K+/Cl- co-transporter KCC2 renders GABA hyperpolarizing during neuronal maturation. Nature 397:251-255.

Roberts BL, Maslam S, Scholten G, Smit W (1995) Dopaminergic and Gabaergic Cerebrospinal Fluid-Contacting Neurons Along the Central Canal of the Spinal-Cord of the Eel and Trout. Journal of Comparative Neurology 354:423-437.

Rogers SW, Gregori NZ, Carlson N, Gahring LC, Noble M (2001) Neuronal nicotinic acetylcholine receptor expression by O2A/oligodendrocyte progenitor cells. Glia 33:306-313.

Romano C, Goldstein A (1980) Stereospecific nicotine receptors on rat brain membranes. Science 210:647-650.

Roth Y, Kimhi Y, Edery H, Aharonson E, Priel Z (1985) Ciliary motility in brain ventricular system and trachea of hamsters. Brain Res 330:291-297.

Rozzo A, Armellin M, Franzot J, Chiaruttini C, Nistri A, Tongiorgi E (2002) Expression and dendritic mRNA localization of GABAC receptor rho1 and rho2 subunits in developing rat brain and spinal cord. Eur J Neurosci 15:1747-1758.

Russo RE, Reali C, Radmilovich M, Fernandez A, Trujillo-Cenoz O (2008) Connexin 43 delimits functional domains of neurogenic precursors in the spinal cord. Journal of Neuroscience 28:3298-3309.

Sabourin JC, Ackema KB, Ohayon D, Guichet PO, Perrin FE, Garces A, Ripoll C, Charite J, Simonneau L, Kettenmann H, Zine A, Privat A, Valmier J, Pattyn A, Hugnot JP (2009) A Mesenchymal-Like ZEB1(+) Niche Harbors Dorsal Radial Glial Fibrillary Acidic Protein-Positive Stem Cells in the Spinal Cord. Stem Cells 27:2722-2733.

Sargent PB (1993) The diversity of neuronal nicotinic acetylcholine receptors. Annu Rev Neurosci 16:403-443.

Sawamoto K, Wichterle H, Gonzalez-Perez O, Cholfin JA, Yamada M, Spassky N, Murcia NS, Garcia-Verdugo JM, Marin O, Rubenstein JL, Tessier-Lavigne M, Okano H, Alvarez-Buylla A (2006) New neurons follow the flow of cerebrospinal fluid in the adult brain. Science 311:629-632.

Sawchenko PE, Swanson LW (1982) Immunohistochemical Identification of Neurons in the Paraventricular Nucleus of the Hypothalamus That Project to the Medulla or to the Spinal-Cord in the Rat. Journal of Comparative Neurology 205:260-272.

Schoeffter P, Hoyer D (1988) Centrally acting hypotensive agents with affinity for 5-HT1A binding sites inhibit forskolin-stimulated adenylate cyclase activity in calf hippocampus. Br J Pharmacol 95:975-985.

Schweizer C, Balsiger S, Bluethmann H, Mansuy IM, Fritschy JM, Mohler H, Luscher B (2003) The gamma 2 subunit of GABA(A) receptors is required for maintenance of receptors at mature synapses. Mol Cell Neurosci 24:442-450.

Seddik R, Schlichter R, Trouslard J (2006) Modulation of GABAergic synaptic transmission by terminal nicotinic acetylcholine receptors in the central autonomic nucleus of the neonatal rat spinal cord. Neuropharmacology 51:77-89.

Seguela P, Wadiche J, Dineley-Miller K, Dani JA, Patrick JW (1993) Molecular cloning, functional properties, and distribution of rat brain alpha 7: a nicotinic cation channel highly permeable to calcium. J Neurosci 13:596-604.

Sharma G, Vijayaraghavan S (2001) Nicotinic cholinergic signaling in hippocampal astrocytes involves calcium-induced calcium release from intracellular stores. Proc Natl Acad Sci U S A 98:4148-4153.

Sharma G, Vijayaraghavan S (2002) Nicotinic receptor signaling in nonexcitable cells. J Neurobiol 53:524-534.

Shechter R, Ziv Y, Schwartz M (2007) New GABAergic Interneurons supported by myelin-specific T cells are formed in intact adult spinal cord. Stem Cells 25:2277-2282.

Shechter R, Baruch K, Schwartz M, Rolls A (2011) Touch gives new life: mechanosensation modulates spinal cord adult neurogenesis. Mol Psychiatr 16:342-352.

Shen JX, Yakel JL (2012) Functional alpha7 Nicotinic ACh Receptors on Astrocytes in Rat Hippocampal CA1 Slices. J Mol Neurosci 48:14-21.

Sherriff FE, Henderson Z (1994) A Cholinergic Propriospinal Innervation of the Rat Spinal-Cord. Brain Research 634:150-154.

Shihabuddin LS, Horner PJ, Ray J, Gage FH (2000) Adult spinal cord stem cells generate neurons after transplantation in the adult dentate gyrus. Journal of Neuroscience 20:8727-8735.

Shimosegawa T, Koizumi M, Toyota T, Goto Y, Yanaihara C, Yanaihara N (1986) An Immunohistochemical Study of Methionine-Enkephalin-Arg6-Gly7-Leu8-Like Immunoreactivity-Containing Liquor-Contacting Neurons (Lcns) in the Rat Spinal-Cord. Brain Research 379:1-9.

Silva-Alvarez C, Carrasco M, Balmaceda-Aguilera C, Pastor P, Garcia MD, Reinicke K, Aguayo L, Molina B, Cifuentes M, Medina R, Nualart F (2005) Ependymal cell differentiation and GLUT1 expression is a synchronous process in the ventricular wall. Neurochem Res 30:1227-1236.

Simon J, Wakimoto H, Fujita N, Lalande M, Barnard EA (2004) Analysis of the set of GABA(A) receptor genes in the human genome. J Biol Chem 279:41422-41435.

Sine SM, Engel AG (2006) Recent advances in Cys-loop receptor structure and function. Nature 440:448-455.

Skipor J, Thiery JC (2008) The choroid plexus--cerebrospinal fluid system: undervaluated pathway of neuroendocrine signaling into the brain. Acta Neurobiol Exp (Wars) 68:414-428.

Soumier A, Banasr M, Goff LK, Daszuta A (2010) Region- and phase-dependent effects of 5-HT(1A) and 5-HT(2C) receptor activation on adult neurogenesis. Eur Neuropsychopharmacol 20:336-345.

Soumier A, Banasr M, Lortet S, Masmejean F, Bernard N, Kerkerian-Le-Goff L, Gabriel C, Millan MJ, Mocaer E, Daszuta A (2009) Mechanisms contributing to the phase-dependent regulation of neurogenesis by the novel antidepressant, agomelatine, in the adult rat hippocampus. Neuropsychopharmacology 34:2390-2403.

Spector R, Johanson CE (1989) The mammalian choroid plexus. Sci Am 261:68-74.

Staley KJ, Soldo BL, Proctor WR (1995) Ionic mechanisms of neuronal excitation by inhibitory GABAA receptors. Science 269:977-981.

Stell BM, Brickley SG, Tang CY, Farrant M, Mody I (2003) Neuroactive steroids reduce neuronal excitability by selectively enhancing tonic inhibition mediated by delta subunit-containing GABAA receptors. Proc Natl Acad Sci U S A 100:14439-14444.

Stepien AE, Tripodi M, Arber S (2010) Monosynaptic Rabies Virus Reveals Premotor Network Organization and Synaptic Specificity of Cholinergic Partition Cells. Neuron 68:456-472.

Stoeckel ME, Uhl-Bronner S, Hugel S, Veinante P, Klein MJ, Mutterer J, Freund-Mercier MJ, Schlichter R (2003) Cerebrospinal fluid-contacting neurons in the rat spinal cord, a gamma-aminobutyric acidergic system expressing the P2X(2) subunit of purinergic receptors, PSA-NCAM, and GAP-43 immunoreactivities: Light and electron microscopic study. Journal of Comparative Neurology 457:159-174.

Stoop R, Surprenant A, North RA (1997) Different sensitivities to pH of ATP-induced currents at four cloned P2X receptors. J Neurophysiol 78:1837-1840.

Strack AM, Sawyer WB, Marubio LM, Loewy AD (1988) Spinal origin of sympathetic preganglionic neurons in the rat. Brain Res 455:187-191.

Strack AM, Sawyer WB, Platt KB, Loewy AD (1989) CNS cell groups regulating the sympathetic outflow to adrenal gland as revealed by transneuronal cell body labeling with pseudorabies virus. Brain Research 491:274-296.

Sun XP, Supplisson S, Mayer E (1993) Chloride channels in myocytes from rabbit colon are regulated by a pertussis toxin-sensitive G protein. Am J Physiol 264:G774-785.

Swanson LW, Mckellar S (1979) Distribution of Oxytocin-Stained and Neurophysin-Stained Fibers in the Spinal-Cord of the Rat and Monkey. Journal of Comparative Neurology 188:87-106.

Takai T, Noda M, Mishina M, Shimizu S, Furutani Y, Kayano T, Ikeda T, Kubo T, Takahashi H, Takahashi T, et al. (1985) Cloning, sequencing and expression of cDNA for a novel subunit of acetylcholine receptor from calf muscle. Nature 315:761-764.

Takeda Y, Blount P, Sachais BS, Hershey AD, Raddatz R, Krause JE (1992) Ligand binding kinetics of substance P and neurokinin A receptors stably expressed in Chinese hamster ovary cells and evidence for differential stimulation of inositol 1,4,5-trisphosphate and cyclic AMP second messenger responses. J Neurochem 59:740-745.

Takeoka A, Kubasak MD, Zhong H, Roy RR, Phelps PE (2009) Serotonergic Innervation of the Caudal Spinal Stump in Rats After Complete Spinal Transection: Effect of Olfactory Ensheathing Glia. Journal of Comparative Neurology 515:664-676.

Takeoka A, Kubasak MD, Zhong H, Kaplan J, Roy RR, Phelps PE (2010) Noradrenergic innervation of the rat spinal cord caudal to a complete spinal cord transection: Effects of olfactory ensheathing glia. Experimental Neurology 222:59-69.

Tamamaki N, Yanagawa Y, Tomioka R, Miyazaki J, Obata K, Kaneko T (2003) Green fluorescent protein expression and colocalization with calretinin, parvalbumin, and somatostatin in the GAD67-GFP knock-in mouse. J Comp Neurol 467:60-79.

Tavazoie M, Van der Veken L, Silva-Vargas V, Louissaint M, Colonna L, Zaidi B, Garcia-Verdugo JM, Doetsch F (2008) A specialized vascular niche for adult neural stem cells. Cell Stem Cell 3:279-288.

Telgkamp P, Padgett DE, Ledoux VA, Woolley CS, Raman IM (2004) Maintenance of high-frequency transmission at purkinje to cerebellar nuclear synapses by spillover from boutons with multiple release sites. Neuron 41:113-126.

Terao S, Sobue G, Hashizume Y, Li M, Inagaki T, Mitsuma T (1996) Age-related changes in human spinal ventral horn cells with special reference to the loss of small neurons in the intermediate zone: a quantitative analysis. Acta Neuropathol 92:109-114.

Theodosis DT, Rougon G, Poulain DA (1991) Retention of Embryonic Features by an Adult Neuronal System Capable of Plasticity - Polysialylated Neural Cell-Adhesion Molecule in the Hypothalamo Neurohypophyseal System. P Natl Acad Sci USA 88:5494-5498.

Theodosis DT, Bonfanti L, Olive S, Rougon G, Poulain DA (1994) Adhesion Molecules and Structural Plasticity of the Adult Hypothalamoneurohypophyseal System. Psychoneuroendocrino 19:455-462.

Thomas KE, Moon LD (2011) Will stem cell therapies be safe and effective for treating spinal cord injuries? British medical bulletin 98:127-142.

Tohgi H, Abe T, Hashiguchi K, Saheki M, Takahashi S (1994) Remarkable reduction in acetylcholine concentration in the cerebrospinal fluid from patients with Alzheimer type dementia. Neurosci Lett 177:139-142.

Towers S, Princivalle A, Billinton A, Edmunds M, Bettler B, Urban L, Castro-Lopes J, Bowery NG (2000) GABAB receptor protein and mRNA distribution in rat spinal cord and dorsal root ganglia. Eur J Neurosci 12:3201-3210.

Tozuka Y, Fukuda S, Namba T, Seki T, Hisatsune T (2005) GABAergic excitation promotes neuronal differentiation in adult hippocampal progenitor cells. Neuron 47:803-815.

Tredway TL, Guo JZ, Chiappinelli VA (1999) N-type voltage-dependent calcium channels mediate the nicotinic enhancement of GABA release in chick brain. J Neurophysiol 81:447-454.

Uchida I, Cestari IN, Yang J (1996) The differential antagonism by bicuculline and SR95531 of pentobarbitone-induced currents in cultured hippocampal neurons. European Journal of Pharmacology 307:89-96.

Ugrumov MV (2009) Non-dopaminergic neurons partly expressing dopaminergic phenotype: Distribution in the brain, development and functional significance. J Chem Neuroanat 38:241-256.

Umbriaco D, Watkins KC, Descarries L, Cozzari C, Hartman BK (1994) Ultrastructural and morphometric features of the acetylcholine innervation in adult rat parietal cortex: an electron microscopic study in serial sections. J Comp Neurol 348:351-373.

Unwin N (1993) Nicotinic acetylcholine receptor at 9 A resolution. J Mol Biol 229:1101-1124.

Unwin N (2005) Refined structure of the nicotinic acetylcholine receptor at 4A resolution. J Mol Biol 346:967-989.

Vallejo YF, Buisson B, Bertrand D, Green WN (2005) Chronic nicotine exposure upregulates nicotinic receptors by a novel mechanism. J Neurosci 25:5563-5572.

van den Pol AN (1999) Hypothalamic hypocretin (orexin): Robust innervation of the spinal cord. Journal of Neuroscience 19:3171-3182.

Vaney DI (1991) Many diverse types of retinal neurons show tracer coupling when injected with biocytin or Neurobiotin. Neurosci Lett 125:187-190.

Veening JG, Barendregt HP (2010) The regulation of brain states by neuroactive substances distributed via the cerebrospinal fluid; a review. Cerebrospinal Fluid Res 7:1.

Velez-Fort M, Audinat E, Angulo MC (2009) Functional alpha 7-containing nicotinic receptors of NG2-expressing cells in the hippocampus. Glia 57:1104-1114.

Vessal M, Aycock A, Garton MT, Ciferri M, Darian-Smith C (2007) Adult neurogenesis in primate and rodent spinal cord: comparing a cervical dorsal rhizotomy with a dorsal column transection. Eur J Neurosci 26:2777-2794.

Vigh B, Vighteichmann I, Aros B (1977) Special Dendritic and Axonal Endings Formed by Cerebrospinal-Fluid Contacting Neurons of Spinal-Cord. Cell and Tissue Research 183:541-552.

Vigh B, Vighteichmann I, Silva MJME, Vandenpol AN (1983) Cerebrospinal Fluid-Contacting Neurons of the Central Canal and Terminal Ventricle in Various Vertebrates. Cell and Tissue Research 231:615-621.

Vigh B, Silva MJME, Frank CL, Vincze C, Czirok SJ, Szabo A, Lukats A, Szel A (2004) The system of cerebrospinal fluid-contacting neurons. Its supposed role in the nonsynaptic signal transmission of the brain. Histol Histopathol 19:607-628.

Vitalis T, Fouquet C, Alvarez C, Seif I, Price D, Gaspar P, Cases O (2002) Developmental expression of monoamine oxidases A and B in the central and peripheral nervous systems of the mouse. J Comp Neurol 442:331-347.

Wada E, Wada K, Boulter J, Deneris E, Heinemann S, Patrick J, Swanson LW (1989) Distribution of alpha 2, alpha 3, alpha 4, and beta 2 neuronal nicotinic

receptor subunit mRNAs in the central nervous system: a hybridization histochemical study in the rat. J Comp Neurol 284:314-335.

Wang DD, Krueger DD, Bordey A (2003) GABA depolarizes neuronal progenitors of the postnatal subventricular zone via GABAA receptor activation. J Physiol 550:785-800.

Wang HZ, Veenstra RD (1997) Monovalent ion selectivity sequences of the rat connexin43 gap junction channel. The Journal of general physiology 109:491-507.

Wang L, Spary E, Deuchars J, Deuchars SA (2008) Tonic GABAergic inhibition of sympathetic preganglionic neurons: a novel substrate for sympathetic control. J Neurosci 28:12445-12452.

Wang L, Bruce G, Spary E, Deuchars J, Deuchars SA (2010) GABA(B) Mediated Regulation of Sympathetic Preganglionic Neurons: Pre- and Postsynaptic Sites of Action. Frontiers in neurology 1:142.

Wang LP, Kempermann G, Kettenmann H (2005) A subpopulation of precursor cells in the mouse dentate gyrus receives synaptic GABAergic input. Mol Cell Neurosci 29:181-189.

Wang MY, Dun NJ (1990) 5-Hydroxytryptamine Responses in Neonate Rat Motoneurons Invitro. J Physiol-London 430:87-103.

Watanabe M, Fukaya M, Sakimura K, Manabe T, Mishina M, Inoue Y (1998) Selective scarcity of NMDA receptor channel subunits in the stratum lucidum (mossy fibre-recipient layer) of the mouse hippocampal CA3 subfield. Eur J Neurosci 10:478-487.

Weiss S, Dunne C, Hewson J, Wohl C, Wheatley M, Peterson AC, Reynolds BA (1996) Multipotent CNS stem cells are present in the adult mammalian spinal cord and ventricular neuroaxis. Journal of Neuroscience 16:7599-7609.

Weissman TA, Riquelme PA, Ivic L, Flint AC, Kriegstein AR (2004) Calcium waves propagate through radial glial cells and modulate proliferation in the developing neocortex. Neuron 43:647-661.

Wessler I, Kirkpatrick CJ (2008) Acetylcholine beyond neurons: the non-neuronal cholinergic system in humans. Br J Pharmacol 154:1558-1571.

Wilson JM, Hartley R, Maxwell DJ, Todd AJ, Lieberam I, Kaltschmidt JA, Yoshida Y, Jessell TM, Brownstone RM (2005) Conditional rhythmicity of ventral spinal interneurons defined by expression of the Hb9 homeodomain protein. Journal of Neuroscience 25:5710-5719.

Wisden W, Gundlach AL, Barnard EA, Seeburg PH, Hunt SP (1991) Distribution of GABAA receptor subunit mRNAs in rat lumbar spinal cord. Brain Res Mol Brain Res 10:179-183.

Wojtowicz JM, Kee N (2006) BrdU assay for neurogenesis in rodents. Nature Protocols 1:1399-1405.

Wong DT, Bymaster FP, Horng JS, Molloy BB (1975) A new selective inhibitor for uptake of serotonin into synaptosomes of rat brain: 3-(p-trifluoromethylphenoxy). N-methyl-3-phenylpropylamine. J Pharmacol Exp Ther 193:804-811.

Wonnacott S (1997) Presynaptic nicotinic ACh receptors. Trends Neurosci 20:92-98.

Wonnacott SA, X; Bertrand, D. (1993) Methyllcaconitine: A new probe that discriminates between nicotinic acetylcholine receptor subclasses. Methods in Neurosciences 12:263-275.

Wooltorton JR, Pidoplichko VI, Broide RS, Dani JA (2003) Differential desensitization and distribution of nicotinic acetylcholine receptor subtypes in midbrain dopamine areas. J Neurosci 23:3176-3185.

Wu SY, Dun NJ (1992) Presynaptic Gaba-B Receptor Activation Attenuates Synaptic Transmission to Rat Sympathetic Preganglionic Neurons Invitro. Brain Research 572:94-102.

Yokota Y, Sasai Y, Tanaka K, Fujiwara T, Tsuchida K, Shigemoto R, Kakizuka A, Ohkubo H, Nakanishi S (1989) Molecular characterization of a functional cDNA for rat substance P receptor. J Biol Chem 264:17649-17652.

Young SZ, Taylor MM, Bordey A (2011) Neurotransmitters couple brain activity to subventricular zone neurogenesis. Eur J Neurosci 33:1123-1132.

Yu S, Tooyama I, Ding WG, Kitasato H, Kimura H (1995) Immunohistochemical localization of glucose transporters (GLUT1 and GLUT3) in the rat hypothalamus. Obes Res 3:S753-S760.

Yu Y, Ugawa S, Ueda T, Ishida Y, Inoue K, Kyaw Nyunt A, Umemura A, Mase M, Yamada K, Shimada S (2008) Cellular localization of P2X7 receptor mRNA in the rat brain. Brain Research 1194:45-55.

Zagoraiou L, Akay T, Martin JF, Brownstone RM, Jessell TM, Miles GB (2009) A Cluster of Cholinergic Premotor Interneurons Modulates Mouse Locomotor Activity. Neuron 64:645-662.

Zappaterra MD, Lisgo SN, Lindsay S, Gygi SP, Walsh CA, Ballif BA (2007) A comparative proteomic analysis of human and rat embryonic cerebrospinal fluid. J Proteome Res 6:3537-3548.

Zhang Y, Lu L, Furlonger C, Wu GE, Paige CJ (2000) Hemokinin is a hematopoietic-specific tachykinin that regulates B lymphopoiesis. Nat Immunol 1:392-397.

Zheng JQ, Felder M, Connor JA, Poo MM (1994) Turning of nerve growth cones induced by neurotransmitters. Nature 368:140-144.